Understanding the impact of hypoxia on therapeutic response in breast cancer

---



Athanasios Patsalias

Wolfson College

Thesis submitted to the University of Oxford in accordance with the requirements for the degree of Doctor of Philosophy (DPhil)

Supervisor: Prof. Ester M. Hammond

University of Oxford
Department of Oncology
Michaelmas Term, 2024

ABSTRACT

Hypoxia, one of the most common features of the tumour microenvironment, is known to mediate anticancer treatment resistance and is highly associated with poor patient prognosis and relapse. Breast tumours are known to be amongst the most hypoxic ones, with more than 40% of breast adenocarcinomas, exhibiting regions of variable conditions of low oxygen. Despite numerous studies describing mechanisms of hypoxia-mediated increases in breast cancer cell aggressiveness and metastatic capacity, the impact of hypoxia on the breast cancer response to therapeutics, has not been adequately characterised. Our study aimed to investigate the response of triple-negative breast cancer cells, exposed to different levels of oxygen, towards the PARP inhibitor (PARPi) Olaparib, reporting an oxygen dependency of the cytotoxic effect of this anticancer agent. Preliminary data suggest the same observation with the more novel and yet non-deeply characterised in the context of hypoxia, polymerase theta inhibitor, ART558. Results of a systematic review, on the effects of PARPi in hypoxic cells supported this oxygen-dependency which we report. Furthermore, we analysed hypoxia-mediated transcriptional changes in genes associated with important biological processes of hypoxic cells. We assessed the oxygen dependency of such genes and their prognostic potential. Our work identified *RIMKLA*, a hypoxia-inducible gene, as a potential prognostic and predictive biomarker in breast cancer, putatively able to prognosticate outcomes in other types of cancer, as well. We further examined the biological role of *RIMKLA in vitro*, using breast cancer cells. We found that *RIMKLA* depletion by means of siRNA-mediated knockdown, resulted in a hypoxia-specific reduction of intracellular glutathione levels, upregulation of intracellular reactive oxygen species (ROS), and sensitisation of cells exposed to hypoxia. This sensitisation was significantly rescued after treatment with chemical antioxidants, suggesting a ROS-dependent mechanism. Reoxygenation of hypoxic, *RIMKLA*-depleted breast cancer cells, drove them into apoptosis and accumulation of DNA damage.

Thesis word count: 46,864

To all my dear friends and to my beloved family...
To those who decided to believe in their dreams...
And to those who believed in them...

Acknowledgments

It feels almost unreal writing these lines since this signifies the end of the most impactful era of my entire life. Only one emotion is greater than the excitement I feel for what the future holds, and it is that of immense GRATITUDE. When I began my DPhil journey, I was told that it takes all the help you can get to accomplish it, and I can confidently say that this was the biggest truth I have ever been told! It would have been impossible to do this without massive support from friends, colleagues, and family members. This work is devoted to all the people that helped me to accomplish my aspirations and to quench my scientific thirst, and I shall try my best to thank them in the small space of this section.

First and foremost, I would like to thank my supervisor, Prof. Ester Hammond. Ester, there are no words, in any human language, which can be used to express the gratitude which I feel for you and all that you have done for me. I couldn't have dreamed of having a better supervisor, mentor and, in many instances, a friend, than you. You taught me how to be a ture scientist by showing intelligence and rigor, by exemplifying professionalism, by training me to be critical of data, to be simple yet impactful (well, at least you tried, lol) and to be resilient. But above all you believed in me, even when I did not believe in myself, and for that I will never stop being thankful. I feel honored and blessed to have collaborated with you, and massively thankful to you, for granting me the opportunity to work in your lab, to learn a metric ton of stuff, and to accomplish my dreams. For this, and many other reasons, I will always hold you in my heart as one of the most impactful persons in my life, second only to my (actual) parents! All I can wish is that one day I get to be half of the great scientist that you are! P.S.: I'm sorry for all the times we made your blood pressure rise in the lab – but, honestly, it was lots of fun (lol)! Massive thanks for everything, boss!

Many thanks must also go to all the amazing colleagues that I had the honor to work with, during my time as a DPhil student: Sam, Natalie, Tiffany, Çağla, Charlotte, Sophie, Kat, Edward, Chumin, Louise, Conor, Jakub, Graham, Megan, Lina, Oliver, Bozhena, Akiko, Ricardo – it was a

great privilege to work with you all! Special thanks go to Hala Estephan, the most amazing Postdoc that a student can wish for. Hala, I will always be grateful for the skills you passed on to me, for always being there when anyone needed your help, and for being an example of quintessential teamwork in science!

A big thank you to all the people who helped me by assessing and improving my work during my studentship in the department. To Eric O'Neil – Eric, it was a massive help to know that you are always there when students needed you. We couldn't have wished for a better DGS! Thank you for helping me keep it together (multiple times)! Many thanks to Eileen Parkes, Geoff Hggins, Andy Blackford, and Nicola Sibson, for being my assessors. I will always be grateful for the constructive input on my research, and for being blessed to get expert advice from such great scientists. A warm thank you to my second supervisor, Amato Giaccia, for positive reinforcement during our brief talks – it was a pleasure to meet you and get to be your student. Many thanks to Monica Olcina and Iosifina Foskolou for providing useful information about life in Oxford. A big thank you to Mark Hill, for being the only radiation expert you might possibly ever need, especially when you need to fit a curve!

Massive thanks are also due to all my friends in the department, since life would not have been the same and a DPhil would not have been possible, if I hadn't had the blessing of meeting them! To Alice, Annamaria, Irene, Nuria, Pauline, Susan, Sahad, Alex, Vasso, David, Dominika, Tatsuya, Kelly, Tess, Su, Simei, Maxim, Gonzalo, Puru, Fariha, Yuri, Florian, Aswhin, Sophia, Matt, Bruno, Jamie, Ignacio, Wei, Remko, Linda, Sovan, Christian, Salome, Lana, Jennifer, Iain, Nathalie, Ed, Callum, Ftoon, Gwennie, Hongbin, Kate, Yhizou, Christiano, Flurin, Richard, Sam, Scott, Mahnaz, Kristoffer, Angela, Ben, Sovan, Rhod, Constantinos, Rathi, Rebecca, Teressa, Ian, Eleyna, Jiyoung, Caroline, Nikki, Heather, Fiona, Salwa, Shannon, Alexander, Arussa, Julius - It brings me tears of joy that I have the privilege of calling you my friends!

Special thanks are due to the people in the department I got to call my second family. Pash, thanks for always being a warm hug in the department, always willing to chat and listen, and for

being the affectionate secret Santa that you are! Swati, my sister from another mother, you know how much I love you, and that I feel blessed to call you family! This DPhil would have been practically impossible without you supporting me, in so many ways (especially by keeping my list updated) and surviving the "dance with the Satan," together! Asmita, you will always be my Lab Sunshine, the dearest and most loyal friend anyone can ask for! Thank you for your love and friendship, for your massive support, for your calm and practical advice and for being the kindest soul on this planet, always there for me. Paul, I am honored to be your friend (yes, suck it up) – you made this journey exciting, fun and cool, millions of times! You are the cleverest man I have met, with a pure soul and a witty sense of humor, and I feel blessed to get to call you friend! Lastly, a thank you is due to Tim Humphrey, for excellent positive reinforcement at times of great need! Tim – thank you for being the kind person and the great scientist that you are!

A great thank you also goes to my College President, Sir Tim Hitchens, for being an amazing mentor and a dear friend! Sir Tim – you know I'm your biggest fan, now it is written on my thesis as well – can't get any more official (lol)! To all my college friends, my choir friends, my Oxford friends and all my friends back home – thank you guys for being there for me, even when science was coming to get me! I love you all, so much. Basil and Adam – thank you for being brothers from another mother! Matt, Emily, Caroline (and family, lol), Callum and Livi, Tein - massive thanks for blessing me with your friendship! Lastly, to my dear family – a huge, massive, Gargantuan thank you, for all your love and support! You have no idea what it means to me to know that you're there, every step of the way. My cousin Eleni – thank you for all the late-night talks in times of need. My beloved auntie – thank you for your kind wishes and your love! My dear grandma, thank you for being the proudest person for me. And finally, Mum and Dad – I feel the luckiest boy on earth, just because I get to say that I am your son! You have set so many great examples for me in life, and I hope that I get to be as worthy and as kind as you are! Your selfless love and your massive support are the biggest blessings of my life! I really hope I made you proud!

THANK you all for making my DPhil, an amazing journey!

Table of Contents

ABSTRACT **2**

Acknowledgments **4**

List of figures **14**

List of tables **19**

Chapter 1 Introduction **24**

1.1. Cancer as a disease 24

1.1.1. The basic features of cancer 24

1.1.2. The hallmarks of cancer 25

1.1.3. DNA damage: types and causes 26

1.1.4. The DNA Damage Response: Sensor, transducers, and mediators of DNA damage 28

1.1.5. The DNA damage response: mechanisms of genomic damage repair 31

1.1.6. DDR in cancer: defects and implications in targeted cancer therapy 35

1.1.7. PARP inhibitors (PARPi) and the concept of synthetic lethality 37

1.1.8. Determinants of resistance to PARPi 42

1.2. Breast cancer 46

1.2.1. Basic pathology, classification, and molecular subtypes of breast cancer 46

1.2.2. The genetic background of breast cancer 49

1.3. Tumour Hypoxia 52

1.3.1. Tumour microenvironment and hypoxia 52

1.3.2. Defining hypoxia terms and types according to O_2 levels 54

1.4. The biological response to hypoxia 56

1.4.1. HIF-signalling in hypoxic cells and the transcriptional response to hypoxia 56

1.4.2. The DDR and the replication stress response in hypoxic cells 59

1.4.3. The impact of hypoxia on DNA damage repair 62

1.4.4. Hypoxia and the response to anticancer therapeutic modalities 63

1.4.5. The impact of hypoxia on the effects of DDRi 65

1.4.6. Hypoxia-mediated metabolic adaptations 67

1.5. ROS in cancer and their relationship with tumour hypoxia 68

1.5.1. ROS metabolism and detoxification 68

1.5.2. Cancer cell responses to excessive ROS levels 72

1.5.3. ROS and their relationship to tumour hypoxia 74

1.5.4. RIMKLA 78

1.6. AIMS OF STUDY 81

2.1. Methods 82

2.1.1. Cell culture 82

2.1.2. Mycoplasma testing of cell cultures 82

2.1.3. Cryopreservation of cells 82

2.1.4. Cell Thawing 83

2.1.5. Hypoxia treatment 83

2.1.6. Immunofluorescence 84

2.1.7. Preparation of protein lysates 84

2.1.8. Western blot assay 85

2.1.9. RNA extraction and purification 86
2.1.10. cDNA preparation 86
2.1.11. Real-time quantitative polymerase chain reaction (RT-qPCR) 87
2.1.12. 3-(4,5-dimethylthiazol-2-yl)-2,5-diphenyl-2H-tetrazolium bromide (MTT) assay ... 87
2.1.13. Short interfering RNA (siRNA) transfection 88
2.1.14. Clonogenic survival assay 88
2.1.15. Cell cycle analysis by Flow Cytometry 89
2.1.16. Measurement of Glutathione (GSH) levels using FL1 probe 89
2.1.17. CellROX Green assay for measurement of Reactive Oxygen Species (ROS) 90
2.1.18. Transformation of competent bacterial cells 91
2.1.19. Purification of plasmid DNA 91
2.1.20. Plasmid DNA transfection 92
2.1.21. Irradiation using a Caesium-source Irradiator 92
2.1.22. IC_{50} calculation 93
2.2. Bioinformatic methods 94
2.2.1. Analysis of mRNA levels in patient samples from publicly available datasets 94
2.2.2. Hypoxia signature correlation analyses 95
2.3. Statistical analyses 97
2.4. Materials 98
2.4.1. Cell lines 98
2.4.2. Solutions, buffers, and cell culture reagents 99
2.4.3. Drugs and chemicals 100

2.4.4. Primary Antibodies 101

2.4.5. Secondary Antibodies 103

2.4.6. Primers 104

2.4.7. siRNA sequences 105

2.4.8. Plasmids 105

Chapter 3 The impact of hypoxia on the effect of DDR inhibitors in breast cancer cells .. 106

3.1. Introduction 106

3.2. Results 107

3.2.1. Oxygen-dependent changes in cell cycle 107

3.2.2. The mitotic cell population changes in response to different hypoxia treatments . 108

3.2.3. Viability response to hypoxia 110

3.2.4. Hypoxia does not induce detectable DNA damage in breast cancer cells..... 111

3.2.5. Specific hypoxic conditions induce replication stress 113

3.2.6. Systematic review of the use and effects of PARP inhibitors (PARPi) in hypoxia 116

3.2.7. PARPi exhibit oxygen-dependent effects in breast cancer cells 132

3.2.8. Treatment with 2% O_2 decreases sensitivity to Olaparib 133

3.2.9. RAD51 levels decrease only in <0.1% O_2 135

3.2.10. Sensitivity/resistance to PARPi in hypoxia is not ROS-dependent..... 136

3.2.11. Quantification of ROS in hypoxic cells using ROS-sensor expressing plasmids... 138

3.2.12. Sensitivity to PolQi is oxygen-dependent 140

3.3. Discussion 142

Chapter 4 Hypoxia-induced changes in gene expression 148

4.1. Introduction 148

4.2. Results 151

4.2.1. *EPHA3* 151

4.2.2. *EFNA3* 153

4.2.3. *PPFIA4* 155

4.2.4. PPFIA4 protein levels in response to hypoxia 157

4.2.5. *RIMKLA* 159

4.2.6. *RIMKLA* mRNA levels exhibit differential correlations with hypoxia associated gene signatures 161

4.2.7. Correlation analysis of *RIMKLA* mRNA levels with all three clinically validated hypoxia signatures in all TCGA cancer datasets 163

4.2.8. Expression of *RIMKLA* in publicly available datasets of breast cancer patient samples 165

4.2.9. Analysis of RIMKLA protein levels in publicly available breast tumour and normal breast tissue samples 166

4.2.10. Validation of *RIMKLA* induction in hypoxia using additional breast cancer cell lines 168

4.2.11. Protein levels of RIMKLA increase in hypoxia 170

4.2.12. Validation of a RIMKLA antibody for immunofluorescence 171

4.2.13. Quantification and localisation of RIMKLA in hypoxic cells using phalloidin 173

4.2.14. Nucleolar expression of RIMKLA increases in hypoxia 175

4.2.15. Expression levels of *RIMKLA* correlate with breast cancer patient survival status and resistance to chemotherapy 177

4.2.16. Analysis of *RIMKLA* levels in breast tumour subtypes 179

4.2.17. *RIMKLA* mRNA levels correlate with worse survival in multiple cancer types 181

4.2.18. Homology analysis of RIMKLA with RIMKLB active sites 183

4.2.19. *RIMKLB* is not induced in response to hypoxia 185

4.2.20. Published data suggest that *RIMKLA* has an HRE 187

4.2.21. *RIMKLA* is induced in response to hypoxia mimetics 188

4.2.22. *RIMKLA* is more highly expressed in VHL null RCC 190

4.2.23. *RIMKLA* is not induced in a HIF-2α dependent manner 192

4.2.24. Loss of HIF-1α abrogates *RIMKLA* induction in hypoxia 194

4.3. Discussion 195

Chapter 5 Investigating the biological role of *RIMKLA* in hypoxic cells 201

5.1. Introduction 201

5.2. Results 202

5.2.1. Analysis of the impact of *RIMKLA* on intracellular GSH levels 202

5.2.2. Depletion of *RIMKLA* increases ROS levels in hypoxic and normoxic cells 204

5.2.3. Protein levels of *RIMKLA* are upregulated in response to ROS-inducing agents 206

5.2.4. Loss of *RIMKLA* does not lead to detectable DSBs in hypoxia 208

5.2.5. Loss of *RIMKLA* reduces levels of γH2AX 210

5.2.6. Loss of *RIMKLA* decreases the levels of hypoxia-induced replication stress 212

5.2.7. Loss of *RIMKLA* reduces cell number in response to hypoxia 214

5.2.8. Loss of *RIMKLA* in hypoxia decreases survival of cancer cells 216

5.2.9. Loss of *RIMKLA* does not induce apoptotic nuclear morphology in hypoxic cells .. 218

5.2.10. Loss of *RIMKLA* does not appear to increase activation of Caspase-3 220

5.2.11. Depletion of *RIMKLA* drives reoxygenated cells to apoptosis 222

5.2.12. Reoxygenation of *RIMKLA*-depleted cells drives them into apoptosis without p53-stabilisation..... 224

5.2.13. Reoxygenation of *RIMKLA*-depleted cells leads to higher levels of DSBs 226

5.2.14. Depletion of *RIMKLA* results in induction of apoptosis and decreased cell number in response to treatment with H_2O_2 228

5.2.15. Treatment with ROS scavengers rescues the reduced viability of hypoxic *RIMKLA*-depleted cells..... 230

5.2.16. High expression levels of *RIMKLA* correlate with worse survival outcomes in patients with hypoxic breast cancers, *vs*. patients with non-hypoxic breast tumours 232

5.2.17. Depletion of *RIMKLA* leads to radioresistance in normoxic cells without changing the sensitivity of hypoxic cells to ionising radiation 234

5.2.18. RIMKLA levels appear upregulated and diffusing outside the nucleoli in response to ionising radiation 236

5.2.19. High *RIMKLA* mRNA levels are associated with worse survival in breast cancer patients who received radiotherapy..... 238

5.3. Discussion 240

Chapter 6 Final Discussion..... 246

Chapter 7 References..... 256

Appendix 1 Thematic grouping of papers filtered from our systematic review screen 332

Appendix 2 Data from CCLE for status of key HR protein encoding genes - oncoprint diagrams 340

Appendix 3 Genes mostly upregulated in cyclic hypoxic conditions – RNAseq data (Hammond EM, 2020, unpublished)..... 342

Appendix 4 Analyses of the correlative power of top-15 genes from hypoxia-associated signatures used in the study..... 345

Appendix 5 Tumour *vs*. normal tissue analysis of *RIMKLA* expression levels (TCGA datasets) 350

Appendix 6 Correlation analysis of published breast cancer HIF-target genes with the Buffa hypoxia signature in TCGA BRCA publicly available transcriptomic datasets..... 351

Appendix 7 FIJI/Image J script used for image analysis (foci quantification)..... 354

Appendix 8 Presentations from this Thesis..... 355

List of figures

Figure 1.1. The progression of cancer. 25

Figure 1.2. The main types of DNA damage and their common causes. 28

Figure 1.3. The three apical kinases of the DDR. 31

Figure 1.4. DNA repair mechanisms. 35

Figure 1.5. Synthetic lethality between PARP inhibitors and homologous recombination deficiency. 41

Figure 1.6. The mechanisms of resistance to PARPi. 45

Figure 1.7. The pathology of breast cancer. 47

Figure 1.8. The Molecular subtypes of breast cancer. 49

Figure 1.10. The different types of tumour hypoxia. 53

Figure 1.11. Approximate oxygen levels reported in different tissues in mmHg and $\%O_2$ values. 56

Figure 1.12. The HIF-signalling and the VHL-dependent degradation systems. 59

Figure 1.13. The DDR in hypoxic cells. 61

Figure 1.14. Hypoxia and the response to anticancer therapeutic modalities 65

Figure 1.15. Redox homeostasis in the cell. 72

Figure 1.16. The HIF-mediated response to hypoxic ROS. 77

Figure 1.17. The biological role of *RIMKLA*. 80

Figure 2.1. Hypoxia treatments in our study. 83

Figure 2.2. The FL1-GSH probe. 90

Figure 3.1. Oxygen-dependent changes in cell cycle. 108

Figure 3.2. The mitotic population changes in response to different hypoxia treatments. 109

Figure 3.3. Exposure to hypoxia did not impact cell viability. 110

Figure 3.4. Hypoxia does not induce detectable DNA damage. 112

Figure 3.5. Hypoxia (<0.1% O_2) induces replication stress. 114

Figure 3.6. Hypoxia (<0.1% O_2) induces RPA foci 116

Figure 3.7. Boolean search strategy used for search terms. 117

Figure 3.8. PRISMA flow diagram of the systematic literature exclusion process. 119

Figure 3.9. The thematic distribution of the 35 papers identified from the systematic review process. 120

Figure 3.10. Oxygen-dependent response to Olaparib. 133

Figure 3.11. Treatment with 2% O_2 decreases sensitivity to Olaparib. 134

Figure 3.12. RAD51 levels decrease only in <0.1% O_2. 136

Figure 3.13. Treatment with NAC results in decreased sensitivity to Olaparib in cells exposed to <0.1% O_2 and increased sensitivity in cells treated with 2% O_2 or cyclic hypoxia. 137

Figure 3.14. Hypoxia leads to an increase in cellular ROS levels. 139

Figure 3.15. Oxygen-dependent response to the PolQ inhibitor ART 558. 141

Figure 4.1. Selecting genes of interest. 150

Figure 4.2. The oxygen-dependency of *EPHA3*. 152

Figure 4.3. The oxygen-dependency of *EFNA3*. 154

Figure 4.4. The oxygen-dependency of *PPFIA4*..... 156

Figure 4.5. Analysis of mRNA and protein levels of PPFIA4 in hypoxia. 158

Figure 4.6. The oxygen-dependency of *RIMKLA*. 160

Figure 4.7. Correlation analysis of *RIMKLA* with hypoxia-associated gene signatures in publicly available breast cancer datasets. 162

Figure 4.8. *RIMKLA* mRNA increases in breast tumours..... 165

Figure 4.9. Analysis of RIMKLA protein levels in publicly available breast tumour and normal breast tissue samples. 167

Figure 4.10. Validation of *RIMKLA* induction in hypoxia using additional breast cancer cell lines. 169

Figure 4.11. RIMKLA protein levels increase in hypoxia. 170

Figure 4.12. Validation of a RIMKLA antibody for immunofluorescence. 172

Figure 4.13. Quantification and localisation of RIMKLA in hypoxic cells using phalloidin. 174

Figure 4.14. Nucleolar expression of RIMKLA increases in hypoxia. 176

Figure 4.15. Expression levels of *RIMKLA* correlate with breast cancer patient survival status and resistance to chemotherapy. 178

Figure 4.16. Analysis of *RIMKLA* levels in breast tumour subtypes. 180

Figure 4.17. Kaplan-Meier curves for tumour types where high expression of *RIMKLA* is associated with significantly decreased overall survival probability.. 182

Figure 4.18. Homology analysis of RIMKLA with RIMKLB active sites. 184

Figure 4.19. *RIMKLB* is not induced in response to hypoxia. 186

Figure 4.20. Published data suggest that *RIMKLA* has an HRE. 187

Figure 4.21. Hypoxia mimetics induce *RIMKLA*. 189

Figure 4.22. *RIMKLA* is more highly expressed, in *VHL* null RRC4 cells. 191

Figure 4.23. Stabilisation of HIF-2α does not induce *RIMKLA*. 193

Figure 4.24. Loss of *HIF-1α* abrogates *RIMKLA* induction in hypoxia. 194

Figure 5.1. Analysis of the impact of *RIMKLA* on intracellular GSH levels. 203

Figure 5.2. Loss of *RIMKLA* increases ROS levels in hypoxic and normoxic cells. 205

Figure 5.3. Protein levels of RIMKLA are increased, in response to ROS-inducing agents. 207

Figure 5.4. Loss of *RIMKLA* does not lead to detectable DNA damage in hypoxia. 209

Figure 5.5. Loss of *RIMKLA* reduces levels of γH2AX in hypoxic cells. 211

Figure 5.6. Loss of *RIMKLA* decreases the levels of hypoxia-induced replication stress. 213

Figure 5.7. Loss of *RIMKLA* reduces cell number in response to hypoxia. 215

Figure 5.8. Loss of *RIMKLA* sensitises CAL-51 cells to hypoxia. 217

Figure 5.9. Loss of *RIMKLA* does not induce apoptotic nuclear morphology in hypoxic cells. 219

Figure 5.10. Loss of *RIMKLA* does not appear to lead to activation of Caspase-3. 221

Figure 5.11. The impact of *RIMKLA* loss on nuclear morphology and number of reoxygenated cancer cells. 223

Figure 5.12. Reoxygenation of *RIMKLA*-depleted cells drives them into apoptosis without p53-stabilisation. 225

Figure 5.13. Reoxygenation of *RIMKLA*-depleted cells leads to higher levels of DSBs. 227

Figure 5.14. Depletion of *RIMKLA* results in induction of apoptosis and decreased cell number in response to treatment with H_2O_2. 229

Figure 5.15. Treatment with ROS scavengers rescues the reduced viability of hypoxic *RIMKLA*-depleted cells. 231

Figure 5.16. High levels of *RIMKLA* correlate with worse survival outcomes in patients with hypoxic breast cancers, vs. patients with non-hypoxic breast tumours. 233

Figure 5.17. Depletion of *RIMKLA* leads to radioresistance in normoxic cells without changing the sensitivity of hypoxic cells to ionising radiation. 235

Figure 5.18. RIMKLA levels appear to be upregulated and diffusing outside the nucleoli in response to ionising radiation. 237

Figure 5.19. High *RIMKLA* mRNA levels are associated with worse survival in breast cancer patients who received radiotherapy. 239

Figure 5.20. Proposed model for the biological role of *RIMKLA* in hypoxic cell viability. 245

List of tables

Table 2.1. Cell lines used in this study. Listed below are cell lines, tissue type, culture media and their origin. 98

Table 2.2. List of solutions, buffers, and cell culture reagents. The names and origin of solutions buffers and cell culture reagents. 99

Table 2.3. Drugs and Chemicals. Listed below are drugs and chemicals used in experiments, as well as their abbreviations, their stock concentrations, and their sources of origin. 100

Table 2.4. List of Primary antibodies and related information. 101

Table 2.5. List of Secondary antibodies used and related information. 103

Table 2.6. List of primers used and related information..... 104

Table 2.7. siRNA sequences. List of targets, sequences and manufacturers of siRNAs used in this study. 105

Table 2.8. Plasmids. Name and origin of plasmids used to transfect mammalian cells in our study. 105

Table 3.1. Eligible standards for inclusion or exclusion according to the SPIDER framework . 118

Table 3.2. Summary of studies reporting data PARPi effect on viability of hypoxic cells. 121

Table 3.3. Summary of studies reporting data on viability of hypoxic cells with PARPi combined with other treatment(s)..... 124

Table 4.1 Correlation analysis of *RIMKLA* mRNA levels with all three clinically validated hypoxia signatures in all TCGA cancer datasets. 164

List of Abbreviations and Symbols

8-oxoG	8-oxoguanine
18S	18S ribosomal RNA
47S	precursor rRNA
53BP1	p53 binding protein 1
% O_2	percentage of oxygen
°C	degree Celsius
ΔΔCt	delta delta Ct
γ-H2AX	phosphorylation of the serine-139 residue of H2AX histone family member X AKT
APE1	Apurinic/Apyrimidinic Endodeoxyribonuclease 1 APH
ARNT	Aryl hydrocarbon Receptor Nuclear Translocator ATCC
ATG12	Autophagy Related 12
atm	standard atmosphere
ATM	Ataxia Telangiectasia Mutated
ATMIN	ATM Interactor
ATR	Ataxia Telangiectasia mutated and Rad3-related protein ATRIP
BCL-2	B-cell lymphoma 2
BCL-XL	B-cell lymphoma -extra-large BECN1
BER	base excision repair
BRCA	BReast CAncer gene
BRCA1	Breast Cancer gene 1
BRCA2	Breast Cancer gene 2
BrdU	bromo-2'-deoxyuridine
CAIX	Carbonic Anhydrase 9
CAFs	cancer-associated fibroblasts
CBP	CREB-binding protein
cDNA	complementary DNA
ChIP	chromatin immunoprecipitation
CHK1	Checkpoint Kinase 1

CHK1-S345	phosphorylation of CHK1 at serine 345 CHK2
CO2	carbon dioxide
DEPC water	Diethyl pyrocarbonate water DDR
DMEM	Dulbecco's modified Eagle's medium DMSO
DNA	deoxyribonucleic acid
DNA-PK	DNA-dependent protein kinase
DNA-PKcs	DNA-dependent protein kinase catalytic subunit dNTP
DRB	5,6-Dichlorobenzimidazole 1-β-D-ribofuranoside DRIP
DSBs	double-strand breaks
dsDNA	double-stranded DNA
dU	deoxyuridine
E2F	E2 factor
ECM	extracellular matrix
EdU	5-ethynyl-2'-deoxyuridine
eIF2α	eukaryotic initiation factor 2 alpha EMT
EPO	erythropoietin
ER	endoplasmic reticulum
ERAD	ER-associated degradation
ERCC1	Excision Repair Cross-Complementation Group 1 ERO-1α
ETP	etoposide
FACS	fluorescence-activated cell sorting
FANCD2	Fanconi anemia complementation group D2 FBS
FDA	Food and Drug Administration
FIH	factor-inhibiting HIF
G1 phase	growth 1 phase
G2 phase	growth 2 phase
H2AX	H2A histone family member X
H2O2	hydrogen peroxide
H3K9me3	trimethylation of the 9th lysine residue on histone H3 protein
Hu	hydroxyurea
HCl	hydrochloric acid
HIF	Hypoxia-Inducible Factor
HIF-1	Hypoxia-Inducible Factor-1
HIF-2	Hypoxia-Inducible Factor-2
HIF-1α	Hypoxia-Inducible Factor-1 alpha
HR	homologous recombination
HRE	Hypoxia Responsive Elements
IF	immunofluorescence
IP	immunoprecipitation
IRE1α	inositol-requiring enzyme 1 alpha IRE1αi
JNK	JUN N-terminal kinase
kb	kilobase
KEAP1	Kelch Like ECH Associated Protein 1 kPa

LIG4	DNA Ligase IV
lncRNA	long non-coding RNA
MAPK	Mitogen-Activated Protein kinase MDSC
MEM	Minimum Essential Media
miRNA	microRNA
MLH1	MutL protein homolog 1
mmHg	millimetre of mercury
MMR	mismatch repair
MRE11	Meiotic Recombination 11 Homolog 1
MRN	MRE11-RAD50-NBS1
MRP1	Multidrug Resistance-Associated Protein 1 mRNA
MSH2	MutS homolog 2
MSH6	MutShomolog 6
MTH1	MutT Human Homolog 1
mTORC1	mammalian target of rapamycin complex 1 MYH1
NaCl	Sodium chloride
NAC	*N*-acetylcysteine
NADPH	nicotinamide adenine dinucleotide phosphate NBS1
NCS	neocarzinostatin
NER	nucleotide excision repair
NF-κB	nuclear factor-κB
NHEJ	non-homologous end-joining
NMP1	nucleophosmin
NOX4	NADPH oxidase subunit 4
NRF2	Nuclear Factor Erythroid 2-Related Factor 2
OGG1	8-oxogoaunine DNA glycosylase P/S
p300	histone acetyltransferase p300
p53	tumour protein p53
PARP1	poly(ADP-ribose) polymerase 1 PBS
PCR	polymerase chain reaction
PERK	protein kinase RNA-like endoplasmic reticulum kinase
PERKi	PERK inhibitor
PET	positron emission tomography
PFA	paraformaldehyde
PHD	Prolyl-Hydroxylase Domain protein
PI3K	phosphatidylinositol-3 kinase
PIF1	Petite Integration Frequency 1
PIKK	phosphatidylinositol-3 kinase-like kinase Pol ι
PRISMA	Preferred Reporting Items for Systematic Reviews and Meta-Analyses qPCR
RAD50	RAD50 Double Strand Break Repair Protein RAD51
rDNA	ribosomal DNA
RNA	ribonucleic acid RNA Pol I
RNase H	ribonuclease H RNaseH1
RNR	ribonucleotide reductase

ROS	reactive oxygen species
RPA	Replication Protein A
RPA-S33	phosphorylation of RPA at serine 33 rRNA
RT	room temperature
SDS	sodium dodecyl sulphate
SERCA	sarco/endoplasmic reticulum Ca2+-ATPase SETX
siRNA	small interfering RNA
SOD	superoxide dismutase
SSBs	single-strand breaks
ssDNA	single-stranded DNA
*t*BHP	*tert*-Butyl hydroperoxide
TBS	Tris-Buffered Saline
TCF21	transcription factor 21
TC-NER	transcription-coupled nucleotide excision repair TE
TH-302	evofosfamide
TLS	translesion synthesis
TME	tumour microenvironment
TOP1	topoisomerase I
TopBP1	DNA topoisomerase II binding protein 1 TPZ
TRCs	transcription-replication collisions
Treg	T-regulatory cells
Tuni	tunicamycin
UBF	Upstream Binding Factor
UPR	unfolded protein response
UTB	urea Tris buffer
UV	ultraviolet
VEGF	Vascular Endothelial Growth Factor A VHL
VitC	vitamin C
WB	western blot
WEE1	WEE1 G2 Checkpoint Kinase
WHO	World Health Organisation
x *g*	times gravity
XRCC4	X-ray repair cross-complementing protein 4 XBP1

Chapter 1 Introduction

1.1. Cancer as a disease

1.1.1. The basic features of cancer

Neoplasia, commonly known as cancer, is a group of more than 100 diseases that develop progressively and are characterised by the uncontrolled division of the body's cells (McKinnell RG 1998). Although cancer can develop in virtually any of the body's tissues, and each type of cancer has its unique features, the basic processes that produce cancer are quite similar in all forms of the disease: cancer begins when a cell evades the normal restraints of cell division and starts proliferating uncontrollably (Figure 1.1). All the cells produced by division of this first, "transformed" cell and its progeny, will also display inappropriate proliferation (Greenwald and Dunn 2009).

A tumour, or mass of cells, formed by these abnormal cells may remain within the tissue in which it originated (a condition called *in situ* carcinoma), or it may begin to invade nearby tissues (a condition known as invasive carcinoma) (NIH 2007). An invasive tumour is said to be malignant, and cells that pass into the blood or lymph from a malignant tumour, are likely to establish new tumours (metastases) throughout the body. Malignant tumours threaten an individual's life when their growth disrupts the normal function of tissues and organs (McKinnell RG 1998; NIH 2007; Trichopoulos *et al.* 1996).

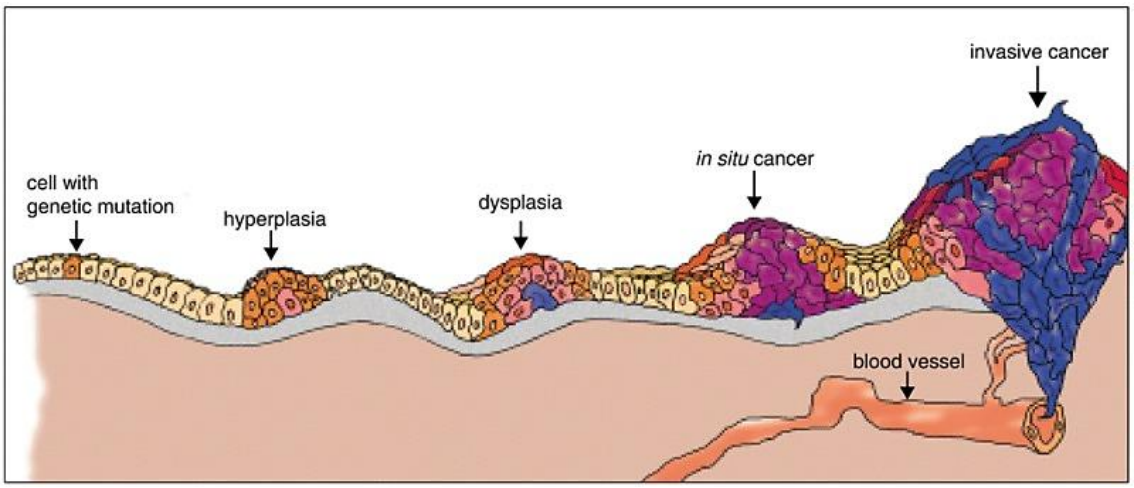

Figure 1.1. The progression of cancer. A diagram of the process of cancer development, from a single cell with a genetic mutation which promotes cell growth and proliferation, forming what is known as hyperplastic lesions. Accumulation of further mutations lead to loss of differentiation and dysplasia. Abnormal growth localised in the tissue of origin (*in situ* carcinoma) ultimately gives rise to an invasive carcinoma, with the ability to metastasise to remote tissues and organs. Reprinted from: "The cell: cell microenvironment and cell handling" (Ganguin *et al*. 2023). Licence No.: 5870270442993.

1.1.2. The hallmarks of cancer

Two decades ago, Hanahan and Weinberg distilled the myriad alterations in cancer cells into six "hallmarks" that collectively enable tumour initiation, progression, and metastasis: sustained proliferative signaling; evasion of growth suppressors; resistance to cell death; replicative immortality; induction of angiogenesis; and activation of invasion and metastasis (Hanahan and Weinberg 2000). A subsequent update in 2011 added two further core capabilities - deregulated energetics and immune evasion - and highlighted two "enabling characteristics": genome instability and tumour-promoting inflammation (Hanahan and Weinberg 2011). More recently, Hanahan (2022) proposed additional dimensions - phenotypic plasticity, non-mutational epigenetic reprogramming, polymorphic microbiomes, and senescent cells - that modulate or facilitate hallmark acquisition (Hanahan 2022).

Out of the emerging hallmarks characterised as enabling, genome instability is considered to be

the most important one. Genome instability refers to a high frequency of mutations within the genome of cancer cells, a characteristic that enables the acquisition of other hallmarks. Some of the most common examples of such genomic changes include increased rates of point mutations, chromosomal rearrangements, and gene amplifications, which occur partly due to mechanisms such as, defects in DNA repair pathways, telomeric dysfunction and epigenetic modifications. Genome instability importance in cancer is thus depicted in is ability to drive tumour evolution, contribute to heterogeneity within tumours and enable rapid adaptation of cancer cells to selective pressures (Negrini *et al.* 2010; Shen 2011; Tubbs and Nussenzweig 2017; Vogelstein *et al.* 2013).

1.1.3. DNA damage: types and causes

As described in previous sections, genomic instability is a common characteristic of most cancer cells with DNA damage accumulation being a primary driver of genomic instability. DNA stability is crucial for the execution of inerrant replication and transcription processes, ultimately aiming to maintain genome integrity for normal cell functions. The molecular mechanisms by which cells maintain genome stability and the consequences of genomic instability are therefore areas of high importance in cancer research (Huang and Zhou 2021).

DNA damage can be divided into two main classes depending on its origin: endogenous and exogenous. The majority of the endogenous DNA damage occurs, when the chemically active DNA engages in hydrolytic and oxidative reactions with water and reactive oxygen species (ROS) respectively, all of which are naturally present within the cells (Chatterjee and Walker 2017). Endogenous DNA damage can also arise from the occasionally error-prone action of the various enzymes which take part in DNA synthesis and transcription, such as DNA polymerases, topoisomerases and DNA glycosylases (Chatterjee and Walker 2017; Huang and Zhou 2021; Reuter *et al.* 2010). Exogenous DNA damage, on the other hand, happens when environmental

physical and chemical agents, damage the DNA (Chatterjee and Walker 2017). Examples of this exogenous hazards include, UV and ionising radiation, heavy metals, alkylating and crosslinking agents (e.g. aromatic amines, nitrosamines), natural toxins (e.g. aflatoxins) and others (Huang *et al*. 2018; Huang and Zhou 2021; Maremonti *et al*. 2020; Wu *et al*. 2020).

The main types of DNA lesions in mammalian cells include, nitrogenous base lesions, such as base mismatches or formation of abasic sites (AP sites), single (SSBs) or double strand breaks (DSBs) and inter-or intrastrand crosslinks (ICLs) (figure 1.2) (Ceccaldi *et al*. 2016; Frankenberg-Schwager 1990). Specifically, the enzymatic machinery of the cell, employed during DNA replication can be prone to errors, leading thus to occasional mismatched base pairing due to the incorporation of incorrect nucleotides (Tubbs and Nussenzweig 2017). Furthermore, ROS and Reactive Nitrogen Species (RNS), common byproducts of physiological activities, can cause DNA lesions from oxidative stress, including AP sites, strand breaks, and base substitutions. Natural decay processes like alkylation, oxidation, and deamination can also lead to mutagenic base substitutions during replication. SSBs can occur spontaneously during replication, or due to certain types of irradiation, potentially leading to DSBs, the most dangerous type of DNA damage. If not properly repaired DSBs can lead to carcinogenesis or cell death (figure 1.2). Nonetheless, all types of the above-described DNA lesions, can have severe consequences for the cell's structural and functional integrity and must be repaired, for the cells to maintain genomic stability and prevent the accumulation of mutations (Carusillo and Mussolino 2020; Ceccaldi *et al*. 2016; Chatterjee and Walker 2017; Hossain *et al*. 2018).

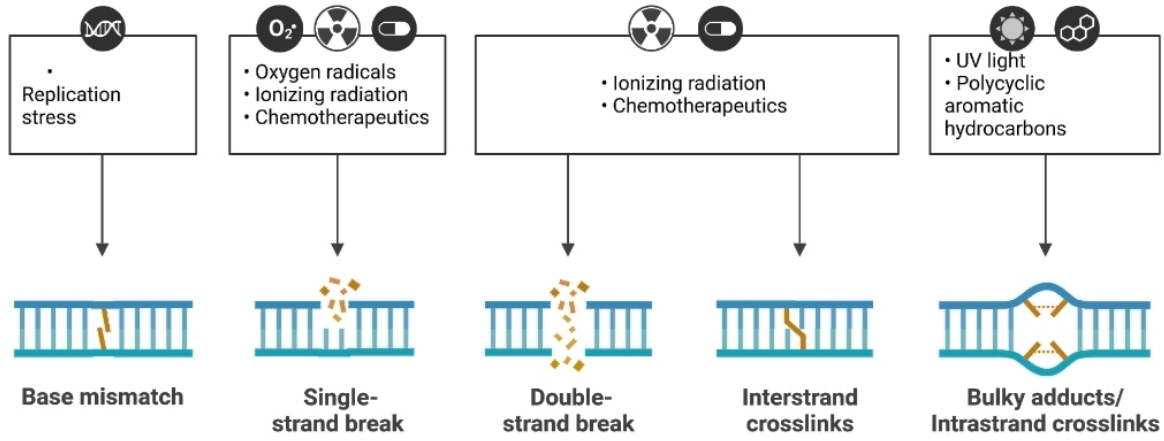

Figure 1.2. The main types of DNA damage and their common causes. The main sources of DNA damage, both endogenous and exogenous are shown, associated with the respective form of DNA lesion they are known to result in. Challenges such as replication stress cause base lesions, including mismatch errors; ROS, ionising radiation, and chemotherapeutics, are mostly associated with single strand breaks, while UV light and aromatic hydrocarbons are associated with the formation of intrastrand crosslinks. All of these lesions if not thoroughly and properly repaired can however result in the formation of toxic double-strand breaks. Reprinted from: "Common causes of DNA Damage," BioRender (2024). Retrieved from: https://app.biorender.com/biorender-templates.

1.1.4. The DNA Damage Response: Sensor, transducers, and mediators of DNA damage

Genomic integrity is safeguarded by a hierarchical DNA damage response (DDR) network that rapidly detects lesions, propagates signalling cascades, and orchestrates appropriate repair or checkpoint outcomes. At its core are three apical phosphoinositide-3-kinase-related kinases (PIKKs) - ATM, ATR and DNA-PKcs - each activated by distinct DNA structures and each mobilising a cohort of transducers and effectors to maintain chromosomal stability (Lord and Ashworth 2012).

Following DNA damage, specialised sensor complexes recognise aberrant DNA termini or single-stranded DNA (ssDNA) tracts and recruit their cognate PIKK. The activated kinase then phosphorylates mediator proteins and downstream checkpoint kinases, culminating in cell-cycle arrest, DNA repair factor recruitment or, if damage is irreparable, apoptotic or senescence cascades. Three coordinated modules can be delineated: i. Detection by sensor

proteins (MRN for DSBs; RPA/9-1-1 for ssDNA; Ku70/80 for DSB ends), ii. Signal transduction *via* PIKK activation (ATM, ATR, DNA-PKcs) and phosphorylation of mediators (MDC1, TOPBP1, 53BP1) and iii. Effector execution through checkpoint kinases 1 and 2 (CHK1, CHK2), repair enzymes (BRCA1/2, RAD51, DNA ligase IV) and chromatin remodelers (figure 1.3) (Blackford and Jackson 2017; Ciccia and Elledge 2010; Jackson and Bartek 2009).

ATM exists as an inactive homodimer tethered by interaction of its FAT (FRAP–ATM–TRRAP) domains. Upon DSB recognition, the MRE11–RAD50–NBS1 (MRN) complex binds broken ends and recruits ATM through an interaction between NBS1's FHA and tandem BRCT domains and ATM's C-terminal FATC region. MRN then promotes ATM autophosphorylation at Ser1981, which triggers dimer dissociation and catalytic activation. Activated ATM phosphorylates histone H2AX on Ser139 (γH2AX) within megabase regions flanking the break, creating binding sites for MDC1. MDC1 amplifies the signal by recruiting RNF8/RNF168 ubiquitin ligases, which in turn facilitate 53BP1 and BRCA1 accumulation - key determinants of repair pathway choice (Blackford and Jackson 2017; Lee and Paull 2004). ATM also directly phosphorylates the checkpoint kinase CHK2 on Thr68, enabling CHK2 dimerisation and activation; phosphorylated CHK2 further targets p53 at Ser20, stabilising this master regulator and enforcing G1 arrest (Matsuoka *et al*. 2000). Through these orchestrated events, ATM both scaffolds repair factor assembly and engages cell-cycle checkpoints to afford time for error-free DSB resolution integrity (Mirza-Aghazadeh-Attari *et al*. 2018).

ATR is activated by ssDNA–RPA complexes that accumulate at stalled replication forks or excision repair intermediates. RPA-coated ssDNA recruits ATR *via* its obligate partner ATRIP, which binds directly to RPA70's basic cleft (Blackford and Jackson 2017). Concurrently, the RAD17–RFC clamp loader assembles the 9-1-1 complex (RAD9–RAD1–HUS1) at junctions of ssDNA and dsDNA. The loaded clamp then interacts with TOPBP1's ATR-activation domain, allosterically stimulating ATR's kinase activity. Once active, ATR phosphorylates CHK1 on Ser317 and Ser345, provoking CHK1 autophosphorylation and full activation. CHK1 phosphorylates

CDC25A, targeting it for ubiquitin-mediated degradation, thereby preventing CDK2 activation and intra-S-phase origin firing (Delacroix *et al.* 2007). ATR also phosphorylates members of the Fanconi anaemia network (e.g. FANCI), integrating interstrand crosslink repair with replication fork stability. Through this axis, ATR preserves replication integrity and forestalls fork collapse into DSBs, particularly under elevated genotoxic stress conditions (Andreassen *et al.* 2004; Blackford and Jackson 2017).

DNA-PKcs, the catalytic subunit of the DNA-PK holoenzyme, is recruited to DSB ends by the Ku70–Ku80 heterodimer, which slides onto DNA termini as a pre-formed ring. Ku binding, exposes the Ku80 C-terminus, docking DNA-PKcs *via* HEAT repeats that encircle the kinase domain. Upon assembly, DNA-PKcs undergoes autophosphorylation at multiple clusters (notably the ABCDE and PQR sites), which modulates end-tethering dynamics and accessibility of end-processing nucleases such as Artemis (Ochi *et al.* 2015; Polo *et al.* 2012). Classical Non-homologous end joining (NHEJ) proceeds as DNA-PKcs–Artemis mediates limited end trimming or gap filling, after which the Ligase IV–XRCC4–XLF–PAXX scaffold aligns DNA termini for ligation. Although rapid and cell-cycle-independent, NHEJ often incurs small insertions or deletions at junctions - tolerable in G1 but potentially oncogenic, if mis-rejoined (Lieber 2008).

Although ATM, ATR and DNA-PKcs initiate distinct repair programmes, substantial cross-regulation exists. For example, ATM-mediated γH2AX deposition facilitates ATR recruitment at DSB-resection forks, and ATR can phosphorylate ATM at Ser1981 under replication stress conditions. Likewise, competition between Ku and MRN for DNA ends, influences pathway choice: Ku depletion enhances resection and homology-assisted repair, whereas overabundant Ku biases repair to NHEJ. Tight spatial and temporal coordination of these PIKKs ensures that the most appropriate repair mechanism is deployed according to lesion type, cell-cycle stage and chromatin context (figure 1.3) (Bartek *et al.* 2004; Liu *et al.* 2000; Ruiz *et al.* 2016).

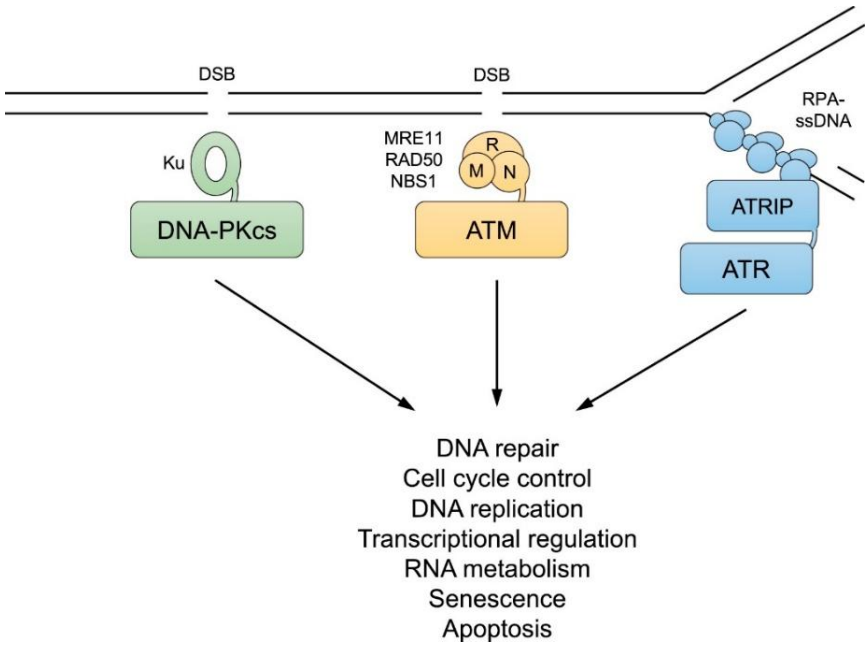

Figure 1.3. The three apical kinases of the DDR. The three kinases orchestrating the DDR are shown with the main types of DNA damages they respond to, and the key proteins involved in the recognition/activation processes. DNA-PKcs is recruited and activated by Ku-bound DSB ends. ATM is activated and recruited to DSBs by the MRE11-RAD50-NBS1 (MRN) complex. ATR is recruited to RPA-coated ssDNA by its stable binding partner ATRIP (Blackford and Jackson 2017). Activation of the DDR kinases can initiate cascades leading to DNA repair, cell cycle arrest, programmed cell death, senescence, replication modulation, or changes in transcriptional regulation. Reprinted from: ATM, ATR, and DNA-PK: The Trinity at the Heart of the DNA Damage Response (Blackford and Jackson 2017). License No.: 5861931090367.

1.1.5. The DNA damage response: mechanisms of genomic damage repair

When DNA damage is encountered, specific, highly regulated and well conserved responses are elicited by the cell, aiming to either repair the damage, or in cases of extreme genomic instability, to control the spread of potentially harmful mutations to cell progenies, by initiating biological processes like apoptosis or senescence (Alhmoud *et al.* 2020; Huang *et al.* 2018).

When it comes to damage repair the majority of minor DNA lesions, such as oxidative damage-associated ones, alkylation products, and SSBs, are repaired through a set of processes collectively known as base excision repair (BER) mechanisms. During BER, damaged bases are initially excised from the double helix, and the damaged part of the DNA backbone is

subsequently cut out and substituted with newly synthesised DNA. The enzymes poly (ADP-ribose) polymerase 1 and 2 (PARP1 and PARP2), play a crucial role in this process by functioning as detectors and communicators for the DNA damage to be repaired (figure 1.4) (Dianov and Hubscher 2013; Parsons and Dianov 2013; Whitaker and Freudenthal 2018). Besides BER, the pool of deoxynucleotides deoxyadenosine triphosphate (dATP), deoxythymidine triphosphate (dTTP), deoxyguanosine triphosphate (dGTP) and deoxycytidine triphosphate (dCTP), essential for DNA synthesis, can also undergo chemical alterations prior to being integrated into the double helix, part of a repair process known as direct damage reversal (Couve *et al*. 2013; Eker *et al*. 2009).

DSBs represent the most deleterious form of DNA damage, as loss of both strands can precipitate chromosomal translocations, oncogenic rearrangements, or apoptosis. Eukaryotic cells deploy two principal DSB repair pathways - homologous recombination (HR) and classical NHEJ - each finely regulated by cell-cycle cues, chromatin context and the interplay of sensor, transducer and effector proteins (figure 1.4)(Chatterjee and Walker 2017; Huang and Zhou 2021).

In G0/G1, when sister chromatids are absent, NHEJ predominates. The Ku70–Ku80 heterodimer binds DSB ends within seconds of break induction, encircling DNA in a sequence-independent fashion to shield termini from nucleolytic degradation. Ku recruits the catalytic subunit DNA-PKcs, forming the DNA-PK holoenzyme. Autophosphorylation of DNA-PKcs elicits conformational changes that permit recruitment of end-processing factors - Artemis, polynucleotide kinase phosphatase (PNKP) and TDP1 - to trim overhangs or convert blocked ends into 5'-phosphate/3'-hydroxyl termini. Final ligation is executed by the Ligase IV–XRCC4–XLF–PAXX complex, which juxtaposes termini and covalently seals breaks, typically with minimal nucleotide loss but with occasional micro-indels sites (figure 1.4)(Chen *et al*. 2024b; Kumar *et al*. 2016; Trenner and Sartori 2019).

As cells progress into S and G2, cyclin-dependent kinase (CDK) activity, phosphorylates CtIP on Ser327 and Thr847, promoting its interaction with the MRN complex (MRE11–RAD50–NBS1). Activated CtIP endonucleolytically nicks DNA adjacent to the break, enabling MRN's exonuclease activity to resect DNA bidirectionally, generating 3' ssDNA overhangs. This resection marks the commitment to HR and simultaneously suppresses NHEJ by precluding Ku re-binding (Gu *et al*. 2023; Kuwahara 2023).

The ssDNA overhangs are immediately coated by replication protein A (RPA), stabilising the ssDNA and preventing secondary structure formation. Transition from RPA to RAD51 filaments is mediated by BRCA1–PALB2–BRCA2: BRCA1 interacts with CtIP and facilitates resection, while PALB2 bridges BRCA1 to BRCA2. BRCA2's eight BRC repeats bind RAD51 monomers, chaperoning them onto RPA-coated ssDNA to form a right-hand-shaped nucleoprotein filament. This RAD51 filament conducts homology search by sampling duplex DNA in 8-nucleotide increments, probing for perfect sequence complementarity. Once homology is located, the invading 3' end primes DNA synthesis by polymerases δ and ε, using the intact sister chromatid as template. Resolution of the resulting joint molecules occurs either *via* dissolution - through the BLM–TOP3α–RMI1/2 complex, which disentangles Holliday junctions without crossover - or by cleavage by structure-specific endonucleases (GEN1, MUS81–EME1), potentially yielding crossovers (figure 1.4) (Ali *et al*. 2021; Savage and Harkin 2015; Trenner and Sartori 2019).

The balance between HR and NHEJ is further modulated by factors that recognise chromatin modifications around DSBs. RNF8/RNF168-mediated ubiquitination of histone H2A at Lys13/15 recruits 53BP1 which, together with its effector Shieldin, inhibits end resection and biases repair toward NHEJ. Conversely, BRCA1 counteracts this bias by recruiting the deubiquitinase BAP1 and promoting resection, thus favouring HR in S/G2 (Ceccaldi *et al*. 2016; Gomes *et al*. 2010; Ochi *et al*. 2015). Similarly, the chromatin remodelers CHD1 and SMARCAD1 facilitate nucleosome eviction to allow resection, while histone methylation marks (mainly H3K36me3) guide

recruitment of CtIP, linking transcriptional activity to repair pathway selection (Gomes *et al.* 2010; Reed 2010).

When the NHEJ repair pathway is compromised due to loss or inactivation of one or more of its key protein components, the activity of the other end joining pathways becomes apparent, which typically involve much more extensive resection of the DNA ends to reveal sequence homology, the annealing of which stabilises the two ends of a break, to allow for more efficient joining and ligation. Microhomology-mediated end joining (MMEJ) requires microhomology, ranging between 2 bp and 20 bp, and the key enzyme known as Polymerase theta (PolQ). PolQ, is encoded by the *POLQ* gene and belongs to the A family of DNA polymerases (Chang *et al.* 2017). It has been shown to stabilise the annealing of two long 3' ssDNA overhangs (often known as 3' tails) with as little as 2 bp of homology, extending one 3' DNA end, by using the annealing partner as a template. This creates a more stable annealed intermediate which can be sealed by either DNA ligase I or DNA ligase III; The polymerase activity of PolQ probably prevents further extensive resection of ends, thereby minimising the potential formation of large deletions (Zhou *et al.* 2021). PolQ has also been shown to exhibit terminal transferase activity and can thus add nucleotides to provide microhomology when that is not already present (Ahrabi *et al.* 2016; Rodriguez-Berriguete *et al.* 2023; Sallmyr and Tomkinson 2018).

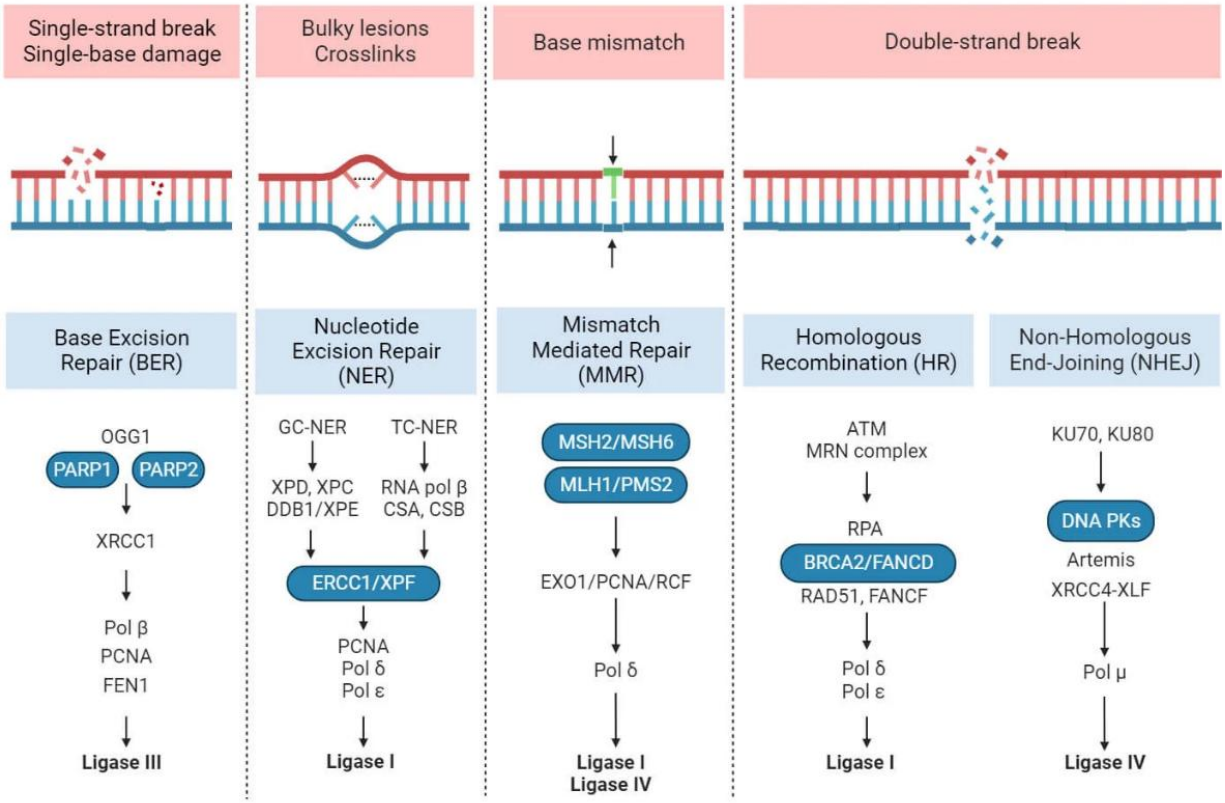

Figure 1.4. DNA repair mechanisms. The main mechanisms of genomic damage repair and the key proteins involved are shown. Specialised cellular machinery is employed for repair, according to the type of DNA lesion. Abbreviations not included in main text: OGG1 = 8-oxoguanine glycosylase-1; XRCC1 = X-ray repair cross-complementing protein; pol β = DNA polymerase beta; PCNA = Proliferating cell nuclear antigen; FEN1 = Flap Structure-Specific Endonuclease 1; XPD = Xeroderma Pigmentosum Group D Protein; XPC = Xeroderma Pigmentosum Group C Protein; XPE = Xeroderma Pigmentosum Group E Protein; DDB1 = Damage Specific DNA Binding Protein 1; CSA = Cockayne Syndrome WD-Repeat Protein A; CSB = Cockayne Syndrome B Protein; pol δ/ε = DNA polymerase delta/epsilon; MLH1 = MutL Homolog 1; PMS2 = Postmeiotic Segregation Increased 2; ATM = Ataxia-telangiectasia mutated; MRN = Mre11-Rad50-Nbs1complex; RPA = Replication protein A. Reprinted from: "DNA repair mechanisms", BioRender (2024). Retrieved from: https://app.biorender.com/biorender-templates.

1.1.6. DDR in cancer: defects and implications in targeted cancer therapy

The majority of carcinogens function by creating DNA damage and inducing mutations. Moreover, genetic abnormalities in DDR pathways, often increase the risk of cancer, play a role in specific genotypes commonly encountered in various cancers, and can promote the survival and growth of tumour cells, despite higher mutation rates and their unstable genomes. Significantly, abnormal cell growth, resulting from the activation of oncogenes or the deactivation of specific

tumour suppressors, induces DNA replication stress and continuous formation of DNA damage (Jin *et al*. 2024; Meena *et al*. 2024; Peripolli *et al*. 2024). This type of injury triggers ATR/ATM-mediated communication, leading to cell death or senescence in laboratory cell cultures, and in the development of tumours in living organisms. In fact, the DDR is frequently triggered in early neoplastic lesions and most likely serves as a defence against cancer. Mutational or epigenetic inactivation of DDR components may lead to breaches in the barrier, which are commonly selected for during tumour development, promoting malignant progression. This explanation of DDR functioning as a barrier against cancer, helps clarify why DDR defects are common in human cancers (Blackford and Jackson 2017; Cecconi 2020; Samstein *et al*. 2021).

With many DDR key proteins mutated and with DDR and repair defects being selected for in tumours, it seems counterintuitive to target those pathways as a strategy for cancer therapy. Nonetheless, it has been shown from standard cancer chemotherapy and radiotherapy that tumour cells are indeed, inherently vulnerable to additional/excessive levels of replication stress, DNA damage, and genomic instability. Inhibition of the DDR can sensitise cancer cells by hampering their ability to cope with such excessive threats to their genome (Huang and Zhou 2021; Jurkovicova *et al*. 2022).

Small molecule inhibitors are now available against all three PIKKs and have entered phase I or II clinical trials, both as single agents and in combination with radiotherapy or traditional chemotherapeutics. Other important kinases and enzymes of the DDR, apart from the three apical kinases, have been also identified as “druggable” targets for anticancer treatment, including PARP1/2, CHK1, WEE1, PolQ and others, with several ongoing preclinical and clinical studies investigating their potential in the treatment of various cancer types (Cerrato *et al*. 2016; Cheng *et al*. 2022; Nasioudis *et al*. 2023; Zhou *et al*. 2021).

1.1.7. PARP inhibitors (PARPi) and the concept of synthetic lethality

By far the most clinically successful case of small molecule-mediated DDRi in oncology, is the use of PARPi for the treatment of malignancies, taking advantage of their genetic background to maximise the treatment outcome – a concept known as synthetic lethality. This concept is based on the fact that, genomic instability in many tumours is caused by defects in certain DNA repair pathways, such as HR. This offers the potential for targeted therapies to exploit the concept of synthetic lethality, whereby loss of one repair pathway, results in high reliance on another pathway that is not essential under normal settings (Slade 2020). Cancer cells that exhibit defects in repairing DNA DSBs, such as those lacking the *BRCA1/2* or *PALB2* genes, depend greatly on BER-mediated repair of DNA damage. Targeting the PARP1/2 proteins with small molecule inhibitors can, hence, induce cytotoxicity and enhance the effectiveness of chemotherapy and radiotherapy, by means of synthetic lethality (figure 1.5) (Ali *et al*. 2021; Farmer *et al*. 2005; Muvaffak and Coleman 2024; Tsang *et al*. 2024). Poly(ADP-ribose) polymerase (PARP) enzymes, particularly PARP1 and PARP2, play central roles in the detection and repair of SSBs, the coordination of BER, the stabilisation of stalled replication forks, and regulation of replication stress signalling. Pharmacological inhibition of PARP enzymes in HR-deficient cells thus induces unrepairable replication-associated DSBs, ultimately culminating in mitotic catastrophe and cell death (Muvaffak and Coleman 2024).

PARP1, the founding and most abundant member of the PARP (or ARTD) family, is a 116 kDa nuclear protein comprising of multiple domains: three N-terminal zinc finger DNA-binding motifs (Zn1, Zn2, Zn3), a central automodification domain (AMD), a BRCT-like domain involved in protein–protein interactions, and a C-terminal catalytic domain. The latter contains the ADP-ribosyl transferase (ART) fold, which catalyses the synthesis of linear or branched poly(ADP-ribose) (PAR) chains from NAD^+. These modifications are attached to PARP itself (auto-PARylation), histones (e.g. H2A, H2AX), and various DDR effectors. PARP1's recruitment to DNA

damage is highly dynamic and governed by its DNA-binding domains, which confer affinity for both SSBs and certain DSB configurations (Herceg and Wang 2001; Kun and Bauer 2001). PARP2 and PARP3, which share 69% and 42% sequence similarity with PARP1 in the catalytic domain, respectively, are also implicated in DNA repair but have more specialised roles (Hanzlikova *et al.* 2017). Like PARP1, PARP2 is activated by SSBs and functions in base excision repair (BER), where it synthesises PAR chains to recruit scaffold proteins, such as XRCC1 and DNA ligase III (van Beek *et al.* 2021). PARP2 also contributes to the stabilisation of stalled replication forks: upon fork stalling it PARylates histone H3 and histone chaperones, promoting chromatin relaxation and facilitating access of fork-restart factors (Muoio *et al.* 2024). PARP3 is the smallest PARP family member (~60 kDa) and is selectively activated by blunt-ended DSBs. Upon activation, PARP3 catalyses predominantly mono-ADP-ribosylation, which accelerates classical NHEJ, by recruiting the APLF scaffold and promoting Ligase IV accumulation at break sites (Beck *et al.* 2014; Rulten *et al.* 2011). Beyond DSB repair, PARP3 localises to centrosomes and the mitotic spindle, where its PARylation activity is required for proper spindle assembly and chromosome segregation. In human cells, PARP3 depletion leads to delayed DSB repair kinetics, increased reliance on MMEJ, and heightened chromosomal instability - phenotypes that are especially pronounced in the absence of key NHEJ factors (Liu *et al.* 2017; Martinez-Zamudio and Ha 2012). Despite differences in DNA-binding domain structure, all three enzymes share conserved NAD^+-binding residues and can be inhibited by NAD^+-competitive small molecules. This biochemical redundancy, however, has functional limits: knockout studies in murine models show that, while PARP1-null mice are viable, PARP1/PARP2 double mutants exhibit embryonic lethality, highlighting partial overlap but essential cooperative roles in genome maintenance (Ali *et al.* 2016; Vyas *et al.* 2013).

PARP1 is among the first responders to SSBs and replication-associated lesions. Upon binding DNA, PARP1 rapidly PARylates itself and local chromatin components, relaxing chromatin structure and recruiting downstream repair factors such as XRCC1, DNA polymerase β, and DNA

ligase III. Beyond its role in classical BER, PARP1 regulates fork stability during S phase. In response to replication stress - induced by oncogene activation, nucleotide depletion, or exogenous DNA-damaging agents - replication forks stall, leading to helicase–polymerase uncoupling and generation of extensive ssDNA. This ssDNA is coated by RPA, which initiates ATR-CHK1 signalling to delay cell cycle progression and prevent fork collapse (Herceg and Wang 2001; Statz-Geary *et al*. 2025). PARP1 limits origin firing and replication fork progression by antagonising the activity of the RECQ1 helicase, thereby promoting fork reversal and stabilisation. It also protects nascent DNA strands from nucleolytic degradation by MRE11, stabilises RAD51 filaments at stalled forks, and coordinates the recruitment of HR effectors such as BRCA1, BRCA2, MRE11, and EXO1 to facilitate fork restart and resolution. Loss of PARP activity therefore renders replication forks highly susceptible to collapse, particularly in HR-deficient cells that cannot resolve such structures through recombination-mediated restart. This multi-layered involvement in both SSB repair and replication fork dynamics underpins the profound synthetic lethality observed when PARP is inhibited in HR-deficient cancers (Ali *et al*. 2012; Ali *et al*. 2015; Rose *et al*. 2020).

PARPi exert cytotoxicity through two primary, mechanistically distinct actions: (i) inhibition of PARP catalytic activity, thereby blocking SSB repair, and (ii) "PARP trapping", whereby PARPi-bound PARP1 becomes stably associated with DNA and physically blocks replication fork progression. The trapped PARP–DNA complex constitutes a replication-blocking lesion more toxic than unrepaired SSBs. Upon collision of the replication machinery with these lesions, replication forks collapse into DSBs (figure 1.5). In HR-proficient cells, these breaks can be repaired; in HR-deficient cells, they are converted into persistent DNA lesions transmitted into mitosis, resulting in chromosome missegregation, micronuclei formation, and mitotic catastrophe (Abd El-Rehim *et al*. 2004; Buisson *et al*. 2010; McKinnell RG 1998; Pettitt *et al*. 2018; Tattersall *et al*. 2022). Additional cytotoxic outcomes of PARPi arise from dysregulated transcription, chromatin architecture, and ribosome biogenesis, as PARP1 is also known to

modify RNA-binding proteins and regulate nucleolar integrity. Thus, the therapeutic effect of PARPi extends beyond classical DDR inhibition and is modulated by tumour-specific replication dynamics and stress signalling profiles (Reed 2010; Weaver and Yang 2013).

The first demonstrations of PARP inhibition in mammalian cells date to the 1970s, with thymidine-sensitised HeLa cells treated with nicotinamide analogues. Early PARPi, including benzamide derivatives, were hindered by low potency and specificity. Contemporary PARPi - such as Olaparib, Rucaparib, Niraparib and Talazoparib - are NAD^+-competitive molecules that exhibit nanomolar affinity for PARP1/2 and variable potency in PARP trapping. While most current inhibitors target both PARP1 and PARP2, differential affinity and pharmacokinetics contribute to variable off-target effects and therapeutic indices (Bruin *et al.* 2022; Rose *et al.* 2020). PARPi have been approved for the treatment of *BRCA*-mutant breast, ovarian, pancreatic, and prostate cancers. However, the prevalence of germline *BRCA1/2* (gBRCA) mutations is limited (approximately 5–10% in breast cancers; 15-20% in ovarian cancers), constraining the initial patient population eligible for PARPi monotherapy. This has spurred intense interest in expanding PARPi use to HR-deficient, *BRCA*–wild-type tumours *via* genomic scar assays or functional HRD biomarkers (e.g., RAD51 foci formation) (Fenor de la Maza *et al.* 2024; Huang *et al.* 2024; Shahini and Riazalhosseini 2024; Xie *et al.* 2024). Furthermore, emerging evidence suggests that tumours with elevated replication stress - such as those with oncogene activation, ATR pathway dysregulation, or oxidative stress - may exhibit “functional HRD” and respond to PARPi even in the absence of classical HR gene mutations (Rose *et al.* 2020). Combination strategies are also under clinical development. Co-administration of PARPi with chemotherapy, ionising radiation, ATR or WEE1 inhibitors, or immune checkpoint blockade is being trialled to enhance synthetic lethality and prevent resistance (Frezzini *et al.* 2024; Kostos *et al.* 2024; Xiao *et al.* 2024; Xie *et al.* 2024).

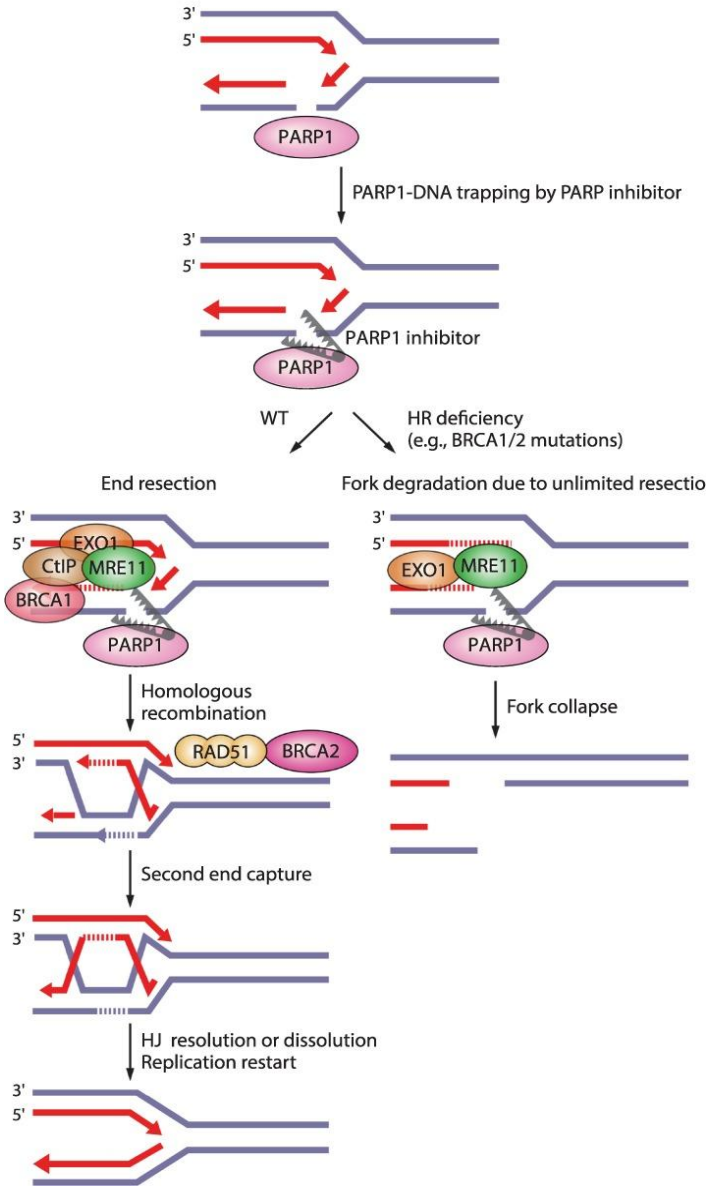

Figure 1.5. Synthetic lethality between PARP inhibitors and homologous recombination deficiency. PARP entrapment on DNA lesions blocks replication machinery and loss of PARP activity prevents fork protection, fork reversal, and fork restart. This results in DSBs that need to be repaired by homologous recombination (Slade 2020). In the case of homologous recombination deficiency due to, for example, mutations in *BRCA1/2*, PARP1-trapping lesions elicit excessive fork degradation by the MRE11 nuclease, the activity of which is unrestrained in the absence of BRCA1/2 and PARP1. This results in fork collapse. Reprinted from: "PARP and PARG inhibitors in cancer treatment through the Genes & Development" Open Access option. License: https://creativecommons.org/licenses/by/4.0/.

1.1.8. Determinants of resistance to PARPi

Resistance to the effect of PARPi arises through a spectrum of interrelated molecular strategies that ultimately restore DNA repair capacity, enhance replication-fork protection, or diminish effective drug engagement. With data from clinical practice showing that, 40–70% of patients have the tendency to develop resistance to PARPi treatment over time, overcoming resistance has thus become a major focus within the oncology research field, prompting comprehensive studies into the molecular biology underlying the resistance mechanisms (figure 1.6) (Kim and Nam 2022).

At the heart of the synthetic-lethal paradigm are germline mutations in *BRCA1* and *BRCA2* - present in approximately 1.8-3.1% and 1.6-3.5%, respectively, of breast cancers - which abrogate, respectively, the initiation of DNA end resection and the nucleation of RAD51 filaments required for high-fidelity repair (Chiappa *et al.* 2021; Turner *et al.* 2004). Somatic alterations in the same genes or in other HR mediators (*PALB2*, *ATM*, *CHEK2*) occur in a further 3–5% of sporadic tumours, often *via* promoter hypermethylation or loss-of-heterozygosity (LOH) and phenocopy germline deficiencies (figure 1.6) (Fang *et al.* 2019; Jaspers *et al.* 2013; Johnson *et al.* 2016; Lappin *et al.* 2022; McCabe *et al.* 2006; Yazinski *et al.* 2017; Yin *et al.* 2018).

Notably, the clinical prevalence of reversion mutations - secondary genetic events that restore the open reading frame of *BRCA1/2* - varies markedly between tumour types, from near zero in certain platinum-naïve ovarian cohorts to as high as 50% in heavily pre-treated breast cancers (Ceccaldi *et al.* 2015). Such variability reflects differences in selective pressures, prior exposure to DNA-damaging agents and the clonal complexity of each malignancy. In several retrospective analyses of next-generation sequencing (NGS) data from 23,375 patients across various common cancer types, the prevalence of multiple pathogenic/likely pathogenic (P/LP) germline mutations in HR genes was analysed. The reversion mutations were detected in *BRCA1* (3.8%), *BRCA2* (3.5%), and *PALB2* (2.0%) after platinum-based chemotherapy and/or PARPi resistance.

The incidence of mutations that restore *BRCA1/2* function in ovarian cancer ranges from 0% to 21%, and as high as 40% to 50% in breast cancer (Fu *et al*. 2024b). Moreover, NGS panels frequently miss large indels or complex genomic rearrangements that underlie many reversion events, resulting in underestimation of true resistance rates and underscoring the need for complementary detection methods such as long-read sequencing or digital droplet PCR (Fu *et al*. 2024a).

Beyond genetic reversion, tumours may reinstate HR-proficiency through upregulation of compensatory factors. ATR activation enhances end resection, while PolQ engages error-prone MMEJ when canonical HR is compromised, thereby diminishing PARPi cytotoxicity (Ceccaldi *et al*. 2015). Simultaneously, replication-fork stabilisation mechanisms, like loss of PTIP or EZH2 to impede MRE11-mediated nascent strand degradation, or downregulation of remodelers like SMARCAL1 and ZRANB3 to prevent fork reversal, preserve fork integrity in *BRCA*-deficient cells and blunt the lethal consequences of PARP trapping (figure 1.6) (Belli *et al*. 2019; Kim and Nam 2022; Yazinski *et al*. 2017).

A further axis of resistance entails rebalancing the competition between NHEJ and HR. A major distinction between NHEJ and HR is that the former, involves minimal end-processing, unlike HR which requires extensive end-resection at the site of the DSB. 53BP1 works with SHLD3 and RIF1 to recruit the shieldin complex to DSBs to prevent end resection, thus committing the cell to NHEJ-mediated DSB repair (Jackson and Moldovan 2022). In *BRCA1*-deficient contexts, loss of *53BP1* or its downstream shieldin complex permits extensive end resection by CtIP and the MRN complex, enabling RAD51 loading in a BRCA1-independent, but BRCA2-dependen manner (figure 1.6). Of note, while *BRCA1* mutations are compatible with HR restoration upon inactivation of NHEJ-promoting factors, restoration of the HR pathway fully depends on functional BRCA2 (Bouwman *et al*. 2010; Chen *et al*. 2020a; Fu *et al*. 2024b; Noordermeer and van Attikum 2019). This adaptive shift highlights the plasticity of DSB repair choice and the

interdependence of pathway regulators (Jackson and Moldovan 2022; Min *et al.* 2013; Nesic *et al.* 2021).

Alterations at the PARP pharmacological target also contribute to resistance. Missense mutations within the WGR domain of PARP1 (for example, R591C) accelerate dissociation of the PARP–DNA complex, reducing the incidence of replication-blocking PARP traps. Loss of poly(ADP-ribose) glycohydrolase (PARG) similarly maintains elevated PAR levels, preserving PARP signalling and negating inhibitor efficacy (figure 1.6) (Gogola *et al.* 2019; Pettitt *et al.* 2018; Slade 2020). Finally, upregulation of ATP-binding cassette transporters (ABCB1, ABCG2) lowers intracellular PARPi concentrations, reflecting a classic drug-efflux–mediated defense (Fried *et al.* 2024; Fu *et al.* 2024b; Jackson and Moldovan 2022; Lloyd *et al.* 2020).

Although genomic scar assays - measuring LOH, telomeric allelic imbalance and large-scale state transitions - offer a high-throughput means of inferring historic HRD, their predictive specificity is compromised by chromosomal instability from non-HR sources, leading to false positives in up to 15–20% of cases (Timms *et al.* 2014). Consequently, functional assays such as RAD51 foci formation, following ionising radiation, remain indispensable for real-time assessment of HR competence and for refining patient selection in PARPi trials (Telli *et al.* 2016). Only by integrating comprehensive genomic profiling with dynamic functional readouts and understanding the mechanistic bases of each resistance route can we optimise PARPi use, anticipate failure modes and design rational combination regimens to forestall or overcome therapeutic escape (Belli *et al.* 2019).

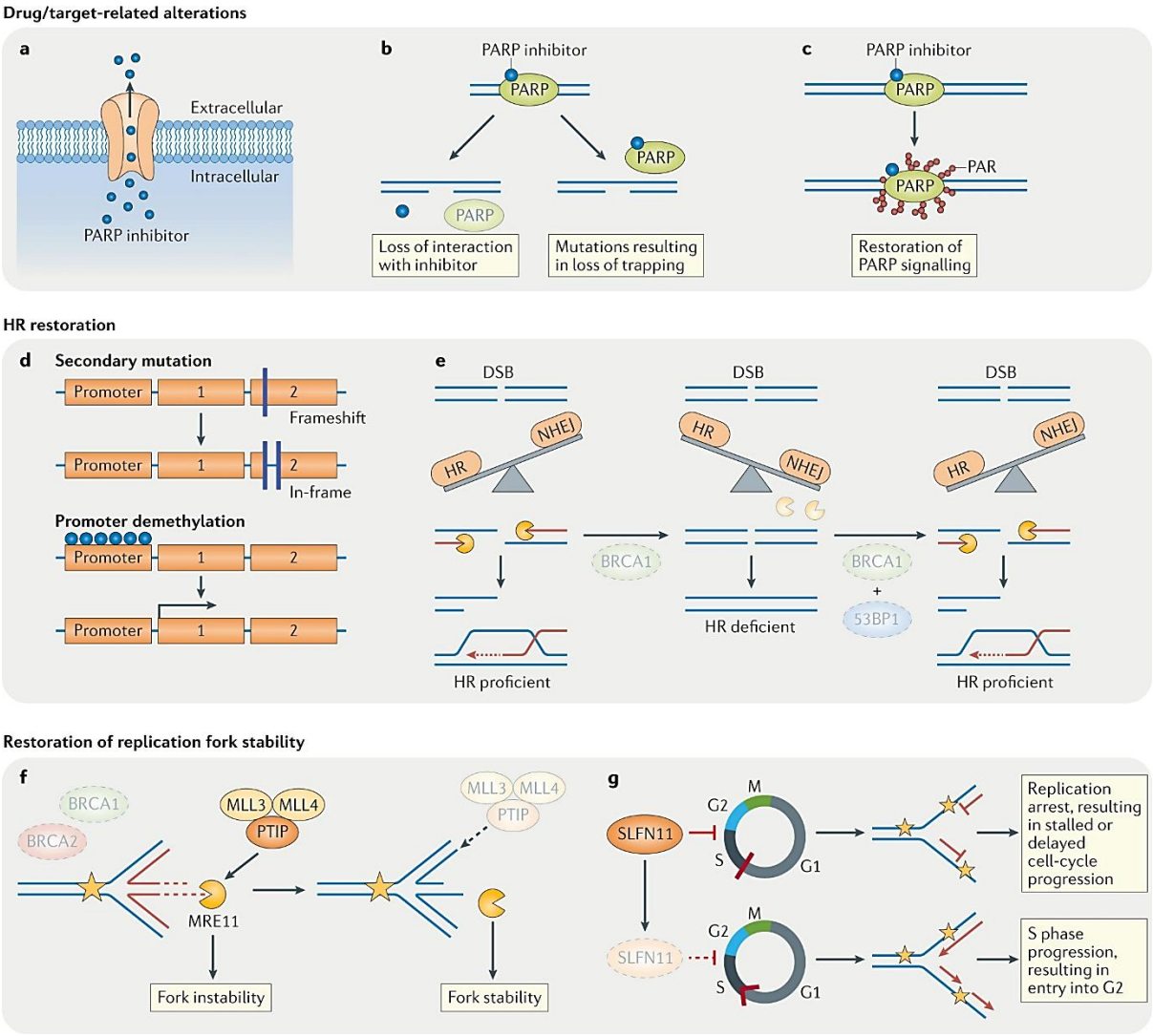

Figure 1.6. The mechanisms of resistance to PARPi. Alterations related to the drug (or target) as observed with chemotherapies, such as upregulation of the efflux transporter P-glycoprotein (a), downregulation of or mutations in PARP1, which is restricted to cells expressing residual levels of BRCA1/2 (b) or loss of polyADP-ribose glycohydrolase (PARG) (c). Restoration of HR, by reactivation of BRCA1/2 function (d) or loss of DNA end-protection (e), restricted to loss of BRCA1 and can occur *via* loss of the non-homologous end-joining (NHEJ) factor 53BP1. Restoration of replication fork stability *via* increased protection from fork degradation (f), for example, by loss of PTIP expression or loss of cell-cycle checkpoint arrest owing to loss of Schlafen 11 (SLFN11) (g). PAR, poly (ADP-ribose); DSB, double-strand break; MLL3, histone-lysine N-methyltransferase 2C; MLL4, histone-lysine N-methyltransferase 2B; MRE11, Meiotic recombination 11; PTIP, Pax2 transactivation domain-interacting protein (Dias *et al.* 2021). Reprinted from: "Understanding and overcoming resistance to PARP inhibitors in cancer therapy." License No.: 5863700058185.

1.2. Breast cancer

1.2.1. Basic pathology, classification, and molecular subtypes of breast cancer

Breast cancer describes a range of malignancies, occurring in the mammary glands, which collectively represent the most prevalent cancer worldwide. It is the most common cancer in the UK, accounting for 55,000 (15%) new cancer cases per year (Harbeck *et al.* 2019). This is predicted to rise by 2% by 2035 Women are overwhelmingly affected, with the incidence increasing with age – more than 80% of breast cancers are diagnosed in women over 50 years old. Breast cancer is the leading cause of cancer deaths, with 685,000 deaths worldwide in 2020 (Katsura *et al.* 2022).

Breast cancers can be generally classified into two broad categories: carcinomas and sarcomas. Carcinomas are arising from the epithelial component of the breast, while sarcomas are rarer and arise from the stromal components of the mammary tissue (blood vessels and myofibroblast cells) (Colditz *et al.* 2012; Polyak 2007). Most breast carcinomas are classified into non-invasive, invasive, and metastatic, based on their pathological features and invasiveness. Accurately distinguishing between breast cancer types is crucial for determining of prognosis and treatment regimens (Hulka 1996). Non-invasive breast carcinomas are commonly classified as ductal carcinoma *in situ* (DCIS), a type of cancer which commonly forms in normal mammary ducts. While DCIS itself is not invasive, it has the potential to become invasive, highlighting the significance of early detection for this cancer type (figure 1.7).

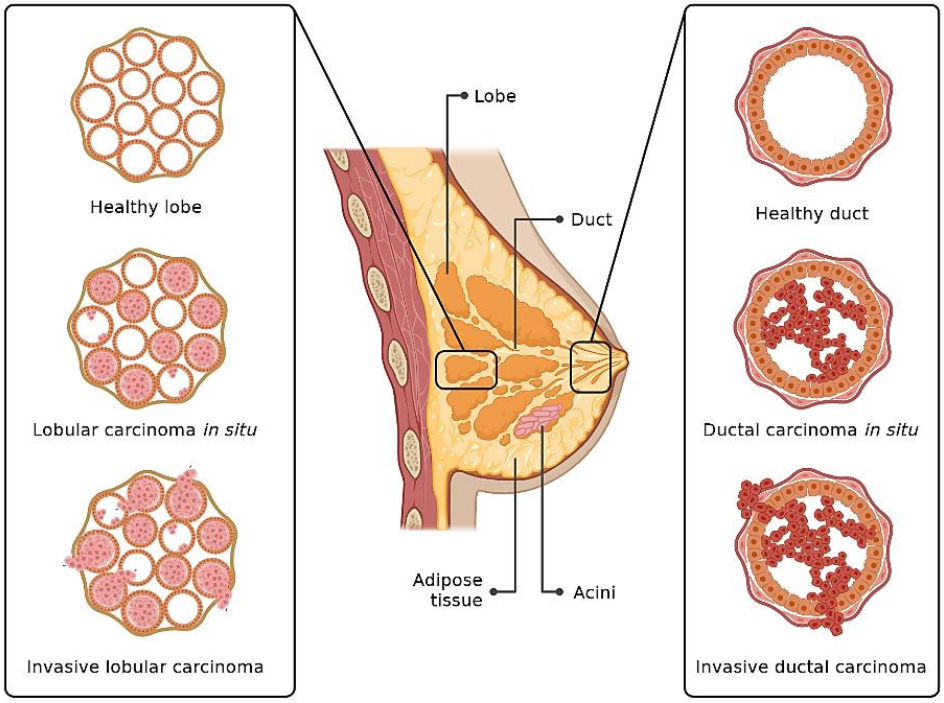

Figure 1.7. The pathology of breast cancer. Mammary ducts and lobules, both in normal and in cancerous states are depicted, with their relative location in the female breast. Reprinted from: "Graphical representation of types of breast cancer," BioRender.com (2024) Retrieved from: https://app.biorender.com/biorender-templates.

Further to the pathological classification of breast cancers, the molecular subtype classification system, where breast cancers are further distinguished into subtypes based on the existence or absence of specific receptors on the surface of tumour cells, has proven to be pivotal in determining the optimal treatment regimen as well as in evaluating prognosis of breast cancer patients (Cancer Genome Atlas 2012; Perou *et al*. 2000). Gene expression studies have identified distinct subtypes based on the expression patterns of certain genes related to oestrogen receptor (ER), human epidermal growth factor-2 (HER-2), proliferation, and basal clusters. The five intrinsic or molecular subtypes include Luminal A, Luminal B, HER-2-enriched, Triple-negative/basal-like (TNBC), and Normal-like breast cancer. Luminal A breast cancer is characterised by being ER/PR positive, HER-2 negative, and has low Ki-67 levels (a commonly

used proliferation marker). Luminal B breast cancer, accounting for less than 20% of all breast cancer cases, is ER/PR positive with either HER-2 positive or negative and high Ki-67 levels. HER2-enriched (or simply known as HER-2 positive) breast cancer, comprising 10-15% of cases, lacks ER/PR expression but has high HER-2 and Ki-67 gene expression. TNBC, representing around 20% of breast cancer cases, is ER/PR/HER-2 negative and associated with highly aggressive phenotype. Normal-like breast cancer is similar to Luminal A but with slightly worse prognosis (figure 1.8) (Abd El-Rehim *et al*. 2004; Allison 2012; Feng *et al*. 2018; Sotiriou *et al*. 2003).

This vast heterogeneity of breast cancers is the reason why, transcriptomic analyses and NGS methods have become of such high importance in the successful treatment of the disease: studies have identified subtypes with distinct prognoses and therapeutic targets, particularly related to hormone receptor expression profiles. Genome wide analyses and transcriptomic profiling have massively contributed to the understanding of molecular classifications of breast cancers, leading to the development of both diagnostic and prognostic panels such as Oncotype Dx, Breast Cancer Index, PAM50 Risk of Recurrence score, Amsterdam 70-gene prognostic profile, and Genomic Grade Index. Understanding these breast cancer subtypes, and their genetic profiles is, hence, crucial for the development and implementation of personalised treatment strategies, aiming to improved patient outcomes (Krop *et al*. 2017; Laenkholm *et al*. 2018; Nielsen *et al*. 2010; Parker *et al*. 2009).

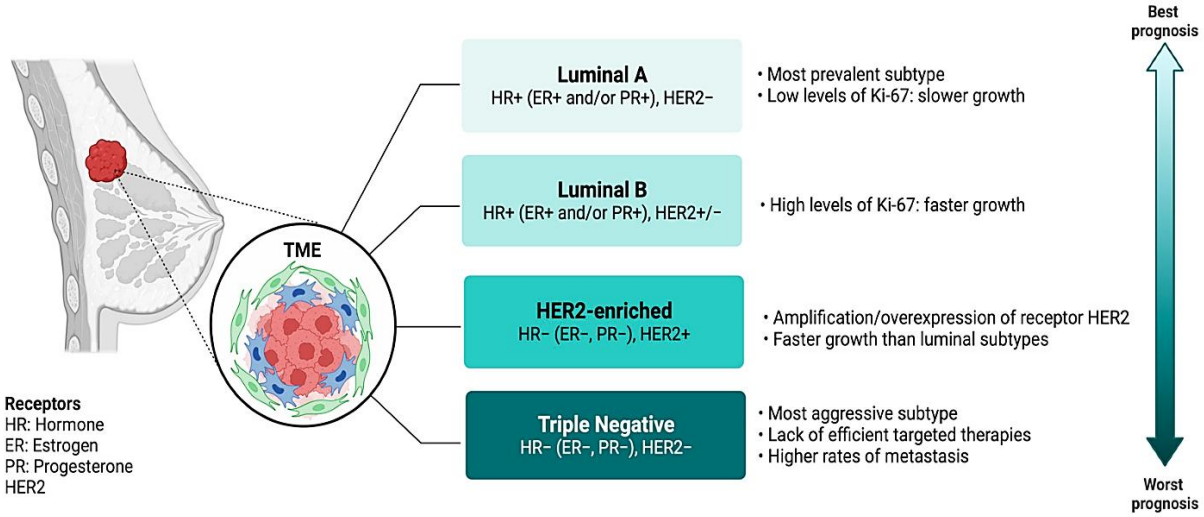

Figure 1.8. The Molecular subtypes of breast cancer. The four main subtypes of breast cancer, classified according to their receptor status are shown, with details on their relative clinical manifestations and subtype-based prognosis. Reprinted from: "BC molecular subtypes classification" (Nogueras Pérez *et al.* 2023). Reproduction License: https://creativecommons.org/licenses/by/4.0/

1.2.2. The genetic background of breast cancer

Breast cancer susceptibility reflects a continuum of inherited and acquired genomic alterations, ranging from rare, high-penetrance mutations in key DNA-repair genes to common, low-penetrance single-nucleotide polymorphisms (SNPs) that cumulatively modulate risk. Germline mutations in *BRCA1* and *BRCA2* remain the paradigmatic drivers of hereditary breast–ovarian cancer syndrome, conferring lifetime risks of approximately 60–80% and 40–60%, respectively (Kotsopoulos *et al.* 2007; Lalloo and Evans 2012a; Mahdavi *et al.* 2019). Mechanistically, BRCA1 functions as an E3 ubiquitin ligase and chromatin remodeler that recruits the CtIP–MRN complex to initiate 5'→3' end resection at DNA double-strand breaks, whereas BRCA2 contains multiple BRC repeats that chaperone RAD51 nucleoprotein filament formation on single-stranded DNA, thereby facilitating homology search and strand invasion (Telli *et al.* 2018). Loss of *BRCA1* abrogates resection and forces repair *via* error-prone NHEJ, while *BRCA2* deficiency permits resection but stalls HR at the strand-invasion step, both

culminating in chromosomal instability (Fang *et al.* 2018). Clinically, *BRCA1*-associated tumours are predominantly triple-negative and display medullary-like histopathology, whereas *BRCA2*-associated cancers more often retain oestrogen-receptor expression and resemble sporadic luminal subtypes. In addition, somatic alterations - promoter hypermethylation of *BRCA1*, LOH at both loci or truncating mutations - occur in 3–5% of sporadic tumours and phenocopy germline defects, further broadening the pool of HRD cancers (Kurian 2010; Lalloo and Evans 2012b) .

Beyond *BRCA1/2*, germline mutations in *TP53* underlie Li–Fraumeni syndrome in which affected individuals develop early-onset breast cancer alongside diverse paediatric malignancies. *TP53* encodes a transcription factor that orchestrates DNA-damage-induced cell-cycle arrest, DNA repair and apoptosis; somatic *TP53* mutations - particularly hotspot missense changes in the DNA-binding domain - are detected in approximately 30–40% of breast cancers, predominantly within basal-like subgroups, and abrogate critical G1/S and G2/M checkpoints, thereby compounding genomic instability (Turnbull *et al.* 2010) .

Moderate-penetrance genes, including *PALB2*, *ATM*, *CHEK2* and *BRIP1*, confer intermediate lifetime risks of ~20–40%. PALB2 tethers BRCA2 to chromatin and is essential for RAD51 filament stabilisation; heterozygous truncating mutations in *PALB2* impart a ~ 35% breast-cancer risk by age 70 (Antoniou *et al.* 2014). ATM, the apical kinase of the double-strand-break response, when heterozygously inactivated, increases breast-cancer susceptibility two- to four-fold, whereas biallelic loss causes ataxia-telangiectasia with profound radiosensitivity (Tew *et al.* 2023). *CHEK2* encodes CHK2, which phosphorylates p53 and BRCA1 to enforce checkpoint arrest; the *c.1100delC* founder variant approximately doubles breast-cancer risk (Fang *et al.* 2018). *BRIP1* (*FANCJ*), encodes a DNA helicase interacting with BRCA1 and carries a ~10–15% risk when truncated (Seal *et al.* 2006). Collectively, these moderate-penetrance genes occupy discrete nodes of the DNA-damage-response network - in damage sensing, checkpoint signalling and homologous recombination - illustrating how partial attenuation of repair pathways yields

intermediate oncogenic potential. At the opposite end of the spectrum, genome-wide association studies have uncovered over 200 common SNPs that individually confer modest relative risks (<1.5-fold) but together explain ~20% of familial breast cancer aggregation (Michailidou *et al.* 2017). These low-penetrance loci frequently map to regulatory elements near genes involved in hormone signalling (*ESR1*, *FOXA1*), cell-cycle regulation (*CCND1*) and immune–microenvironment interactions, and even to *RAD51C*/*D*, suggesting subtle modulation of HR efficiency. Polygenic risk scores, which integrate these SNP effects, now stratify asymptomatic individuals in the general population, informing risk-adapted screening protocols (Borresen *et al.* 1990; Lalloo and Evans 2012a; Swift *et al.* 1987).

In clinical practice, genetic testing focuses primarily on *BRCA1/2* (and, less commonly, *TP53*) to guide risk-reducing strategies such as enhanced surveillance, chemoprevention, and prophylactic surgery. The advent of NGS permits multi-gene panels of 30–100 predisposition loci, yet interpretation of moderate- and low-penetrance findings remains challenging, owing to variants of uncertain significance and the influence of genetic–environmental interactions. Future efforts must refine the classification of novel variants, integrate polygenic risk with lifestyle and hormonal factors, and elucidate how germline genotype shapes tumour evolution, therapeutic sensitivity - particularly to DDRi - and ultimately patient outcomes (Baliakas *et al.* 2024; Kast *et al.* 2024; Liu *et al.* 2024; Wang *et al.* 2024).

1.3. Tumour Hypoxia

1.3.1. Tumour microenvironment and hypoxia

Oncology nowadays acknowledges the fact that a tumour is made up of more than just cancer cells. Instead, it is a diverse mix of tumour cells, infiltrating cells, components of the extracellular matrix (ECM), and secreted factors (Babar *et al*. 2023). Because of their abnormal metabolic behaviour, cancer cells cause physical alterations in the surrounding tissues, resulting in the development of a hypoxic and acidic tumour microenvironment (TME) with disorganised/aberrant blood vessels, which are prone to occlusion, vasospasm, and leakage. While the components of the TME differ among types of tumours, they consistently include immune cells, stromal cells, non-cellular elements, exosomes and secreted factors, as well as changes in vasculature structure, and environmental factors like oxygen, pH, and nutrient levels (Babar *et al*. 2023; Huang *et al*. 2021a; Swanton *et al*. 2024).

Hypoxia is one of the most significant features of the TME, occurring in over 90% of solid tumours and is a key characteristic of cancer biology, with numerous impacts on treatment response and patient prognosis (Vaupel and Mayer 2007). Determining the exact hypoxic state in tumours is still challenging, nonetheless, due to variations in oxygen levels between tissues, tumour size, measurement methods, and tissue oxygenation variability within different organs. Several studies on this topic, however, show that measuring tumour O_2 levels in patients using polarographic techniques, has revealed low values (<10 mmHg / <0.5% O_2) in various cancer types like pancreatic, head and neck, breast, cervical, and melanoma (Hammond *et al*. 2014; McKeown 2014) .

The high rate of proliferation of cancer cells, as well as the remodelling of stromal tissue and ECM in the TME setting, are factors known to contribute to the formation of an oxygen gradient within tumours. Cells in the TME closer to the vasculature are more oxygenated, whereas, what is known

as chronic hypoxia (or diffusion-limited hypoxia) occurs, as cancer cells move farther away from blood vessels, a fact first-validated in experiments using breast cancer mouse models (Vaupel *et al.* 1987). Additionally, in most solid tumours, hypoxia has been shown occur in areas 100-200 μM from a functional blood supply (Vaupel *et al.* 1987; Vaupel *et al.* 1991). Vaso-responsive peritumoral vasculature is a second factor causing, and/or exacerbating hypoxia in the TME: abnormal blood vessels formed in response to angiogenesis in the tumour setting, malfunction significantly, leading thus to acute and dynamic (or perfusion-limited) hypoxia and the formation of diverse oxygen gradient within tumours (figure 1.10) (McKeown 2014; Nagy *et al.* 2010; Nagy and Dvorak 2012; Patel *et al.* 2012; Zhu *et al.* 2014).

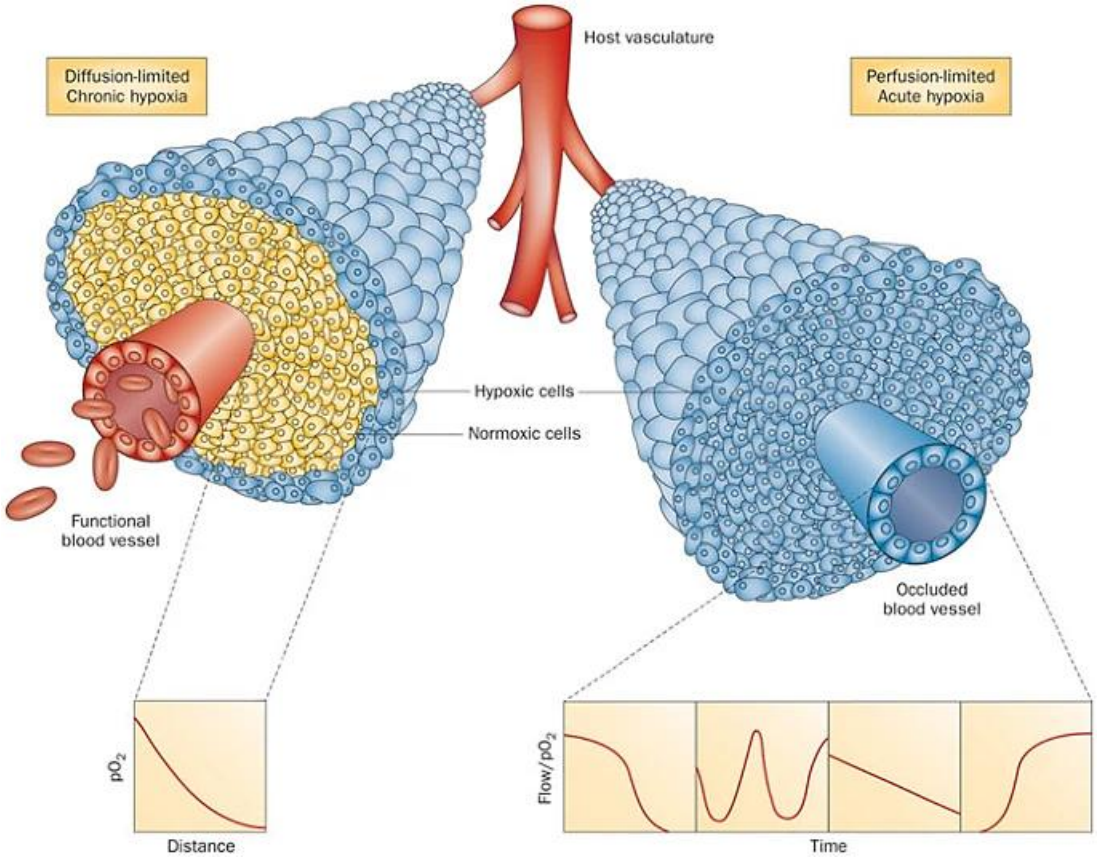

Figure 1.10. The different types of tumour hypoxia. Left side: oxygen diffuses from the vessels, it is used by the nearest tumour cells, which results in a decrease in oxygen partial pressure (pO2) as shown. This decrease in oxygen eventually results in the development of chronically hypoxic cells, farther from the vessels. Right side: perfusion through the vessel has been transiently

compromised and cells around become acutely hypoxic, potentially due to vasospasm, leakage, or occlusion (partial or full) of the aberrant tumour vessels. Examples of the flow and relative pO2 changes reported during a 60 min period are shown in the four panels at the right, which illustrate a rapid and complete shutdown (panel 1) and recovery (panel 4), a gradual decrease with time (panel 3), and repeated fluctuations (panel 2). Reprinted from: "Imaging hypoxia to improve radiotherapy outcome" (Horsman *et al.* 2012). Licence No.: 5870330178549.

1.3.2. Defining hypoxia terms and types according to O_2 levels

In the field of hypoxia, disambiguation of the various terms used in scientific and medical literature to explain the various oxygen levels is crucial. The term normoxia is employed to describe to tissue culture-levels of oxygen, i.e., 21% O_2, which is commonly utilised by the majority of researchers for culturing mammalian cells and conducting experiments in this area of research. This oxygen level, however, is obviously not representative of body-tissue levels in any organ, a fact that makes the term normoxia somewhat criticised, as non-physiologically relevant (Hammond *et al.* 2014; McKeown 2014). Therefore, physoxia is the term which refers to the range of oxygen levels found within different tissues and organs throughout the body. The general term hypoxia refers to a decrease in oxygen levels in a specific tissue or organ, enough to result in the stabilisation of the transcription factor HIF-1α under such conditions. More specifically, the term radiobiological hypoxia, commonly discussed in relation to cancer treatment with radiation therapy, refers to the extent of oxygen deprivation needed to observe radiation resistance. Lastly, the term anoxia refers to a total absence of oxygen in the atmosphere, meaning 0% O_2 (Giaccia *et al.* 2004; Hammond *et al.* 2014). In conclusion, the threshold for hypoxia is determined by comparing the oxygen levels in a specific tissue or organ to the usual oxygen levels in that same tissue or organ. In the normal breast tissue, for instance, the usual oxygen level is approximately 7%, while in the liver it is 5.2% (Carreau *et al.* 2011; McKeown 2014). Therefore, the definition of hypoxia may vary between these two organs (figure 1.11).

Hypoxia can be also classified according to either its duration, into chronic, acute, and dynamic (also known as cyclic hypoxia), or according to its "severity." Oxygen levels are used to quantify

the severity and due to the diverse nature of the TME, regions of “mild” hypoxia (0.5-2% O_2) and “severe” hypoxia, also known as radiobiological hypoxia (<0.1% O_2), can coexist in the various tumours. While mild and severe hypoxia both trigger HIF-1 signaling, only severe hypoxia additionally activates other stress response pathways within the cell, like DDR and the unfolded protein response (UPR) (Bader *et al.* 2021; Bolland *et al.* 2021; Hammond *et al.* 2014). In terms of differences in duration, the different types of hypoxia described above, have also been associated with different responses in the TME. For instance, sudden lack of oxygen, known as acute hypoxia, is associated with higher metastatic capacity of tumour cells, compared to chronic hypoxia, which results from restricted oxygen transfer through blood vessels and its duration is uncertain (Saxena and Jolly 2019). Moreover, studies indicate that sudden lack of oxygen is more likely to promote tumour growth than prolonged lack of oxygen. Additionally, research has showed that chronically hypoxic cells remain viable for more than 96 h, whereas acutely hypoxic cells lose viability after 24 h, while both types of cells have similar phenotypes of resistance to radiation (Bigos *et al.* 2024; Pires *et al.* 2010; Rofstad *et al.* 2010).

Broady, periods of inadequate oxygen levels are classified as acute if they last less than 48 h and as chronic if they exceed 48 h (Saxena and Jolly 2019). Cyclic hypoxia, also known as dynamic hypoxia, consists of alternating periods of low oxygen levels and reoxygenation, which could result in DNA damage in cancer cells caused by ROS. This type of hypoxia is linked to the aberrant blood circulation in tumours and varies highly in oxygen levels and time periods (Bader *et al.* 2020; Bader *et al.* 2021; Michiels *et al.* 2016). In general, hypoxia in its different forms, can greatly affect the growth of tumours, their ability spread, and the status of DNA damage in cancer cells (Hammond and Giaccia 2005; Oren *et al.* 2021).

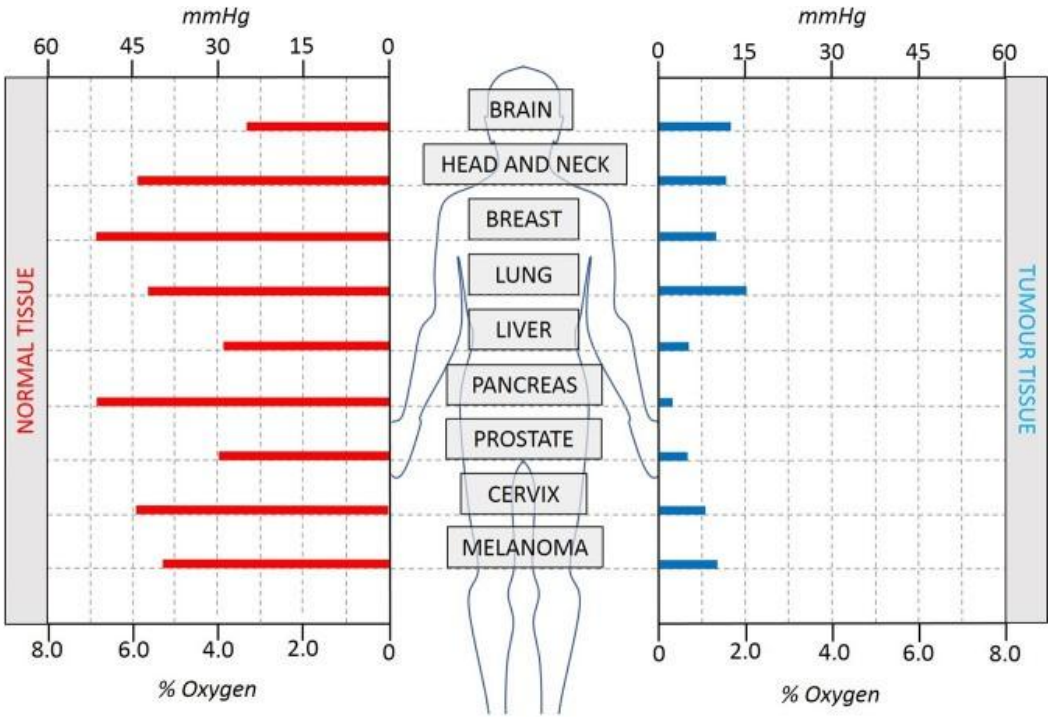

Figure 1.11. Approximate oxygen levels reported in different tissues in mmHg and %O_2 values. The left side depicts oxygen levels, reported from various studies, in normal tissues, while the right side depicts oxygen levels reported in tumour tissue. Of note, all reported oxygen levels are much lower than 21% O_2 which is defined as normoxia in *in vitro* studies. Reprinted from: " Inside the hypoxic tumour: reprogramming of the DDR and radioresistance" (Begg and Tavassoli 2020). Reproduction Licence: https://creativecommons.org/licenses/by/4.0/

1.4. The biological response to hypoxia

1.4.1. HIF-signalling in hypoxic cells and the transcriptional response to hypoxia

The HIF family of transcription factors is crucial in controlling how cells respond to low oxygen levels. HIFs control the expression of genes coding for proteins involved in various functions such as cell proliferation, apoptosis/survival, metabolic adaptation, angiogenesis, metastasis and invasion of cancer cells, inflammation, immune response regulation and pH-modulation (Brahimi-Horn and Pouyssegur 2009). HIF signalling is pivotal in all these processes in hypoxic cells, by controlling the expression levels of numerous (in the order of thousands) genes (Basheeruddin and Qausain 2024). The HIF transcription factor functions as a heterodimer, which consists of two proteins: an unstable α subunit (HIF-1α, HIF-2α, or HIF-3α, in humans) and

a constitutive β//aryl hydrocarbon receptor nuclear translocator (ARNT) subunit. HIF-1α, HIF-2α and HIF-3α combined with HIF-1β/ARNT, are respectively denoted as HIF-1, HIF-2, and HIF-3. The α subunit, which is sensitive to oxygen, is degraded when sufficient oxygen levels are present in the cell but stabilised in low-oxygen conditions (McKinnell RG 1998; Swift *et al*. 1987).

The stability of HIF-α subunits is governed by prolyl-hydroxylase domain (PHD) enzymes (PHD1–3) that belong to the 2-oxoglutarate (2-OG)–dependent, non-haem iron oxygenase superfamily. PHD2, the predominant isoform in most tissues, has a Michaelis–Menten(K_m) constant for O_2 of ~230μM (~20% O_2), conferring high sensitivity to even mild hypoxia. In normoxia, PHDs hydroxylate conserved proline residues (Pro402, Pro564 in HIF-1α), enabling the von Hippel–Lindau (VHL) E3-ubiquitin ligase complex, to ubiquitylate HIF-α for proteasomal degradation. Concurrently, factor-inhibiting HIF (FIH) hydroxylates Asn803 within HIF-1α's C-terminal transactivation domain (*C-TAD*), preventing interaction with co-activator p300/CBP. Oncometabolites - succinate, fumarate and R-2-hydroxyglutarate - competitively inhibit PHDs by mimicking 2-OG, thus stabilising HIF-α in tumours with *SDH*, *FH* or *IDH* mutations (figure 1.12) (Hampton-Smith *et al*. 2019; Lee 2019; Martin-Puig *et al*. 2015; Webb *et al*. 2009).

Upon <5% O_2 (~38 μM O_2), inactive PHDs and FIH, permit HIF-α accumulation. HIF-1α and HIF-2α heterodimerise with HIF-1β and bind hypoxia response elements (HREs; 5'-[A/G]CGTG-3') in target promoters. Co-activator recruitment requires displacement of FIH and binding of p300/CBP *via* the *N-TAD* and *C-TAD* interfaces. Classic HIF targets include *VEGF*, *GLUT1* and *LDHA*, and others. (Freedman *et al*. 2002; Loboda *et al*. 2010).

HIF-1α accumulates within 30–60 minutes of hypoxia onset, peaking by 4 h, then declines during prolonged hypoxia, whereas HIF-2α induction is slower (4–8 h) but more sustained, persisting for 24 h. Their target repertoires overlap but diverge: HIF-1α preferentially regulates glycolytic enzymes and acute stress responders, whereas HIF-2α controls genes involved in stemness (*Oct4*), angiogenesis (*VEGFR2*) and chronic adaptation. Notably, HIF-2α binds a distinct

high-affinity HRE motif (*RCGTG*), influencing differential gene expression under prolonged hypoxia (Hu *et al*. 2003; Semenza 2012).

In addition to HIF-1α and HIF-2α, HIF-3α contributes to the fine-tuning of transcriptional responses under hypoxia. Unlike its counterparts, HIF-3α possesses multiple splice variants - some lacking transactivation domains - which can function as dominant-negative regulators of HIF-1/2 activity. The full-length HIF-3α isoform (IPAS) binds HREs without recruiting p300/CBP, thereby competing with HIF-1α for DNA occupancy and dampening target-gene induction, particularly under prolonged or cyclic hypoxia. Although less is known about canonical HIF-3α targets, studies implicate it in restraining *VEGF* and *EPO* expression, preventing over-exuberant angiogenesis once a minimal hypoxic adaptation has been achieved (Makino *et al*. 2002; Pasanen *et al*. 2010; Yang *et al*. 2015).

Beyond HIFs, hypoxia interfaces with NF-κB, NRF2 and STAT pathways. Hypoxia triggers IKKβ-mediated NF-κB activation *via* ROS, promoting expression of anti-apoptotic factors. Nrf2 is stabilised by Keap1 oxidation and induces expression of antioxidant genes. Moreover, STAT3 is phosphorylated under hypoxia *via* JAK2, enhancing transcription of downstream genes. This multilayered network ensures coordinated regulation of energy-intensive biological processes in fluctuating oxygen environment (Beitner-Johnson and Millhorn 1998; Cai *et al*. 1996; Gray *et al*. 2005; Malec *et al*. 2010; Nakayama and Kataoka 2019; Sarada *et al*. 2008).

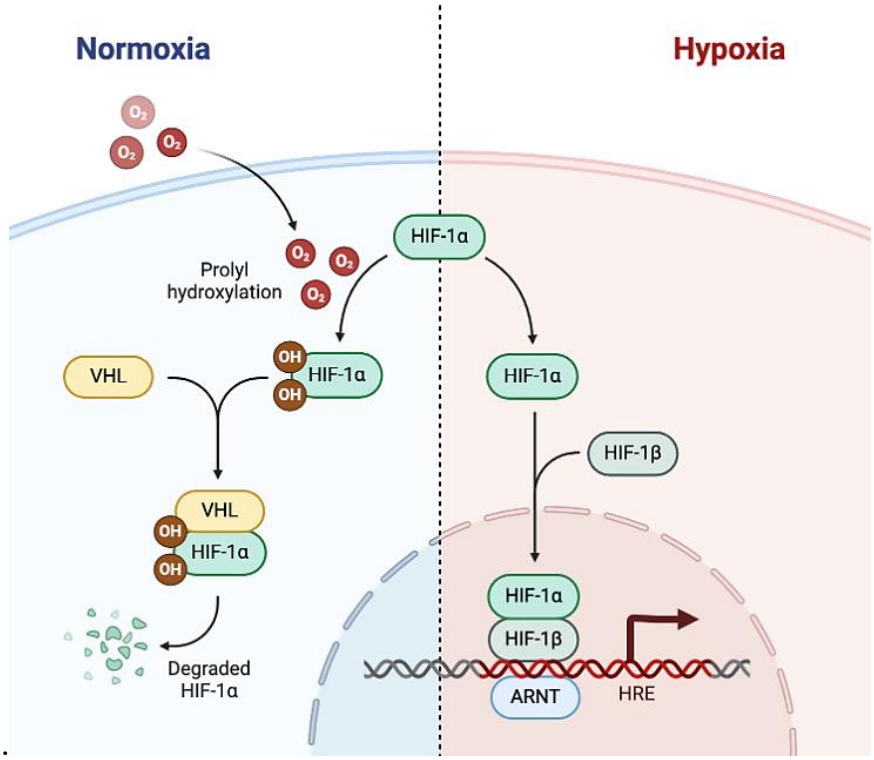

Figure 1.12. The HIF-signalling and the VHL-dependent degradation systems. In the presence of sufficient levels of oxygen, iron (II), and 2-oxoglutarate, HIF-α is hydroxylated by PHD and FIH under normal oxygen levels. Hydroxylation permits VHL, the recognition part of an E3-ubiquitin ligase complex, to attach to HIF-α, directing it for proteasomal breakdown. On the contrary, in conditions of insufficient oxygen, PHD and FIH become inactive and do not add hydroxyl groups to HIF-α. After binding with HIF-1β/ARNT, HIF-α moves to the nucleus and binds to hypoxia responsive element promoters to activate target genes through transcription. Reprinted from: "HIF signalling pathway" BioRender.com (2024) Retrieved from https://app.biorender.com/biorender-templates.

1.4.2. The DDR and the replication stress response in hypoxic cells

Under radiobiological hypoxia (<0.1% O_2), DNA synthesis is effectively abolished. Early ^3H-thymidine incorporation assays revealed >95% reduction in nucleotide uptake at these oxygen levels (Hammond *et al.* 2002). More granular BrdU labelling demonstrated that active replication persists unchanged down to ~0.15% O_2 but is extinguished below this oxygen threshold (Brahimi-Horn and Pouyssegur 2009; Hammond *et al.* 2003b). Single-molecule DNA fibre assays have since resolved the underlying dynamics: forks slow-down by >50%, stall frequency increases three-fold, and origin firing is suppressed by ~ 60% at <0.1% O_2, whereas at

2% O_2 replication kinetics are indistinguishable from normoxia (Foskolou *et al.* 2016; Pires *et al.* 2010). Mechanistically, this phenotype stems from compromised deoxyribonucleotide triphosphate (dNTP) supply. Ribonucleotide reductase (RNR) catalyses the rate-limiting conversion of ribonucleoside diphosphates to deoxyribonucleotides *via* a stable tyrosyl radical housed in its RRM2 subunit. Structural and kinetic studies demonstrate that re-oxidation of this radical - *via* an iron-oxo cluster - requires molecular oxygen, and under hypoxia the radical decays, reducing catalytic turnover by >80%. The resultant dNTP paucity precipitates polymerase–helicase uncoupling, extensive RPA-coated ssDNA tracts and replication fork reversal (Foskolou *et al.* 2017; Foskolou and Hammond 2017; Hogbom *et al.* 2003; Scearce *et al.* 1993).

Accumulation of RPA-coated ssDNA rapidly recruits ATR through ATRIP's RPA70-interaction domain, complemented by RAD17–RFC–9-1-1 clamp loading and TOPBP1-mediated allosteric activation (Foskolou *et al.* 2016; Olcina *et al.* 2013; Pires *et al.* 2010). Activated ATR phosphorylates CHK1 on Ser317 and Ser345, triggering CHK1 autophosphorylation at Ser296, which in turn targets CDC25A for SCFβTrCP-mediated proteolysis, suppressing CDK2 activity and origin firing (Zhang *et al.* 2005). ATR also phosphorylates H2AX on Ser139 - directly and *via* CHK1 - producing γH2AX which nucleates MDC1, RNF8/RNF168 ubiquitination and recruitment of downstream repair mediators (figure 1.13) (Hammond *et al.* 2002; Pires *et al.* 2012).

Concurrently, the MRN complex recognises reversed fork structures and engages ATM *via* NBS1's FHA/BRCT domains, inducing ATM Ser1981 autophosphorylation. ATM phosphorylates CHK2 on Thr68, enabling CHK2 dimerisation and activation, and directly stabilises p53 through Ser15 phosphorylation, reinforcing G_1/S arrest (Lee and Paull 2005; Matsuoka *et al.* 2007). Intriguingly, this ATM activation occurs in the absence of DSBs: alkaline comet assays reveal no significant increase in tail moment under hypoxia, highlighting the limitations of strand-break detection and suggesting that ATM may sense topological or chromatin alterations at stalled forks (figure 1.) (Bencokova *et al.* 2009; Hammond *et al.* 2002; Olcina *et al.* 2013). Dual inhibition

of ATR and ATM in severely hypoxic cells precipitates rampant fork collapse, replication-associated DSBs and apoptotic cell death, underscoring their non-redundant roles in fork stabilisation and origin suppression (Olcina *et al.* 2013; Pires *et al.* 2012). However, reliance on comet assays and endpoint kinase assays risks underestimating low-level oxidative lesions or transient fork reversal intermediates. High-resolution approaches, such as γH2AX ChIP-seq, to map subnucleosomal damage, or electron microscopy of replication intermediates, are required to fully characterise hypoxia-induced DNA perturbations. Finally, reoxygenation after chronic hypoxia unleashes ROS bursts that oxidatively damage nascent and parental DNA, generating 8-oxoguanine lesions and DSBs upon fork restart, and further activating ATR/ATM axes (Freiberg *et al.* 2006; Hammond *et al.* 2004; Hammond *et al.* 2006a). These findings highlight the dynamic interplay between oxygen fluctuations, nucleotide metabolism, and checkpoint signalling, and suggest that therapeutic targeting of ATR/ATM in hypoxic tumour niches may potentiate replication catastrophe selectively in cancer cells.

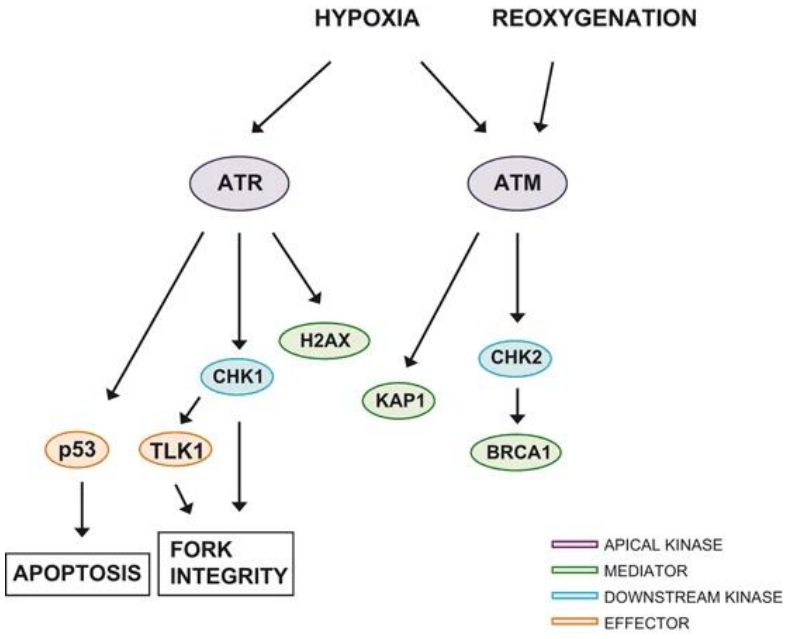

Figure 1.13. The DDR in hypoxic cells. Schematic representation of the hypoxia-induced DDR. In hypoxic conditions, stalled replication initiate a DDR (both ATR- and ATM-dependent). In reoxygenation, DSBs are detected and activate ATM signaling. Reprinted from: "Hypoxia and the DNA Damage Response" (Olcina and Hammond 2014). Licence No.: 5870801450755.

1.4.3. The impact of hypoxia on DNA damage repair

Under hypoxic stress, the most profound and consistently observed defect in DNA-damage responses pertains to HR, reflecting the pathway's high energetic demands and stringent co-factor requirements. In severely hypoxic conditions (<0.1% O_2), cells impose multilayered suppression of HR core factors, leading to a decrease of high-fidelity DSB repair and heightened genomic instability.

Central to this repression is the hypoxia-induced formation of a repressive E2F4–p130 complex at E2F recognition motifs within the *RAD51* and *BRCA1* promoters. Hypoxia stabilises p130 by inhibiting CDK-mediated phosphorylation, enabling E2F4 binding and displacement of activating E2F1 complexes, which in turn silences transcription of these essential HR mediators - an effect demonstrable within hours of oxygen withdrawal and independent of HIF-1α accumulation or S-phase fraction. Chromatin immunoprecipitation assays, reveal sharp reductions in histone H3 acetylation and RNAPII occupancy at the *RAD51* locus under <0.1% O_2, confirming direct transcriptional repression (Bindra *et al.* 2005; Bindra and Glazer 2007a). Concurrently, hypoxia remodels the epigenetic landscape at HR gene promoters: HIF-1α up-regulates the H3K9 methyltransferases G9a and GLP, increasing H3K9me2 at both *BRCA1* and *RAD51* promoters. This mark recruits HP1γ, condensing local chromatin and further occluding access by transcriptional activators. Functionally, HR reporter assays in multiple tumour cell lines demonstrate >70% reduction in HR repair events under severe hypoxia (Mihaylova *et al.* 2003; Nakamura *et al.* 2008). Post-transcriptional mechanisms reinforce HR suppression: hypoxia-induced micro-RNAs (miR-210, miR-373) target *RAD52* and *RPA1* mRNAs, reducing protein stability and impairing end-resection and RAD51 filament stability (Crosby *et al.* 2009). Moreover, the deubiquitinase UCHL1 - required for BRCA1 stability - is downregulated by HIF-1α-dependent repression, accelerating proteasomal degradation of residual BRCA1 under low-oxygen conditions (Xu *et al.* 2024b).

While HR endures the most severe attenuation, other repair pathways are also modulated by hypoxia, albeit to a lesser extent. Mismatch Repair (MMR) is suppressed *via* H3K9me2 deposition at the *MLH1* promoter, mediated by G9a/GLP up-regulation, leading to ~ 50% reduction in MLH1 protein and reduced G:T mismatch correction under <0.1% O_2 (Bindra and Glazer 2007b). BER components - including glycosylases NEIL2 and OGG1, AP endonuclease APE1 and the dNTP sanitiser MTH1 - are transcriptionally and translationally downregulated in hypoxia, yielding a ~40% decrease in oxidised base excision activity (Chan *et al*. 2014; Leszczynska *et al*. 2016). NER exhibits an oxygen-dependent dichotomy: at <0.2% O_2, ERCC1 expression falls by ~ 30% with concomitant impairment of UV lesion removal, whereas at milder hypoxia (~1.8 % O_2), up-regulation of XPC partially restores global genome NER, suggesting a dynamic transcriptional response *via* HREs in NER gene promoters (Liu *et al*. 2012; Yuan *et al*. 2000). Finally, NHEJ displays cell-type and assay-dependent variability: some models report modest induction of Ku70/80 and DNA-PKcs under hypoxia, whereas others observe a 20–30% decrease in end-joining efficiency, underscoring the need for standardised, single-molecule assays to resolve hypoxia's true impact on NHEJ (Jongen *et al*. 2017; Madan *et al*. 2012). While PolQ and PARP1 are the core catalytic and scaffolding factors for MMEJ in HR-deficient cells (Ceccaldi *et al*. 2015; Mateos-Gomez *et al*. 2017), direct measurement of MMEJ activity under hypoxia has not yet been reported. It therefore remains an important avenue for future investigation to determine whether hypoxic silencing of HR is accompanied by a compensatory shift toward PolQ-dependent MMEJ.

1.4.4. Hypoxia and the response to anticancer therapeutic modalities

Several impactful studies have demonstrated the importance of tumour hypoxia in determining patient prognosis. The findings from such studies suggest that tumour cells with lower oxygen levels are harder to treat with current cancer therapies such as, chemotherapy, radiation, and surgery (Hammond *et al*. 2014; Jing *et al*. 2019; Vaupel and Mayer 2007).

There are multiple reasons underlying the resistant phenotype of hypoxic cancer cells to chemotherapy. Such reasons include the distance from operational blood vessels which impedes drug delivery and diffusion, the slow cell proliferation rates in oxygen-deprived regions of the tumours, and the selection pressure, which results in loss of p53-mediated apoptosis in cancer cells (Gardner *et al*. 2001; Hammond and Giaccia 2005; Ho *et al*. 2022). Collectively, hypoxic cancer cells can increase their chemotherapy resistance, by triggering various pro-survival and adaptive mechanisms: HIF-mediated signaling is particularly responsible for causing drug resistance in hypoxic tumours by triggering various events including, the upregulation of genes encoding for proteins associated with multidrug resistance, the overexpression of drug efflux pumps, the evasion of cell death, the stimulation of self-autophagy, neovascularisation stimulation *via* Vascular Endothelial Growth Factor A (VEGF) activity, and mitochondrial metabolism modulation (Chen *et al*. 2014; Pugh and Ratcliffe 2003; Zhao *et al*. 2024). Regrettably, the development of small molecule inhibitors that target HIF-1α for cancer treatment, has not advanced to clinical trials, due to poor overall efficacy in living organisms, while combination of HIF-modulating agents with traditional and advancer anticancer therapeutic agents, is still being explored (Li *et al*. 2019; McAleese *et al*. 2021).

Approximately half of all cancer patients, undergo radiation therapy either by itself or in conjunction with some other treatment method. Numerous advancements have been achieved in enhancing the results of radiotherapy, which can be categorised into two main groups: those that enhance the impact on the actual malignancy and those that safeguard the healthy tissue (Abd El-Rehim *et al*. 2004; Wachsberger *et al*. 2004; Wicker *et al*. 2022). Mechanistically, the presence of oxygen during ionising radiation, is commonly known to cause the formation of free radicals, leading to the formation of stable organic peroxides that can ultimately result in DNA damage, challenging the cells with its repair. This results in an oxygen enhancement effect which makes hypoxic cells, up to three times more resistant to radiation, compared to cells at higher oxygen levels (Baumann *et al*. 2016; Horsman and Overgaard 1992; Possenti *et al*. 2024).

Furthermore, poor prognosis can also be expected when tumours are surgically resected due to increased invasion and metastasis caused by tumour hypoxia (Brown and Wilson 2004). The summary of hypoxia-associated impacts on anticancer therapeutic modalities is summarised below (figure 1.14).

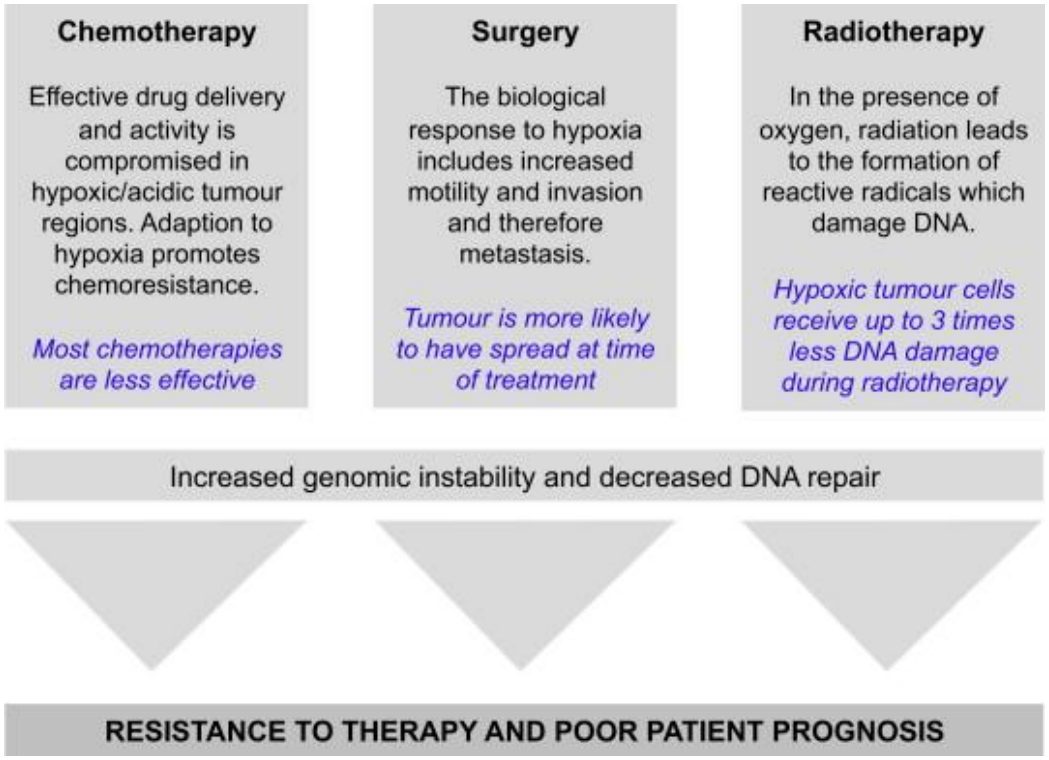

Figure 1.14. Hypoxia and the response to anticancer therapeutic modalities. Hypoxic tumour cells exhibit resistance to all common forms of anticancer treatment: chemotherapy, radiotherapy, and surgery. The figure summarises the main mechanisms of hypoxia-mediated treatment resistance, which leads to poor prognosis in cancer patients with hypoxic tumours. Reprinted from: "The Meaning, Measurement and Modification of Hypoxia in the Laboratory and the Clinic" (Hammond *et al.* 2014). Licence: https://creativecommons.org/licenses/by/3.0/

1.4.5. The impact of hypoxia on the effects of DDRi

Radiobiological hypoxia mediates the activation of DDR as an "adaptive response" where, its pro-survival signaling contributes to the hypoxia-mediated drug resistance which observed in tumour

cells. Hypoxia activates ATR-CHK1 and ATM-CHK2 checkpoints - sensing stalled forks and chromatin perturbations - to suppress origin firing, stabilise replication forks, and forestall catastrophic DSBs (Olcina *et al*. 2013; Olcina *et al*. 2014; Pires *et al*. 2012). Inhibition of these kinases abrogates the hypoxia-induced checkpoint: ATR, CHK1 or CHK2 blockade in cells subjected to hypoxia/reoxygenation triggers unscheduled origin firing amid dNTP scarcity, precipitating fork collapse, replication-associated DSBs and apoptotic death (Freiberg *et al*. 2006; Hammond *et al*. 2006b; Hammond and Giaccia 2006; Hammond *et al*. 2006a).

In the same field of the effects of DDRi in hypoxia, the use of PARPi to selectively kill hypoxic cells, due to the hypoxia-mediated suppression of HR led to the development of the contextual synthetic lethality concept. Work published almost a decade ago, highlighted the impact of hypoxia as a phenomenon of the TME, on the efficacy of PARPi supported by both, *in vitro* and *in vivo* findings. Specifically, it was reported that, cancer cells exposed to either severe acute hypoxia (16 h with 0.02% O_2) followed by reoxygenation or moderate chronic hypoxia (72 h with 0.2% O_2), showed reduced HR protein expression and HR function. This hypoxia mediated HR-repression conferred synthetic lethality, sensitising the hypoxic cells to the cytotoxic effects PARPi. This findings was further supported by reports of increased levels of DNA damage in hypoxic subregions of PARPi treated tumour xenografts and *ex vivo* clonogenic assays with these tumour cells, followed by radiotherapy (Chan *et al*. 2010). These findings suggest a clear sensitising effect of hypoxia to PARPi cytotoxicity and a contextual radiosensitising effect. Interestingly, nonetheless, more recent research on the same field, has suggested that hypoxia, being more accurately examined as an oxygen-gradient within malignant tumours and their microenvironment, can actually elicit different responses to PARPi, depending on oxygen levels – a finding that highlights a higher complexity in the relationship between DDRi and hypoxia. Specifically, a study published in 2021, investigated the impact of different oxygen levels in the response of HR-proficient and HR-deficient cells to PARPi. Their findings showed that, while oxygen levels as low as <0.5% sensitised those cell models to the effects of PARPi, higher oxygen

levels (2% O_2) resulted in resistance to PARPi treatment. An absence of adequate ROS levels and therefore, a ROS-dependent mechanism of resistance was hypothesised in this study. In this context, this same work reported an improved response to PARPi after the selective elimination of hypoxic tumour cells with the use of the hypoxic cytotoxin Tirapazamine (TPZ) (Mehibel *et al*. 2021). In support of this observation, another study published in 2022, identified biomarkers of resistance to the effects of the PARPi talazoparib, analysing g*BRCA*-mutant tumour samples, from patients who had received neoadjuvant talazoparib as a monotherapy. Transcriptomic analyses of such samples resulted in the identification of pathways associated with resistance to this PARPi, showed that hypoxia was one the most significantly enriched pathways, in tumours resistant to talazoparib (Liu *et al*. 2022b). Together, these reports highlight a significant gap in our current understanding of the impact of hypoxia and the TME, on the efficacy of PARPi and suggest a much more complex conceptualisation of context synthetic lethality, potentially extending to the efficacy other of types of DDRi, as well.

1.4.6. Hypoxia-mediated metabolic adaptations

Oxygen is well-known to play a crucial role in cell metabolism. In hypoxic regions of malignant tumours, however, the cancer cells need to survive and proliferate in areas with limited oxygen and nutrients (Chakraborty 2020; Pereira *et al*. 2013). In order to sustain growth, cancer cells "rewire" their metabolic pathways and employ alternative methods to maintain their proliferation. The Warburg effect, controlled by HIF-1 transcriptional activity, is an essentially metabolic reprogramming process. The key nutrients in the TME that support cell growth and proliferation are glucose, and glutamine. Hypoxia-driven mutations like those known to occur in isocitrate dehydrogenase-1 and 2 (*IDH1* and *IDH2*), both key enzymes of the Krebs cycle as well as HIF-1-mediated triggering of transcriptional processes that promote glucose absorption and

glycolysis and glutamine metabolism and uptake, function in conjunction to maintain the cancer cell energetic demands (Chen *et al.* 2013a; Semenza 2011; Warburg 1956).

Glutamine is the primary amino acid in cancer cell metabolism and has been shown to be essential for providing energy and vital metabolic substrates for cancer cells, including non-essential amino acids, metabolic intermediates of the Krebs cycle, glutathione and of course ATP (Pan *et al.* 2022; Reinfeld *et al.* 2021). HIF-1 and HIF-2, can upregulate the expression of *SLC1A5* to support ATP and glutathione production in pancreatic cancer cells, rendering them thus resistant to gemcitabine. Reduced glucose availability in hypoxic areas increases the reliance on alternative carbon sources like L-glutamine (Yoo *et al.* 2020). Furthermore, a lack of the Autophagy-related 12 (*ATG12*) gene, results in reduced L-glutamine levels in cells under hypoxic conditions and cancer cell death was observed following L-glutamine depletion. Analysis of the TME, revealed that targeting *ATG12* led to reduced tolerance to low oxygen levels, increased necrosis levels, and a significantly better response to anticancer treatment (Keulers *et al.* 2022).

1.5. ROS in cancer and their relationship with tumour hypoxia

1.5.1. ROS metabolism and detoxification

ROS are short-lived, highly reactive derivatives of molecular oxygen that function both as signaling mediators and as oxidants capable of modifying proteins, lipids, and nucleic acids. (Galadari *et al.* 2017; Xing *et al.* 2022). ROS can be generally grouped into radical and non-radical forms. Oxygen radicals, include superoxide (O_2^{-}), hydroxyl radical ($^{\cdot}OH$), nitric oxide ($NO^{\cdot}$), organic radicals ($R^{\cdot}$), peroxyl radicals ($ROO^{\cdot}$), alkoxyl radicals ($RO^{\cdot}$), thiyl radicals ($RS^{\cdot}$), sulphonyl radicals ($ROS^{\cdot}$), thiyl peroxyl radicals ($RSOO^{\cdot}$) and disulphides (RSSR). Non-radical ROS include, hydrogen peroxide (H_2O_2), singlet oxygen ($^1O_2$), ozone(O_3), organic hydroperoxides (ROOH), hypochloride (HOCl), peroxynitrite (ONO^{-}), nitrosoperoxycarbonate anion ($O{=}NOOCO_2^{-}$), nitrocarbonate anion

(O_2NOCO_{2-}), dinitrogen dioxide (N_2O_2), nitronium (NO_2^+) and highly reactive lipid- or carbohydrate-derived, carbonyl compounds. Among them, superoxide, hydrogen peroxide, and hydroxyl radicals are the most well studied ROS in cancer (Galadari *et al*. 2017; Liou and Storz 2010).

ROS can be produced by various endogenous and exogenous factors. Specifically, mitochondria are found to be the most significant source of endogenous ROS (Xing *et al*. 2022). Mitochondrial ROS are formed during the process of oxidative phosphorylation, which involves the electron transfer chain, comprising of four enzyme complexes. Complexes I and III are the main sites of mitochondrial ROS production, with electron leakage leading to the generation of superoxide radicals. Additionally, mutations in complex II can increase mitochondrial ROS generation, causing oxidative stress and potential cellular transformation into malignant phenotypes. Other contributors to ROS production in mitochondria, include glycerol 3-phosphate dehydrogenase, pyruvate dehydrogenase (PDH), and 2-oxoglutarate dehydrogenase (Han *et al*. 2001; Liou and Storz 2010; Storz 2006). Manganese superoxide dismutase (MnSOD) converts O_2^- to H_2O_2 in the mitochondrial matrix (Hoidy *et al*. 2022; Liu *et al*. 2022a; Pan *et al*. 2022). H_2O_2 in the mitochondrial matrix can be further turned to •OH by mitochondrial aconitase *via* the Fenton reaction (Xing *et al*. 2022). During the Fenton reaction process, Iron (II) (Fe^{2+}), reacts with H_2O_2 to generate •OH, which can in turn inflict damage to important biological macromolecules of the cell such as DNA, lipids, and proteins. Therefore, iron is recognised as an important source of endogenous ROS and is shown to be taking part in various biological processes and many pathological conditions through the production of ROS (Chen *et al*. 2024a; Shiota *et al*. 2024). Furthermore, many other enzymes have been found to contribute to the production of endogenous ROS, like those of the nicotinamide adenine dinucleotide phosphate (NADPH) oxidase (NOX) family, consisting of 7 members: NOX1, NOX2, NOX3, NOX4, NOX5, dual oxidase 1 (DUOX1), and DUOX2. NOXs are membrane-bound enzymes which function by reducing oxygen to O_2^- by transferring one electron from NADPH to flavin adenine dinucleotide (FAD), across biological membranes (Bedard and Krause 2007; Landry and Cotter 2014). Other endogenous,

ROS-linked enzymes, include diamine oxidase (DAO), cyclooxygenases (COXs), and lipoxygenases (LOX). Peroxisomes and endoplasmic reticulum stress can further contribute to ROS production (figure 1.15) (Abd El-Rehim *et al.* 2004; Chen *et al.* 2024a; Shiota *et al.* 2024).

Exogenous sources of ROS, include multiple external triggers, such as air pollutants, tobacco smoke, ionising, and non-ionising radiations (e.g. UV-radiation), foods, and drugs, as well as various xenobiotics. Moreover, chemical agents like quinones, heavy metals such as lead, arsenic, mercury, chromium, and cadmium, organic solvents, and pesticides are also known as common exogenous sources of ROS (Bhattacharyya *et al.* 2014; Juan *et al.* 2021).

Under physiological conditions, low levels of ROS fine-tune kinase cascades (e.g., MAPK, PI3K/AKT), modulate transcription factor activity (e.g., NF-κB, Nrf2), and participate in host defense. However, when in excess (a condition known as "oxidative stress") ROS have the potential to inflict widespread cellular damage by oxidising and altering essential macromolecules within the cells, thereby hindering their intended functions. This indicates that ROS can have multiple functions, serving as either protective (e.g. in antimicrobial defences), signalling, or even harmful molecules, depending on the equilibrium, between ROS generation and removal, at the cell cycle phase and cellular compartment they are located in (de Almeida *et al.* 2022; Klaunig *et al.* 2010).

To ensure proper cellular and metabolic functions and thence, survival, the cell employs a tightly regulated system of intracellular ROS levels control, which consists of several mechanisms that work collectively, to achieve what is known as "redox homeostasis" (figure 1.15) (Juan *et al.* 2021; Xing *et al.* 2022). This metabolic system, also known as the antioxidant system, plays a crucial role in maintaining the balance of ROS in normal cells, preserving the integrity of cellular structure and function. The antioxidant system basically transforms ROS into less reactive molecules in order to "neutralise" the damaging impact of excessive ROS (Snezhkina *et al.* 2019). Cellular antioxidants, include any molecule that counteracts, restricts, or inhibits the creation of

ROS, neutralises those already formed by giving providing electrons, and consequently prevents the harmful effects of potentially dangerous oxidisers. In line with their function, action site, and source, antioxidants are categorised into endogenous and exogenous, enzymatic and nonenzymatic antioxidants. The endogenous enzymatic antioxidant system includes enzymes such as superoxide dismutase (SOD), glutathione reductase (GSR), glutathione peroxidase (GPX), glutathione S-transferase (GST), catalase (CAT), heme oxygenase (HO), peroxiredoxin (PRX), thioredoxin (TRX), and paraoxonase (PON). The nonenzymatic antioxidant system comprises of moth endogenous and exogenous molecules such as, glutathione (GSH), NADPH, nicotinamide dehydrogenase (NADH), vitamin C (ascorbic acid), vitamin E (α-tocopherol), and melatonin, among others (figure 1.15) (Asgari *et al*. 2024; Moller *et al*. 2023; Nir *et al*. 2022; Rudenko *et al*. 2023).

By far the most important cellular antioxidant system, employed to control ROS levels, is the GSH system. The GSH system consists of GSH, GSR, GPX, and GST. Specifically, GSH guards cells against oxidative stress by converting oxidised disulphide bonds in cytoplasmic proteins to cysteine residues. In this process, GSH undergoes oxidation to form glutathione disulphide (GSSG). GPX enzymes, are responsible for breaking down hydrogen peroxide and organic hydroperoxides GSR, in turn, helps in reducing GSSG levels and replenishing GSH intracellular levels (GSH pool). Under homeostatic circumstances, GSH remains mostly in its reduced state due to the constant action of GSR in cells. GST are enzymes involved in detoxification, combining GSH with different external and internal electrophilic substances (Brigelius-Flohe 1999; Cassier-Chauvat *et al*. 2023; de Baat *et al*. 2023; Townsend and Tew 2003; Ursini *et al*. 1995; Xing *et al*. 2022).

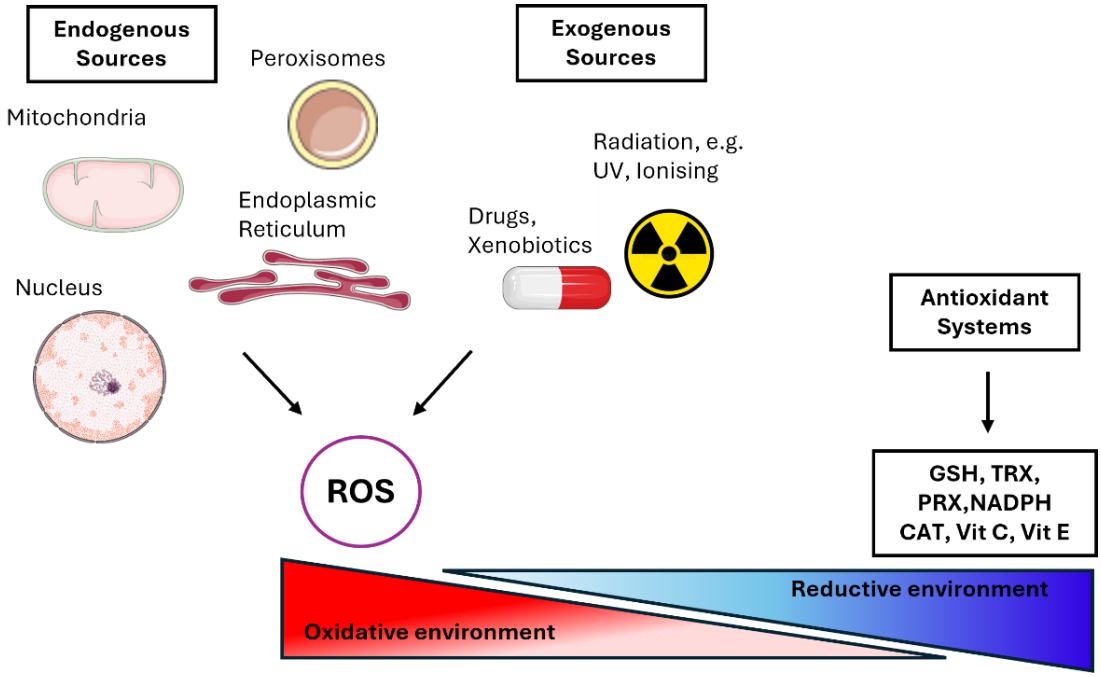

Figure 1.15. Redox homeostasis in the cell. Endogenous and exogenous sources of cellular ROS are illustrated. A balance between ROS and antioxidants in the cells is known as redox homeostasis. An imbalance between the cellular ROS levels and the capacity of antioxidant systems shift the intracellular environment to an oxidised state, known as oxidative stress, which thence, threatens essential macromolecules and ultimately the cell's functional and structural integrity. GSH = glutathione; TRX = thioredoxin; CAT = catalase; NADPH = nicotinamide adenine dinucleotide phosphate oxidase; Vit C = vitamin C; Vit E = vitamin E. Image created with Microsoft PowerPoint and Servier Medical Art. Licence: https://creativecommons.org/licenses/by/4.0/

1.5.2. Cancer cell responses to excessive ROS levels

Cancer cells maintain elevated - but precisely regulated - ROS levels to drive proliferation *via* redox-sensitive signalling pathways (Aggarwal *et al.* 2019; Xing *et al.* 2022). At low concentrations, H_2O_2 or $O_2^{\bullet -}$ cause reversible oxidation of critical cysteine residues in phosphatases such as PTEN, thereby sustaining PI3K/AKT and MAPK cascade activation and promoting cell-cycle progression (Sarmiento-Salinas *et al.* 2021; Storz 2005). MnSOD functions as a mitochondrial redox rheostat: reduced MnSOD activity elevates superoxide levels, which can enhance NF-κB-mediated transcriptional programmes and proliferation, whereas MnSOD overexpression increases H_2O_2, activates p38 MAPK and induces a quiescent state (Cullen *et al.* 2003; Felty *et al.* 2005).

When ROS production exceeds the buffering capacity of antioxidant systems - typically above tens of micromolar H_2O_2 - cancer cells engage in programmed cell death pathways. Oxidative peroxidation of cardiolipin and thiol oxidation of mitochondrial permeability transition components, facilitate Cytochrome c release, leading to apoptosome assembly and activation of initiator Caspase-9 and effector Caspases-3/6/7 (Nguyen *et al*. 2023; Rauf *et al*. 2024; Yang *et al*. 2024). In parallel, extensive DNA oxidative damage activates ATM/ATR kinases, inducing cell-cycle arrest or senescence through activation of $p21^{CIP1}$ and $p16^{INK4A}$ (Simon *et al*. 2000).

The tumour suppressor p53 integrates redox cues to determine cellular fate. Under moderate oxidative stress, p53 transactivates antioxidant genes - such as SESN1 and GPX1 - to restore homeostasis; under severe stress, p53 induces pro-oxidant PIG family members (PIG3, PIG6), amplifying mitochondrial ROS production and driving apoptosis *via* BAX and PUMA upregulation (Gambino *et al*. 2013; Hayes *et al*. 2020; Liu and Xu 2011).

Ferroptosis - an iron-dependent form of regulated cell death - is characterised by iron-catalysed peroxidation of polyunsaturated phospholipids. Labile Fe^{2+} reacts with H_2O_2 *via* the Fenton reaction, and lipoxygenases propagate lipid radicals, compromising membrane integrity (Dixon *et al*. 2012; Jiang *et al*. 2021). GPX4 and the cystine/glutamate antiporter xCT maintain lipid redox balance; inhibition of GPX4 (e.g. RSL-3) or xCT (e.g. Erastin) induces ferroptosis in RAS-driven cancer models (Kim *et al*. 2023; Wang *et al*. 2022; Yagoda *et al*. 2007). Furthermore, $p14^{ARF}$ augments ferroptotic sensitivity by repressing nuclear factor erythroid 2-related factor 2 (NRF2) and enhancing p53-dependent lipid ROS accumulation (Chen *et al*. 2017).

Across both apoptotic and ferroptotic pathways, redox-mediated post-translational modifications - such as S-glutathionylation of caspases or S-nitrosylation of BAX - modulate the activity of death effectors. The interplay between glutathione- and thioredoxin-dependent systems in directing cell death remains an active area of investigation (Benhar 2020; Hayes *et al*. 2020). Pharmacological targeting of antioxidant enzymes - such as inhibition of GSR or SOD2 - to

disrupt redox homeostasis has demonstrated enhanced sensitivity of tumour cells to chemotherapy and radiotherapy in preclinical models, underscoring therapeutic opportunities in modulating cancer redox biology (Halliwell and J 2022). Additional research is needed, to determine how the GSH and/or TXN antioxidant systems regulate apoptosis and/or ferroptosis and controlled cell death induction, however, it has been previously indicated that depletion of intracellular GSH can activate ferroptosis (Sun *et al.* 2018).

1.5.3. ROS and their relationship to tumour hypoxia

The impact of hypoxia on intracellular ROS levels is somewhat controversial, with some studies demonstrating increased ROS production in normal and malignant cells under hypoxic conditions, whilst others are reporting the opposite, suggesting a complex mechanism, probably dependent on cell line, experimental conditions, and specific ROS subtypes (Chandel *et al.* 2000; Duranteau *et al.* 1998; Sgarbi *et al.* 2017; Tuttle *et al.* 2007; Twigger *et al.* 2024). The majority of research on the field, however, point to a hypoxia-mediated increase in ROS, generated mainly from the mitochondrial complex III, but also from complexes I and II, as well as from the activity of enzymes of the Krebs cycle, such as 2-oxoglutarate dehydrogenase (OGDH) (Kung-Chun Chiu *et al.* 2019; Lu *et al.* 2017; Quinlan *et al.* 2014; Tafani *et al.* 2016; Yan *et al.* 2021). Mechanistically, decreased complex IV activity in the mitochondria of hypoxic cells, has been shown to slow down the electron transfer along the ETC, increasing the production of unintentional electron transfer to molecular oxygen, which produces the highly reactive O_2^- (Brunelle *et al.* 2005). While less understood, hypoxia also triggers the production of ROS by upregulating enzymes that produce them as a byproduct of their main catalytic activity. Following the first surge of mitochondrial ROS, which stops after mitochondrial depolarisation, hypoxia can generate ROS by xanthine oxidase (XO) activity (Abramov *et al.* 2007). Another study demonstrated that hypoxia triggers the mRNA and protein quantities of NOX4, whose function leads to a rise in ROS levels (Li *et al.* 2008).

In conditions of insufficient oxygen, HIF signalling is responsible for mitigating hypoxia-mediated ROS level increases, in a variety of ways. SOD2, the enzyme converting the O_2^- radical to H_2O_2, which can then be further broken down into harmless water and oxygen by catalase enzymes, was found to dependent on HIF-2α expression in research carried out in mice (de Bastos *et al*. 2024; Scortegagna *et al*. 2003). Human cell studies demonstrated that SOD2 expression is induced under hypoxia, in a HIF-2α dependent manner, while in renal carcinoma cells, SOD2 expression is suppressed under hypoxia, in a HIF-1α dependent manner (Befani *et al*. 2013; Gao *et al*. 2013).

GSH, a tripeptide, serves as a major defence against ROS was also found to be also upregulated in hypoxia (Oh *et al*. 2008; Rouschop *et al*. 2013). The recycling of glutathione is facilitated by the reducing power of NADPH through reaction catalysed by GSR. Under hypoxic conditions, key NADPH-producing pathways are upregulated, such as serine synthesis, which generates NADPH. HIF-1α plays a critical role in upregulating enzymes involved in GSH biosynthesis, and the constituent amino acids of glutathione: cysteine, glutamate, and glycine (Amelio *et al*. 2014; Lu *et al*. 2015). Moreover, HIF-1α activity helps to maintain GSH in its reduced form and contributes to increased levels of de novo GSH synthesis by upregulating enzymes involved in GSH biosynthesis and GSH-constituent amino acid synthesis. Specifically, it has been reported that HIF-1α mediated the upregulation of serine synthesis pathway enzymes like phosphoglycerate dehydrogenase (PHGDH) increases serine availability for glycine and cysteine synthesis (Samanta *et al*. 2022; Ye *et al*. 2014). HIF-1 also upregulates solute carrier protein 7A11 (SLC7A11), which is a component of the cysteine import channel, leading to increased cysteine flux into the cell (Lu *et al*. 2015). Additionally, glutamate synthesis from glutamine is increased in response to HIF actions, to counteract the depletion of intracellular glutamate levels. Specifically, HIF-1α stabilisation stimulates glutaminase 1 and 2 (GSL1 and GLS2) expression, increasing thus cellular glutathione levels. Recent work has shown that HIF-1α stabilisation by hypoxia or *EGLN1* (*PHD2*) depletion in periosteal progenitor cells, stimulates GLS1 expression,

and thus increases cellular glutathione levels, which protects these cells from ROS-mediated cell death. Furthermore, HIF-1 has been shown to directly stimulate GSH synthesis in breast cancer cells by upregulating the enzyme responsible for the rate-limiting step in the pathway, namely glutamate–cysteine ligase (GCLM) (figure 1.16)(Lu *et al.* 2015; Stegen *et al.* 2016). Finally, HIFs play a crucial role in minimising ROS production from mitochondria in hypoxic conditions, by reducing mitochondrial mass and regulating the expression of alternative isoforms of subunits of the respiratory complexes. The complex I subunit, NDUFAL2, is induced in hypoxia, in a HIF-1 dependent manner, decreasing ETC activity and mitochondrial ROS production (Thomas and Ashcroft 2019). HIF-1 also upregulates COX4-2, improving electron transfer and oxygen consumption efficiency in hypoxia (Fukuda *et al.* 2007; Tello *et al.* 2011). Overall, HIF signaling plays a key role in regulating mitochondrial ROS production and intracellular ROS detoxification, a function that appears to be essential for cell viability in hypoxia (Thomas and Ashcroft 2019). Interestingly, there has been reports of a reciprocal relationship between HIF signaling and ROS, as ROS have been shown to lead in HIF-α stabilisation under hypoxia (Jin *et al.* 2011; Peng *et al.* 2014; Pouyssegur and Mechta-Grigoriou 2006; Qutub and Popel 2008).

The exact roles of hypoxia-induced ROS in the biological functions of the cell, are still a largely unexplored research field. It is impressive that, though most of the research concludes that hypoxia can indeed upregulate intracellular levels of ROS, hypoxic cells exhibit a significantly radioresistant phenotype, and somehow, the hypoxia-induced ROS do not lead to an increased amount of DSBs and, thus, detectable DNA damage in hypoxia as described in previous sections. These questions are of high significance, and further research is due in order to fully comprehend the complex redox biological mechanisms of hypoxic cells and to fully exploit them for improving hypoxia-targeted therapy. Recently, ROS levels in hypoxia have been shown to contribute to transcriptional stress through the accumulation of DNA:RNA hybrids, R-loops, in the absence of SSBs/DSBs (Ma *et al.* 2023). This is one of the few reports of a specific role of ROS in hypoxic cancer cell biology, with many possible extensions in the mechanisms of oxidative stress

signalling, in hypoxic conditions. It will be interesting to further dissect the oxidative stress response in hypoxic cells and understand, to what extent ROS-signalling mediates the treatment-resistant behaviour of hypoxic cancer cells. Interestingly, another recently published study showed that Ag5, a silver-based molecular cluster which inhibits major cellular antioxidant systems, sensitised hypoxic cancer cells significantly, in a *HIF-1α*/ROS- dependent manner, a finding that highlight the fact that hypoxia-induced redox responses could, indeed, be exploited to improve targeted anticancer therapy (Twigger *et al.* 2024).

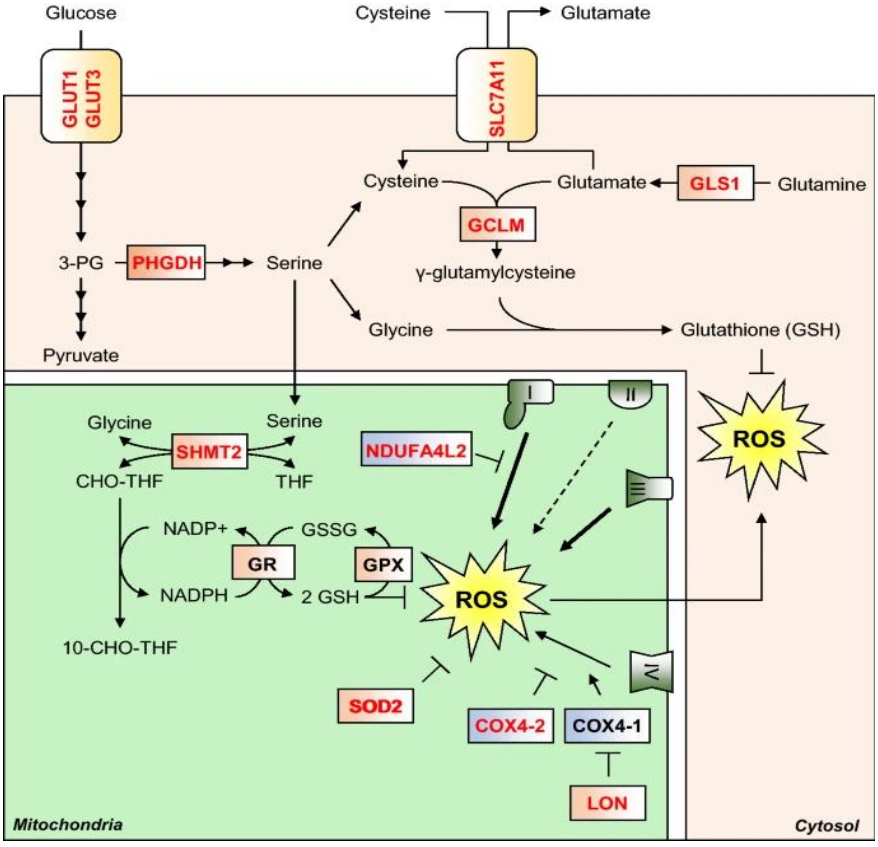

Figure 1.16. The HIF-mediated response to hypoxic ROS. Hypoxia-induced ROS, trigger a HIF-mediated antioxidant response. HIF upregulates the expression of the cellular machinery needed for recycling, as well as *de novo* synthesis of most cellular antioxidant systems, ensuring, thus, the functional and structural integrity of hypoxic cells, buffering excessive hypoxia-induced ROS and their potentially aberrant effects. Reprinted from: "Exploring the molecular interface between hypoxia-inducible factor signalling and mitochondria" (Thomas and Ashcroft 2019). Licence: http://creativecommons.org/licenses/by/4.0/.

1.5.4. RIMKLA

The *Ribosomal modification protein RimK-like A* (*RIMKLA)* codes for an N-acetylaspartylglutamate (NAAG) synthase enzyme, which catalyses the synthesis of NAAG and N-acetylaspartylglutamylglutamate (NAAG2) using the substrates N-acetylaspartate (NAA) and L-glutamate, at the concurrent expense of an ATP molecule (Collard *et al*. 2010; Lodder-Gadaczek *et al*. 2011). Along with its paralogue *RIMKLB,* both have been shown to encode enzymes which catalyse the ligation L-glutamate to NAA or to citrate to synthesise NAAG or NAAG2, respectively, with *RIMKLA* however, encoding an enzyme shown to have approximately 75-fold higher NAAG-synthesising activity compared to NAAG2-synthesising activity, and *RIMKLB* encoding an enzyme shown to display comparable activities for both NAAG and NAAG2 synthesis (Collard *et al*. 2010). Of note, both genes are named after the RimK protein, an ATP-dependent glutamate ligase, first characterised in *E. coli*, decades ago (Kang *et al*. 1989). RimK, is known to be responsible for the addition of glutamic acid residues to the C-terminus of ribosomal protein S6 in *E. coli*, and both *RIMKLA* and *RIMKLB* were named after it, due to the fact that they both contain the same, conserved active site domain with the bacterial RimK, without any evidence of ribosomal modification properties in mammalian cells, nonetheless, and their sole currently identified functions, being limited to the synthesis of the above-described dipeptides (Kang *et al*. 1989; Yan *et al*. 2024). In cancer cells, the role of *RIMKLA* has not been investigated *per se*, it has been, however, identified as part of an amino acid metabolism-associated gene signature, predicting the prognosis and immunotherapy response, of clear-cell renal carcinoma, as well as in a 12-gene metabolism-associated signature, implicated in tumour metastases in clear cell renal carcinoma (Tan *et al*. 2023a; Zhang *et al*. 2022).

Interestingly, the product of *RIMKLA*, NAAG, has been shown to be of high importance in cancer cell metabolism: despite NAAG being known as the most abundant neuropeptide in the mammalian nervous system, high NAAG-content has moreover been associated with advanced

and aggressive cancers where it was shown to function as a glutamate-reservoir for cancer cells promoting ovarian cancer cell growth, as well as promoting proliferation and inhibiting differentiation of glioma stem-like cells (Long *et al*. 2013; Nguyen *et al*. 2019). Additionally, NAAG has been recently identified, as a crucial tumour-promoting metabolite in a specific subtype of triple-negative breast cancer, through metabolomic analyses of tumour samples (Xiao *et al*. 2022).

Another interesting fact, potentially associating *RIMKLA* and *RIMKLB* with cancer biology, is the catabolism of their product NAAG. As shown below (figure 1.17), downstream it synthesis, NAAG is catabolised to L-glutamate and NAA, by the catalytic activity of the key enzymes glutamate carboxypeptidase II (GCP II) and its close homolog GCP III (Vorlova *et al*. 2019). The enzyme GCP II, encoded by the gene folate hydrolase 1 (*FOLH1*), is also known as NAAG peptidase or more commonly as prostate-specific membrane antigen (PSMA), an alias most oncologists are familiar with, due to its high biomarker significance in prostate adenocarcinoma (Mesters *et al*. 2006; Vorlova *et al*. 2019). Furthermore, it has been identified in the neovasculature of most human solid tumours and, therefore, it is being investigated for its potential to serve as an imaging and therapeutic target in other cancers, as well (Abbott *et al*. 2021; Ho *et al*. 2024; Lu *et al*. 2023; Vorlova *et al*. 2019). Most interestingly, however, apart from its established role in diagnosis prostate cancer, GCP II expression has been observed in malignancies from kidney, bladder, breast, colon, and Schwann cells, highlighting its potential as a biomarker for additional cancer models (Barinka *et al*. 2012). Notably, GCP II inhibitors are being extensively investigated as anticancer treatments agents, based on data reporting that GCPII depletion through genetic alteration, or pharmacological inhibition of GCPII resulted in a reduction of both glutamate concentrations and cancer growth (Nguyen *et al*. 2019). These findings together, support the significance of NAAG in malignant tumours and its potential for anticancer treatment development, and by extension, they lay an emphasis on the potential significance of the enzymes that synthesise it. In the context of hypoxia, one study has shown that NAAG pre-

treatment was able to reduce oxidative stress and DNA damage levels, in hypoxic-ischaemic neonatal rat brain cells (Bratek *et al.* 2020).

The biological role of the enzyme NAAGS II, which *RIMKLA* encodes, suggests that by producing NAAG, which can be further catabolised to glutamate, *RIMKLA* might be indirectly contributing to the GSH reservoir within the cells and thus, to the redox homeostasis. This connection has not been investigated or established yet, and its impact on ROS levels and redox equilibria of hypoxic cells is also, yet to be characterised (figure 1.17).

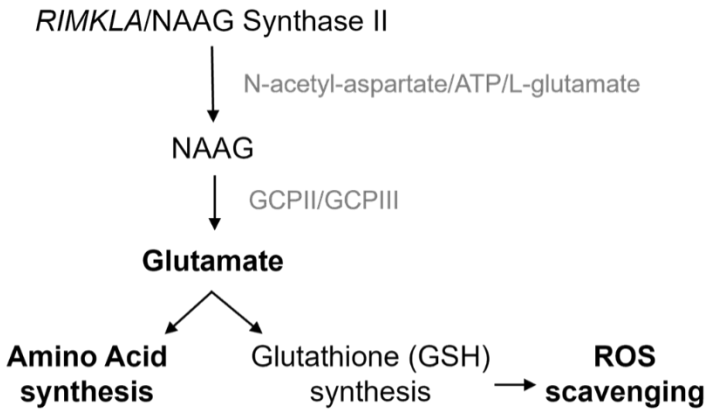

Figure 1.17. The biological role of *RIMKLA*. *The RIMKLA* gene codes for NAAG synthase, an enzyme that produces NAAG. GCPII (glutamate carboxypeptidase II) catabolises NAAG to glutamate which acts as a substrate for synthesis of GSH and other amino acids.

1.6. AIMS OF STUDY

I. To determine the impact of different hypoxic conditions on the efficacy of PARPi, in breast cancer cell lines *in vitro*, and investigate the biological mechanisms underlying responses to therapy with DDRi in hypoxic cells.

II. To characterise transcriptional changes, in response to different levels of oxygen using breast cancer cells and examine the prognostic/predictive potential of hypoxia-inducible genes.

III. To investigate the biological function of *RIMKLA*, a gene we report to be hypoxia-inducible and examine its impact on cellular redox homeostasis, using breast cancer cells.

Chapter 2 Methods and materials

2.1. Methods

2.1.1. Cell culture

Cells were grown in culture media composed of 90% D-MEM, or 90% RPMI, supplemented with 10% Foetal Bovine Serum (FBS). While in culture, cells were maintained in a humidified incubator set at 37^0C and 5% CO_2. Cell lines used in this study and their specifications are listed in table 2.1. Cell culture reagents and related information are listed in table 2.2.

2.1.2. Mycoplasma testing of cell cultures

Testing for mycoplasma infection was routinely carried out in cultured cells using, the HEK-Blue Detection kit (InvivoGen). For this test, cells were grown in antibiotic-free media for, at least 48 hours, before being harvested at 100% confluency. Samples were then heated for 15 min at 100°C, 50 µL of which was added to 200 µL of HEK-Blue cells (1-3.5 x 105 cells/mL) in HEK-Blue detection medium (InvivoGen). Cells were plated in a 96-well plate, along with positive and negative controls (controls were provided by the manufacturer) and incubated for 24 hours, under normal tissue culture conditions. Appearance of a pink colour indicated a negative result for mycoplasma infection, whereas appearance of a blue colour indicated a positive result for mycoplasma infection.

2.1.3. Cryopreservation of cells

Confluent cells were trypsinised and centrifuged at 500 x g for 5 min, in complete media. The cell pellet was then resuspended in 90% D-MEM media supplemented with 10% FBS and 10% dimethyl sulfoxide (DMSO) and aliquoted into cryovials (Fisher Scientific) at a concentration of ~2 x 10^6 cells/mL. The cryovials were temporarily stored at -80°C in a Mr. Frosty container

(Nalgene), which also contained 2-propanol. The cryovials containing the frozen cells were later transferred to liquid nitrogen.

2.1.4. Cell Thawing

Cryovials of frozen cells were thawed quickly in a 37°C water bath. Cells were then resuspended in 5 mL of complete media and centrifuged for 5 min at 500 x g. The pellets obtained were resuspended in complete media before being transferred to a T25 flask and maintained at 37°C in a 5% CO_2 humidified incubator.

2.1.5. Hypoxia treatment

Hypoxia treatments at <0.1% O_2 were carried out in a Bactron II anaerobic chamber (Shel Labs). Conditions of <0.1% to 2% O_2 reoxygenation treatments (cyclic hypoxia) were carried out in an M35 variable atmosphere workstation (Don Whitley Scientific). Specifically, for cyclic hypoxia: cycles of 2 h of <0.1% O_2 followed by 2 h of 2% O_2 were used to treat the cells according to a previously published work (Bader *et al.* 2021). Cells were seeded on glass dishes and/or six well plastic plates and harvested in the chamber, using equilibrated solutions. Details of the hypoxia treatments we applied, are illustrated below (figure 2.1)

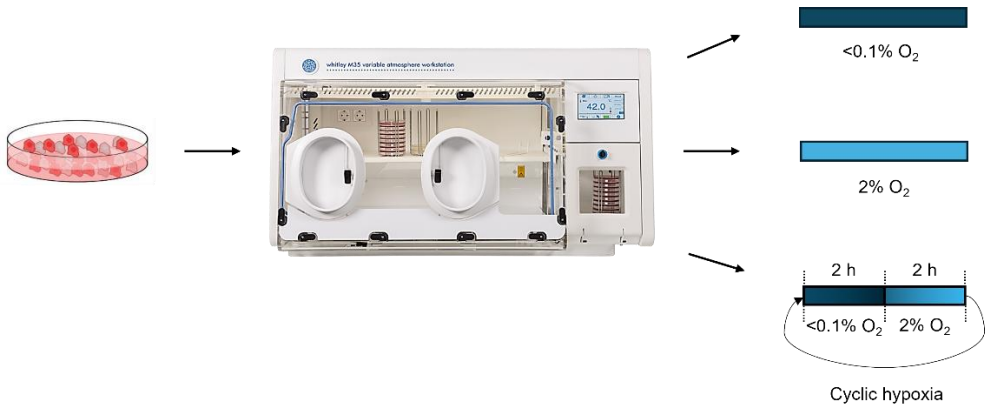

Figure 2.1. Hypoxia treatments in our study. The methods and types of hypoxia treatments used in our experiments are illustrated

2.1.6. Immunofluorescence

Cells were seeded onto autoclaved cover slips (Menzel-Glaser) before treatment. After the treatment endpoint, cells were fixed with 4% (w/v) paraformaldehyde (PFA) fixation buffer, for 10 min. Samples were then washed thoroughly (3 times) in PBS, stored at 4°C. Then, cells were permeabilised with 1% PBS-Triton X-100 (Thermo Fisher) for 15 min, followed by a wash with PBS (room-temperature) they were blocked in 2% (w/v) BSA (Thermo Fisher) in 0.1% PBS-tween, for 1 hour. Proteins were visualised with a LSM710 confocal microscope (Carl Zeiss Microscopy Ltd) and at least 100 cells were imaged and counted per condition. Counting was blinded and at least 3 random fields were imaged. DNA damage and replication stress were quantified by counting cells with >5 53BP1 foci or >5 γH2AX foci and >5 RPA foci, respectively. A specific macro script was used in FIJI/ImageJ for foci quantification (appendix 6). The relevant parameters were determined using the script to quantify each experiment, including: DAPI channel number, foci channel number, and specific prominence. The specific prominence value was determined by testing a range of prominence values. The prominence value which captured none or very few foci in the negative control and an adequately high number of foci in the positive control was selected. The prominence value was kept constant for analysing images from each experimental repeat. Details of primary and secondary antibodies used can be found in tables 2.3 and 2.4, respectively.

2.1.7. Preparation of protein lysates

Cells were scraped into 1 mL of PBS, pelleted, and lysed in 20-60 µL of UTB lysis buffer (9 mol/L Urea, 75 mmol/L Tris-HCl pH 7.5, 0.15 mol/L β-mercaptoethanol). Lysates were sonicated for 30 s 2X with 30 s cooling between before centrifugation at 16,200 x g for 10 min at 4°C. Finally, supernatants were transferred to a 2 mL plastic tube and stored at 20°C.

2.1.8. Western blot assay

Protein concentration of lysates was measured by Nanodrop 1000 (Fisher Scientific), and 20-50 µg of protein were combined with sample buffer (3.3% SDS, 6 mol/L urea, 17 mmol/L Tris-HCl (pH 7.5), 0.07 mol/L β-mercaptoethanol, 0.01% Bromophenol blue) and heated at 100°C for 10 min. 5 µL of dual-colour precision protein ladder (BioRad) were loaded. Samples were electrophoresed in Tris-glycine running buffer (25 mmol/L Tris base, 192 mmol/L glycine, 0.1% (w/v) SDS) on 4-20% Mini-PROTEAN TGX pre-cast gels (BioRad) at 120 V, for 60-90 min. Gels were rinsed with transfer buffer (25 mmol/L Tris base, 150 mmol/L glycine, 20% (v/v) methanol) and then transferred onto 0.4 µm nitrocellulose membranes using a Transblot-Turbo machine (BioRad). The membranes were blocked in Intercept blocking buffer (LI-COR) buffer mixed (1:1) in Tris-Buffered Saline (TBS) (50 mmol/L Tris-HCl pH 7.6, 150 mmol/L NaCl) for 1 h. Membranes were stained with primary antibody (diluted in 1:1 LI-COR buffer: TBS-Tween) overnight at 4°C with shaking. Membranes were washed 3 times, in TBS-Tween for 5 min each time before being incubated with secondary antibody (diluted to 1:10,000 in 1:1 LI-COR buffer: TBS-Tween) for 1-2 h, at room temperature with shaking. The membranes were finally washed 3 times in TBS-Tween and analysed using the Odyssey infrared imaging and detection system. Details of primary and secondary antibodies used can be found in tables 2.3 and 2.4, respectively.

Protein band quantification was performed using ImageStudio Lite software (LI-COR Biosciences). Digital blot images were imported as compressed files. For each sample, the protein of interest signal was normalised to its respective actin signal (Signal_{Protein} / Signal_{Actin}), accounting for loading variations. Relative protein expression was then calculated as the fold change by dividing the normalised value for each experimental condition by the normalised value of the control sample.

2.1.9. RNA extraction and purification

Cells were washed with 2 mL of PBS and then scraped into 1 mL of Trizol (Invitrogen) and stored at -20°C. For RNA extraction, samples were thawed and 200 µL of chloroform was added, samples were vortexed for 15 s and incubated at room temperature for 2 min before centrifugation at 16,200 g for 15 min at 4°C. The supernatant was transferred to a fresh tube and 500 µL of isopropanol was added. The samples were mixed by shaking before centrifugation at 16,200 x g for 10 min at 4°C. The RNA pellet was kept and resuspended in 1 mL 70% ethanol, then vortexed and centrifuged at 7,500 g for 5 min at 4°C. As much supernatant was removed as possible and residual ethanol was left to air dry for approximately 20 min. Once dry, the pellet was resuspended in 60 µL diethylpyrocarbonate (DEPC) water (Thermo Fisher Scientific) and the RNA concentration was measured using the Nanodrop 1000 (Thermo Fisher Scientific). Following this, the samples underwent DNase I treatment to degrade any residual DNA. DNase I (NEB) and DNase I reaction buffer (NEB) were mixed with 10 µg of RNA and then incubated at 37°C for 20 min. The DNase I was then neutralised through adding 1 µL of 0.5 mol/L EDTA before a 10 min incubation at 75°C.

2.1.10. cDNA preparation

A Verso enzyme kit (Thermo Fisher Scientific) was used to carry out reverse transcription of mRNA into cDNA. The reaction master mix consisted of 5X cDNA synthesis buffer, RNA primer, dNTP mix, RT enhancer, verso enzyme, and DEPC water. The RNA sample (2 µg) was combined with the master mix, vortexed and then briefly spun down to ensure even mixing of reagents. The cDNA was then generated through placing the samples in a polymerase chain reaction (PCR) machine (Applied Biosystems) with the following program: 60 min at 42°C, 2 min at 95°C and then 4°C. Samples were stored at -20°C.

2.1.11. Real-time quantitative polymerase chain reaction (RT-qPCR)

For RT-qPCR, cDNA was diluted 1:50 in DEPC-treated water. Master-mixes of the chosen primers (Table 2.6) were then made up with 12.5 µL SYBR green (Applied Biosciences), 2.5 µL forward primer 2.5 µL, reverse primer and 2.5 µL of DEPC water. Then, 5 µL of the diluted cDNA samples were added to 20 µL of the master mixes in a 96 well plate in which three technical replicated for each gene/primer combination were run. The plate was spun down before being analysed using a Step One Real-Time PCR System (Thermo Fisher Scientific) with the following schedule: preparation of 20 s at 50°C and 15 min at 95°C, 40 cycles of 15 s at 95°C, 30 s at 60°C and 30 s at 72°C and finally the melting curve of 15 s at 95°C, 1 min at 60°C, 30 s at 95°C and 15 s at 60°C. The Δ(ΔCT) was used to quantify the fold change of the genes of interest to the endogenous control gene, 18-S. The sequences of all the primers used in RT-qPCR experiments can be found listed in table 2.6.

2.1.12. 3-(4,5-dimethylthiazol-2-yl)-2,5-diphenyl-2H-tetrazolium bromide (MTT) assay

A 5 mg/mL stock solution of MTT was made in PBS and sonicated for 2-3 min, until completely dissolved. The resulting MTT stock solution was then filtered through a 0.22 µm sterilisation filter. The stock was stored at 4°C, protected from light for a maximum of 4 weeks. Cells were plated in 100 µL of cell line-specific media in a 96 well plate and allowed to adhere overnight before being treated. Following treatment, 10 µL of MTT reagent was added to each well and incubated at 37°C for 3 h protected from light. If the treatment involved hypoxia, the MTT incubation was carried out inside the chamber. After 3 h, the MTT-containing media was removed and replaced with 100 µL DMSO per well to solubilise crystals. The plate was then incubated for a further 15-20 min at 37°C protected from light before being read using the MTT programme on the POLARstar Omega plate reader (BMG Labtech), with an absorbance of 570 nm. Blank wells (medium + MTT, no cells) were used to subtract background.

2.1.13. Short interfering RNA (siRNA) transfection

Cells were transfected with siRNA using Lipofectamine RNAiMAX Transfection Reagent (Fischer Scientific) as recommended in the manufacturer's protocol. Specifically, the siRNA was diluted in FBS- and antibiotic-free MEM (OPTI-MEM, Gibco) to a final volume of 250 µL. In a separate tube, the RNAiMAX Transfection reagent was also diluted in FBS- and antibiotic-free MEM to a final volume of 250 µL. Both mixtures were incubated for 5 min, at room temperature. The siRNA mixture was then combined with the transfection reagent mixture and incubated at room temperature, for another 20 min. The siRNA-transfection reagent mixture (500 µL total volume) was added to the plates containing cells, supplemented with 1.5 – 2.5 mL of antibiotic-free, FBS-containing D-MEM. Cells were incubated for 24 hours in standard conditions and then the media was replaced with fresh antibiotic-free, FBS-containing D-MEM. The cells were cultured for another 24 hours before treatment. The siRNA sequences used in experiments, and their specifications, can be found in Table 2.7.

2.1.14. Clonogenic survival assay

A pre-determined number of cells (150 – 500 cells – depending on the plating efficiency of the cell line used) were seeded in each well of a 6-well plate, in triplicate and allowed to adhere for 3 h, in standard tissue culture conditions. Post treatment, the plates were transferred to a standard humidified incubator at 37°C, and 5% CO_2 and colonies were allowed to form for approximately 7-14 days. Cells were then stained with 0.5% (w/v) crystal violet in 50% methanol and 20% ethanol. Colonies comprised of, at least 50 cells were counted using a colony counter. The survival fraction was calculated using the formula: Survival Fraction = [(number of colonies formed after treatment) / (number of cells seeded x plating efficiency)] x 100 plating efficiency = number of colonies obtained in the untreated control / number of cells seeded in the untreated control. The plating efficiency was calculated as: number of colonies obtained / number of cells seeded.

2.1.15. Cell cycle analysis by Flow Cytometry

Following treatment, cells were trypsinised and collected in 1 mL PBS. After collection, cells were washed with PBS and transferred to 15 mL falcons. Centrifugation followed at 500 x g for 5 min and cells were then fixed with 1 mL 70% ethanol added dropwise while vortexing. Samples were placed at -20°C for at least 30 min. Samples were then centrifuged at 250 x g for 5 min and resuspended in 1 mL of 2 mol/L HCl containing 0.1 mg/mL protease inhibitor (Sigma) and incubated at room temperature for 20 min. Samples were then washed once in 2 mL PBS and centrifuged at 350 x g for 5 min and then washed once in 1 mL 2% BSA in PBS and centrifuged at 500 x g for 5 min. Cells were then resuspended in 100 µL of 2% BSA in PBS and were then incubated with the primary antibody diluted 1:100 in 1% BSA in PBS for 90 min at room temperature, followed by the secondary antibody diluted 1:200 in 1% BSA in PBS for 60 min. Finally, the pellets were resuspended in PBS containing Propidium Iodide (PI) (10 µg/mL) and incubated at 37°C for 30 min. Analysis was carried out for 10000 cells per experimental condition using BC CytoFlex flow cytometer (Beckman Coulter). Data were analysed using FlowJo software (FlowJo, LLC, BD Biosciences).

2.1.16. Measurement of Glutathione (GSH) levels using FL1 probe

FL1-GSH probe (figure 2.2) has the ability of increasing its emission of fluorescence, at 485 nm when bound to GSH, thereby enabling the measurement of GSH levels in different conditions. For this assay, 3,000 cells were plated in a flat-bottom 96-well plate and treated after left to adhere. FL1-GSH probe at a concentration of 10 µmol/L was added to the culture media of the treated cells, 2 h before the treatment endpoint. N-ethyl-maleimide (NEM) was used as a negative control at 5 µmol/L for 4 h and N-acetylcysteine (NAC) was used as a positive control, at 6 mmol/L for 4 h. After the end of the treatment, 96-well plates were directly analysed using the fluorescence detection (485 nm) programme of the POLARstar Omega Plate Reader (BMG Labtech).



Figure 2.2. The FL1-GSH probe. The structure and function of the FL1-GSH probe, kindly provided by Dr A. Sedgwick, and used for measurement of GSH in this study, is shown is this figure (Twigger *et al*. 2024).

2.1.17. CellROX Green assay for measurement of Reactive Oxygen Species (ROS)

For the measurement of ROS in different conditions CellROX Green reagent was used. Cell ROX green consists of a proprietary chemical probe structure with the ability to bind DNA or mitochondria, respectively, when oxidised and emitting fluorescence at 488 nm (for CellROX Green). For this assays, 70,000 cells were plated in each chamber of a multi-chamber microscopy slide and allowed to adhere overnight prior to treatment. CellROX Green reagent at 10 µmol/L, was added directly to the culture media of the cells, 30 min before the treatment endpoint. Then, media containing CellROX reagent were discarded, and cell were fixed in 400 µL of 4% w/v PFA. After washing the cells 3 times with ice-cold PBS, the slide chambers were discarded, and cells were stained with DAPI, while coverslips were mounted on each slide. After drying overnight, the samples were analysed using LSM780 confocal microscope (Carl Zeiss Microscopy Ltd) and at least 100 cells were imaged and counted per condition, to determine the mean signal intensity of CellROX Green reagent in each condition. Fluorescence intensities were normalised to cell number and background, and DAPI co-staining was used for segmentation.

2.1.18. Transformation of competent bacterial cells

DH5α competent cells (Invitrogen) were thawed (on ice) for 30 min from -80°C. Next, 1-5 µL of plasmid DNA in mixture with 20-30 µL of competent cells, were added in a microcentrifuge tube. Mixing was accomplished by softly tapping the base of the tube. The mixture of plasmid DNA and competent cells was left to incubate on ice for 20 min. Then, it was subjected to heating at 42°C in a water bath for 45 sec. The tube was once more, placed on ice for a duration of 2 min. Subsequently, 800 µL of SOC media, without antibiotics were added to the tube and placed in a 37°C shaking incubator for 45 min, for incubation. This was followed by plating and spreading 100 µL of the transformation mixture onto 10 cm LB agar plates with the correct antibiotic, then overnight incubation at 37°C, in an upside-down position. Next day, a single colony was picked, with a pipette tip and transferred it to a 15 mL falcon with 5 mL of LB + antibiotic to function as a starter culture. The initial culture was left to incubate in a shaker at 37°C for 8 h. Next, the 5 mL initial culture was transferred into 250 mL of LB with the correct antibiotic in a 500 mL conical flask and left to grow overnight at 37°C on a shaker. The bacterial cultures were subjected to ultra-centrifugation at 6000 x g at 4°C, using ultra-centrifuge tubes. The pellets were either stored at -80°C for an extended period or purified on the same day.

2.1.19. Purification of plasmid DNA

The plasmids used, were purified using the MaxiPrep Plasmid Purification kit from Qiagen. In short, the bacterial pellets were lysed using buffer P1. P2 buffer was added and mixed by inverting forcefully 4-6 times (not vortexed) and then left to incubate at room temperature for 5 minutes. Chilled buffer P3 was combined and stirred vigorously by flipping 4-6 times, then left to incubate on ice for 20 minutes. Next, the blend underwent centrifugation at 20,000 x g for 30 minutes at 4°C. The resulting supernatant was rapidly gathered, blended, and centrifuged again at 20,000 x g for 15 minutes at 4°C. The ensuing supernatant was immediately introduced to a QIAGEN-tip 500 pre-treated with buffer QBT, allowing the column to empty naturally. The QIAGEN-tip was

rinsed two times using buffer QC. Buffer QF was used to elute the DNA, then RT isopropanol was added to precipitate it. The mixture was centrifuged at 15,000 x g for 30 minutes at 4°C. Afterwards, the pellet was washed with RT 70% ethanol and centrifuged again at 15,000 x g for 10 minutes at 4°C. Finally, the pellet was air-dried at RT before being resuspended in Tris-EDTA (TE) buffer or DEPC-treated water.

2.1.20. Plasmid DNA transfection

Lipofectamine 2000 (Invitrogen) transfection reagent, was used to transfect cells with plasmid DNA. In short, cells were plated when they reached 70-80% confluency and were then allowed to adhere overnight on a 6 cm dish. The next day, a mixture of 250 µL of serum-free media mixed with 12.5 µL of lipofectamine 2000 and a second mixture of 2 µg of plasmid DNA in 150 µL of serum-free media, were combined and vortexed for 10 seconds in a microcentrifuge tube and then centrifuged. Then, they were allowed to incubate for 5 min. The lipofectamine 2000-DNA mixture was then directly added onto the adherent cells, complemented by 2 mL of standard growth media. Media were changed after 24 h and the transfected cells were visualised and analysed for transfection efficiency.

2.1.21. Irradiation using a Caesium-source Irradiator

Cells were exposed to Caesium (Cs) radiation at a specified dose (Gy) using a Gamma-Service Medical GmbHGSR D1 irradiator, delivering a rate of 1.5 Gy/min. Radiation boxes were used to irradiate cells under hypoxic conditions. These boxes possess airtight seals and thus do not allow changes in oxygen tensions to which the cells are exposed, during transport out of the hypoxia chambers and during irradiation. The above-described radiation boxes have been previously used and validated, to deliver radiation whilst maintaining hypoxic conditions (Anbalagan *et al*. 2015).

2.1.22. IC_{50} calculation

Dose-response data, expressed as percentage of inhibition relative to positive (untreated) and negative (background) controls, were analyzed using GraphPad Prism v.8.0.0 (GraphPad Software, San Diego, CA). Inhibitor concentrations (logarithmically spaced across ≥8 doses, tested in triplicate) were transformed to $\log_{10}$ values within Prism. A four-parameter logistic nonlinear regression model [log(inhibitor) *vs*. response – Variable slope] was fitted to the normalised data, using the equation: *Y = Bottom + (Top – Bottom) / (1 + 10^{((LogIC$_{50}$ – X) × HillSlope)})*,where *Y* = response, *X* = $\log_{10}$(concentration), *Top* and *Bottom* = asymptotic plateaus (constrained to 100% and 0% unless data indicated otherwise), and *HillSlope* = curve steepness. When full inhibition (≥50%) was not achieved experimentally, Prism still calculated an IC_{50} by mathematically extrapolating the fitted curve beyond the tested concentration range to identify the theoretical concentration achieving 50% inhibition, based on the constrained *Top* plateau (100%) and the curve's fitted slope. Importantly, such extrapolated IC_{50} values were interpreted with caution as they represent estimates rather than experimentally observed values and were explicitly noted in reporting. Model adequacy was validated by R^2 > 0.90 and residual distribution analysis. IC_{50} values (the concentration yielding 50% inhibition) and their 95% confidence intervals were directly computed by Prism from the fitted curve parameters. Results were excluded if confidence intervals exceeded one order of magnitude, Hill slopes fell outside the expected range (−0.5 to −1.5), or if significant extrapolation was required without biological justification.

2.2. Bioinformatic methods

2.2.1. Analysis of mRNA levels in patient samples from publicly available datasets

Publicly available normal sample omics data from GTEx were accessed and downloaded from the GTEx portal (www.gtexportal.org). Publicly available patient sample omics data from The Cancer Genome Atlas (TCGA) (Cancer Genome Atlas Research *et al*. 2013) and the Molecular Taxonomy of Breast Cancer International Consortium (METABRIC) (Curtis *et al*. 2012) studies, were accessed and downloaded from cBioportal (www.cbioportal.org). The data was used to analyse mRNA levels of specific genes, in different patient groups according to tumour type/subtype, stage of disease, receptor status, patient's vital status. Raw counts were normalised to transcripts per million (TPM) and $\log_2$-transformed prior to analysis. Patients were stratified into quartiles based on mRNA expression of each gene. In primary analyses, we compared the highest quartile (Q4 - *high*) against the combined lower three quartiles (Q1–Q3 - *low*), to contrast extreme overexpression with the broader cohort, enhancing detection of threshold effects and statistical power in large, heterogeneous datasets (Haller *et al*. 2019; Heffernan *et al*. 2014; Ingebriktsen *et al*. 2022; Pothuri *et al*. 2024; Scott *et al*. 2018). For subtype-specific or other filtered analyses with smaller number of events (*n*), we compared Q1 *vs*. Q4 or employed an upper-quartile split when either arm contained $n \leq 50$ patients (Curtis *et al*. 2012; Ingebriktsen *et al*. 2022; Omar *et al*. 2024)..

Kaplan–Meier curves for percent overall survival (%OS) and progression-free survival (%PFS) (for TCGA) or %OS and percent relapse-free survival (%RFS) (for METABRIC) were generated in R 4.2.0 using the survival (v3.3-1) and survminer (v0.4.9) packages. Graphs were plotted using GraphPad PRISM (v8.0.0). Patients were censored at last follow-up if no event occurred. A two sided log-rank test (Mentel-Cox) was used to determine statistical significance (*p* values) and HR – high *vs*. low (B/A) – both reported (Kaplan and and Meier 1958). Benjamini–Hochberg correction across

all quartile comparisons (α = 0.05) to control the false discovery rate (FDR). Together, these strategies allow for the robust identification of survival associations while accounting for cohort-specific data distributions and statistical constraints (Cortes-Ibanez *et al.* 2023; Kaplan and and Meier 1958; Kumar *et al.* 2023).

For neoadjuvant chemotherapy response analysis, pre-treatment tumour biopsies (GEO accession *GSE163882*) provided *RIMKLA* TPM values. We compared patients achieving pathological complete response (pCR) *versus* those with residual disease (RD) using the Wilcoxon rank-sum test on raw TPM values; data were $\log_2$-transformed for visualisation.

2.2.2. Hypoxia signature correlation analyses

Transcriptomic data from TCGA and METABRIC datasets was accessed through www.cbioportal.org. The raw mRNA expression values of the top-15 genes within three clinically validated hypoxia-associated signatures, known as the hypoxia metagene, (Buffa, *et al*., 2010), the pimonidazole-specific signature (Ragnum, *et al*., 2015) and the Winter signature (Winter, *et al*. 2007) in addition to the mRNA levels of genes of interest, were downloaded from each dataset. First, the median expression of each of the top-15 genes was calculated across all samples of each dataset. The expression of each gene in each sample was then normalised over the median expression of that same gene in the whole dataset. Then, the median of each of the top-15 normalised gene mRNA values within a given sample was calculated and the log10 value of this was taken. This log10 values ("hypoxia score") are then plotted against the respective log10 values of each of the studied genes, which were calculated in the same manner. A Pearson coefficient (Pearson R) was used to determine the strength of the correlation, and a log-rank test was applied to determine the statistical significance.

Principal component analysis (PCA) was performed using ClustVis (Metsalu and Vilo 2015) to evaluate the dimensionality and variance captured by both the full and reduced (top-15 gene) versions of the Buffa and Ragnum hypoxia gene signatures**.** Expression matrices were generated

for each signature using TCGA-BRCA transcriptomic data, and variance explained by the first two principal components (PC1 and PC2) served as a metric for assessing information retention. The top-15 gene subsets were selected based on published rankings and evaluated to determine whether reduced gene sets maintained the overall expression structure of the full signatures (appendix 4). In parallel, pathway enrichment analysis was conducted using Enrichr to compare the functional coherence of the full and reduced gene sets and observed preservation of key biological processes (Chen *et al*. 2013b; Kuleshov *et al*. 2016; Xie *et al*. 2021)(appendix 4).

The top-15 genes from the hypoxia metagene (Buffa *et al*. 2010) were selected for correlation analyses because this subset represents the most consistently co-expressed and prognostically informative genes across multiple tumour datasets, as determined by the $\pi\hat{C}$ connectivity score. This reduced panel has been independently validated in several cancer types (e.g., breast, HNSCC, HCC) and is widely used in the literature for hypoxia scoring, known as "reduced hypoxia metagene" or "reduced Buffa signature." (Buffa *et al*. 2010; Zeng *et al*. 2022; Zhang *et al*. 2020; Zhang *et al*. 2021). Using this compact, well-characterised subset reduces noise, simplifies interpretation, and enhances comparability with previous studies.

To validate the robustness of using the top-15 genes from both the hypoxia metagene and the pimonidazole signature for correlation analyses, we performed enrichment analysis and observed preservation of key biological processes (Appendix 4). Correlation patterns of these genes with the full gene sets, were reproducible across independent datasets. PCA performed on both the full 51-gene Buffa hypoxia signature and a reduced top-15 gene subset revealed that the top-15 gene set preserved and even improved variance capture in the first two principal components (PC1+PC2 = 64.6%) compared to the full signature (PC1+PC2 = 60.4%) (Appendix 4). This indicates that the top-ranked genes maintain the core expression structure and may serve as a robust proxy for the full signature in correlation-based analyses. PCA analysis of the Ragnum hypoxia gene signature showed that a top-15 gene subset explained more total variance in sample expression patterns than the full gene set (69.3% *vs*. 54.4% for PC1+PC2) (Appendix 4).

This suggests that the top-15 genes are highly co-expressed and represent the most informative component of the signature. The increase in both PC1 and especially PC2 indicates that the reduced gene set retains - and may even enhance - biological structure and discriminatory power, supporting its use in downstream correlation and classification analyses.

2.3. Statistical analyses

Statistical analyses were carried out by GraphPad Prism software, version 8.0. Specifically, unless otherwise stated, a two-way ANOVA test or Student-t test (two-tailed) were applied to determine significance in situations where more than two means were affected by more than one independent factor, and a one-way ANOVA in cases where means were affected by only one factor. Error bars represent mean ± standard deviation (SD). Statistical significance was assumed if $p<0.05$, with the following significance indicators used: * $p<0.05$, ** $p<0.01$, *** $p<0.001$, **** $p<0.0001$.

The *n* number stated in each experiment (figure legend), defines the number of independent biological repeats (e.g., n = 3, indicate 3 independent biological repeats, with at least 3 technical replicates). Where *n = 3*, statistical analyses are carried out, designated by *n* and the *p* value indicators described above. Error bars represent ±SD from the biological repeats. Where *n = 1*, statistical analyses are not carried out, designated by *n* and absence of significance indicators and error bars represent ±SD from averages of the technical replicates. Where *n = 2*, statistical analyses are not carried out, designated by *n* and absence of significance indicators and error bars represent ±SD from averages of the 2 independent biological repeats.

In cases of multiple testing, we controlled the error rate by Benjamini-Hochberg correction ($\alpha adj = 0.05/$no. of tests) using MS Excel v.2505, and the false discovery rate (FDR) using the Benjamini–Hochberg procedure at $q < 0.05$. In such instances adjusted *p* values are reported.

2.4. Materials

2.4.1. Cell lines

Cell lines used in experiments are listed below (table 2.1).

Table 2.1. Cell lines used in this study. Listed below are cell lines, tissue type, culture media and their origin.

Cell line	Type of tissue	Culture media	Origin
CAL-51	Human breast adenocarcinoma	D-MEM, 10% FBS	Prof. M. Tarsounas
MDA-MB-231	Human breast adenocarcinoma	D-MEM, 10% FBS	Dr A. Coutts
MCF-7	Human breast adenocarcinoma	D-MEM, 10% FBS	Prof. K. Ramadan
BT-549	Human breast adenocarcinoma	RPMI, 10% FBS	Prof. K. Vallis
T47D	Human breast adenocarcinoma	D-MEM, 10% FBS	Prof. K. Vallis
RKO$^{HIF1+/+}$	Human colorectal adenocarcinoma	D-MEM, 10% FBS	Dr D. Chan
RKO$^{HIF1\alpha-/-}$	Human colorectal adenocarcinoma	D-MEM, 10% FBS	Dr D. Chan
RCC4$^{VHL+/+}$	Human renal clear cell carcinoma	D-MEM, 10% FBS	Prof. P. Ratcliffe
RCC4$^{VHL-/-}$	Human renal clear cell carcinoma	D-MEM, 10% FBS	Prof. P. Ratcliffe
786-O	Human renal adenocarcinoma	D-MEM, 10% FBS	Prof. V. Macaulay

2.4.2. Solutions, buffers, and cell culture reagents

Listed below are the solutions, buffers, and cell culture reagents (table 2.2).

Table 2.2. List of solutions, buffers, and cell culture reagents. The names and origin of solutions buffers and cell culture reagents.

Name	Origin
β-mercaptoethanol	Fisher Scientific
Blocking Buffer	LI-COR
Bromodeoxyuridine (BrdU)	Millipore
Dulbecco's modified Eagle's medium (D-MEM)	Sigma-Aldrich, Gibco
Diethyl pyrocarbonate water (DEPC water)	Fisher Scientific
Dimethylsulphoxide (DMSO)	Fisher Scientific
DL-Dithiothreitol (DTT)	Sigma Aldrich
Ethanol	Fisher Scientific
Fetal bovine serum (FBS)	Gibco
Formaldehyde	Sigma-Aldrich
Gel Loading Buffer	Fisher Scientific
Glycerol	Fisher Scientific
Glycine	Sigma-Aldrich
Hydrochloride acid (HCl)	Sigma-Aldrich
Methanol	Fisher Scientific
Phalloidin	Invitrogen
Phosphate buffer saline (PBS)	Fisher Scientific
ProLong® Gold 4',6-diamidino-2-phenylinodole (DAPI)	Invitrogen/ Life Technologies
Propidium iodide (PI)	Sigma-Aldrich
Protease inhibitor	Roche
RNAse A (ribonuclease A)	Sigma-Aldrich
Roswell Park Memorial Institute (RPMI)	Sigma-Aldrich

Sodium dodecyl sulphate (SDS)	Fisher Scientific
Hydrochloric acid 36% w/v (HCl)	Sigma-Aldrich
SYBR® Green	Applied Biosystems
Tris-Base	Sigma-Aldrich
Triton-X-100	Fisher Scientific
TRIzol®	Invitrogen/ Life Technologies
Trypan blue	Invitrogen
Trypsin 0.05% EDTA	Sigma-Aldrich
Tween 20	Fisher Scientific
Urea	Fisher Scientific

2.4.3. Drugs and chemicals

Drugs and chemicals used, are listed below (table 2.3).

Table 2.3. Drugs and Chemicals. Listed below are drugs and chemicals used in experiments, as well as their abbreviations, their stock concentrations, and their sources of origin.

Drug / Chemical	Concentration	Origin
Hydroxyurea (Hu)	1 mol/L	Sigma Aldrich
Etoposide (ETP)	25 mmol/L	Sigma Aldrich
Neocarzinostatin (NCS)	200 ng/µL	Sigma Aldrich
Olaparib (Opal)	1-10 µmol/L	Calbiochem
ART555	1-10 µmol/L	From Prof. G. Higgins
N-acetylcysteine (NAC)	6-20 mmol/L	Sigma Aldrich
N-ethylmaleimide	5 µmol/L	Promega
Hydrogen Peroxide (H_2O_2)	5 mmol/L	Merck
Desferrioxamine (DFO)	100 µmol/L	Sigma Aldrich
Dimethyloxalylglycine (DMOG)	50 µmol/L	Sigma Aldrich
Cobalt Chloride ($CoCl_2$)	150 µmol/L	Merck
F1- GSH probe	10 µmol/L	From Dr A. Sedgwick

CellROX green	10 µmol/L	Invitrogen

2.4.4. Primary Antibodies

Primary antibodies used are listed in table 2.4, below.

Table 2.4. List of Primary antibodies and related information.

Name	Species	Dilution	Manufacturer	Catalogue No.	Application
β-actin	mouse	1:10000	Santa Cruz	sc-69879	WB
HIF-1α	mouse	1:500	BD Biosciences	610958	WB
53BP1	rabbit	1:250	Novus Biologicals	NB100-904	IF
H2AX-S139	mouse	1:500	Millipore	05-636	WB, IF
GRP78	mouse	1:2000	BD Biosciences	610978	WB
RPA (4E4)	rat	1:500	Cell Signaling	2208	WB, IF
p53-DO1	mouse	1:2000	Santa Cruz	sc-126	WB
RIMKLA	rabbit	1:1000-1:100	Fisher Scientific	PA5-101852	WB, IF

H3	rabbit	1:1000	Abcam	ab1791	WB
H3-S10	mouse	1:1000	Cell Signaling	9701	WB
BrDU	mouse	1:50	BD Biosciences	347580	FACS
RAD51	rabbit	1:2000	Dr A. Blackford	-	WB
VHL	rabbit	1:500	Cell Signaling	68547	WB
PPFIA4	mouse	1:1000	Abnova	H00008497-M10	WB
HIF-2α	rabbit	1:500	Novus Biologicals	NB100-122	WB
Fibrillarin	mouse	1:100	Abcam	ab-4566	IF
NFκ-β-Ser536	rabbit	1:1000	Cell Signaling	3031	WB
NFκ-β	rabbit	1:1000	Abcam	ab16502	WB
p38	rabbit	1:1000	Cell Signaling	9212	WB
p38-Thr180/Tyr182	rabbit	1:1000	Cell Signaling	9211	WB

Caspase 3	rabbit	1:500	Cell Signaling	9661	WB

2.4.5. Secondary Antibodies

The list of Secondary antibodies used is given in table 2.5.

Table 2.5. List of Secondary antibodies used and related information.

Name	Species	Dillution	Manufacturer	Catalogue No.	Application
Alexa Fluor 680 goat rabbit IgG (H+L)	rabbit	1:200	Invitrogen	A21076	IF
Alexa Fluor 488 goat mouse	mouse	1:200	Invitrogen	A11017	IF
Alexa Fluor 488 goat rabbit	rabbit	1:200	Invitrogen	A11072	IF
Alexa Fluor 594 goat mouse	mouse	1:200	Invitrogen	A11020	IF
Alexa Fluor 594 goat rabbit	rabbit	1:250	Invitrogen	A11007	IF
IRDye 680 goat mouse	mouse	1:10000	Li-COR	926-68073	WB
IRDye 800 goat mouse	mouse	1:10000	Li-COR	926-32212	WB
Alexa Fluor® 680 goat anti-rat IgG (H+L)	rat	1:10000	Invitrogen	A21096	WB, IF

2.4.6. Primers

The primers used in RT-qPCR analyses are listed below (table 2.6).

Table 2.6. List of primers used and related information.

Gene	Forward/ Reverse Sequence	Sequence	Working concentration	Manufacturer
18S	*18S*-F	TAGAGGGACAAGTGGCGTTC	10 µmol/L	Sigma Aldrich
	18S-R	CGGACATCTAAGGGCATCAC		
RIMKLA	*RIMKLA*-F	GGTAGGGGGCCAGGTCATAG	100 µmol/L	Sigma Aldrich
	RIMKLA-R	GAGTCAGTGCCTTAGCGTCA		
RIMKLB	*RIMKLB*-F	CATTGTTGTGGGAGGTCGTGT	100 µmol/L	Sigma Aldrich
	RIMKLB-R	GATAGCCAGCTGCTTTCCTTG		

2.4.7. siRNA sequences

Below (table 2.7.) are listed the sequences of the siRNAs used in this study.

Table 2.7. siRNA sequences. List of targets, sequences and manufacturers of siRNAs used in this study.

siRNA target name	Type	Sequence(s)	Manufacturer
RIMKLA	Smart pool	GUCCAAGGGAGAAGAACGA	Horizon Ltd
		UCAACAAAUUCUGGACGUU	
		UGUGUGAGGCAAAUGCUAA	
		GAACCUGGCUACAACAUUA	
RIMKLA	Single sequence		Fischer Scientific
Non-template control (Scramble)	Smart pool	UGGUUUACAUGUCGACUAA	Horizon Ltd
		UGGUUUACAUGUUGUGUGA	
		UGGUUUACAUGUUUUCUGA	
		UGGUUUACAUGUUUUCCUA	

2.4.8. Plasmids

Below (table 2.8.) are the plasmids used for ROS quantification and localisation, in this study.

Table 2.8. Plasmids. Name and origin of plasmids used to transfect mammalian cells in our study.

Plasmid name	Manufacturer	Catalogue No.
pHyPer-Nuc	Evrogen	FP944
pHyPer-dMito	Evrogen	FP942

Chapter 3 The impact of hypoxia on the effect of DDR inhibitors in breast cancer cells

3.1. Introduction

The use of DDRi for the treatment of various malignancies, either alone or in combination with other anticancer therapies, has been a prominent area of cancer research for the last decade (Brandsma *et al.* 2017; Javed *et al.* 2024; Nicum *et al.* 2024; Saha *et al.* 2022). A specific focus remains the impact of TME and its features, on the effects of DDRi.

Hypoxia elicits a unique biological response in cancer cells therefore we aimed to characterise the impact of this response on the effects of two DDRi: PARPi and PolQi, using a breast cancer *in vitro* model. It has been shown from previous work, that the hypoxic TME is a heterogenous one. Different tumour cells simultaneously experience different oxygen levels, depending on their relative location in the tumour, in terms of their proximity to vasculature, as well as the functional quality of vessels nearby (Ge *et al.* 2022; Zhang *et al.* 2023). For this reason, we carried out our experiments testing different oxygen levels.

In this part of our work, we aimed to test the relationship between hypoxia and the response to PARPi, a well-established DDRi with high clinical significance and a newer, less characterised PolQi agent, ART558. We asked how their activity is impacted by conditions that mimic the hypoxic tumour microenvironment, while additionally characterising previously described, hypoxia-induced changes in biological processes known to affect the response to many anticancer treatments (Bannik *et al.* 2021; Saha *et al.* 2022; Sahgal *et al.* 2023; Zeman and Cimprich 2014). We decided to carry out our work using mainly triple-negative breast cancer (TNBC) *in vitro* models, considering the previously described hypoxic nature of this breast cancer subtype (Bernardi and Gianni 2014; Srivastava *et al.* 2023; Zheng *et al.* 2020).

3.2. Results

3.2.1. Oxygen-dependent changes in cell cycle

First, we investigated changes in cell cycle that occur in response to treatment with different levels of oxygen. CAL-51 (TNBC) cells were exposed to different oxygen levels and co-stained with BrDU – a thymidine analogue commonly used for analysis of DNA synthesis and PI, a dye which binds to DNA and can be used quantify it, enabling the analysis of cell cycle phases (Cecchini *et al*. 2012). Exposure to radiobiological hypoxia (<0.1% O_2) caused a halt in progression of cell cycle from G1- to S-phase with a concomitant arrest of DNA synthesis (figure 3.1). This has been previously observed in relevant studies (Hammond *et al*. 2002; Pires *et al*. 2010). In contrast, treatment with 2% O_2 did not appear to cause changes in cell cycle, compared to normoxic conditions (21% O_2). Finally, cyclic hypoxia resulted in a statistically significant G1-phase arrest and an S-phase fraction enrichment in agreement with previous reports (Bader *et al*. 2021), suggesting that despite ongoing DNA synthesis either cells were rendered unable to proceed to G2-phase or a prolongation of S-phase of the cell cycle occurred (figure 3.1., A and B).

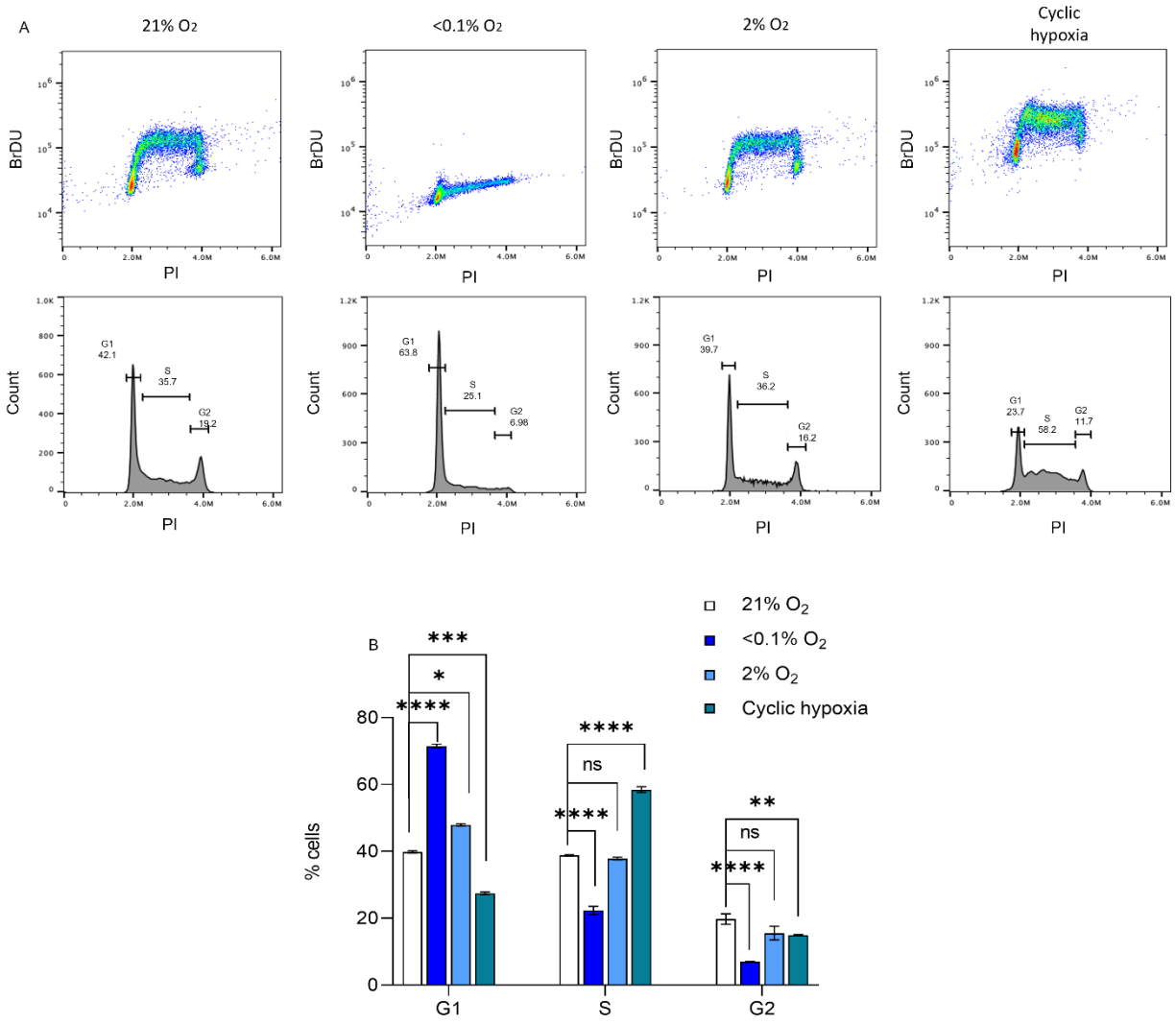

Figure 3.1. Oxygen-dependent changes in cell cycle. CAL-51 cells were exposed to the indicated treatments for 16 h, (A) Representative FACS images from BrDU and PI-stained CAL-51 cells. (B) Quantification of cell count in each phase of the cell cycle from part A. n = 3.

3.2.2. The mitotic cell population changes in response to different hypoxia treatments

We then investigated the oxygen-dependency of the mitotic fraction, using a pool of unsynchronised cells. To do so, we exposed two TNBC cell lines to different oxygen levels and protein samples were analysed for H3-Ser10, a well-known mitotic marker (Gurley *et al.* 1978; Hans and Dimitrov 2001). As expected from our previously described cell cycle analysis data, we observed a statistically significant decrease of H3-Ser10 protein levels in CAL-51 cells treated

with <0.1% O_2 and with cyclic hypoxia (figure 3.2, A, B). Using MDA-MB-231 cells we found a decrease in H3-Ser10 protein levels in response to all hypoxia treatments, with a significant decrease seen in cells exposed to <0.1% O_2 and cyclic hypoxia (figure 3.2, C and D).

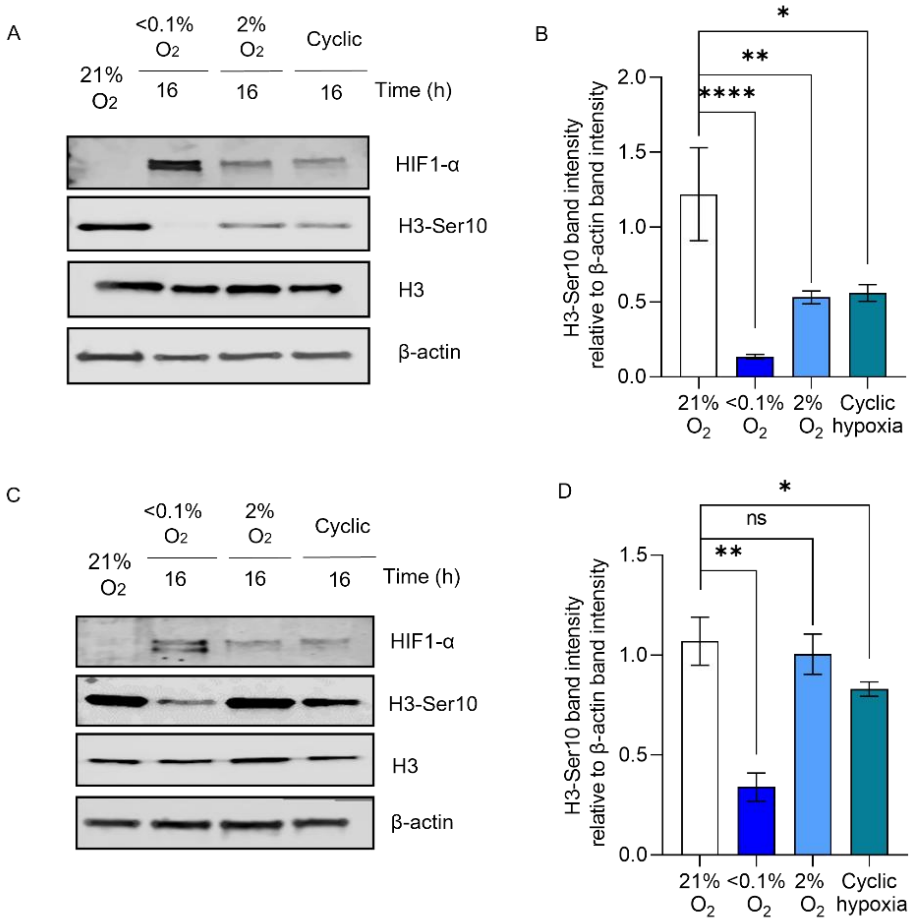

Figure 3.2. The mitotic population changes in response to different hypoxia treatments. (A) CAL-51 cells were exposed to the indicated hypoxia treatments for 16 h. Samples were analysed by western blot assay for H3-Ser10 protein levels. Total H3 and β-actin are used as controls. (B) Quantification of H3-ser10 protein level changes in CAL-51 cells from part B. n = 3. (C) MDA-MB-231 cells were exposed to the indicated hypoxia treatments for 16 h. Samples were analysed by western blot assay for H3-Ser10 protein levels. (D) Quantification of H3-ser10 protein level changes in MDA-MB-231 cells from part C. n = 2. Total H3 and β-actin are used as controls.

3.2.3. Viability response to hypoxia

After investigating the oxygen-dependency of the cell cycle and considering the changes which we observed, we asked how might cell viability be affected upon exposure to different oxygen levels. Colony survival assays with CAL-51 (TNBC) cells treated with different types of hypoxia, showed no significant change in cell viability (figure 3.3, A, B). Interestingly, even though treatment with <0.1% O_2 decreased the mitotic cell fraction, as reported previously (figure 3.2, A, B) there was no change in the cell viability. Using some additional breast cancer cell lines to validate these findings, specifically MDA-MB-231 (TNBC) and MCF-7 (Luminal A), we found that cell viability did not significantly change in response to any of the oxygen levels tested, compared to 21% O_2 (figure 3.3, C and D).

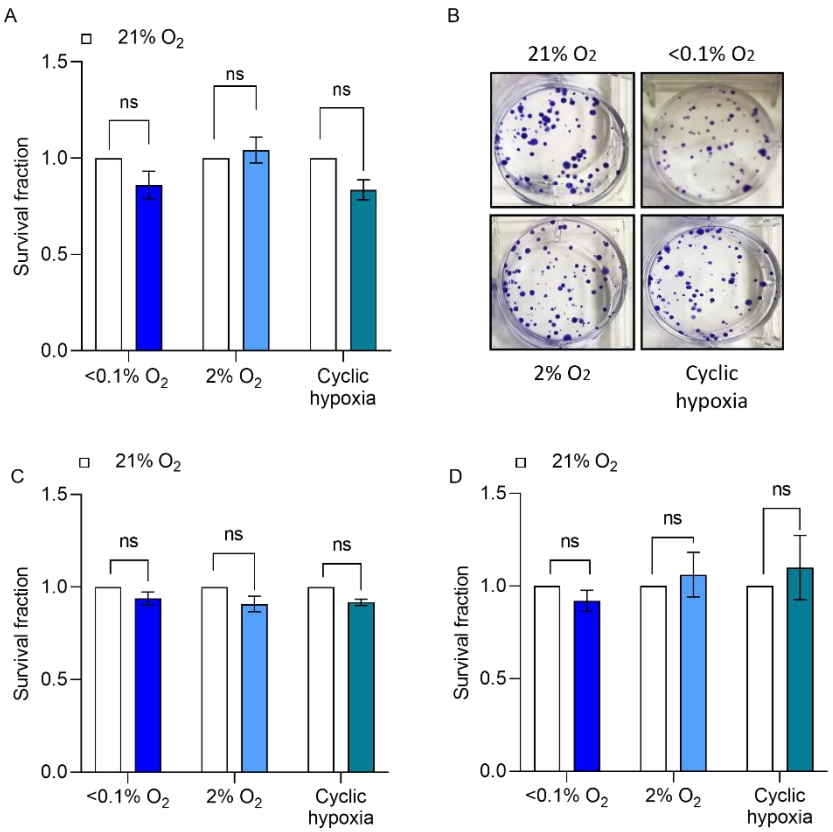

Figure 3.3. Exposure to hypoxia did not impact cell viability. (A) CAL-51 cells were exposed to the indicated hypoxia treatments for 16 h. Cell viability was quantified normalised to non-treated control. n = 3. (B) Representative images of clonogenic assay in part A. (C) MDA-MB-231 cells were exposed to the indicated hypoxia treatments for 16 h. Cell viability was quantified normalised to non-treated control. n = 3. (D) MCF-7 cells were exposed to the indicated hypoxia treatments for 16 h. Cell viability was quantified normalised to non-treated control. n = 3.

3.2.4. Hypoxia does not induce detectable DNA damage in breast cancer cells

Next, we investigated the oxygen-dependency of DNA damage. For that purpose, cells exposed to different hypoxia levels were analysed by immunofluorescence assay for the DNA damage marker, 53BP1. This DNA repair protein localises on areas of DNA double strand breaks, to initiate their repair cascade. The formation of 53BP1 foci, can thus be observed on sites of DNA damage and these foci can be fluorescently labelled and quantified (Djuzenova *et al*. 2015; Panier and Boulton 2014). As expected, compared to cells treated with the potent DNA-damaging agent, Neocarzinostatin (Schonlau *et al*. 1997; Tanoue *et al*. 1998), no detectable DNA damage was observed in cells exposed to <0.1% or 2% O_2, *via* 53BP1 foci immunofluorescence analysis, but surprisingly neither in cells exposed to cyclic hypoxic conditions, despite previous reports (Bader *et al*. 2021)(figure 3.4, A, B). Another marker of several cellular stresses, including DNA damage and replication stress, γH2AX, was used to further analyse the oxygen-dependency of DNA damage and replication stress: foci formation of the phosphorylated histone H2AX in the gamma position (γH2AX) can be observed under such conditions (Djuzenova *et al*. 2015; Kuo and Yang 2008). Immunofluorescence analysis of γH2AX foci in CAL-51 cells treated with different oxygen levels showed a pan-nuclear increase of γH2AX, in the absence of distinct foci upon treatment with <0.1% O_2 – a phenomenon that has been previously reported in specific levels of oxygen (Olcina *et al*. 2013), and previously associated to DNA replication stress (Gagou *et al*. 2010; Parsels *et al*. 2018), with approximately 40% of the total cell population corresponding to this phenotype (figure 3.4, A, D). Exposure to 2% O_2 and cyclic hypoxia did not increase levels of γH2AX or lead to formation of distinct foci. Of note, some levels of endogenous damage and replication stress, were repeatedly observed in untreated normoxic controls (figure 3.4, A, C).

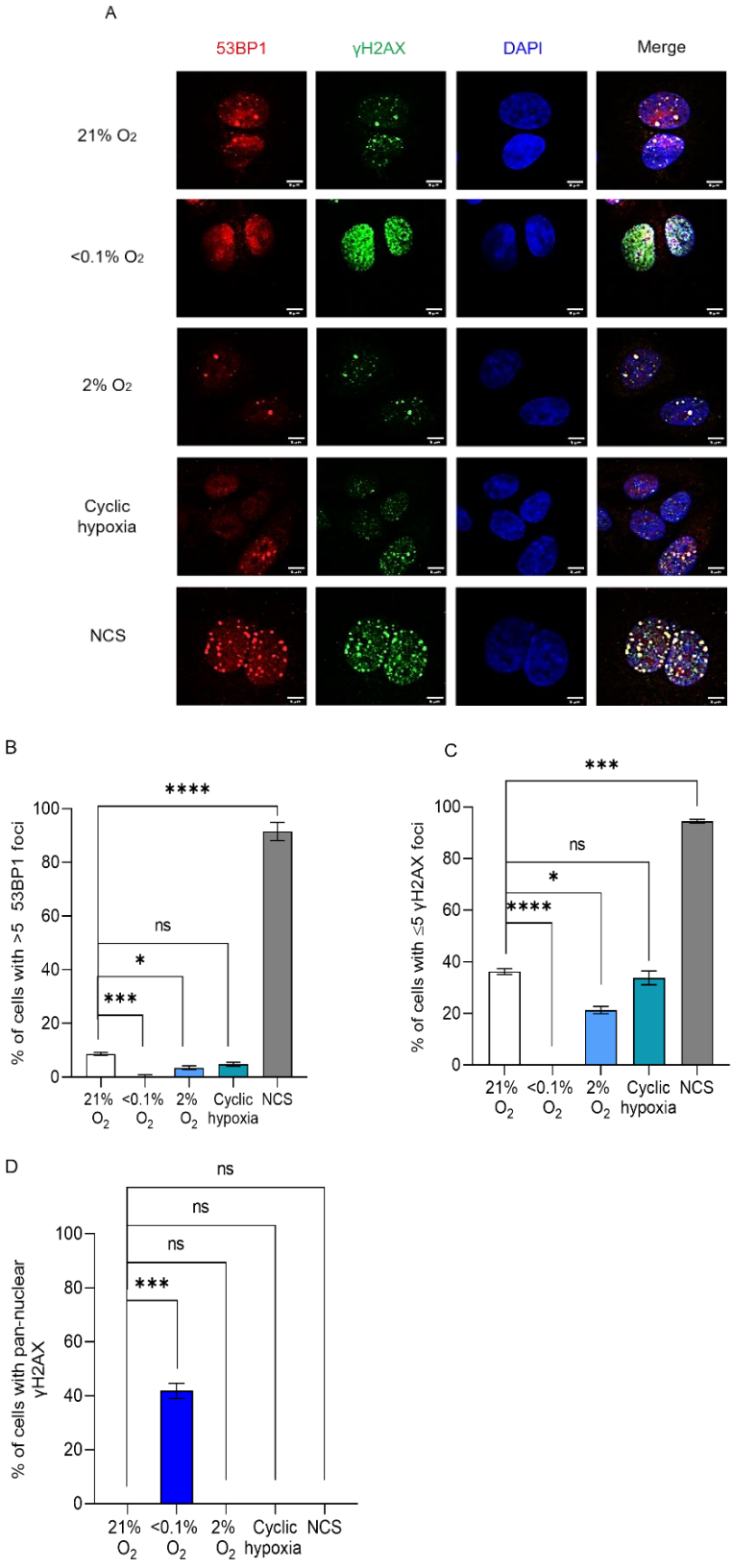

Figure 3.4. Hypoxia does not induce detectable DNA damage. CAL-51 cells were exposed to the indicated treatments for 16 h (A) Representative microscopy images of 53BP1 (red) and γH2AX (green) colocalised foci with DAPI (blue). Scale bar = 5 μm. (B) Quantification of 53BP1 and (C) of γH2AX foci, in CAL-51 cells. NCS = Neocarzinostatin, 200 ng/μL for 6 h. n = 3. (D) Quantification of cells with pan-nuclear γH2AX in cells exposed to hypoxia. n = 3.

3.2.5. Specific hypoxic conditions induce replication stress

Taking note of several previous studies reporting findings on hypoxia-induced replication stress (Hammond *et al*. 2014; Ma *et al*. 2023; Olcina *et al*. 2013; Wouters and Koritzinsky 2008), we wanted to investigate the oxygen-dependency of this phenomenon. The phosphorylation of RPA is a golden standard method for quantitative analysis of replication stress levels (Vassin *et al*. 2009), hence protein samples of cells treated with different oxygen levels were analysed for total and phosphorylated RPA protein levels by western blot assay. As shown in the western blots of figure 3.5, CAL-51 cells (figure 3.5, A) and MDA-MB-231 cells (figure 3.5, B) increase their phosphorylated RPA protein levels, only upon exposure to radiobiological hypoxia (<0.1% O_2). For this experiment we used radiobiological hypoxia (<0.1% O_2) as a positive control of replication stress, as it has been previously shown to induce such conditions (Foskolou *et al*. 2016; Foskolou *et al*. 2017). Furthermore, the same protein samples were analysed for the levels of the cellular stress sensor protein, p53. Significant stabilisation of p53 was seen using p53 wild-type CAL-51 cells, only in radiobiological hypoxic conditions (<0.1% O_2) (figure 3.5, A).

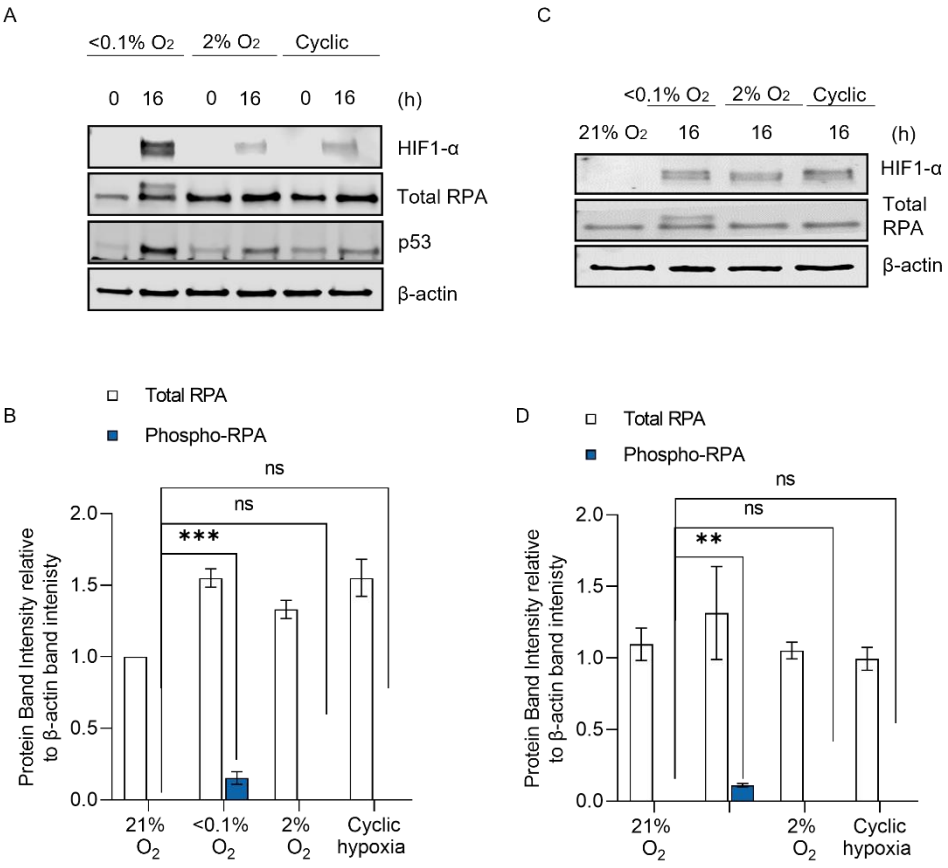

Figure 3.5. Hypoxia (<0.1% O_2) induces replication stress. CAL-51 and MDA-MB-231 cells were exposed to the indicated treatments for 16 h (A) Western blot analysis of total (lower band) and phosphorylated (upper band) RPA and p53 levels in CAL-51 cells. (B) Quantification of total and phosphorylated RPA levels from part A, as band intensity over β-actin, normalised to 21% O_2. n = 3. (C) Western blot analysis of total (lower band) and phosphorylated (upper band) RPA in MDA-MB-231 cells. β-actin used as a loading control and HIF1-α as a hypoxia control. (D) Quantification of total and phosphorylated RPA levels from part C, as band intensity over β-actin, normalised to 21% O_2. n = 3.

In addition, we wanted to further analyse the oxygen-dependency of replication stress, with a higher-resolution assay to confirm our above described western blot data, considering the significant impact of replication stress levels on the response to DDRi, which has been the focus of several studies in this research field (Abel *et al.* 2023; Durinikova *et al.* 2022; Lappin *et al.* 2022; O'Connor and Forment 2023). To be more thorough, we decided to add a second control for DNA replication stress for this assay, by treating cells with Hydroxyurea (Hu), a well-established inhibitor of the enzyme Ribonucleotide reductase (RNR), commonly used to induce detectable replication stress. We carried out immunofluorescence analysis of RPA foci, in cells treated with different oxygen levels, comparing to normoxic and hydroxyurea-treated controls. Upon phosphorylation, RPA forms distinct foci on regions of ssDNA, indicative of replication stress (Okamoto *et al.* 2018). Using two TNBC cell lines we observed formation of distinct RPA foci only in cells exposed to radiobiological hypoxia (<0.1% O_2), while treatment with 2% O_2 or cyclic hypoxia did not result in the formation of RPA foci (figure 3.6, A, B).

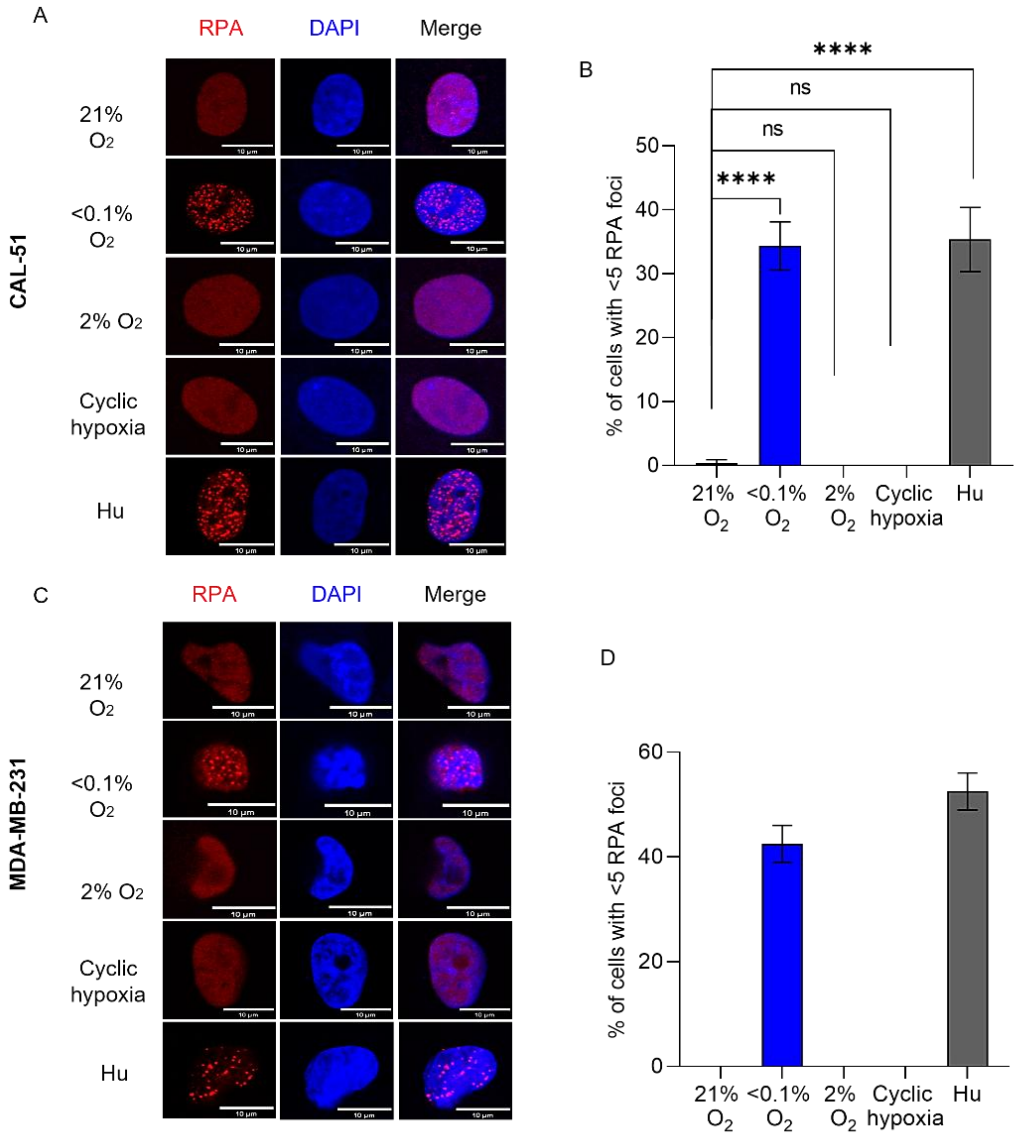

Figure 3.6. Hypoxia (<0.1% O_2) induces RPA foci. CAL-51 and MDA-MB-231 cells were exposed to the indicated hypoxia treatments for 16 h (A) Immunofluorescence analysis of RPA foci (red) in the nuclei stained with DAPI (blue) of CAL-51 cells. Scale bar = 10 μm (B) Quantification of RPA foci in part A. n = 3. (C) Immunofluorescence analysis of RPA foci (red) in DAPI-stained (blue) nuclei of MDA-MB-231 cells. Scale bar = 10 μm (D) Quantification of RPA foci in part C. n = 2. Hu = Hydroxyurea, 2 mmol/L for 8 h, used as a second positive control, apart from <0.1% O_2.

3.2.6. Systematic review of the use and effects of PARP inhibitors (PARPi) in hypoxia

Thus far, we have investigated the oxygen-dependency of biological processes which can affect the cellular response to anticancer agents. As a next step, we carried out a systematic review of the published literature regarding the effects of PARPi – our DDRi of interest – in hypoxia, following

the guidelines set by PRISMA (Preferred reporting Items for Systematic reviews and Meta-analyses)(Page *et al.* 2021). The methodology and outcomes of this review are presented in the following sub-chapters. The rationale for conducting this systematic review was to inform us about the observations published previously in this field of research, before testing the impact of hypoxia on the effects of PARPi in our own experimental settings.

3.2.6.1. Systematic review: Search methodology

For our systematic review, we designed a search methodology around one phenomenon of interest: use of PARPi in hypoxic conditions. The search terms used are depicted in figure 3.7, with similar or closely related terms identified and truncated as derivational affixes to maximise the search sensitivity. The Ovid MEDLINE index was used to source any relevant articles published between 1st Jan 2010 and 1st July 2023 - the specific time-period being chosen, to cover all at the time recently published studies for review.

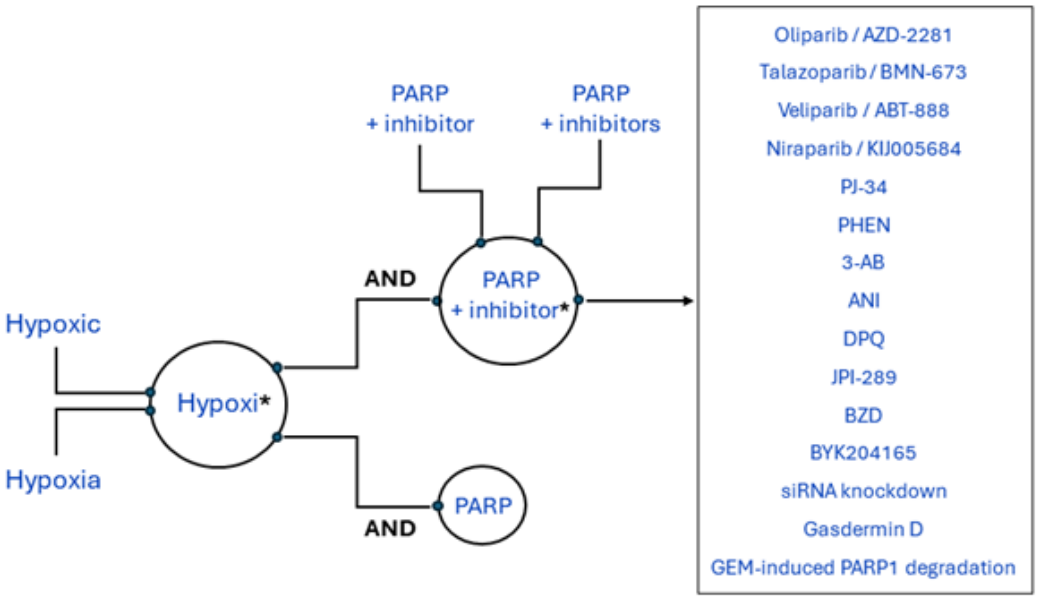

Figure 3.7. Boolean search strategy used for search terms. Similarly related search words were identified as affixes.

3.2.6.2. Systematic review: Screen

The sum of studies gathered from the search output described in the previous sub-chapter, were screened for duplicates. Then, eligibility criteria determined according to the SPIDER (Sample, Phenomenon of Interest, Design, Evaluation and Research type) framework (table 3.1) were used, to review the remaining papers, as follows: first on the Title and Abstract level and then, eligible shortlisted papers, on the full text level, to decide if they could proceed to the qualitative review stage. The detailed screen methodology we used, with inclusion and exclusion criteria set, as well as the individual review stages, are shown below (figure 3.8).

Table 3.1. Eligible standards for inclusion or exclusion according to the SPIDER framework

	Inclusion criteria	**Exclusion criteria**
Date	2010-2023	Published outside of 2010-2023
Sample	Human cell line(s)	Study exclusively in non-human cell line(s)
Phenomenon of Interest	Study relevant to the use of PARP inhibitors in hypoxic conditions	Study not relevant to inhibition of PARP in hypoxia. For example, studies which use the cleavage of PARP as a measurement of apoptosis in hypoxia. No hypoxia experiments carried out; hypoxia is just mentioned in the paper (introduction for example).
Design	Cell lines were treated in specified hypoxic conditions ≤ 2% O_2	Cell lines treated in hypoxic conditions >2% O_2. No details provided of the exact oxygen concentration used. Experiments rely on hypoxia mimetic agents such as $CoCl_2$, DFO, DMOG etc.
Research type	Empirical research	Secondary sources and non-empirical research including review texts, conference proceedings, textbook contents; non-English text

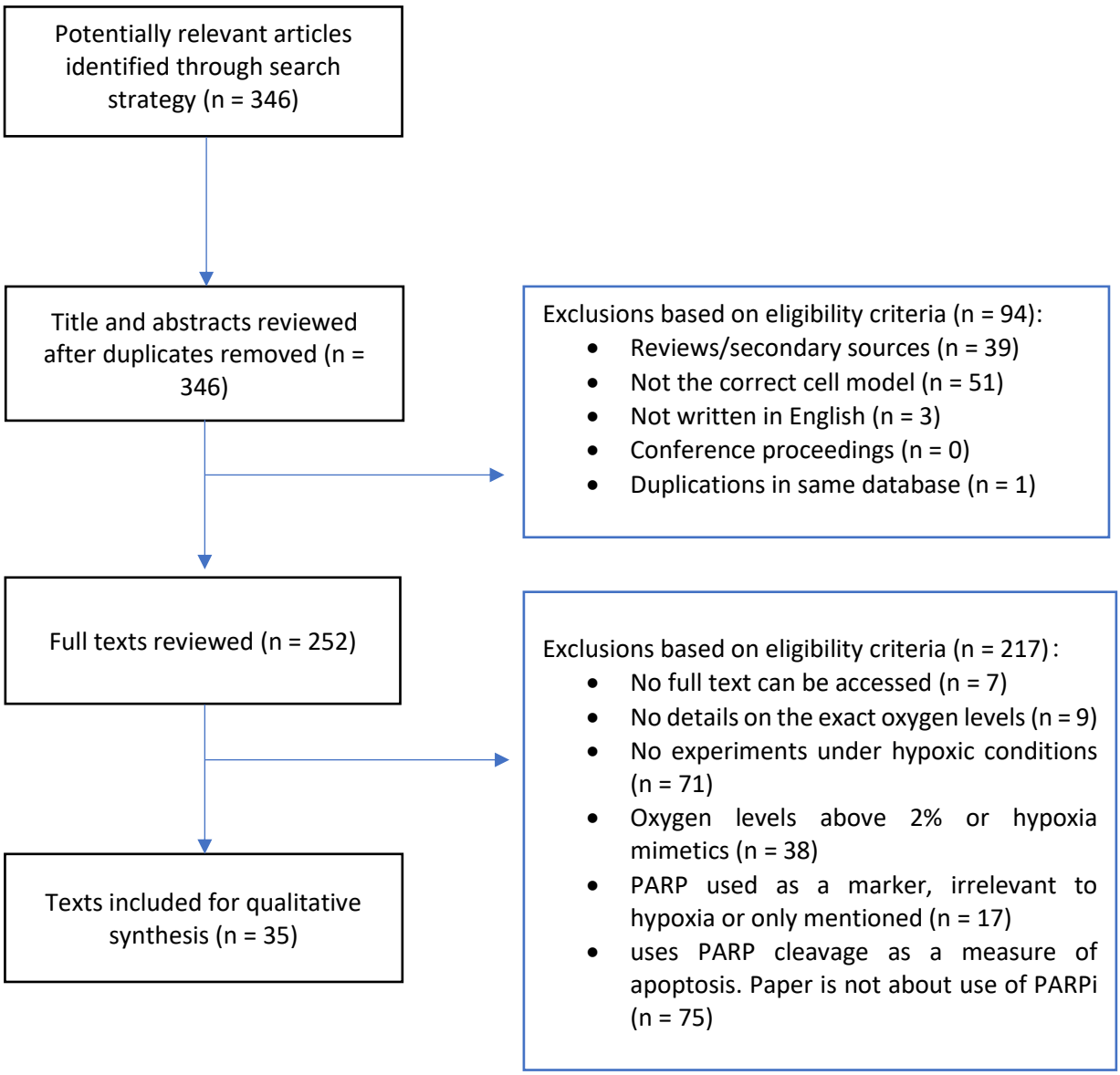

Figure 3.8. PRISMA flow diagram of the systematic literature exclusion process. The Ovid MEDLINE index was used to find potentially relevant published studies between 2010 and 2023. We screened 346 papers; 252 were qualified for critical assessment, resulting in a total of 35 articles included in this study.

3.2.6.3. Systematic review: Synthesis

In this systematic review we mainly focused on the existing data about PARPi cytotoxicity in hypoxia. For this purpose, we thematically categorised the 35 papers which occurred from the screen, into two groups: papers which reported explicit findings regarding the efficacy of PARPi in hypoxic cells and papers which investigated other effects of PARPi in hypoxia (appendix 1). In the first group, we further distinguished studies testing PARPi sensitivity in hypoxia alone and studies investigating PARPi cytotoxicity in hypoxia, plus other treatment(s). Findings regarding cell sensitivity to PARPi in hypoxia were found in 26 out of 35 papers (tables 3.2 and 3.3). The remaining 9 papers reported findings on different biological processes including the relationship between PARPi and hypoxia inducible factors (HIFs), cell migration, and angiogenesis (figure 3.9 and appendix 1).

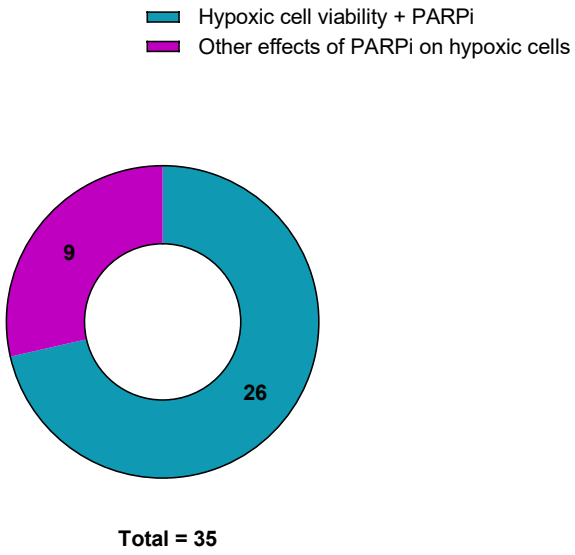

Figure 3.9. The thematic distribution of the 35 papers identified from the systematic review process. Parts of whole representation of the number of papers in each of the qualitative themes, identified during full-text review stage.

Out of the 26 papers which reported findings, regarding the cytotoxicity of different PARPi on cells exposed to hypoxia, 17 of them tested PARPi in hypoxia alone (table 3.2) and 9 investigated the effects of PARPi in hypoxia, plus some other combined treatment (table 3.3). Out of the 17 papers studying the cytotoxic effects of PARPi in hypoxia alone, 8 observed increased viability of hypoxic cells upon treatment with PARPi and another 6, reported reduced viability. Interestingly, another 3 studies investigated PARPi cytotoxicity in a range of oxygen levels or other conditions and reported both decreased and increased viability findings. A direct comparison of the study models and the oxygen levels used in each study can be seen in table 3.2, along with the key observations of each study regarding the impact of PARPi on hypoxic cell viability.

Table 3.2. Summary of studies reporting data PARPi effect on viability of hypoxic cells.

Study ID	Study model	Level of O_2	PARPi	Viability effect of PARPi in hypoxia	Viability assay used
Shafiq M., *et al*. Pulm Pharmacol Ther, 2023	Human pulmonary endothelial cells (HPAEC)	1%	siRNA	Decrease	Cell counting
Wong WW., *et al*. RSC Med Chem, 2023	HR proficient and deficient CRC cell lines	0.1%	Olaparib, talazoparib and HAP of phenolic Olaparib analogues	Decrease	Sulforhodamine B (SRB)
Peng X., *et al*. Oncogene, 2022	CRC cell lines	1%	Gasdermin D	Decrease	Ki67 and CCK8
Yang Y., *et al*. Front Cell Dev Biol, 2022	R28 retinal cells	0.2%	Olaparib	Increase	RBPMS staining

Liu X., *et al.* NPJ Breast Cancer, 2022	Treatment naïve gBRCA^{+} patient samples	Hypoxia signatures	Talazoparib	Increase	Survival analysis of patient samples
Haga S., *et al.* J Surg Res, 2022	AML12 cells transgenic for human TGFβ	<1%	PJ-34	Increase	xCELLigence, LDH cytotoxicity kit
Marcus JM., *et al.* Neurochem Int, 2021	Primary Cortical neurons	<1%	BMN 673	Increase	Almar blue, Hoechst, and Propidium Iodide staining
Marti JM., *et al.* Redox Biol, 2021	HEK 293T	1%	Olaparib PARP1 KO (CRISPR-Cas9)	No change with Olaparib Decreased viability with PARP1 KO	Cell proliferation assay (counting)
Mehibel M., *et al.* J Clin Invest, 2021	Various HR proficient and HR deficient cell lines	0.1% and 2%	Olaparib, Talazoparib	Decrease at 0.1%, and Increase at 2%	Colony survival assay, Tumour growth measurement
Jang HR., *et al.* Front Immunol, 2020	HK-2 cells	1%	JPI-289	Increase	Cell titer 96
Cao S., *et al.* J Cell Mol Med, 2019	AC16 cells	1%	DPQ	Increase	TUNNEL assay, PI/Annexin V staining
Giovannini S., *et al.* Nucleic Acids Res, 2019	A2780 and SUM149PT cell lines	1%	Olaparib	Increase	Colony survival assay
Saki M., *et al.* Mol Cancer Res, 2017	NSCLC cell lines	0.1%	Veliparib (ABT-888)	Decrease	Colony survival assay
Kim Y., *et al.* Clin Exp	Primary cortical neurons	<1%	JPI-289	Increase	Trypan blue staining, CCK-8, Annexin-V

Pharmacol Physiol, 2017					
Kumareswaran R., *et al*. Radiother Oncol, 2015	H1299 and ME180 cell lines	0%, 0.2%, 1%, H/R cycles (cyclic hypoxia)	Olaparib (AZD-2281)	Decrease at 0%, moderate decrease at 0.2 and 1%, increase at cyclic hypoxia	Colony survival assay
Chan N., *et al*. Cancer Res, 2010	MEF, RKO, DU145 and H1299 cell lines and tumour xenografts	0.2% and 0.02%	Veliparib (ABT-888), ANI	Decrease at 0.02%, moderate decrease at 0.2%, reduced hypoxic fraction of tumour xenografts (EF5 staining)	Colony survival assay, IHC for apoptotic markers
Hegan DC., *et al*. Proc Natl Acad Sci U S A, 2010	RKO, A549, H460 cell lines	0.1%	siRNA, KU0058684, BZD, ANI, PHEN, ABT-888, 3-AB	Decrease	Colony survival assay

A smaller number of studies which were identified by our screen, investigated the cytotoxic effects of PARPi in hypoxia in combination with other forms of treatment. Most of these studies focused on the radiosensitising effect of PARPi in hypoxic cells, *in vitro* and/or *in vivo*. Furthermore, several studies tested cell viability using PARPi in hypoxia, in combination with other chemical compounds. The reported outcomes of these studies, regarding cell viability, both in hypoxia alone and in combination with other treatment(s), as well as the levels of oxygen tested, and further details can be found summarised, in table 3.3, below.

Table 3.3. Summary of studies reporting data on viability of hypoxic cells with PARPi combined with other treatment(s).

Study ID	Study model	Level of O_2	PARPi	Combined treatment	Reported outcomes	Viability assay used
Lee TW., *et al.* Int J Radiat Biol, 2019	Various HNSCC cell lines, HEK-293, and WI-38/Va-13 cell lines	<0.01% and 0.2%	Olaparib, Veliparib	Radiation	Decreased viability and radiosensitisation at both <0.01% and 0.2%	Regrowth assays, colony survival assays
Borst GR., *et al.* Oncotarget, 2017	Tumour xenografts	EF5 staining	Olaparib	Radiation	Decreased tumour hypoxic fraction	IHC for EF5 and EdU
Jiang Y., *et al.* Int J Radiat Oncol Biol Phys, 2016	Calu-3, Calu-6, and tumour xenografts	1%	Olaparib	Radiation	Radiosensitisation of hypoxic cells, and of hypoxic tumour xenografts	Colony survival assay, IHC for apoptotic markers, tumour growth
Zhan L., *et al.* Dis Esophagus, 2016	ECA109 and TE13 ESCC cell lines	0.2%	Olaparib	Radiation	Decreased viability and radiosensitisation in chronic hypoxia	Colony survival assay
Gani C., *et al.* Radiother Oncol, 2015	22Rv1 cells	0.2%	Olaparib	Radiation	Decreased viability and radiosensitisation of cells in normoxic, acute and chronic hypoxic conditions	Colony survival assay
Geng H, *et al. In Vitro* Cell Dev Biol Anim, 2021	Primary cardiac myocytes	<1%	siRNA	Sp1 inhibitor (Mithramycin A)	Increased viability in hypoxia	MTT, caspase-3 activity assays

Le BV., *et al.* Cell Rep, 2020	Various malignant and normal hematopoietic cell lines	1%	Olaparib, Talazopa-rib	Recombinant TGFβ1	Increased viability of hypoxic cells	Colony survival assay
Erdélyi K., *et al.* Int J Mol Med, 2013	A549 cells	<1%	shRNA	Hydrogen Peroxide (H_2O_2)	Increased viability of hypoxic cells	MTT assay
Pan R., *et al.* CNS Neurosci Ther, 2013	C8-D1A cells	1%	siRNA	Zinc Chloride (ZnCl)	Increased viability of hypoxic cells	Cytotox96 nonradioactive assay kit

Fourteen studies used oxygen tensions of ≤1 % O_2, while several probed lower oxygen levels - down to 0.2% (Yang *et al.* 2022) or 0.1 % (Wong *et al.* 2023), or even severe hypoxia (<0.1% O_2) like in the studies of Mehibel *et al*. and Chan *et al*. Liu *et al.* categorised breast tumours by hypoxia-associated gene signatures rather than a fixed oxygen set-point. Across these conditions, Olaparib emerged as the most widely used PARPi (24/35 studies), with Talazoparib appearing in eight studies. A handful of studies employed alternative inhibitors - PJ-34 or used PARP1 siRNA as a surrogate (tables 3.2 and 3.3).

Overall, although experimental systems and specific oxygen tensions vary in our review dataset, a recurrent finding is that hypoxia often increases cancer cell sensitivity to PARPi, whereas in some non-malignant contexts, PARP blockade can be protective, and in smaller set of study models, "moderate" hypoxia can even blunt PARPi efficacy.

In eight, cancer-focussed reports, hypoxia amplified PARPi–induced cytotoxicity. Wong *et al.* synthesised phenolic prodrugs of Olaparib and Talazoparib and showed that, in DLD-1 and DLD-$1^{BRCA2-/-}$ cells, these prodrugs remained inert under normoxia but became potently cytotoxic under hypoxia (0.1% O_2), reducing viability, far more than the parent compounds (Wong *et al.*

2023). Mehibel *et al.* cultured carcinoma cells at both 0.1 % and 2 % O_2 and found that, at 0.1 % O_2 cells became two- to three-fold more sensitive to PARPi - demonstrating a threshold effect in which severe hypoxia (<0.1% O_2) represses repair capacity and primes cells for PARPi-driven death (Mehibel *et al.* 2021). These data reproduced those reported earlier by Chan *et al.* who confirmed this sensitisation response, using several cell lines exposed to 0.2% and 0.02% O_2. Specifically, they reported that the cytotoxicity of veliparib was double upon treatment with 0.2 % O_2, and at 0.02 % O_2, veliparib toxicity was more than tripled, compared to 21 % O_2 (Chan *et al.* 2010). Hegan *et al.* similarly observed that, in cells exposed to 0.01% O_2, PARPi produced near-absolute loss of viability, consistent with the finding that severe hypoxia induces a functional HRD, reported by the same group and others (Hegan *et al.* 2010). Peng *et al.* found that hypoxia or chemotherapy induce nuclear translocation of Gasdermin D, a protein which further interacts with and inhibits PARP1 in a manner identical to Olaparib, leading to blockade of DNA damage repair-related functions and induction of DNA damage-related apoptosis (Peng *et al.* 2022). *In vivo*, Borst *et al.* used EF5 staining to identify hypoxic regions in syngeneic, HR-proficient breast cancer models: when Olaparib was combined with radiation, hypoxic areas exhibited a delay advantage over radiation alone as well as and decreased *ex vivo* clonogenic survival (Borst *et al.* 2017). Finally, Jiang *et al.* demonstrated *in vivo* that, Calu-6 tumors showed low oxygen areas linked to lower RAD51 protein levels. Additionally, they showed that Olaparib treatment boosted DNA damage and cell death and resulted in significant growth inhibition in Calu-6 tumors but not in well-oxygenated Calu-3 tumors (Jiang *et al.* 2016). Collectively, these studies show that cancer cells experiencing hypoxia at or below ~0.1% O_2 become roughly 2- to 5-times more vulnerable to PARPi, than under normoxic conditions.

By contrast, some reports describe PARPi as protective under hypoxia, in non-malignant contexts. Yang *et al.* treated retinal pigment epithelial cells at 0.2% O_2 with Olaparib and found that, although hypoxia alone reduced viability by ~30%, PARPi rescued roughly half of that viability and decreased mitochondrial-associated endoplasmic reticulum membrane dysregulation.

Additionally, some indicators of mitochondrial performance, such ROS accumulation, mitochondrial Ca^{2+} influx and mitochondrial membrane potential collapse, decreased after Olaparib treatment while treatment with Olaparib attenuated the hypoxia-induced upregulation of the inflammasome protein NLRP3 levels as well as the phosphorylation of ERK1/2 and histone H2AX (Yang *et al*. 2022). Zhou *et al*. studied a diabetic ischaemic wound model - where tissue oxygen falls to ~2% - and showed that the PARPi, PJ-34, markedly accelerated wound closure (~25% improvement) in hypoxic *in vitro* models. Specifically, PARPi enhanced HUVEC migration and invasion in Boyden chamber assays by 80% and 180%, respectively. In the animal models of the same study, wound healing was significantly enhanced from with the addition of PJ-34, which promoted angiogenesis at the ischemic and diabetic wound beds, as evidenced by significantly higher levels of endothelial cell markers (VEGFR2 and eNOS) in mice treated with PJ-34, compared to controls (Zhou *et al*. 2017). Geng *et al*. silenced PARP in primary cardiomyocytes exposed to <1% O_2 and reported that while hypoxia decreased cell viability, PARP knockdown reduced hypoxia-induced cell death and PARP overexpression increased hypoxia-mediated apoptosis *via* direct interaction with the protein SP1 (Geng *et al*. 2021). Similar protective effects were observed in neuronal systems, where veliparib (BMN 673), attenuated hypoxic apoptosis by preventing PARP1 overactivation and TDP-43 mislocalisation (Marcus *et al*. 2021), and in renal and myocardial tissue, where the PARPi, JPI-289, mitigated ischemia-reperfusion injury by modulating inflammatory signaling and apoptotic pathways (Cao *et al*. 2019; Jang *et al*. 2020). Finally, Marti *et al*., reported no significant change in viability of HEK 293T cells at 1% O_2 in response to Olaparib, compared to normoxia, but a significant reduction in viability of hypoxic cells at the same oxygen levels, in response to PARP1 KO *via* CRISPR-cas9 genome editing (Marti *et al*. 2021). These studies together illustrate that, in non-transformed cells the use of PARPi under low oxygen conditions can be beneficial, by conserving metabolic functions, reducing apoptosis and overall cellular damage.

Another set of investigations identified contexts of hypoxia-driven PARPi resistance in tumours and cancer cells. Liu *et al*. showed that g*BRCA*$^{+}$ breast tumours with high hypoxia signature scores were found to be less sensitive to neoadjuvant Talazoparib treatment (Liu *et al*. 2022b). *In vitro*, Mehibel *et al.*, observed that carcinoma cell lines exposed to 2% O_2 were ~30% less susceptible to Olaparib or Talazoparib than cells in normoxia, suggesting that "moderate" hypoxia confers resistance to PARPi, while hypothesising that reduced ROS levels at milder oxygen tensions where underpinning this phenotype (Mehibel *et al*. 2021). Giovannini *et al.*, reported that *BRCA1*-deficient breast cancer cells at 1% O_2, stabilised truncated *BRCA1* splice variants, resulting in restored HR function, enough to diminish Olaparib cytotoxicity rate by 50%, compared to normoxia (Giovannini *et al*. 2019). These three examples underscore that "moderate" hypoxia or adaptive DDR responses, can mitigate PARPi efficacy in certain TME contexts. The respective oxygen level, emerges as a critical determinant of these outcomes, with radiobiological hypoxia (<0.01% O_2) maximising synthetic lethality in cancer models, while moderate hypoxia (<1-2% O_2) fostering resistance through, either HIF-1α/TGFβ-dependent, HR-dependent or ROS-dependent mechanisms (Chan *et al*. 2010; Giovannini *et al*. 2019; Le *et al*. 2020; Mehibel *et al*. 2021).

The methodological approaches across these studies reveal both strengths and limitations in current research paradigms. Hypoxia modeling varies widely, ranging from severe (<0.01% O_2) to moderate (2% O_2) conditions, with exposure durations spanning acute (6-24 h) to chronic (>72 h) periods. While these models have proven valuable, they often lack the complexity of actual TMEs, and the clinical relevance of oxygen concentrations tested remains debated. Viability assessment predominantly relies on clonogenic assays for radiosensitisation studies, metabolic readouts like CCK-8 and MTT for general cytotoxicity, and apoptosis markers such as TUNEL and Caspase-3 activation, each with inherent limitations in specificity and throughput (tables 3.2, 3.3). Only a minority of studies (4/30) included *in vivo* validation, though these provided critical insights, such as the reduction of hypoxic tumor fractions by Olaparib in breast cancer xenografts

(Borst *et al.* 2017) and the tumor-selective chemosensitisation achieved by hypoxia-activated Olaparib prodrugs (Wong *et al.* 2023). A significant methodological gap remains in correlating *in vitro* oxygen levels with *in vivo* tumor hypoxia metrics, which could substantially improve translational relevance. Moreover, quantification of HR-proficiency is infrequent and indirect; only a minority observe RAD51 foci or measure HR transcripts, while no studies use DR-GFP or equivalent reporters. Although Olaparib and Talazoparib are extensively profiled, newer PARPi like Niraparib and Rucaparib, have not been systematically compared under hypoxic conditions. Finally, while nonapoptotic cell-death pathways such as pyroptosis (Peng *et al.* 2022) appear in some studies, downstream consequences of PARPi in hypoxic conditions for antitumour immunity, remain largely unexplored.

At the mechanistic level, beyond cell survival outcomes, the PARP-HIF axis emerges as a central regulator of cellular responses to hypoxia. PARP1 directly modulates HIF stability and activity through isoform-specific interactions, PARylating HIF-1α to facilitate chromatin recruitment and transcriptional activation of hypoxic response genes (Marti *et al.* 2021) while forming complexes with HIF-2α that are disrupted by PARPi (PJ-34), leading to VHL-mediated degradation (Gonzalez-Flores *et al.* 2013). These PARP-HIF interactions have been shown to foster diverse downstream consequences, from Notch3 induction in hypoxic conditions being decreased by PARPi (Nakamura *et al.* 2022) to bidirectional modulation of angiogenesis, with PARPi inhibiting pathological angiogenesis in retinal models (Mao *et al.* 2016) while promoting wound healing in diabetic contexts (Zhou *et al.* 2017). Hypoxia also profoundly reprograms DNA repair pathways, creating opportunities for contextual synthetic lethality through transcriptional repression of HR genes *via* E2F4/p130-mediated downregulation (Hegan *et al.* 2010), hypoxia-dependent epigenetic silencing (Lu *et al.* 2011), and VHL deficiency-induced HR suppression (Scanlon *et al.* 2018). Together these findings imply that such vulnerabilities can be exploited therapeutically, even in tumors without germline HR defects, expanding the potential applications of PARPi beyond classical *BRCA*-mutated cancers.

Therapeutic innovation in this field has yielded several promising strategies, particularly hypoxia-activated prodrugs (HAPs) of PARPi. Wong *et al*. developed phenolic Olaparib derivatives that showed >5-fold increased toxicity in hypoxic (0.2% O_2) versus normoxic conditions in colorectal cancer models, while maintaining tumor-selective chemosensitisation when combined with Temozolomide (Wong *et al*. 2023). Radiosensitisation approaches have also benefited from insights into hypoxia-PARPi interactions, with studies demonstrating enhanced radiation efficacy through impaired DSB repair (Jiang *et al*. 2016) and reduced RAD51 foci formation in hypoxic tumor subregions and hypoxic cells, respectively. Interestingly, DNA-PKi outperformed PARPi in HNSCC radiosensitisation, particularly under hypoxia (Lee *et al*. 2019), suggesting potential combination strategies. Biomarker development has progressed with hypoxia signatures correlating with Talazoparib response in g*BRCA*+ breast cancer (Liu *et al*. 2022b) and HIF-1α/PARP1 co-expression emerging as a potential predictor for Notch3-targeted approaches (Nakamura *et al*. 2022), though no PARPi trial has incorporated tumor hypoxia status as a stratification factor.

In the context of PARPi effects on the viability of hypoxic cells, several critical knowledge gaps must be addressed to advance this field. The relationship between oxygen gradients and PARPi dose-response remains poorly characterised, particularly for physiologically relevant O_2 levels that commonly occur in human tumors. The role of TME components, especially cancer-associated fibroblasts, in modulating hypoxia-induced PARPi response has been largely overlooked in current research. While pan-PARPi, like Olaparib and PJ34 dominate existing studies, the potential of isoform-specific agents targeting PARP1 versus PARP2/3 remains virtually unexplored despite their likely differential effects in hypoxic contexts. Clinical translation faces substantial barriers, including the lack of standardised hypoxia imaging protocols for trials and insufficient validation of hypoxia biomarkers in patient-derived xenograft (PDX) models. These gaps represent both challenges and opportunities for future research aimed at harnessing the complex interplay between PARPi and hypoxic stress for therapeutic benefit.

The current evidence paints a picture of hypoxia as a double-edged sword in PARPi therapy – creating vulnerabilities in some malignant contexts, while fostering resistance in others and consistently protecting normal tissues from ischemic damage. This “bifurcated” impact stems from hypoxia's multifaceted disruption of DNA repair fidelity, transcriptional networks, and metabolic homeostasis, which apparently are all intersecting with PARP activity in cell-type specific ways. While innovations like HAPs and biomarker-driven combinations show promise for targeting hypoxic tumour niches, realising their full potential will require overcoming methodological heterogeneity and deepening our understanding of tumour-stromal interactions in oxygen-deprived microenvironments. The path forward must prioritise rigorous standardisation of hypoxia models, development of predictive biomarkers, and innovative clinical trial designs that account for the dynamic nature of tumour hypoxia, ultimately enabling more precise and effective study of PARPi effects, across the spectrum of hypoxic stress.

3.2.7. PARPi exhibit oxygen-dependent effects in breast cancer cells

As a next step, we wanted to investigate the effects of PARPi on the sensitivity of hypoxic cells, in our own experimental settings.

We, therefore, decided to test the cytotoxic effects of the PARPi Olaparib, in a range of oxygen levels, using two breast cancer cell lines. We decided to continue the work with TNBC *in vitro* models, based on the previously reported finding that establish this type of breast cancer as one of the most hypoxic (Bernardi and Gianni 2014; Srivastava *et al*. 2023; Zheng *et al*. 2020). The TNBC cell lines we used to evaluate the effects of the PARPi Olaparib were selected according to convenience of culture, duplication rates, plating efficiencies and clonogenicity, which we evaluated during their use. Based on these, we chose to continue to work with CAL-51 and MDA-MB-231 cells for this part of our work.

The viability of hypoxic cells in the presence or absence of the PARPi Olaparib, was determined by colony survival assays (figure 3.10, A).

Our findings showed that, CAL-51 cells were more sensitive (figure 3.10, B) than MDA-MB-231 cells (figure 3.10, C) in normoxic conditions, consistently with previous reports (De Soto *et al*. 2006; Farmer *et al*. 2005). Exposure to <0.1% O_2 sensitised both cell lines to Olaparib (figure 3.10, A, B). Interestingly, both breast cancer cell lines exposed to either 2% O_2 or cyclic hypoxia, showed a resistance to the cytotoxic effects of Olaparib (figure 3.10, B, C).

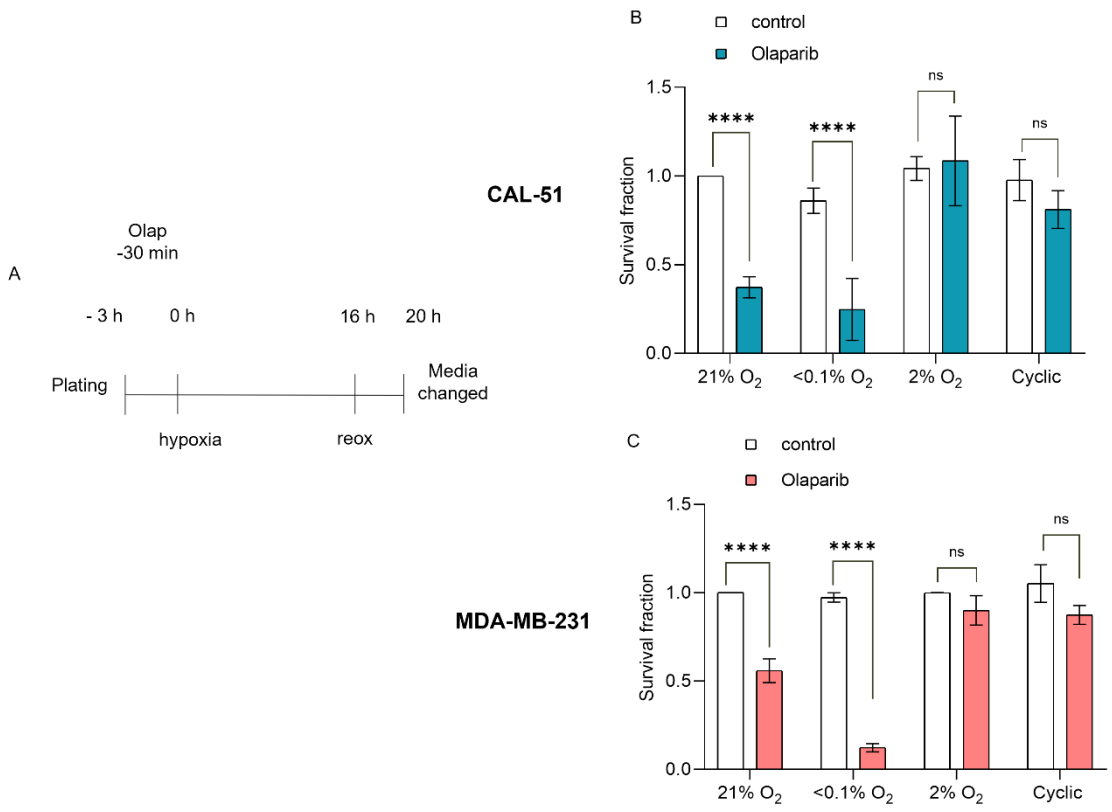

Figure 3.10. Oxygen-dependent response to Olaparib. CAL-51 and MDA-MB-231 cells were exposed to the indicated oxygen levels for 16 h. (A) A schematic representation of the experimental timeline is shown. (B) Colony survival assay of CAL-51 cells pre-treated with Olaparib (1 µmol/L) for 30 min. Olaparib was removed 4 h after reoxygenation, i.e., at 20 h. n = 3. (C) Colony survival assay of MDA-MB-231 cells were pre-treated with Olaparib (10 µmol/L) for 30 min. Media was removed 4 h after reoxygenation, i.e., at 20 h. n = 3.

3.2.8. Treatment with 2% O_2 decreases sensitivity to Olaparib

To validate the oxygen-dependency of Olaparib we observed with colony survival assays, we carried out an additional viability assay with both TNBC cell lines we previously used. The MTT assay is a colorimetric assay for assessing cell metabolic activity. NAD(P)H-dependent cellular oxidoreductase enzymes may, under defined conditions, reflect the number of viable cells present (Levitz and Diamond 1985). For this experiment, CAL-51 and MDA-MB-231 cells were exposed to 2% O_2 after treatment with a range of Olaparib concentrations (figure 3.11, A). Compared to normoxic cells treated with the same PARPi dosages, the IC50 for Olaparib was

significantly higher for cells exposed to 2% O_2 (figure 3.11, B, C and D), validating the oxygen-dependent cytotoxicity of Olaparib that we previously observed in colony survival assays. Of note, IC50 values of Olaparib in MDA-MB-231 cells exposed to 2% O_2 were not achieved in the used dose range, and the relative IC_{50} value was extrapolated in this case (section 2.1.22).

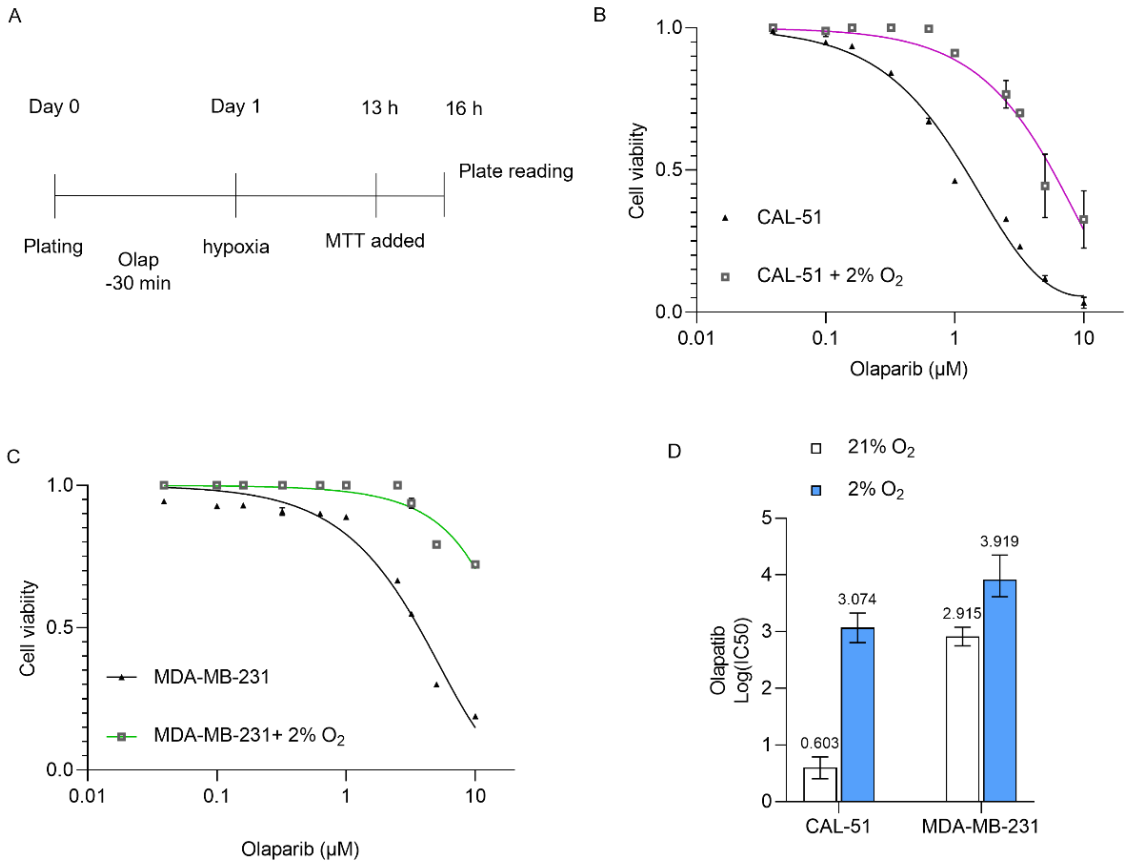

Figure 3.11. Treatment with 2% O_2 decreases sensitivity to Olaparib. (A) Schematic representation of experimental timeline. (B) CAL-51 cells were exposed to the indicated hypoxia treatment for 16 h and pre-treated with the indicated doses of Olaparib, for 30 min. Viability was analysed by MTT assay. n = 1. (C) MDA-MB-231 cells were exposed to the indicated hypoxia treatment and pre-treated with Olaparib with the indicted doses for 30 min. Cell viability was analysed by MTT absorbance measurement. (D) Olaparib Log_{10} (IC50) values (displayed above error bars) from parts B and C, calculated and plotted with GraphPad prism. n = 1.

3.2.9. RAD51 levels decrease only in <0.1% O_2

One of the mechanisms of hypoxia-mediated sensitisation to PARPi is the functional suppression of the HR-pathway of DNA repair shown to be mediated by a decrease of RAD51 protein levels, in conditions of <0.1% O_2 (Chan *et al*. 2010). We investigated, if this key HR protein RAD51 levels change in response to the oxygen levels we tested in our experimental settings (Graeser *et al*. 2010). Using both breast cancer cell lines previously described, we analysed protein samples of cells exposed to different oxygen levels by western blot assay. The levels of RAD51 decreased upon treatment with all the oxygen levels tested, with a significant decrease, however, observed only in cells exposed to <0.1% O_2 (figure 3.12, A, B, C and D). This observation is consistent with previous reports (Chan *et al*. 2010) and could potentially explain the resistance to Olaparib, observed in cells exposed to 2% or cyclic hypoxia.

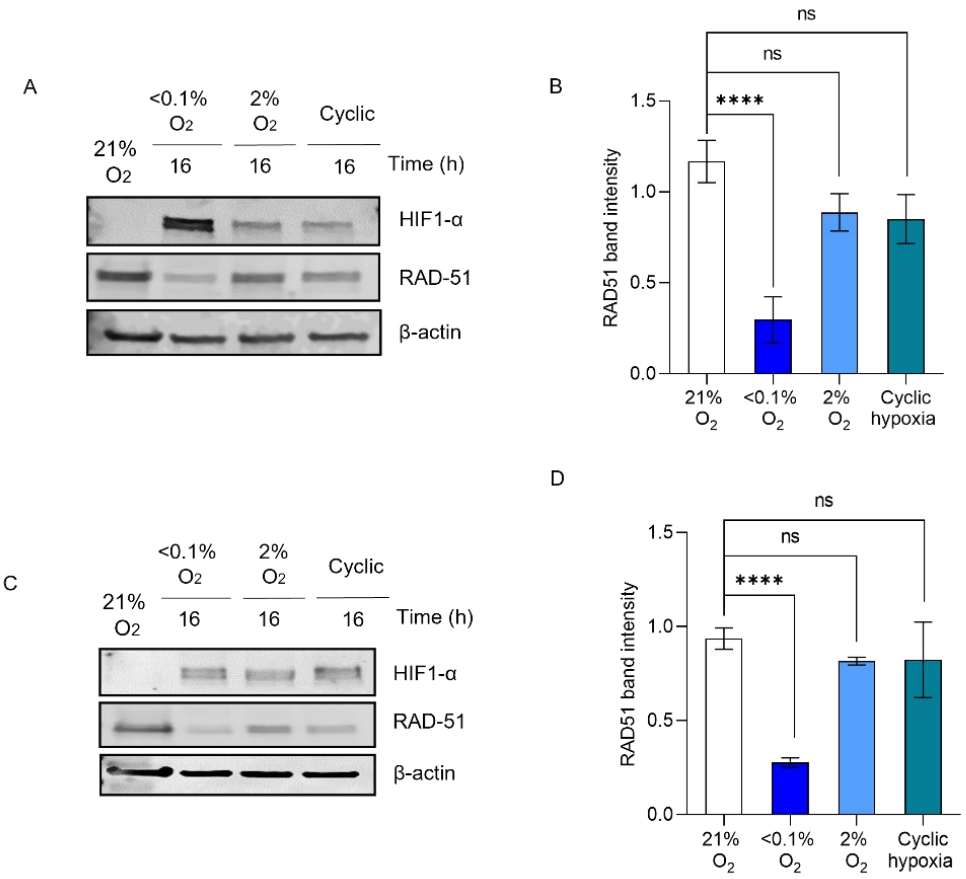

Figure 3.12. RAD51 levels decrease only in <0.1% O_2. (A) Western blot analysis of RAD-51 levels in CAL-51 cells, exposed to the indicated hypoxia treatments for 16 h. (B) Quantification of RAD51 band intensity / β-actin band intensity in CAL-51 cells from part A. n = 3. (C) Western blot analysis of RAD51 levels in MDA-MB-231 cells, exposed to the indicated hypoxia treatments for 16 h. (D) Quantification of RAD51 band intensity / β-actin band intensity, in CAL-51 cells from part C. n = 3. β-actin was used as loading control and HIF-1α, as a hypoxia control.

3.2.10. Sensitivity/resistance to PARPi in hypoxia is not ROS-dependent

A recent study Reporting findings matching our data which showed an oxygen-dependency of Olaparib cytotoxic effects, hypothesised that a decrease in ROS levels under mild hypoxic conditions (2% O_2) was the mechanism of resistance of these cells to PARPi (Mehibel *et al.* 2021). For that reason, we tested this hypothesis by carrying out colony survival assays, using the two breast cancer cell lines previously described (figure 3.13, A). Cells were exposed to hypoxia and in the presence or absence of Olaparib and/or NAC, a commonly used ROS scavenger (Zhang *et*

al. 2011). The presence of NAC in Olaparib-treated cells increased the drug's cytotoxicity towards cells exposed to 2% O_2 and cyclic hypoxia – both conditions under which resistance to Olaparib was previously seen. Interestingly, the addition of NAC, reduced the cytotoxic effects of Olaparib in cells exposed to <0.1% O_2 (figure 3.13, B and C).

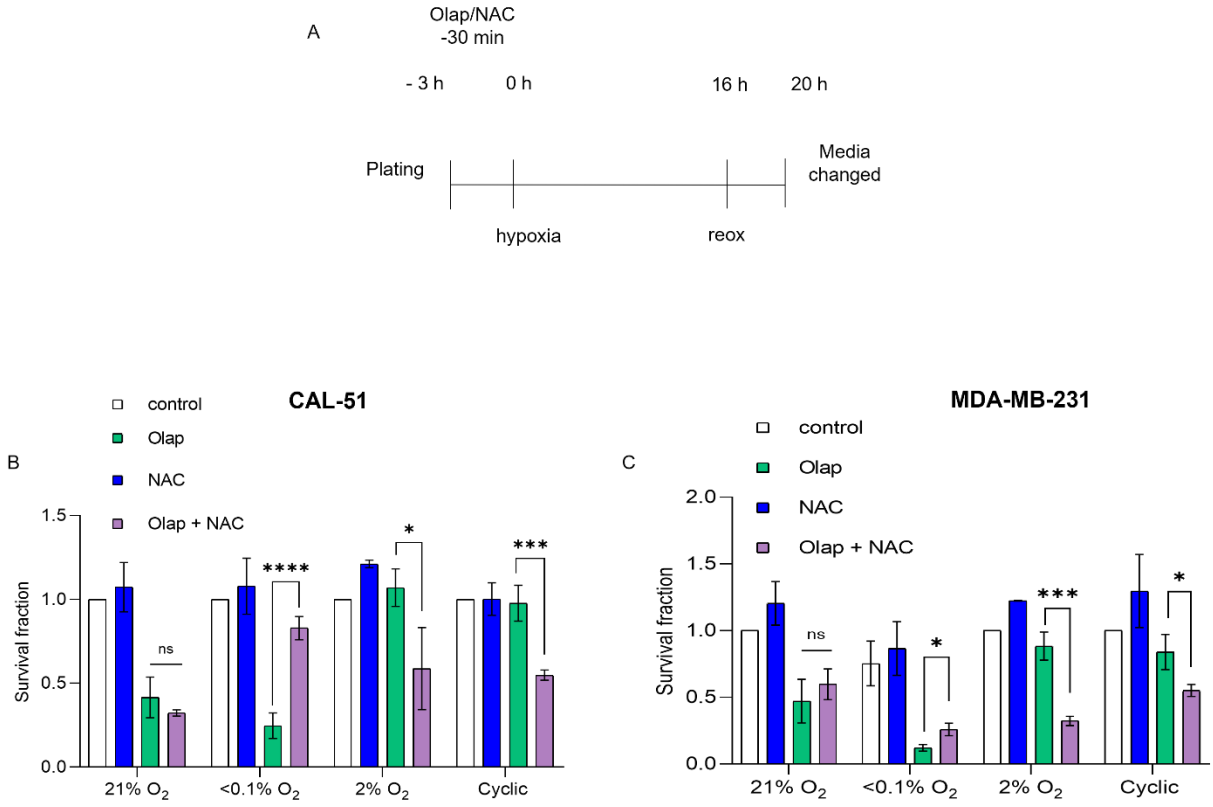

Figure 3.13. Treatment with NAC results in decreased sensitivity to Olaparib in cells exposed to <0.1% O_2 and increased sensitivity in cells treated with 2% O_2 or cyclic hypoxia. (A) Experimental timeline: Olaparib and/or NAC were added 30 min before hypoxia treatments. Media were changed 4 h after reoxygenation. (B) Colony survival assay quantification of CAL-51 cells treated with Olaparib (1 µmol/L), plus/minus NAC (20 mmol/L), at either normoxia or at the indicated hypoxia treatments. n = 3. (B) Clonogenic assay quantification on MDA-MB-231 cells, treated with Olaparib (10 µmol/L) plus/minus NAC (20 mmol/L), at normoxia or at the indicated hypoxia treatments. n = 3.

3.2.11. Quantification of ROS in hypoxic cells using ROS-sensor expressing plasmids

Following the previously described results, we wanted to characterise the oxidative stress response to hypoxia and quantify ROS levels in hypoxic cells. To do so, we used a ROS-sensor plasmid-based assay where CAL-51 cells where transfected with pHyPer-Nuc and pHyPer-Mito plasmids before exposure to hypoxia. The pHyPer-Nuc and pHyPer-Mito plasmids express a nuclear-targeted and a mitochondrially-targeted, GFP-based H_2O_2 sensor protein respectively, which upon oxidation by H_2O_2 emits fluorescence, which can be used to quantify levels of H_2O_2 in the nucleus and the mitochondria of cells (figure 3.14, A) (Fischer-Fantuzzi and Vesco 1988; Gorman *et al.* 1984; Haas *et al.* 1996). Treatment with <0.1% O_2 lead to significant increases in both nuclear and mitochondrial H_2O_2 levels, whereas exposure to 2% O_2 increased H_2O_2 levels in the nucleus but non-significantly in the mitochondria, compared to normoxic cells (figure 3.14, B, C, D and E). These findings conclude that ROS in the form of H_2O_2 accumulate in cells under hypoxic conditions in both radiobiological hypoxia and 2% O_2 and point to an oxygen-dependency of mitochondrial H_2O_2 levels in these cells.

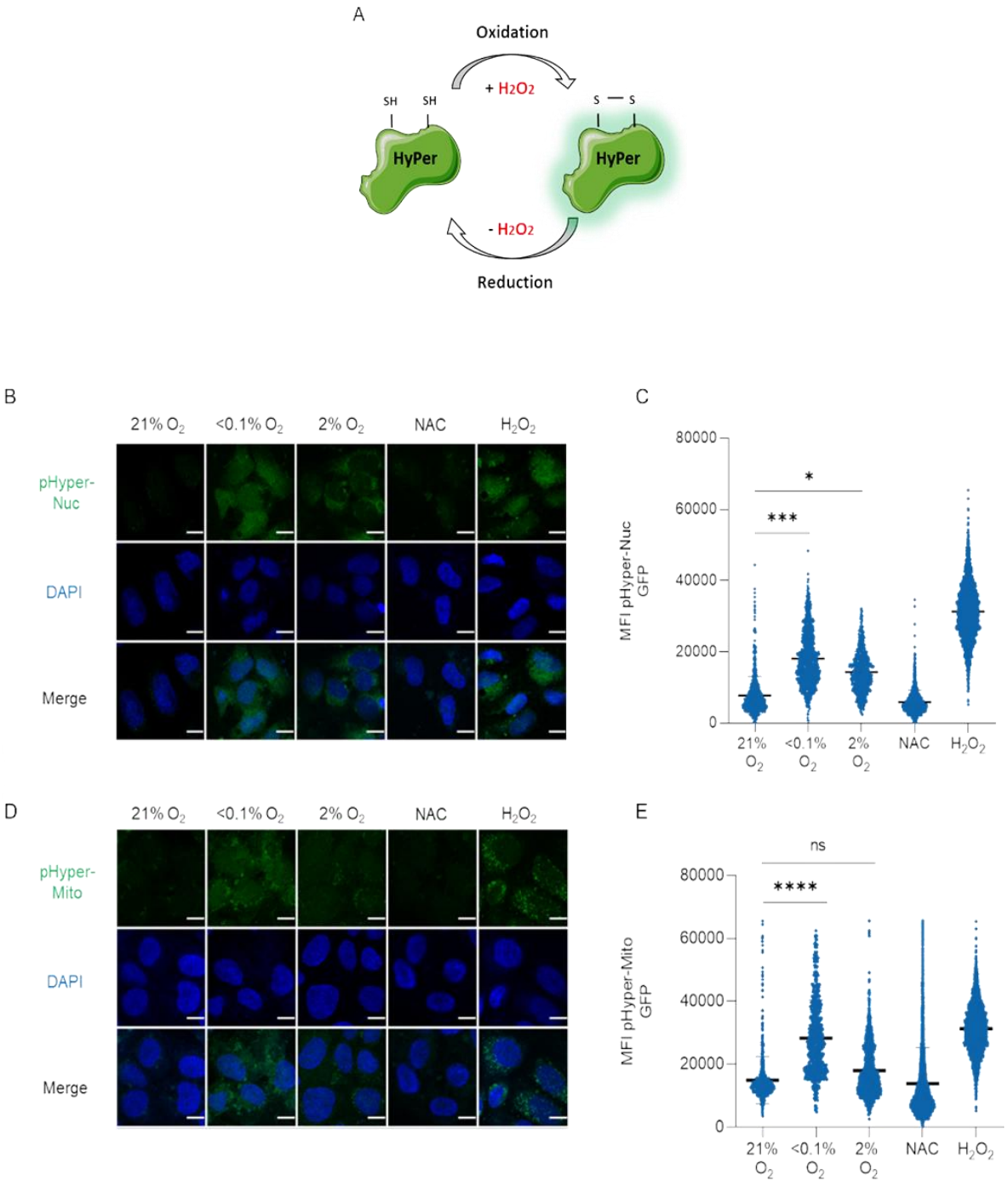

Figure 3.14. Hypoxia leads to an increase in cellular ROS levels. CAL-51 cells were exposed to the indicated O_2 levels, for 8 h. (A) Illustration of the mechanism of function of the pHyPer-Nuc and pHyPer-Mito plasmids. (B) Representative images from fluorescence microscopy analysis of GFP Mean fluorescence intensity (MFI) in CAL-51 cells exposed to hypoxia, after transfection with pHyPer-Nuc plasmid. Scale bar = 10 µm. (C) Quantification of nuclear H_2O_2 levels from part B. n = 3. (D) Representative images from microscopic analysis of GFP Mean fluorescence intensity (MFI) in CAL-51 cells exposed to hypoxia after, transfection with pHyPer-Mito plasmid. Scale bar = 10 µm. (E) Quantification of mitochondrial H_2O_2 levels from part D. n = 3. H_2O_2 (6 mmol/L for 30 min), used as a positive control and NAC (20 mmol/L for 5 h), used as negative control.

3.2.12. Sensitivity to PolQi is oxygen-dependent

Further exploring the effects of DDRi on sensitivity of hypoxic cells we tested the oxygen-dependency of PolQi, a novel class of drugs showing great potential in the treatment of malignancies (Rodriguez-Berriguete *et al*. 2023). Recently, PolQi have been shown to exhibit positive outcomes in treatment of HR-deficient tumours (Ceccaldi *et al*. 2015; Dai *et al*. 2016) and combination treatment with PARPi has proven to be additively beneficial (Zatreanu *et al*. 2021).

For this purpose, we used the previously described TNBC breast cancer cell model to carry out some preliminary experiments, carrying out colony survival assays, in the presence or absence of PolQi, testing cell survival in a range of oxygen levels (figure 3.15, A).

These experiments suggested that the PolQi, ART558, showed increased cytotoxicity towards CAL-51 cells in comparison to MDA-MB-231 cells, under normoxic conditions (figure 3.15, B, C).

Preliminary data showed that treatment with <0.1% O_2 sensitised CAL-51 cells to the effects of ART558 but did not have the same effect on MDA-MB-231 cells (figure 3.15, B, C). The inverse phenotype was observed with cells exposed to 2% O_2, with CAL-51 cells being resistant to ART588 and MDA-MB-231 cells appearing to be more sensitive compared to their normoxic counterparts. Finally, preliminary data in cells exposed to cyclic hypoxia suggested resistance to the effects of ART558 in both breast cancer cell lines, except in the case of higher drug concentrations tested on CAL-51 cells (figure 3.15, B, C). This preliminary set of data is reported considering the novelty of PolQi but interpreted with caution, as our reports require further validation.

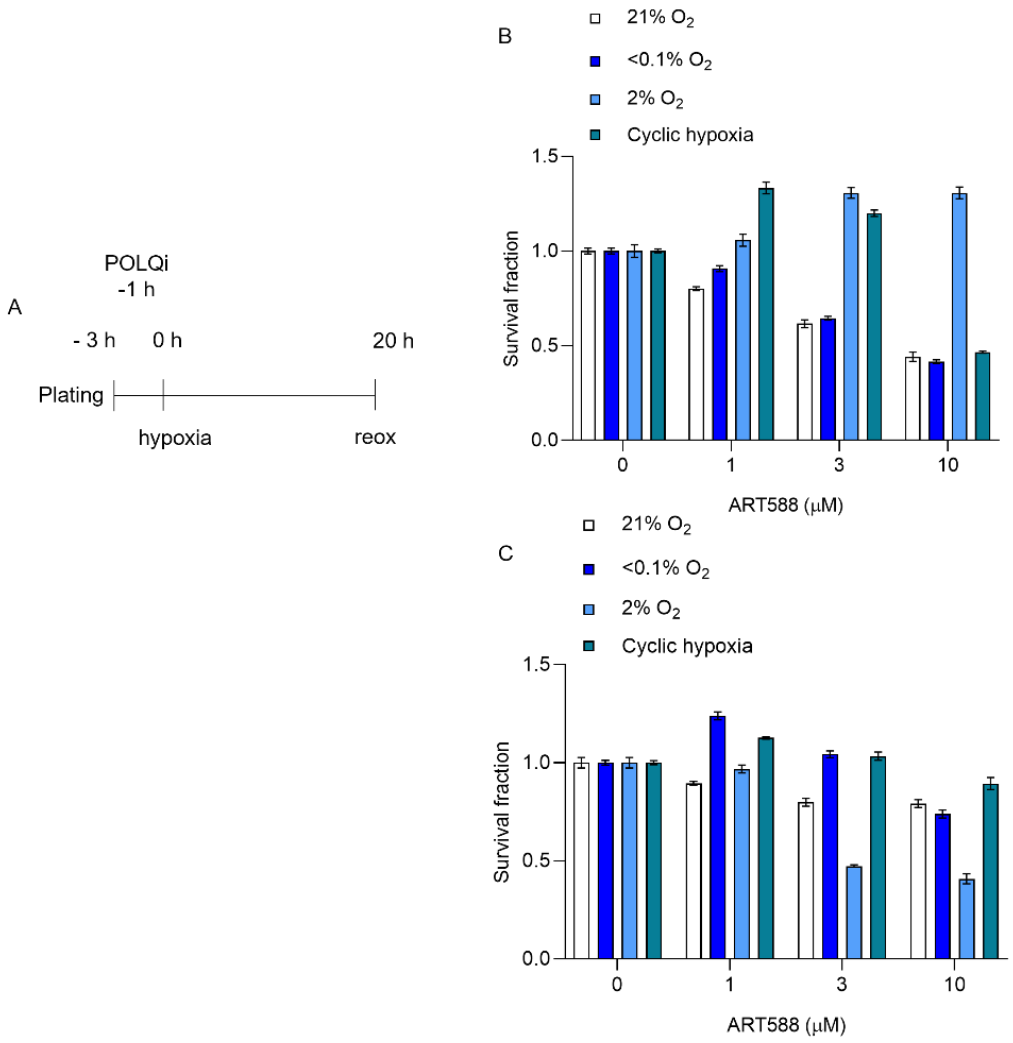

Figure 3.15. Oxygen-dependent response to the POLQ inhibitor ART 558. (A) Schematic representation of experimental timeline. (B) CAL-51 cells were exposed to the indicated hypoxia treatments for 20 h and pre-treated with the indicated doses of ART558 (PolQi) for 1 h. Cell viability was assessed with colony survival assay. n = 2. (C) MDA-MB-231 cells were exposed to the indicated hypoxia treatments for 20 h and pre-treated with the indicated doses of ART558 (PolQi) for 1 h. Cell viability was assessed with colony survival assay. n = 2.

3.3. Discussion

This part of our study investigated the intricate interplay between hypoxia, a pervasive feature of the TME, and cellular responses to DDRi, specifically the PARPi, Olaparib, and the novel PolQi, ART558. Our primary objective was to decipher how low oxygen conditions sculpt the vulnerability of breast cancer cells to these targeted agents, moving beyond descriptive observations to elucidate underlying mechanisms and contextualise findings within the established paradigm of hypoxia-induced therapy resistance.

Part of our investigation focused on characterising hypoxia-induced cellular adaptations. Consistent with prior studies (Hammond *et al.* 2002; Pires *et al.* 2010), severe hypoxia (<0.1% O_2) triggered a pronounced G1-phase arrest and suppression of DNA synthesis in CAL-51 cells, as evidenced by BrdU/PI analysis. This aligns with the canonical view of hypoxia as a potent cell cycle modulator. Intriguingly, however, cyclic hypoxia induced a distinct S-phase enrichment, suggestive of an S/G2 arrest, contrasting with the reported H3-Ser10 reduction in RKO cells under similar conditions (Bader *et al.* 2021). The persistence of H3-Ser10 phosphorylation in our cyclic hypoxia model, despite S-phase accumulation, underscores a critical cell-line dependency in the execution of hypoxic cell cycle checkpoints. This heterogeneity likely stems from intrinsic genetic backgrounds, including mutational burden and the status of key oncogenes/tumour suppressors (Olivieri *et al.* 2020; Stewart-Ornstein and Lahav 2017), which fundamentally shape stress response pathways. Importantly, despite significant cell cycle perturbations under severe hypoxia, clonogenic survival remained unaffected across all hypoxic regimens in all breast cancer cell lines tested. This finding highlights the remarkable capacity of cancer cells to recover proliferative potential upon reoxygenation (Pires *et al.* 2010), a crucial factor in tumour repopulation post-therapy.

The absence of detectable 53BP1 foci under all hypoxic conditions, coupled with the induction of DNA damage/replication stress markers only upon exposure to <0.1% O_2, further emphasises

the graded nature of hypoxia's impact. This finding partially diverges from reports implicating cyclic hypoxia in DNA damage accumulation (Bader *et al*. 2021), again pointing to significant cell-line-specific and perhaps even cancer model variations in managing hypoxic stress. This context is vital for interpreting differential DDRi responses.

Our exploration of PARPi sensitivity of hypoxic cells revealed a striking oxygen-dependent dichotomy. As anticipated based on hypoxia-induced HR repression (Chan *et al*. 2010; Lu *et al*. 2011), treatment with <0.1% O_2 sensitised breast cancer cells to Olaparib, correlating with diminished RAD51 levels–a key mediator of HR. However, a clinically relevant resistance phenotype emerged in cells exposed to 2% O_2 and cyclic hypoxia, both conditions where we report unaltered RAD51 protein levels. This suggests that RAD51 abundance alone is an insufficient predictor of functional HR competency under these oxygen tensions. Perhaps, investigation of RAD51 foci levels in such conditions would provide more useful insight into this mechanistic aspect. Nonetheless, the resistance observed aligns with reports where RAD51 protein levels remained stable and PARPi cytotoxicity decreased (Kumareswaran *et al*. 2015), implying that HR may remain functionally adequate, or alternative repair pathways are engaged, to confer survival under moderate/cyclic hypoxia. Notably, our findings represent the first report of a cyclic hypoxia–driven resistance phenotype to PARP inhibition, unveiling a previously unrecognised adaptive mechanism that may compromise therapeutic efficacy within fluctuating tumour oxygen microenvironments.

The reversal of this resistance phenotype by the antioxidant N-acetylcysteine (NAC) implicates reactive oxygen species (ROS) as a mediator. This finding seemingly contradicts the hypothesis that resistance in conditions of 2% O_2 stems from reduced ROS levels (Mehibel *et al*. 2021). Our concurrent detection of nuclear H_2O_2 accumulation at both <0.1% and 2% O_2 using a plasmid-based sensor suggests a more complex redox landscape. We propose that the kinetics, cellular compartmentalisation, and/or signalling functions of hypoxia-induced ROS, rather than

mere presence or absence, critically influence PARPi response. NAC may disrupt pro-survival ROS signalling cascades activated specifically under moderate/cyclic hypoxia, thereby re-sensitising cells. While confirming NAC's ROS-scavenging efficacy within our specific assays is a noted limitation, the concordance between the functional rescue by NAC and measurable H_2O_2 accumulation provides compelling, albeit preliminary, evidence for ROS involvement. Furthermore, emerging clinical data links PARPi resistance to hypoxia pathways alongside EMT and Myc/E2F signalling (Liu *et al*. 2022b), suggesting multifactorial resistance mechanisms operating in moderate hypoxia that extend beyond HR status, potentially involving altered cell fate decisions or survival pathway activation.

Preliminary investigation into the novel PolQi, ART558, revealed intriguing cell-line and oxygen-context dependent cytotoxicity. The differential normoxic sensitivity between CAL-51 and MDA-MB-231 cells aligns with the concept of PolQi synthetic lethality in specific genetic contexts (Zatreanu *et al*. 2021). Hypoxia further modulated this response: severe hypoxia sensitised CAL-51 but not MDA-MB-231, while moderate hypoxia induced resistance in CAL-51 and potential sensitisation in MDA-MB-231. Critically, cyclic hypoxia promoted resistance in both lines. This complex pattern underscores the profound influence of the hypoxic spectrum on the therapeutic window of emerging DDRi like PolQi. It suggests that hypoxia may alter the reliance on PolQ-mediated repair (e.g., MMEJ) or create synthetic lethal vulnerabilities unique to specific oxygen tensions and genetic backgrounds. Further mechanistic dissection is warranted to unravel these interactions.

Aligning with previous reports directly testing cytotoxicity of Olaparib towards the same two TNBC cells lines we modelled (Zhao *et al*. 2018) our data show a higher IC50 of Olaparib in CAL-51 cells compared to MDA-MB-231 cells, in normoxic conditions. Further investigation into the status of the genes encoding the key proteins known to confer HR functional deficiencies, including *BRCA1/2*, *RAD51C*, *ATM*, *ATRX*, *PALB2*, *ARID1A*, *BARD1* and others (Nakamura *et al*. 2025;

Yamamoto and Hirasawa 2021), using publicly available cell line sequencing data from the Cancer Cell Line Encyclopaedia (CCLE) dataset accessed *via* cBioportal (Cerami *et al.* 2012), revealed that a number of those genes in CAL-51 cells carry pathogenic mutations, in contrast to the fully wild-type status of all the key HR protein encoding genes in MDA-MB-231 cells, as it can be seen in the respective oncoprint diagrams (appendix 2). This suggests that CAL-51 cells have a lower functional capacity than MDA-MB-231 cells, as further supported by the same phenotype in normoxic conditions upon treatment with the PolQi, ART558. Despite the fact that some of the key HR genes are known to exhibit haploinsufficiency (Ahuja *et al.* 2008; Minello and Carreira 2024; Warren *et al.* 2003), even monoallelic mutations are able to cause partial HR deficiencies, reducing to variable extends, the functional capacity of this repair pathway (Cousineau and Belmaaza 2007; Minello and Carreira 2024; Smith *et al.* 2019). Aligning with this hypothesis, CAL-51 cells formed distinctively less RAD51 foci in response to ionising radiation (IR) treatment, compared to a fully wild-type cell line, but more foci compared to a fully null *BRCA1* cell line, in a relevant study (Graeser *et al.* 2010), supportive of partial deficiency of HR in CAL-51 cells. It would be interesting, nonetheless, to test the HR functional capacity using golden- standard reporter assays for HR capacity, to fully elucidate the mechanism of the differential sensitivity, towards DDRi.

While this part of our study provides significant insights into the oxygen-dependent modulation of DDRi responses, several limitations warrant consideration**.** Firstly, the mechanistic link between ROS and Olaparib resistance in conditions of 2% O_2/cyclic hypoxia, though strongly suggested by the NAC rescue and H_2O_2 detection, requires further validation. The absence of direct, concurrent measurement of NAC's ROS-scavenging efficacy within the specific clonogenic survival assays limits our ability to definitively attribute the sensitisation effect solely to ROS ablation. Secondly, the data concerning the novel PolQi ART558, while revealing intriguing oxygen- and cell-line-dependent effects, remain preliminary. A more comprehensive assessment, including mechanistic studies on PolQ function, DNA repair

pathway engagement (e.g., TMEJ), and replication stress under different hypoxic regimes, is essential to fully understand these complex interactions. Thirdly, our findings are derived primarily from two specific TNBC cell line models (CAL-51, MDA-MB-231). The pronounced cell-line dependency observed in hypoxic responses (e.g., H3-Ser10 dynamics, DNA damage accumulation) underscores the necessity to validate key conclusions across a broader panel of models with diverse genetic backgrounds to assess the generalisability of our observations. Finally, the *in vitro* nature of our experiments, while crucial for controlled mechanistic dissection, cannot fully recapitulate the dynamic complexity of the *in vivo* TME, including stromal interactions, metabolic gradients, and immune influences, which may further modulate hypoxia-DDRi interactions.

Finally, our systematic review crystallises a critical gap in the field: while profound hypoxia (<0.2% O_2) consistently sensitises to PARPi, the impact of the more prevalent moderate hypoxia (≥1% O_2) is significantly understudied. Our data robustly contribute to filling this void, demonstrating that moderate and cyclic hypoxia are potent drivers of PARPi resistance, mediated at least partially by ROS-dependent mechanisms. This reinforces the paramount importance of accurately modelling the spectrum of tumour hypoxia in preclinical studies to predict clinical DDRi efficacy reliably.

Collectively, this part of our work demonstrates that hypoxia is not a single rather entity but a dynamic spectrum eliciting distinct cellular adaptations that profoundly and differentially modulate DDRi sensitivity. The observed resistance to Olaparib under moderate/cyclic hypoxia, potentially orchestrated by nuanced ROS signalling, alongside the complex oxygen-dependent responses to PolQi, highlights the challenges and opportunities in targeting hypoxic tumour subpopulations. The significant cell-line dependency observed throughout our study underscores the necessity of personalised approaches, considering both tumour genetics and the specific characteristics of the hypoxic microenvironment. Moving forward, deciphering the

precise molecular mechanisms linking oxygen tension, ROS dynamics, and DDR pathway functionality will be essential for developing strategies to overcome microenvironment-driven resistance and fully realise the potential of DDRi in cancer treatment.

Chapter 4 Hypoxia-induced changes in gene expression

4.1. Introduction

Hypoxia-mediated changes in gene expression pose an interesting research field. From well-established hypoxia-mediated upregulations of genes like, *CAIX* and *VEGF* (Kaluz *et al*. 2002; Shweiki *et al*. 1992), to the much more newly discovered changes in expression levels of genes, like those of the *APOBEC* family and *SETX* (Bader *et al*. 2021; Ramachandran *et al*. 2021), knowledge on such mechanisms, provides useful tools for unravelling the biology of tumour hypoxia and ultimately, enabling the discovery of targets that can be used to eliminate hypoxic tumour cells.

In this part of our work, we investigated such hypoxia mediated changes in gene expression, starting by validation of data from RNA-sequencing (RNA-seq) of MDA-MB-231 cells, exposed to different oxygen levels (<0.1%, 2% O_2 and cyclic hypoxia) (Simpson, CJ., Hammond, EM., 2020, unpublished). We examined gene expression changes which were suggested by our RNA-seq data. Specifically, we investigated the oxygen-dependency of genes that were mostly upregulated in cyclic hypoxic conditions, due to the physiological relevance of this hypoxia type (appendix 3). We eventually focused on studying four genes, which were filtered down based on a pipeline we created, to identify potential gene-targets of interest. The criteria we set for the gene selection process, are displayed below (figure 4.1). For each one of the four genes we selected, we analysed first the oxygen-dependency of their mRNA levels, using a different cell line to the one used for our RNA-seq, as a validation approach. Then, we carried out survival analyses, comparing survival outcomes in patients with high *vs.* low tumour mRNA levels of each gene, using publicly available data from the TCGA BRCA patient cohort, to get a preliminary view of their potential clinical relevance. Using the same dataset, we also analysed the correlation between a clinically validated, hypoxia-associated gene signature, with the tumour mRNA levels of each one of the four genes. Ax described in our methodology (section 2.2.2), the reduced 15-gene hypoxia

metagene (Buffa *et al*. 2010) was used for this purpose. Consistent with our methodological framework (see Methods), the reduced 15-gene hypoxia metagene retained the core transcriptional structure of the full Buffa signature - capturing 64.6% of variance in PC1+PC2 compared to 60.4% for the full 51-gene set - and showed strong concordance with the full Buffa hypoxia signature across datasets, indicating that the reduced set captures the major transcriptional signal of the full signature. Similarly, principal component analysis of the Ragnum hypoxia signature demonstrated that a top-15 gene subset explained substantially more variance than the full gene set (69.3% vs. 54.4% for PC1+PC2), further supporting the use of reduced, highly co-expressed subsets as biologically informative proxies in downstream correlation analyses (appendix 4).

We used this investigation approach to enable us to further focus our study on genes that have some prognostic potential and preferably, an additional significant correlation with hypoxia in patient tumour samples. Thus, we hoped to identify hypoxia biomarker candidates and further study their biological roles in hypoxic cells.

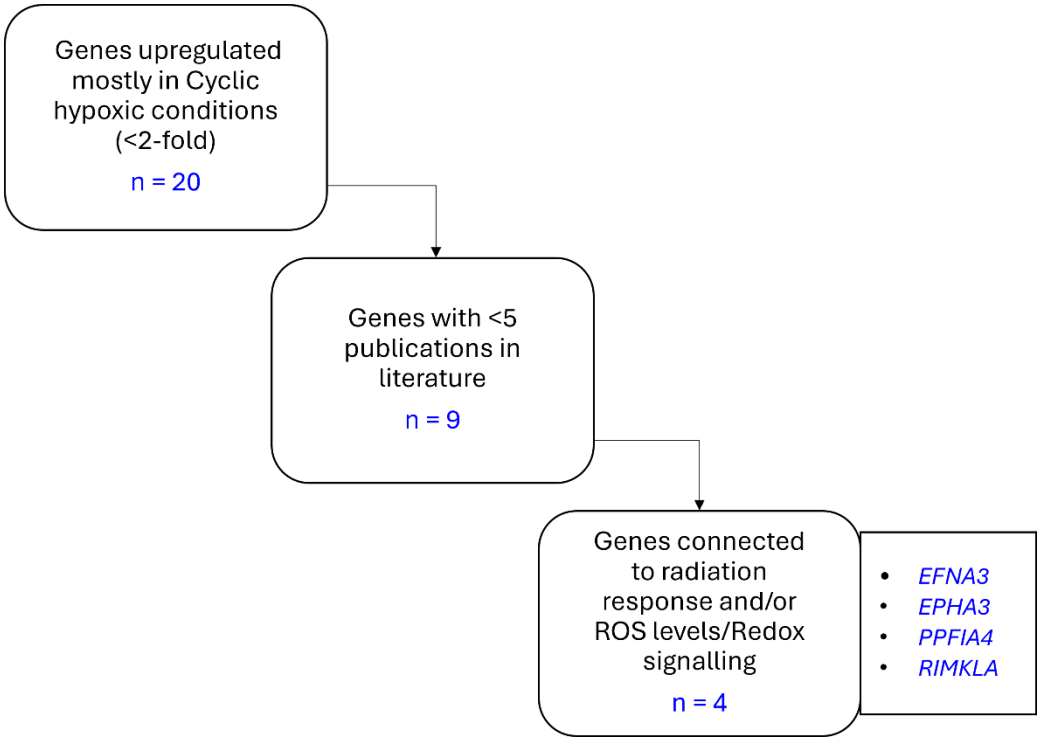

Figure 4.1. Selecting genes of interest. The pipeline we used for the selection of genes to further investigate is shown. A <2-fold increase was the first filtering criterion. Genes with less than 5 PubMed publications were included. This was the second criterion, opting to eliminate well-known hypoxia-inducible genes. Literature connection (i.e., peer-reviewed publication) to radiation response and/or ROS levels/Redox signalling was the final criterion for gene filtering.

4.2. Results

4.2.1. *EPHA3*

The *EPHA3* gene, encodes the Ephrin (EPH)-A3 receptor, a receptor tyrosine-kinase of the EPH subfamily (Beckmann *et al*. 1994). The EPH and EPH-like receptors have been mainly associated with developmental signalling pathways, particularly in the nervous system (Flanagan and Vanderhaeghen 1998). EPHA3, in specific, binds ephrin-A ligands (EFNA) with high preference for EFNA5. Upon activation by EFNA5, downstream signalling regulates cell-cell adhesion, cytoskeletal organisation, and cell migration (Lawrenson *et al*. 2002). Interestingly, in breast cancer, EPHA3 has been shown to facilitate breast cancer cell motility and in head and neck cancer, it has been associated with increasing radiation resistance, *via* the PTEN/Akt/EMT pathway (Beckmann *et al*. 1994; Talia *et al*. 2023).

First, we analysed the mRNA levels of *EPHA3* in hypoxic CAL-51 cells, by RT-qPCR. Our data showed that its expression was significantly upregulated in cells exposed to 2% O_2, but not in response to <0.1% O_2 or cyclic hypoxia (figure 4.2, A, B). Furthermore, correlation analysis of the gene's mRNA levels with the top-15 genes of the hypoxia metagene (Buffa signature) (Buffa *et al*. 2010), using the TCGA BRCA dataset, showed a significant negative correlation, suggestive of a downregulation of *EPHA3* expression in tumour samples from this cohort (figure 4.2, C). Finally, analysis of percent overall survival (%OS) and percent progression-free survival (%PFS) in patients with high *vs*. patients with low mRNA levels of *EPHA3* using data from the TCGA BRCA dataset, did not show any significant difference for disease progression but a significant difference in overall survival (figure 4.2, D and E). Collectively, these findings suggest that *EPHA3* might not be hypoxia-inducible but might have some prognostic potential in breast cancer.

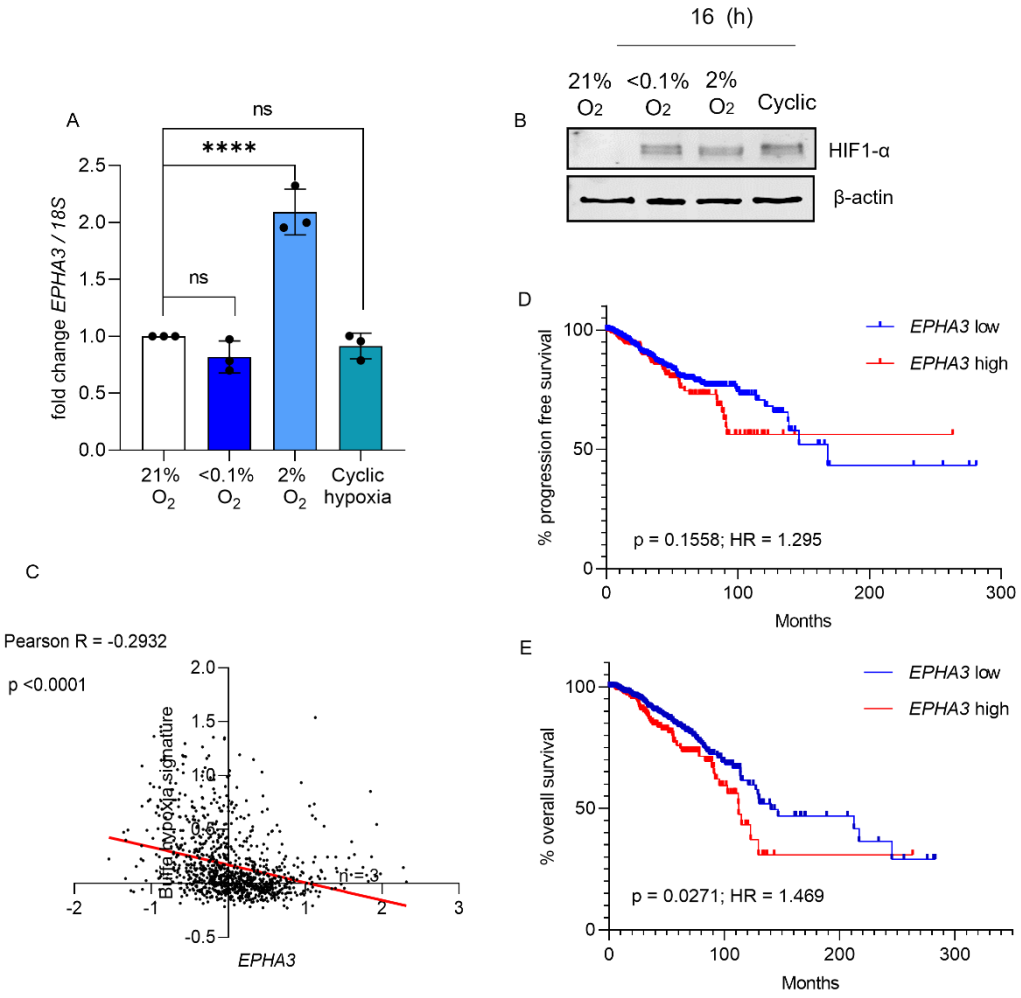

Figure 4.2. The oxygen-dependency of *EPHA3*. (A) CAL-51 cells were exposed to the indicated hypoxia treatments for 16 h. Samples were analysed by RT-qPCR for *EPHA3* mRNA levels. *18S* was used as a housekeeping control. n = 3. (B) Western blot analysis of HIF-1α protein levels from part A, as control of hypoxia induction. (C) Correlation analysis by linear regression, of *EPHA3* mRNA levels from publicly available TCGA BRCA patient sample transcriptomic data (n = 1084), with the mRNA levels of the top-15 genes from the Buffa hypoxia signature, in the same patient samples. The log-mean expression of the top-15 genes from the Buffa hypoxia for each sample dataset is shown, correlated to the log-mean expression of *EPHA3* mRNA. The Pearson R correlation coefficient, and p value are displayed. (D) and (E) TCGA BRCA data were downloaded from cBioportal. Using mRNA expression levels for *EPHA3*, lower quartiles (Q1-Q3) (low) and upper quartile (Q4) (high) groups were identified. Interrogation of clinical data indicated that tumours with high *EPHA3* expression compared to those with low show: in part D., no difference in progression of disease (HR = 1.295; p = 0.1558, Log-rank test) and in part E, significant difference in overall survival (HR = 1.469; p = 0.0271, Log-rank test).

4.2.2. *EFNA3*

This gene encodes Ephrin 3, a protein of the ephrin family. Ephrin 3, is anchored to the cell membrane *via* a glycosylphosphatidylinositol linkage and binds EPH and EPH-like receptor tyrosine-kinases to mediate developmental processes, especially in the nervous system and in erythropoiesis (Davis *et al*. 1994; Zhou 1998). It has been implicated as a prognostic factor in lung adenocarcinoma and gastric cancer (Deng *et al*. 2021; Yiminniyaze *et al*. 2023; Zheng *et al*. 2021) and interestingly it has been shown that the Ephrin-A3/EphA2 axis is a hypoxia-sensitive modulator of hepatocellular carcinoma (HCC) metabolism and a key contributor to HCC initiation and progression (Husain *et al*. 2022). Moreover, downregulation of *EFNA3* by mir-210 has been implicated in radiation response in human hepatoma xenograft experiments (Yang *et al*. 2013).

Using RT-qPCR we investigated the oxygen-dependency of *EFNA3* in CAL-51 cells exposed to different oxygen levels. Our data showed a significant upregulation of its mRNA levels in <0.1% O_2 and cyclic hypoxic conditions but surprisingly, not in response to 2% O_2 (figure 4.3, A). As expected, considering its previously published connection to tumour hypoxia, correlation analysis of *EFNA3* mRNA levels with the top-15 genes of the hypoxia metagene signature was significantly positive, in tumour samples of the TCGA BRCA dataset (figure 4.3, B). Comparison of %OS and %PFS in TCGA BRCA patients with high *vs*. patients with low *EFNA3* levels, did not show a prognostic significance in terms of %OS; it did however hint at a significant difference in the progression of disease (figure 4.3, C and D). Together, this data show that, *EFNA3* expression in breast cancer cells might be upregulated at some oxygen levels (perhaps in an oxygen-dependent manner) and probably possesses some prognostic potential.

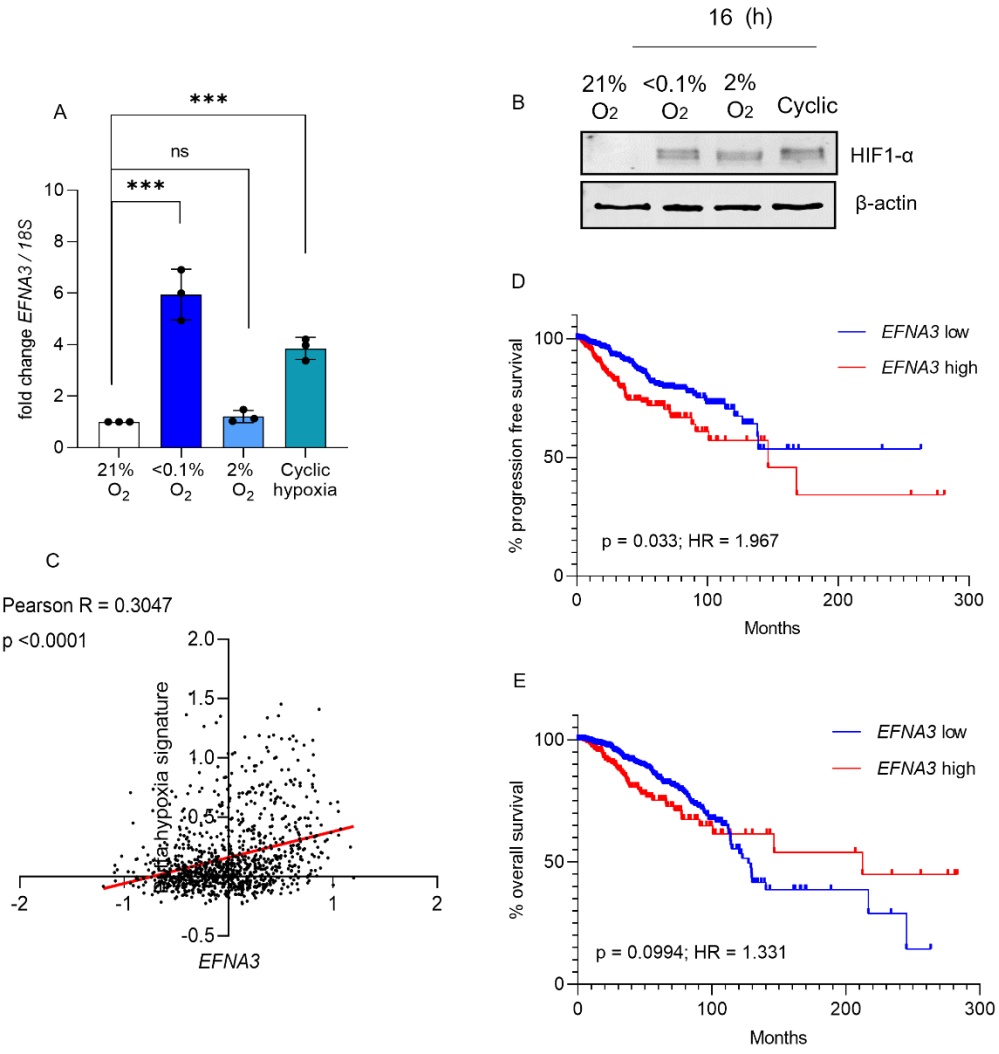

Figure 4.3. The oxygen-dependency of *EFNA3*. (A) CAL-51 cells were exposed to the indicated hypoxia treatments for 16 h. Samples were analysed by RT-qPCR for *EFNA3* mRNA levels. *18S* was used as a housekeeping control. n = 3. (B) Western blot analysis of HIF-1α protein levels from part A, as control of hypoxia induction (Data also shown in fig. 4.2). (C) Correlation analysis by linear regression, of *EFNA3* mRNA levels from publicly available TCGA BRCA patient sample transcriptomic data (n = 1084), with the mRNA levels of the top-15 genes from the Buffa hypoxia signature, in the same patient samples. The log-mean expression of the top-15 genes from the Buffa hypoxia for each sample dataset is shown, correlated to the log mean expression of *EFNA3* mRNA. The Pearson R correlation coefficient, and p value are displayed. (D) and (E) TCGA BRCA data were downloaded from cBioportal. Using mRNA expression levels for *EFNA3*, lower quartiles (Q1-Q3) (low) and upper quartile (Q4) (high) groups were identified. Interrogation of clinical data indicated that tumours with high *EFNA3* expression compared to those with low: in part D., significant difference in progression of disease (HR = 1.967; p = 0.033, Log-rank test) and in part E, no difference in overall survival (HR = 0.1.331; p = 0.0994, Log-rank test).

4.2.3. *PPFIA4*

Also known as *LIPA4*, *PPFIA4* (Protein Tyrosine Phosphatase Receptor Type F Polypeptide-Interacting Protein Alpha-4) encodes the protein Liprin-A4. Liprins, are a group of proteins which interact with transmembrane protein tyrosine phosphatases, mediating developmental processes in mammary tissue, as well as axon guidance (Serra-Pages *et al*. 1995; Serra-Pages *et al*. 1998). The exact biological role of *PPFIA4* in normal cells, has not yet been fully elucidated. The gene and its protein product have been associated, nonetheless, to both cancer and hypoxia by a limited number of studies: it has been shown that HIF-1α mediates an upregulation of *PPFIA4* which in turn promotes proliferation, migration reprogramming of glucose metabolism in ovarian, colon and oesophageal cancer cells (He *et al*. 2023; Huang *et al*. 2021b; Tan *et al*. 2023b). Interestingly, a recent study showed that *PPFIA4* promotes castration-resistant prostate cancer by enhancing mitochondrial metabolism through methylenetetrahydrofolate dehydrogenase 2 (MTHFD2), and showed that depletion of *PPFIA4* impacted ROS levels, $NADP/NADPH^{+}$ ratio and mitochondrial membrane potential (Zhao *et al*. 2022).

Analysis of *PPFIA4* mRNA levels, by RT-qPCR, using CAL-51 cells exposed to different oxygen levels, showed that it was indeed, significantly upregulated in response to all tested oxygen levels (figure 4.4, A). Additionally, in support of the hypoxia-mediated induction of this gene, a significant correlation to the top-15 genes of the hypoxia metagene (Buffa) signature in the TCGA BRCA tumour sample dataset, was also seen in our analysis (figure 4.4, B). Surprisingly, survival analysis of TCGA BRCA data from patients with high compared to those with low tumour mRNA levels of *PPFIA4*, showed a non-significant trend towards better prognosis for those with higher *PPFIA4* levels, both in terms of %OS and %PFS (figure 4.4. C and D).

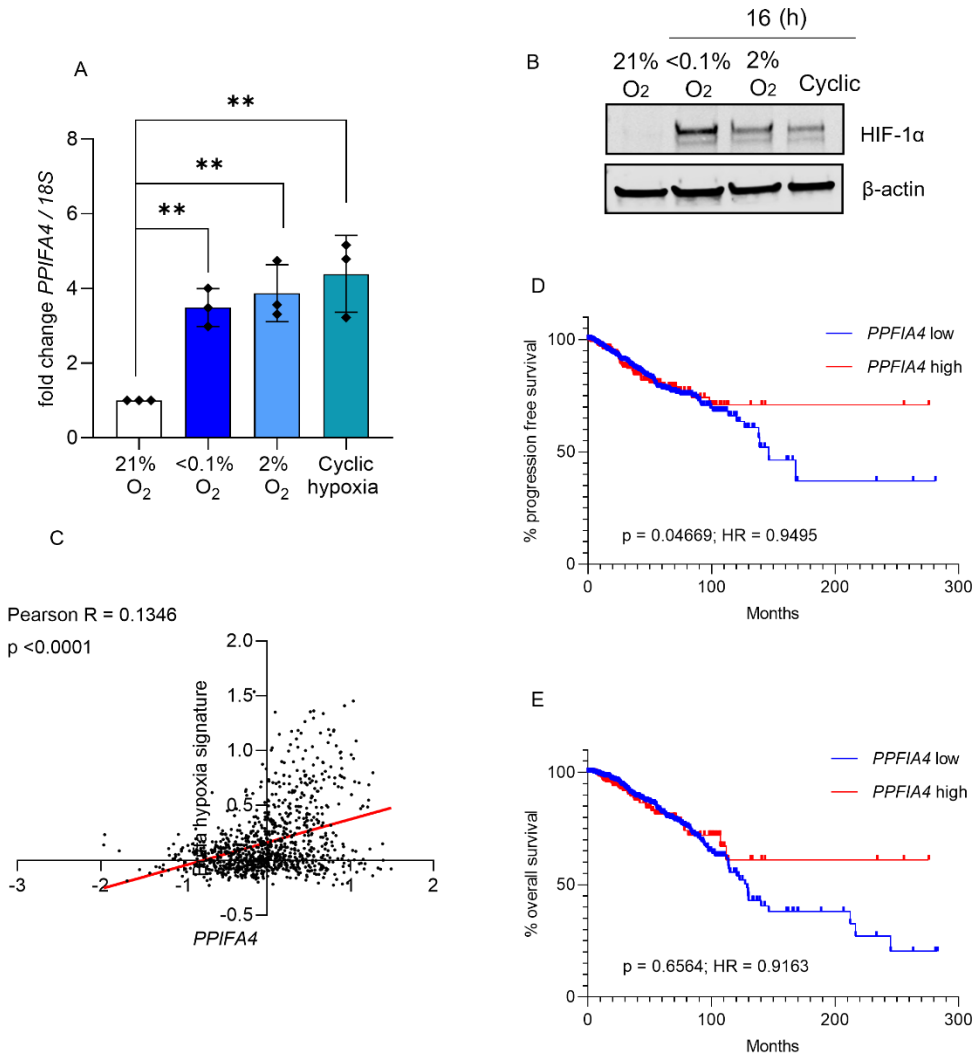

Figure 4.4. The oxygen-dependency of *PPFIA4*. (A) CAL-51 cells were exposed to the indicated hypoxia treatments for 16 h. Samples were analysed by RT-qPCR for *PPFIA4* mRNA levels. *18S* was used as a housekeeping control. n = 3. (B)) Western blot analysis of HIF-1α protein levels from part A, as control of hypoxia induction. (C) Correlation analysis by linear regression, of *PPFIA4* mRNA levels from publicly available TCGA BRCA patient sample transcriptomic data (n = 1084), with the mRNA levels of the top-15 genes from the Buffa hypoxia signature, in the same patient samples. The log-mean expression of the top-15 genes from the Buffa hypoxia for each sample dataset is shown, correlated to the log mean expression of *PPFIA4* mRNA. The Pearson R correlation coefficient, and p value are displayed. (D), (E) TCGA BRCA data were downloaded from cBioportal. Using mRNA expression levels for *PPFIA4*, lower quartiles (Q1-Q3) (low) and upper quartile (Q4) (high) groups were identified. Interrogation of clinical data indicated that tumours with high *PPFIA4* expression compared to those with low: in part D., lower probability of progression of disease (HR = 0.9495; p = 0.04669, Log-rank test) and in part E, better overall survival (HR = 0.9163; p = 0.6564, Log-rank test).

4.2.4. PPFIA4 protein levels in response to hypoxia

The data described in the previous section, placed PPFIA4 as a potentially hypoxia-inducible gene-target in hypoxic cancer cells and tumours. As a next step, we wanted to validate the hypoxia-mediated upregulation in an additional cell line, testing mRNA, and protein levels.

Surprisingly, RT-qPCR analysis of *PPFIA4* mRNA levels in MDA-MB-231 cells treated with different oxygen levels showed a significant upregulation in 2% O_2 and cyclic hypoxic conditions, but not in response to treatment with <0.1% O_2 (figure 4.5, A). In addition, analysis of PPFIA4 protein levels in the same cells showed a detectable protein level increase, only in cells treated with 2% O_2 (figure 4.5, B and C).

These data collectively, suggested that not all hypoxic cells upregulate PPFIA4 levels, despite published data that report *PPFIA4* to be a HIF-1α target (Tan *et al*. 2023b).

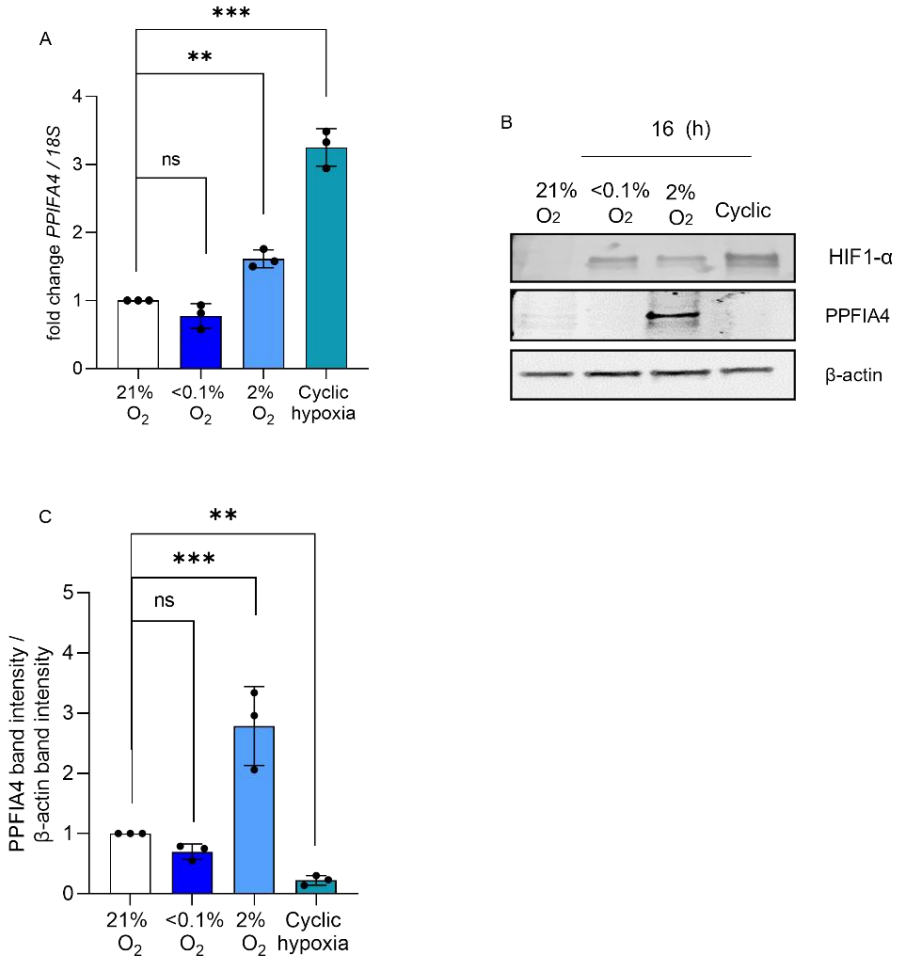

Figure 4.5. Analysis of mRNA and protein levels of PPFIA4 in hypoxia. MDA-MB-231 cells were exposed to the indicated hypoxia treatments for 16 h and samples were harvested for: (A) Analysis of *PPFIA4* mRNA levels by RT-qPCR, using *18S* as a housekeeping gene. (B) Analysis of protein levels of PPFIA4 by western blot, using β-actin as loading control. (C) Quantification of western blot analysis of PPFIA4 protein levels, from part B. n = 3.

4.2.5. *RIMKLA*

The *Ribosomal modification protein RimK-like A* (*RIMKLA)*, its biological role and its associations to cancer biology and hypoxia, are thoroughly described in previous sections (1.5.4). As explained, the enzyme product of *RIMKLA*, has the potential to impact redox signalling in cancer cells, through its function in generating NAAG, which can act as glutamate reservoir in cancer cells, with glutamate being one of the main amino acids associated with redox homeostatic mechanisms of the cell (section 1.5.4 and figure 1.17). Therefore, it satisfied the criteria we set for further investigation.

We started our investigation by analysing the oxygen-dependency of *RIMKLA*, by means of RT-qPCR in CAL-51 cells treated with different oxygen levels. Results showed an increase in *RIMKLA* mRNA levels in response to all tested hypoxia treatments (figure 4.6, A).

Using transcriptomic data from TCGA BRCA patient samples, we analysed the type and degree of correlation between mRNA levels of *RIMKLA* and the top-15 genes of the hypoxia metagene in these tumours, with the analysis showing a significant, albeit quantitatively small, negative correlation (figure 4.6, B).

Comparison of survival outcomes in patients of the TCGA BRCA dataset, comparing high *vs.* low tumour mRNA levels of *RIMKLA* showed a significantly worse prognosis for patients with higher *RIMKLA* tumour levels, both in terms of %OS and %PFS (figure 4.6, C and D).

The above-described findings suggested that *RIMKLA* might be a good prognostic biomarker for patients with invasive breast cancers, but not specific for hypoxic tumours.

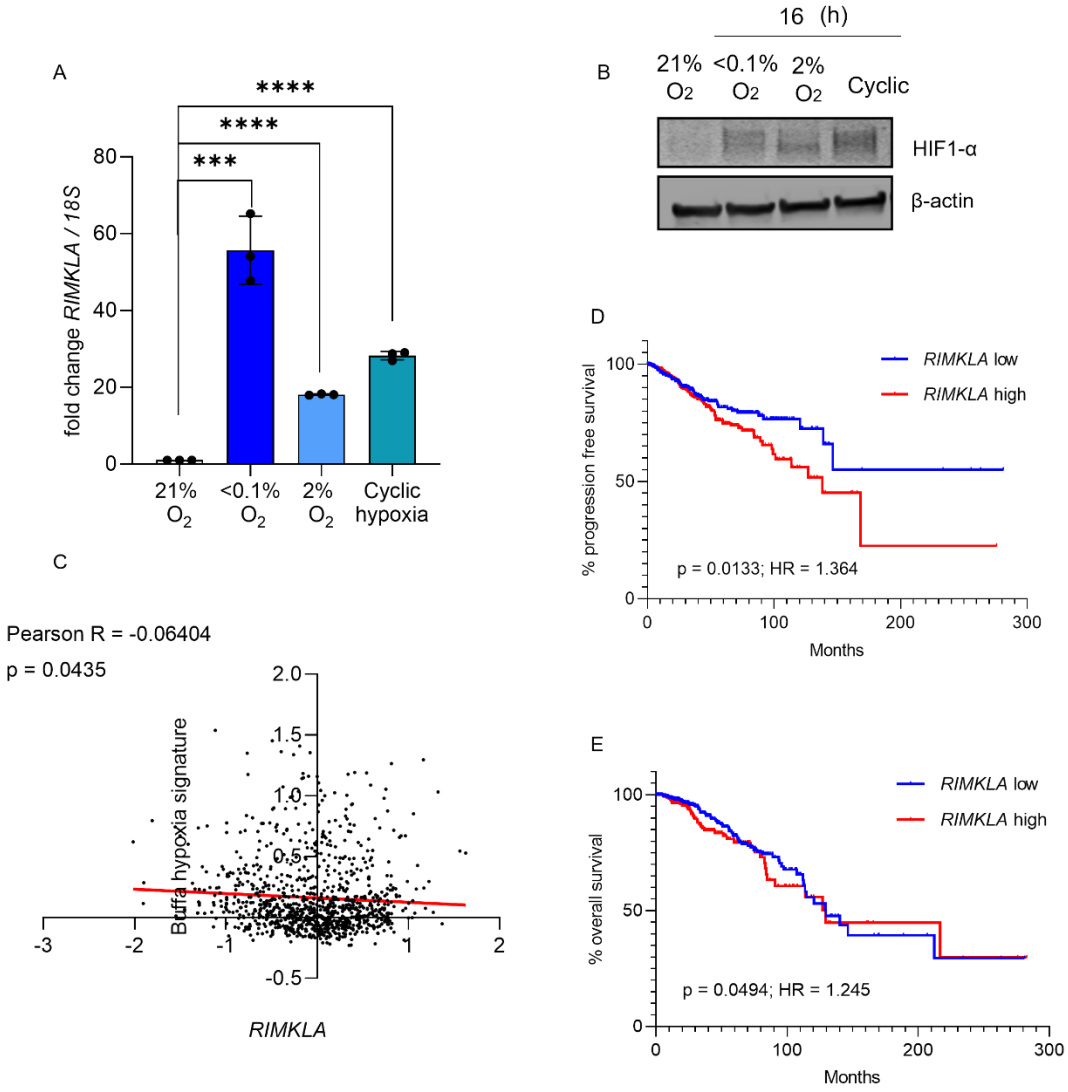

Figure 4.6. The oxygen-dependency of *RIMKLA*. (A) CAL-51 cells were exposed to the indicated hypoxia treatments for 16 h. Samples were analysed by RT-qPCR for *RIMKLA* mRNA levels. *18S* was used as a housekeeping control. n = 3. (B) Western blot analysis of HIF-1α protein levels from part A, as control of hypoxia induction. (C) Correlation analysis by linear regression, of *RIMKLA* mRNA levels from publicly available TCGA BRCA patient sample transcriptomic data (n = 1084), with the mRNA levels of the top-15 genes from the Buffa hypoxia signature, in the same patient samples. The log-mean expression of the top-15 genes from the Buffa hypoxia for each sample dataset is shown, correlated to the log mean expression of *RIMKLA* mRNA. The Pearson R correlation coefficient, and p value are displayed. (D), (E) TCGA BRCA data were downloaded from cBioportal. Using mRNA expression levels for *RIMKLA*, lower quartiles (Q1-Q3) (low) and upper quartile (Q4) (high) groups were identified. Interrogation of clinical data indicated that tumours with high *RIMKLA* expression compared to those with low: in part D., higher probability of progression of disease (HR = 1.364; p = 0.0133, Log-rank test) and in part E, poorer overall survival (HR = 1.245; p = 0.0494, Log-rank test).

4.2.6. *RIMKLA* mRNA levels exhibit differential correlations with hypoxia associated gene signatures

Despite the data from correlation analysis with the hypoxia metagene pointing towards a low hypoxia-specificity for this gene in the TCGA BRCA dataset, its interesting prognostic potential, especially in terms of %PFS in the same patient cohort, seemed promising. Most importantly, the fact that both RNA-seq and RT-qPCR data previously described (appendix 3 and figure 4.6) suggested an upregulation of *RIMKLA* mRNA levels in response to hypoxia, it felt surprising for this gene to have a negative correlation with the hypoxia metagene. Therefore, we expanded our investigation on the correlation of *RIMKLA* with hypoxia-associated signatures in breast cancer patient samples using an additional, hypoxia-associated gene signature of validated prognostic power.

We analysed the type and degree of correlation of *RIMKLA* mRNA levels in patient samples from two breast cancer datasets, TCGA BRCA and METABRIC, with the top-15 genes of the pimonidazole-specific (Ragnum) hypoxia signature (Ragnum *et al.* 2015). Quite interestingly, the results of this analysis showed a statistically significant, positive correlation coefficient for *RIMKLA*, in both breast tumours datasets, in striking contrast to what we observed previously (figure 4.7, A, B, C and D).

These contradicting data suggested the possibility of a differential correlation pattern for this gene, depending on the different hypoxia-associated signatures and potentially depending on the tumour type that each signature was generated from and their different methodological approaches.

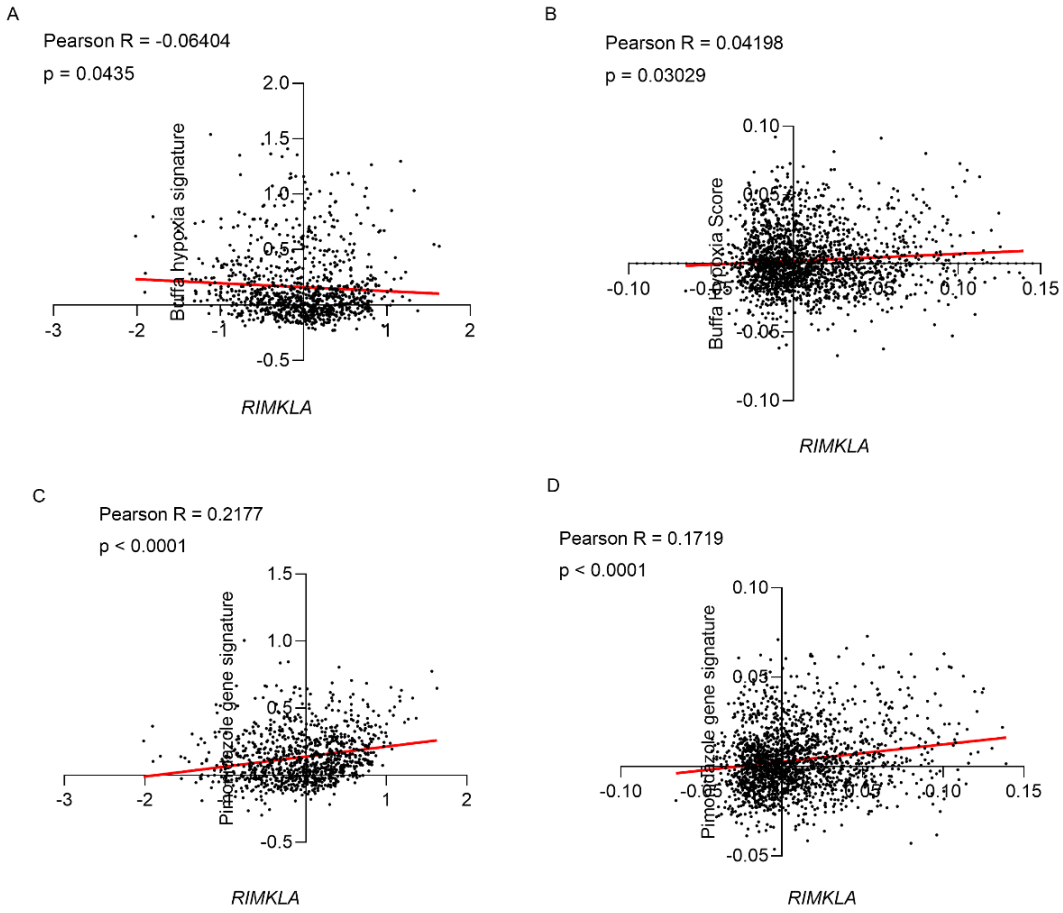

Figure 4.7. Correlation analysis of *RIMKLA* with hypoxia-associated gene signatures in publicly available breast cancer datasets. TCGA BRCA (n = 1084) and METABRIC (n = 2509) gene expression data were accessed and downloaded *via* cBioportal. (A) Pearson's correlation analysis of *RIMKLA* mRNA levels with mRNA levels of the top-15 genes from the hypoxia metagene (Buffa) signature, in samples from patients of the TCGA BRCA dataset. The log-mean expression of the metagene hypoxia signature top-15 genes for each patient dataset is shown, correlated to the log-mean expression of *RIMKLA* mRNA. (B) Pearson's correlation analysis of *RIMKLA* mRNA levels with mRNA levels of the top-15 genes from the hypoxia metagene (Buffa) signature, in samples from patients of the METABRIC dataset. The log-mean expression of the metagene hypoxia signature top-15 genes for each patient dataset is shown, correlated to the log-mean expression of *RIMKLA* mRNA. (Data also shown in figure 4.6) (C) Pearson's correlation analysis of *RIMKLA* mRNA levels with mRNA levels of the top-15 genes from the pimonidazole-specific (Ragnum) signature, in samples from patients of the TCGA BRCA dataset. The log-mean expression of the Ragnum hypoxia signature top-15 genes for each patient dataset is shown, correlated to the log-mean expression of *RIMKLA* mRNA. (D) Pearson's correlation analysis of *RIMKLA* mRNA levels with mRNA levels of the top-15 genes from the pimonidazole-specific (Ragnum) signature, in samples from patients of the METABRIC dataset. The log-mean expression of the metagene hypoxia signature top-15 genes for each patient dataset is shown, correlated to the log-mean expression of *RIMKLA* mRNA.

4.2.7. Correlation analysis of *RIMKLA* mRNA levels with all three clinically validated hypoxia signatures in all TCGA cancer datasets

We thought that the difference in the results of the correlation analysis of *RIMKLA* mRNA levels that we observed between the Buffa and Ragnum hypoxia-associated signatures, in breast cancer patient samples, was very intriguing. Furthermore, a closer look at the Ragnum hypoxia-associated signature revealed that *RIMKLA* was a part of the genes detected in this transcriptomic analysis, although not included in the top-15 genes set. To make sure that we remove biases, we decided to investigate the correlation between *RIMKLA* and hypoxia-inducible genes, using the full gene sets from all three widely known and clinically relevant, hypoxia-associated gene signatures: the hypoxia metagene (Buffa signature), the pimonidazole-specific (Ragnum) hypoxia signature, and the Head-and-neck cancer-specific hypoxia metagene (Winter signature). In addition, we decided to expand our correlation analyses further, using transcriptomic data from all the TCGA cancer types available, to detect if the differential correlation patterns we hypothesised, could be observed in other cancer types, besides breast.

Indeed, a difference in the degree and type correlation of *RIMKLA* levels with the hypoxia-induced genes from all three gene signatures was seen for several cancer types of the TCGA dataset. This finding further supports our previous observation, using different breast cancer datasets. Interestingly, there was no cancer type detected for which all three hypoxia-associated signatures showed a significantly negative correlation with *RIMKLA* mRNA levels. On the other hand, a significantly positive correlation of *RIMKLA* with all three hypoxia-associated gene signatures came up in three cancer types: Liver Hepatocellular Carcinoma (LIHC), Pheochromocytoma and Paraganglioma (PCPG), and Uterine Corpus Endometrial Carcinoma (UCEC). This finding suggests a strong correlation of hypoxia with *RIMKLA,* in patients with these types of cancer.

Table 4.1 Correlation analysis of *RIMKLA* mRNA levels with all three clinically validated hypoxia signatures in all TCGA cancer datasets. TCGA patient sample data were accessed and downloaded from cBioportal. Pearson's R and adjusted p-values after multiple testing correction (Benjamini-Hochberg at FDR = 5%) are presented for all three hypoxia-associated signatures, in all cancer types. Positive R-values and p< 0.05 represent significant positive correlation (purple) whereas, negative R-value and p< 0.05 represent significant negative correlation (green).

	Buffa Hypoxia Score	Ragnum Hypoxia Score	Winter Hypoxia Score
BLCA	R = -0.23 p = 1.995e-6	R = -0.03 p = 0.606	R = -0.30 p = 1.08e-9
LGG	R = -0.05 p = 0.247	R = -0.06 p = 0.174	R = -0.12 p = 7.139e-3
BRCA	R = -0.06 p = 0.0688	R = 0.2177 p = 0.00304	R = -0.01 p = 0.839
CESC	R = -0.25 p = 3.077e-5	R = 0.10 p = 0.109	R = -0.26 p = 1.370e-5
COAD	R = 0.06 p = 0.275	R = 0.11 p = 0.0336	R = 0.07 p = 0.195
GBM	R = 0.04 p = 0.611	R = 0.04 p = 0.671	R = 0.04 p = 0.666
HNSC	R = -0.14 p = 2.348e-3	R = 0.17 p = 2.116e-4	R = -0.17 p = 2.401e-4
KIRC	R = 0.12 p = 0.0212	R = 0.02 p = 0.724	R = -0.08 p = 0.130
KIRP	R = 0.02 p = 0.706	R = 0.03 p = 0.635	R = -0.04 p = 0.526
LIHC	R = 0.19 p = 2.743e-4	R = 0.15 p = 4.151e-3	R = 0.21 p = 1.035e-4
LUAD	R = -0.16 p = 2.099e-4	R = -0.08 p = 0.0827	R = -0.17 p = 1.568e-4
LUSC	R = 0.12 p = 9.499e-3	R = 0.26 p = 1.02e-8	R = 0.06 p = 0.164
OV	R = 0.17 p = 0.0154	R = 0.09 p = 0.198	R = 0.22 p = 1.717e-3
PAAD	R = -0.17 p = 0.0305	R = -0.15 p = 0.0552	R = -0.18 p = 0.0226
PCPG	R = 0.42 p = 4.14e-8	R = 0.22 p = 5.871e-3	R = 0.17 p = 0.0336
PRAD	R = -0.10 p = 0.0647	R = 0.21 p = 1.293e-4	R = -0.12 p = 0.0257
SKCM	R = 0.10 p = 0.0491	R = 0.08 p = 0.110	R = 0.09 p = 0.0736
THCA	R = -0.03 p = 0.506	R = -0.36 p = 3.06e-16	R = -0.02 p = 0.694
UCEC	R = 0.20 p = 9.016e-3	R = 0.25 p = 1.026e-3	R = 0.25 p = 1.211e-3

4.2.8. Expression of *RIMKLA* in publicly available datasets of breast cancer patient samples

The results of the correlation analyses described in the previous section suggested that the differential correlation with the hypoxia-associated signatures might reflect the tumour type that each signature was generated from. Specifically, despite *in vitro* data suggesting the opposite, the mRNA levels of *RIMKLA* in breast tumours could be repressed. To answer this question, we used publicly available transcriptomic data from the TCGA BRCA dataset and analysed the levels of *RIMKLA* in primary breast tumours *vs.* paired normal tissue and *vs*. unpaired normal breast tissue (GTEx data). Results showed that *RIMKLA* was significantly upregulated in primary tumours compared to normal tissue (figure 4.8, A). We further examined the same data, regarding the mRNA levels of *RIMKLA* in breast tumours of the TCGA BRCA cohort, stratified according to tumour stage. Our analysis showed that, advanced disease correlated with higher levels of *RIMKLA* mRNA, with the highest fold-increase being associated with stage IV breast tumours, suggestive of a correlation between *RIMKLA* levels and advanced stages of breast cancer (figure 4.8, B).

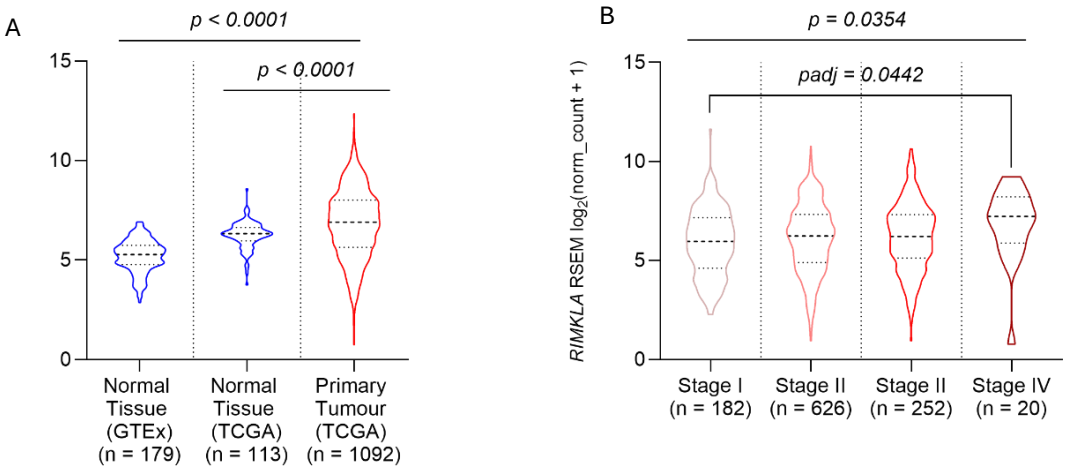

Figure 4.8. *RIMKLA* mRNA increases in breast tumours. TCGA BRCA data (n = 1084) were obtained and analysed from cBioportal. GTEx data were obtained from the GTEx portal (NIH). (A) *RIMKLA* mRNA expression levels, in primary breast cancer samples from TCGA (*n* = 1065) relative to adjacent normal tissue (*n* = 113) and GTEx normal tissue samples (n = 179). (B) *RIMKLA* mRNA expression levels, in primary breast cancer samples (*n* = 1065) relative to adjacent normal tissue (*n* = 114), analysed according to tumour stage. Statistical analysis in part B was performed by one-way ANOVA with Bonferroni's post hoc testing.

4.2.9. Analysis of RIMKLA protein levels in publicly available breast tumour and normal breast tissue samples

To examine if the increase of mRNA levels of *RIMKLA* in breast tumours compared to normal tissue that we described previously corresponds to RIMKLA protein levels as well, we assessed publicly available immunohistochemistry (IHC) data from the Human Protein Atlas (HPA) database.

In this analysis, we compared the extent and the intensity of RIMKLA-positive staining in breast tumour samples and in unpaired, normal breast tissue samples. The number of available samples in each cohort was recorded and plotted for statistical purposes. The histochemistry score (h- score) for RIMKLA staining in both tumour and normal tissue, was calculated according to the following formula: H-Score = (0 x % fraction of no detected) + (1 x % fraction of low intensity) + (2 x % fraction of moderate intensity) + (3 x % fraction of high intensity staining).

Results of this analysis showed a significantly more extensive staining, as well as stronger staining-positivity for RIMKLA in breast tumours, compared to normal tissue samples, as mirrored in the much higher RIMKLA h-score of the former. These data could indicate that protein levels of RIMKLA are also higher in breast cancers compared to normal breast tissue (figure 4.9, A, B and C). Nevertheless, the power of this analysis remains limited, considering the small number of samples available in this repository, and thus the finding are interpreted with caution. Collectively, data from this and the previous section (figure 4.8, A, B) could support that expression of RIMKLA in breast tumours, is higher compared to normal breast tissue.

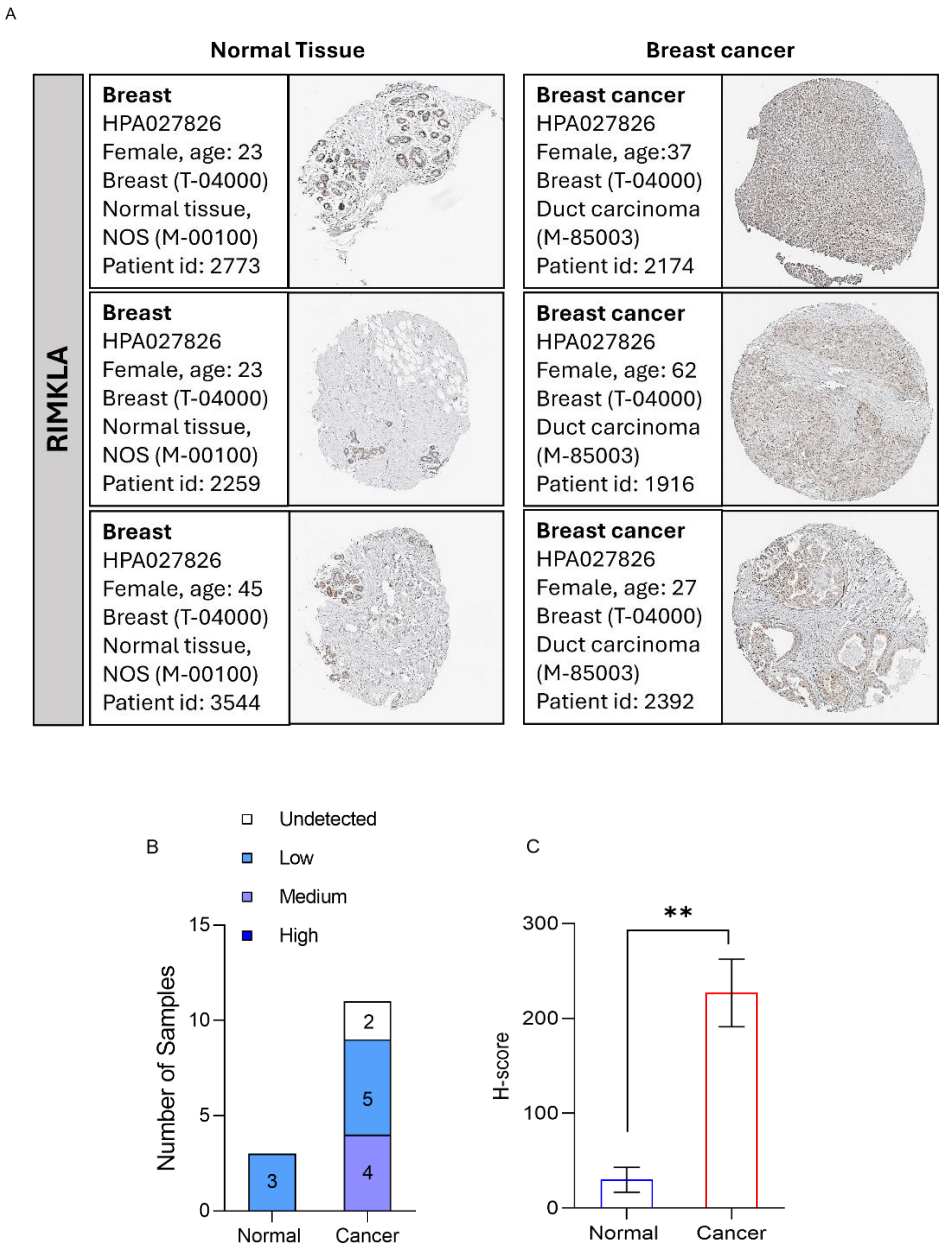

Figure 4.9. Analysis of RIMKLA protein levels in publicly available breast tumour and normal breast tissue samples. Human protein atlas (HPA) IHC data were accessed from www.proteinatlas.org and analysed for RIMKLA staining. (A) Representative images of IHC data from normal (n = 3) and cancerous breast tissue samples (n = 3), stained for RIMKLA. (B) Graphical representation of available samples in normal and breast cancer IHC datasets, on the HPA database. (C) H-score for RIMKLA staining in breast normal and cancerous tissue samples, calculated according to the formula: H-Score = (0 x % fraction of no detected) + (1 x % fraction of low intensity) + (2 x % fraction of moderate intensity) + (3 x % fraction of high intensity staining).

4.2.10. Validation of *RIMKLA* induction in hypoxia using additional breast cancer cell lines

Our findings thus far, suggested that *RIMKLA* might be a good gene-candidate for further research, associated to breast cancer prognosis and hypoxia-specific expression, for several tumour types.

As a next step we aimed to validate the hypoxia-mediated induction of its expression, using additional cancer cell lines. First, the oxygen-dependency of *RIMKLA* was investigated in a second cell line, MDA-MB-231, exposed to different oxygen levels as previously. RT-qPCR analysis of mRNA levels of *RIMKLA* in these cells, showed increased expression levels of the gene, in response to all the tested oxygen levels, with the use of *CAIX* mRNA levels, as a hypoxic control (figure 4.10, A, B). This finding, supports, thus, a cell line-independent, hypoxia-mediated upregulation of *RIMKLA in vitro*.

Since both the cell lines that we have used so far belong to the TNBC type, we wanted to investigate if the hypoxia-mediated gene induction depends on TNBC subtypes or not. For this reason, we used two additional TNBC cell lines, BT549 (TNBC-Mesenchymal) and T47D (Luminal A) which belong to different subtypes from those of CAL-51 (TNBC-Basal-like 2) and MDA-MB-231 (TNBC-Mesenchymal stem-like) cell lines. RT-qPCR analysis of *RIMKLA* mRNA levels in hypoxic BT549 and T74D cells showed an increase in response to both oxygen levels tested (<0.1% and 2% O_2), with *CAIX* mRNA levels analysed simultaneously as a hypoxic control (figure 4.10, C, D). These results are consistent with the hypothesis of the induction of *RIMKLA* in response to hypoxia, suggesting that this finding is moreover, independent of TNBC subtype.

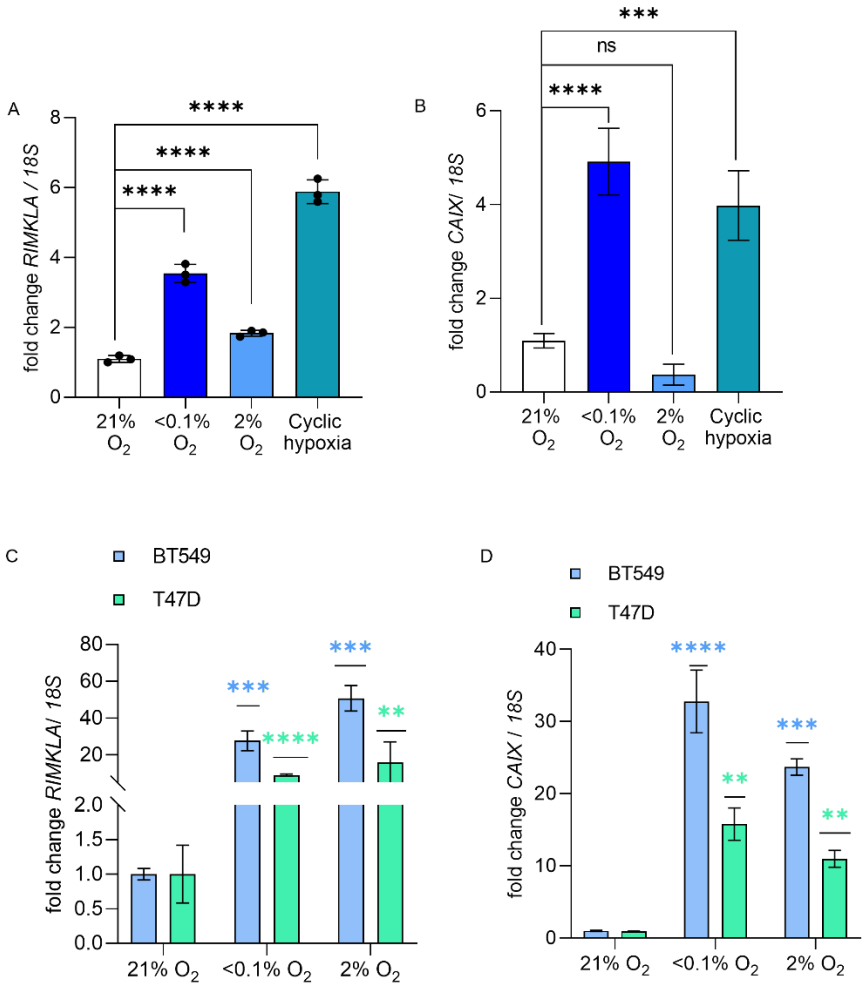

Figure 4.10. Validation of *RIMKLA* induction in hypoxia using additional breast cancer cell lines. (A) MDA-MB-231 cells were exposed to the indicated oxygen levels for 16 h. Samples were used for RT-qPCR analysis of *RIMKLA* mRNA levels, normalised to *18S*. n = 3. (B) RT-qPCR analysis of *CAIX* mRNA levels, normalised to *18S*, used as a hypoxia control for part A. (C) BT549 and T47D cells were exposed to the indicated oxygen levels for 8 h. Samples were used for RT-qPCR analysis of *RIMKLA* mRNA levels, normalised to *18S*. n = 3. (D) RT-qPCR analysis of *CAIX* mRNA levels, normalised to *18S*, as a hypoxia control for part B.

4.2.11. Protein levels of RIMKLA increase in hypoxia

Next, we tested if the induction of *RIMKLA* mRNA levels in response to hypoxia corresponded to a protein level increase, as well. Using CAL-51 and MDA-MB-231 cells exposed to different oxygen levels we carried out a western blot analysis of RIMKLA protein levels.

Results showed that RIMKLA protein levels were indeed, induced in response to hypoxia, compared to normoxic controls (figure 4.11, A, B). Furthermore, an oxygen-dependency of the protein was observed in both cell lines in which protein levels of RIMKLA were tested, coherent with our data from RT-qPCR analysis of *RIMKLA* mRNA levels in the same cell lines, reported in the previous sections, (figure 4.11, A, B, and figures 4.6, A and 4.10, A and C).

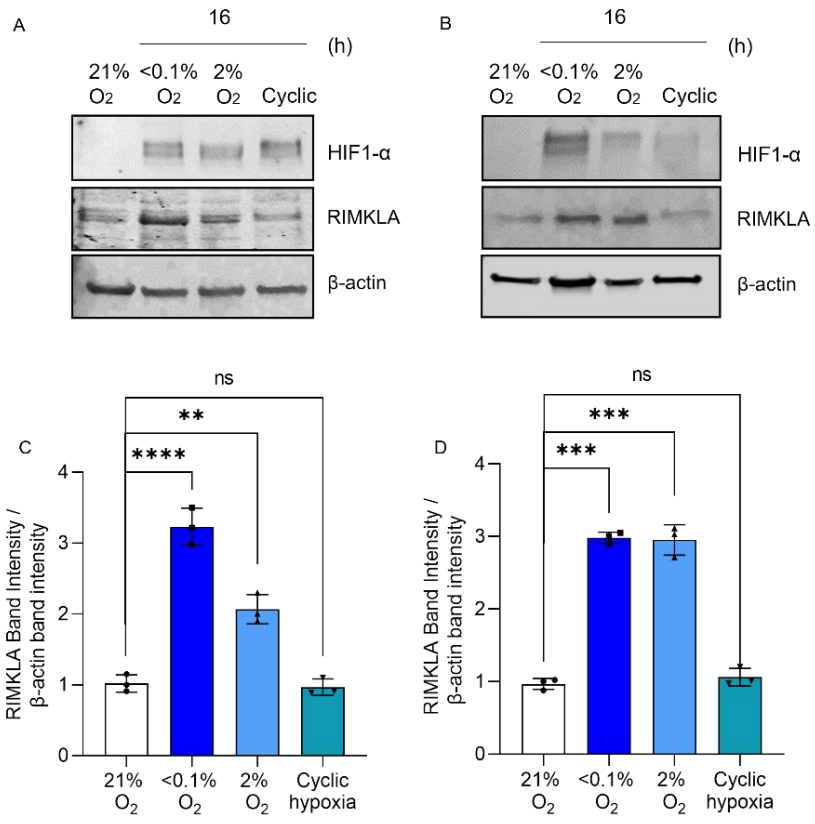

Figure 4.11. RIMKLA protein levels increase in hypoxia. Cells were exposed to the indicated oxygen levels for 16 h. Western blot analysis of RIMKLA protein levels in (A) MDA-MB-231 cells, and (B) CAL-51 cells. HIF-1α was used as a hypoxia control and β-actin, as a loading control. (C) Quantification of RIMKLA levels from MDA-MB-231 cells from part A. (D) Quantification of RIMKLA levels in CAL-51 cells, from part B. n = 3.

4.2.12. Validation of a RIMKLA antibody for immunofluorescence

As a validation for the antibody used for RIMKLA protein levels analyses, we carried out an immunofluorescence assay to determine the accuracy of antibody-mediated detection, with the use of siRNA-mediated knockdown of *RIMKLA* expression (Dana *et al.* 2017). We exposed *Mock*-treated, scramble siRNA (siScr)-transfected, or anti-*RIMKLA* siRNA (si*RIMKLA*)-transfected, CAL-51 cells to <0.1% O_2, which we previously reported (section 4.2.11) to upregulate RIMKLA protein levels. Immunofluorescence analysis of these cells, showed an increase in of RIMKLA protein levels in hypoxic cells that were either treated with mock or were siScr-transfected, compared to the normoxic control. SiRNA-mediated *RIMKLA* knockdown resulted in abrogation of its induction, validating thus, the accuracy of the anti-RIMKLA antibody we used for our experiments (figure 4.12, A). Notably, the antibody we tested exhibited a nucleolar expression of RIMKLA, consistently with previous reports in the HPA data repository (Thul *et al.* 2017). In addition, we carried out a simultaneous RT-qPCR analysis of *RIMKLA* mRNA levels, in *Mock*-treated or *siRIMKLA* transfected CAL-51cells, with samples being harvested 24, 48 and 72 h post-si*RIMKLA* transfection, to determine the optimal time-point efficacy of the siRNA-mediated knockdown (figure 4.12, B).

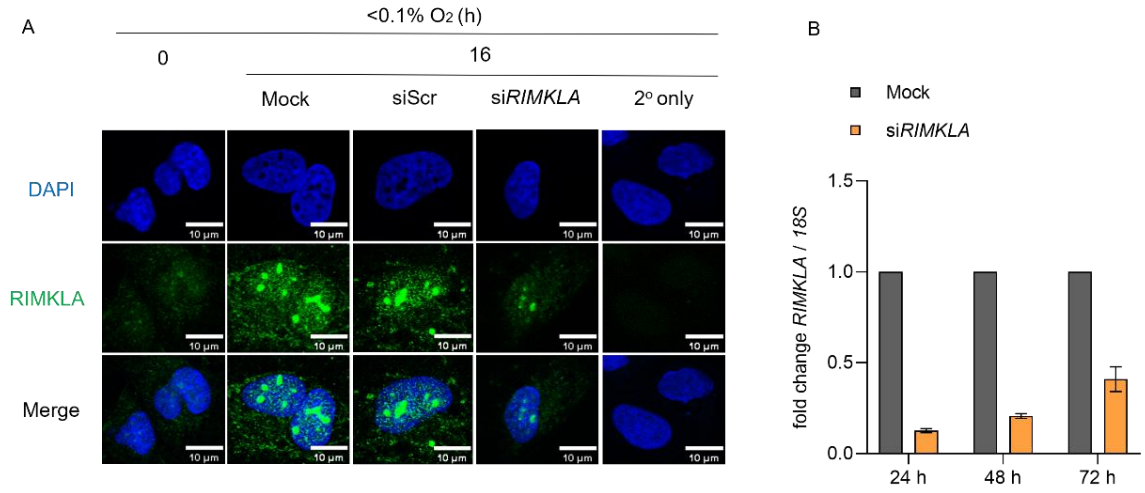

Figure 4.12. Validation of a RIMKLA antibody for immunofluorescence. CAL-51 cells were transfected with either Mock, siScr or si*RIMKLA*, and exposed to <0.1% O_2 for 16 h. (A) Immunofluorescence analysis of RIMKLA (green), for antibody validation. DAPI (blue) used for identification of cell nuclei. Scale bar = 10 µm. (B) RT-qPCR analysis of *RIMKLA* mRNA levels, normalised to *18S*, 24, 48 and 72 h post-transfection, for optimisation of siRNA-mediated knockdown of *RIMKLA*, in samples from part A. n =1.

4.2.13. Quantification and localisation of RIMKLA in hypoxic cells using phalloidin

We previously saw, during immunofluorescence detection of RIMKLA using CAL-51 cells (figure 4.12) that the protein was distributed in the cytoplasmic and nucleolar cellular compartments. To quantify the total-cell increase of RIMKLA in response to hypoxia, we carried out immunofluorescence analysis using CAL-51 and additionally, MDA-MB-231 cells, stained with fluorescently-labelled phalloidin, an established tool for imaging the cell cytoskeleton, due to its F-actin binding abilities (Cooper 1987). The use of phalloidin, enabled us to define the cell margins and quantify the total-cell RIMKLA protein levels.

Results from immunofluorescent detection of RIMKLA in hypoxic phalloidin and anti-RIMKLA co-stained CAL-51 and MDA-MB-231 showed an upregulation of total-cell protein levels, with a 2-fold increase of RIMKLA Mean fluorescence Intensity (MFI) in CAL-51 cells treated with <0.1% O_2 and a 4.2-fold increase in CAL-51 cells treated with 2% O_2.

Treatment of MDA-MB-231 cells with <0.1% O_2 resulted in a 1.8-fold increase in RIMKLA total-cell MFI (figure 4.13, A, B, C and D).

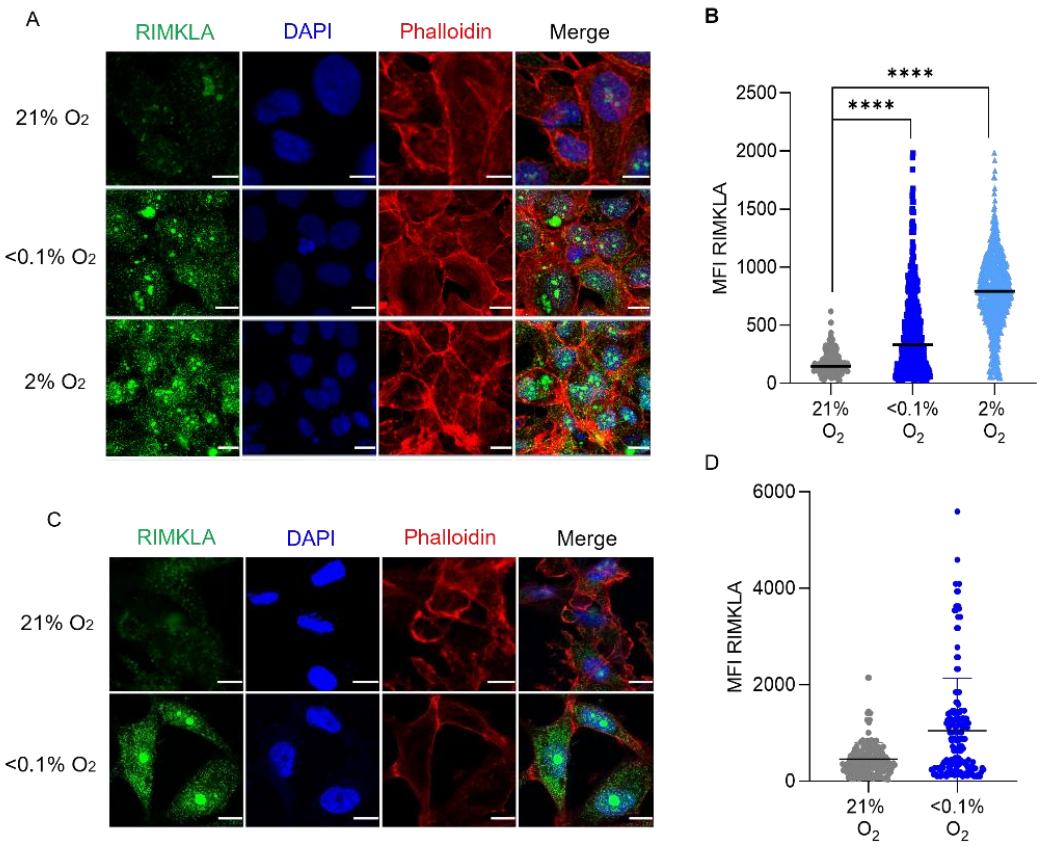

Figure 4.13. Quantification and localisation of RIMKLA in hypoxic cells using phalloidin. Cells were exposed to the indicated oxygen levels for 16 h. (A) Immunofluorescence analysis of total cellular RIMKLA (green) levels in CAL-51 cells stained with (DAPI) and phalloidin (red). Scale bar = 10 µm. (B) Quantification of total cellular levels of RIMKLA from part A. n = 3. (C) Immunofluorescence analysis of total cellular RIMKLA (green) levels in MDA-MB-231 cells stained with (DAPI) and phalloidin (red). Scale bar = 10 µm. (D) Quantification of total cellular levels of RIMKLA from part C. n = 2.

4.2.14. Nucleolar expression of RIMKLA increases in hypoxia

A closer examination of RIMKLA localisation in the cell nuclei, from previous data (figure 4.13, A and C), suggested that a large proportion of the total-cell protein content, resided in the nucleolus, a specialised, distinct compartment of the cell nuclei. This finding was quite interesting, since neither the nucleolar localisation of this protein has been validated previously, nor is the gene's / enzyme product's biological function associated with mammalian nucleoli.

To validate this observation and to confirm the hypoxia-mediated increase of RIMKLA in the nucleolus, we stained hypoxic CAL-51 and MDA-MB-231 cells with an antibody for fibrillarin, a protein which, being expressed exclusively in the nucleoli, can be used as a nucleolar marker (Mucino-Hernandez *et al.* 2023). We co-stained these hypoxic, fibrillarin-stained cells with an antibody for RIMKLA to enable the colocalisation of RIMKLA with fibrillarin and the quantification of the nucleolar fraction of RIMKLA, in response to hypoxia.

We analysed these cells by means of immunofluorescence, which showed a distinct colocalisation of RIMKLA with fibrillarin in both cell lines tested, in both normoxia and hypoxia, confirming the nucleolar localisation of the protein. Furthermore, compared to normoxic controls, the increase of nucleolar RIMKLA fractions in response to both <0.1% and 2% O_2 was validated in both cell lines we used, in terms of nucleolar RIMKLA MFI (figure 4.14 A, B, C and D).

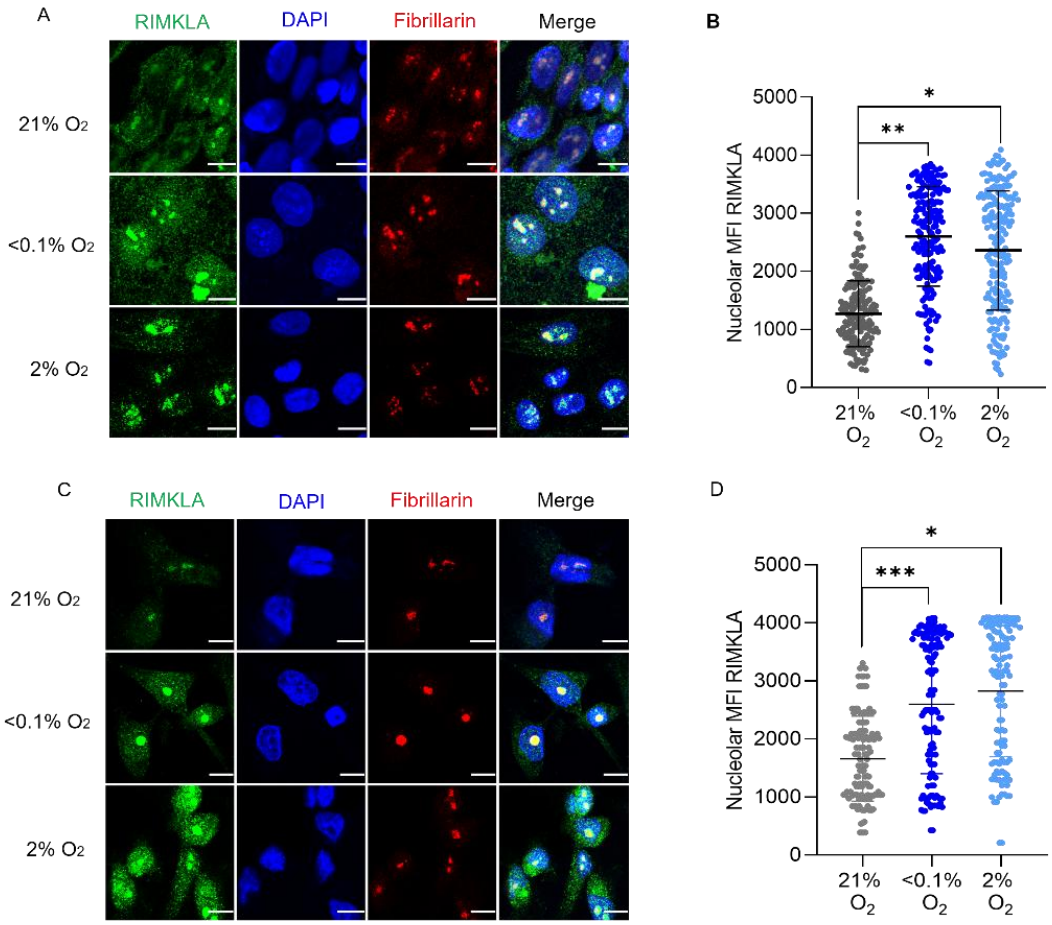

Figure 4.14. Nucleolar expression of RIMKLA increases in hypoxia. Cells were exposed to the indicated oxygen levels for 16 h. (A) Immunofluorescence analysis of RIMKLA (green) and fibrillarin (red), co-localisation in DAPI-stained (blue) CAL-51 cells. Scale bar = 10 μm. (B) Quantification of RIMKLA nucleolar levels from part A. n = 3. (C) Immunofluorescence analysis of RIMKLA (green) and fibrillarin (red), co-localisation in DAPI-stained (blue) MDA-MB-231 cells. Scale bar = 10 μm. (D) Quantification of RIMKLA nucleolar levels from part C. n = 3.

4.2.15. Expression levels of *RIMKLA* correlate with breast cancer patient survival status and resistance to chemotherapy

To expand our understanding of the prognostic significance of *RIMKLA*, we investigated the survival outcomes in terms of %OS and %RFS in an additional breast cancer patient cohort. We chose the METABRIC dataset and interrogated the clinical data for survival outcomes in patients with metastatic tumours having high compared to those having low *RIMKLA* mRNA levels. The analysis showed a significantly poorer %OS and %RFS prognosis for patients with high tumour *RIMKLA* levels over those with low, reinforcing the clinical relevance of *RIMKLA* levels in breast cancer (figure 4.15, A, B).

Further stratification of the clinical data from the METABRIC dataset was carried out, to identify the portion of patients with high and low *RIMKLA* mRNA levels who either survived, died of other causes, or died specifically cause of the disease. A comparison between the high and low *RIMKLA* patient groups revealed that, not only a smaller percentage of surviving patients but also a greater percentage of patients that died specifically of disease, could be found in the group of high compared to those with low *RIMKLA* mRNA levels (figure 4.15, C).

In addition to the prognostic value of *RIMKLA* we also investigated its predictive potential. We did so by analysing the levels of *RIMKLA* using transcriptomic data (obtained pre-treatment), from a cohort of breast cancer patients who received neoadjuvant chemotherapy. Using this data *RIMKLA* mRNA levels between patients exhibiting a pathological complete-response (pCR) *vs.* those exhibiting residual disease outcomes. Results of this analysis showed, a significantly higher *RIMKLA* mRNA content in samples from patients with residual disease, consistent with a potential association of *RIMKLA* with resistance to the effects of chemotherapy, in these patients (figure 4.15, D).

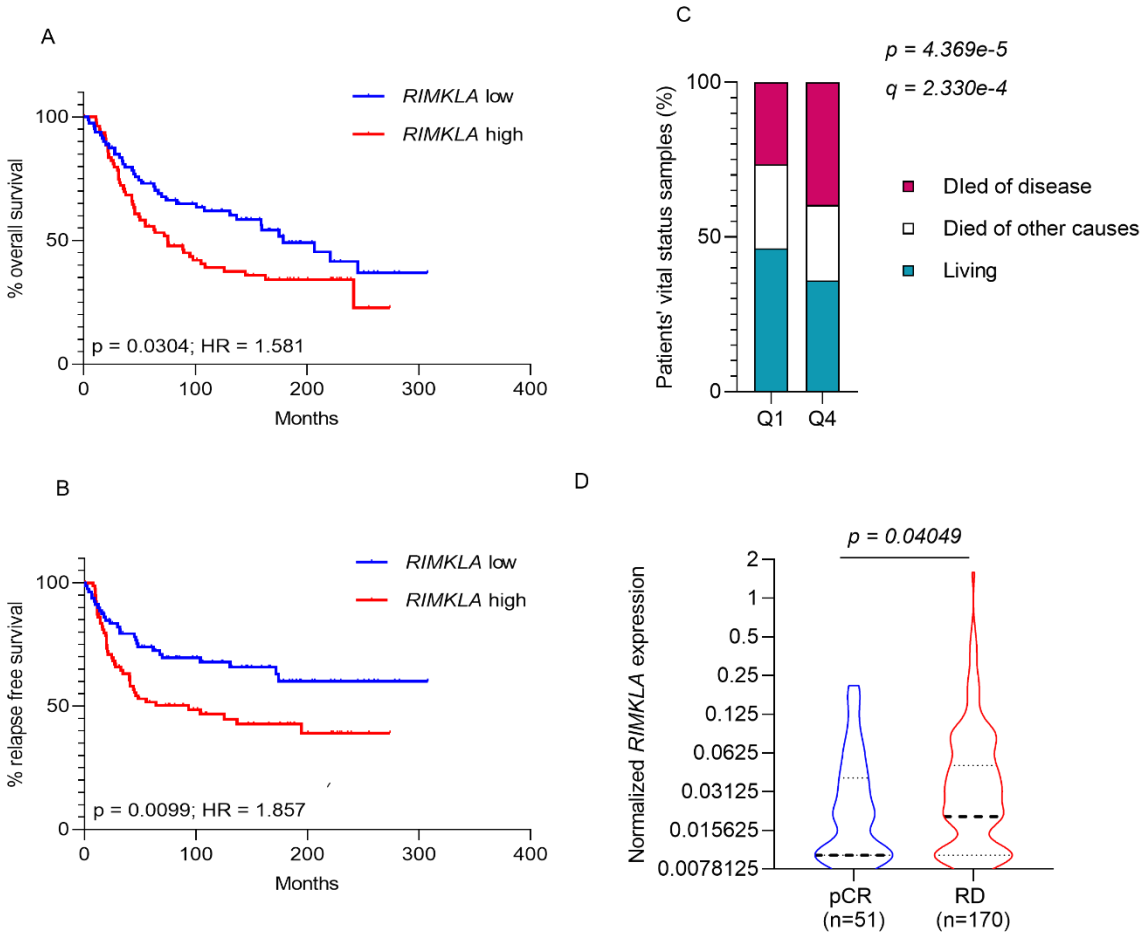

Figure 4.15. Expression levels of *RIMKLA* correlate with breast cancer patient survival status and resistance to chemotherapy. METABRIC patient sample data (n = 2509) were downloaded from cBioportal. Cases were filtered to selected triple negative breast cancers only (n = 299). Using mRNA expression levels for *RIMKLA*, lower quartile (Q1-low) and upper quartile (Q4-high) groups were identified. Interrogation of clinical data for survival outcomes indicated that triple negative tumours with high *RIMKLA* expression had (A) poorer overall survival (HR = 1.581; p = 0.0304) and (B) earlier relapse of disease (HR = 1.857; p = 0.0099) (Log-rank test). (C) *RIMKLA* mRNA levels were obtained from the METABRIC dataset and analysed to identify gene expression quartiles. Q1 and Q4 were compared for patients' vital status. p < 0.0001 (Chi-squared test). (D) *RIMKLA* mRNA levels from pre-treatment tumour biopsies of breast cancer patients, receiving neoadjuvant chemotherapy, were obtained from GEO (Accession: GSE163882). *RIMKLA* expression values (TPM) were extracted and compared between patients with pathological complete response (pCR) versus residual disease (RD) after treatment (p = 0.04049, one-sided Wilcoxon test). Statistical analysis was performed on the raw TPM data. A log2 transformation was applied to the data for visualisation.

4.2.16. Analysis of *RIMKLA* levels in breast tumour subtypes

It was interesting to examine if there was a subtype-dependence of *RIMKLA* mRNA upregulation in breast cancer patients. The most common and widely accepted classification of breast cancer comes from an immunohistochemical perspective, based on the expression of the following hormone receptors: oestrogen (ER), progesterone (PR), and human epidermal growth factor (HER2). Accordingly, the following four subtypes of breast cancer are widely recognised: luminal A, luminal B, HER2-positive, and triple-negative (Orrantia-Borunda *et al*. 2022). Different subtypes are associated with differences in patient survival outcomes, response to therapy, as well as patterns of gene expression (Yersal and Barutca 2014).

For this reason, we used publicly available transcriptomic data from the TCGA BRCA dataset to assess the levels of *RIMKLA*, in the different breast cancer subtypes, compared to its levels in normal breast tissue. Interestingly, *RIMKLA* appeared to be significantly upregulated in Luminal (A and B) and HER2-positive, but not in TNBC (basal-like) breast tumour types (figure 4.16, A). Further dissection of the same dataset into the various molecular subtypes of TNBC (Wang *et al*. 2019) indicated that *RIMKLA* was not significantly upregulated at the mRNA level, in any of the TNBC subtypes examined (figure 4.16, B).

Next, we used the same transcriptomic dataset, to examine the impact of *RIMKLA* levels in progression-free survival (%PFS), filtering the data for patients with luminal (A and B) tumour subtypes and patients with HER2-positve breast tumour subtypes, as these where the subtypes showing a significant upregulation of *RIMKLA*. Survival analysis of the filtered TCGA BRCA data, hinted at a significantly poorer %PFS for patients with high *RIMKLA* levels, in cases of luminal, but not in cases of HER2-positive breast cancer subtypes (figure 4.16, C and D). Nonetheless, the potential confounding factors of this univariate analysis such as, tumour stage, patient age, prior treatment status etc., are acknowledged as limitation of these analyses and therefore the finding are interpreted as preliminary.

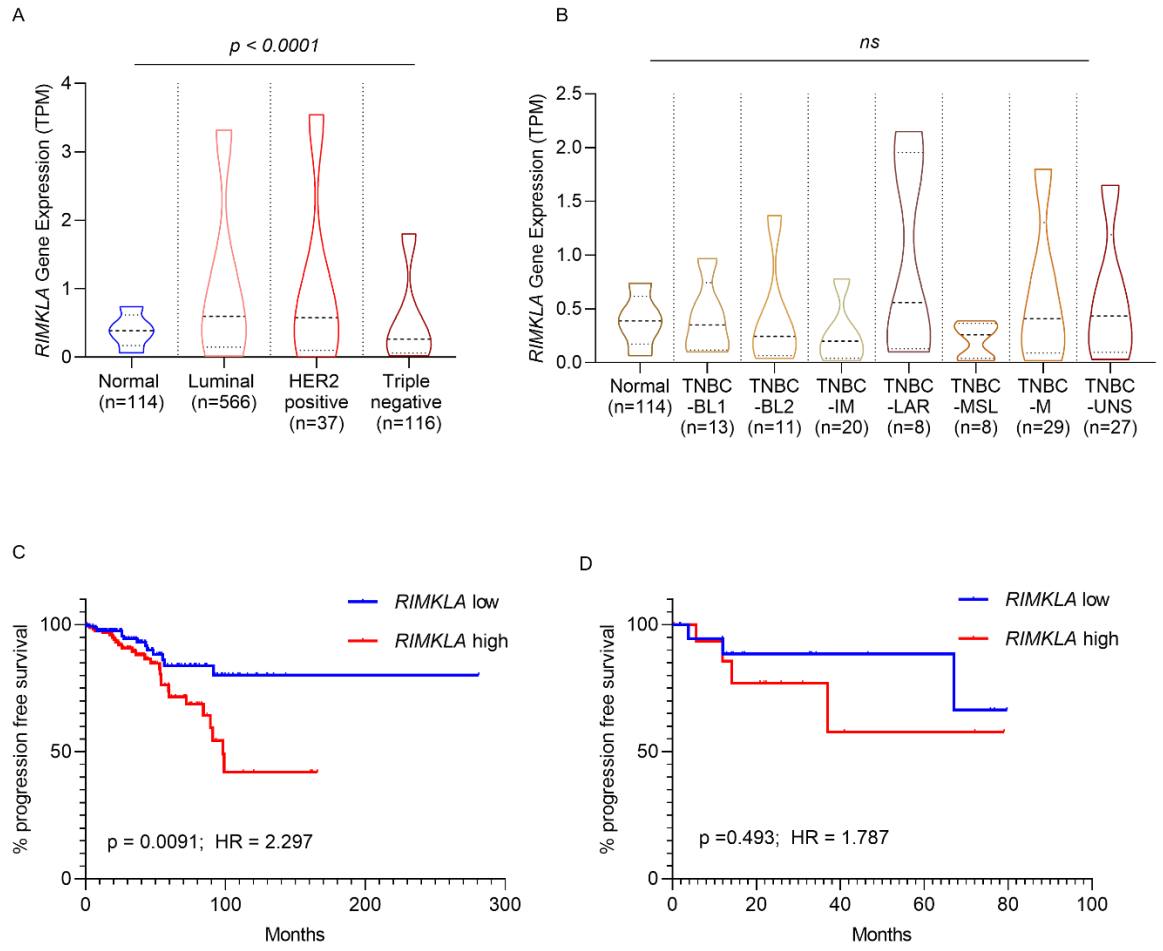

Figure 4.16. Analysis of *RIMKLA* levels in breast tumour subtypes. TCGA BRCA data were accessed and downloaded from cBioportal. (A) Patient samples were filtered according to tumour subtype into luminal (A and B) (n = 566), HER2-positive (n = 37) and triple-negative (n = 116) groups and transcriptomic data were interrogated for levels of *RIMKLA* in each group, compared to normal breast tissue (n = 114). (B) Samples of patients with TNBC tumours were filtered according to TNBC subtypes into: Basal-like 1 (TNBC-BL1, n = 13), basal-like 2 (TNBC-BL2, n = 11), immunomodulatory (TNBC-IM, n = 20), mesenchymal (TNBC-M, n = 29), mesenchymal stem-like (TNBC-MSL, n = 8) and Luminal androgen receptor (TNBC-LAR, n = 8). Transcriptomic data were analysed for *RIMKLA* mRNA levels, compared to normal breast tissue samples (n = 114). (C) Transcriptomic data from patients with luminal (A and B) tumour subtypes were filtered into quartiles according to *RIMKLA* mRNA levels and Q1 (low) was compared to Q4 (high) for %PFS, showing significant poorer outcomes for patients with high *RIMKLA* levels (p = 0.0091; HR = 2.297). (D) Transcriptomic data from patients with HER2-positive tumour subtypes were filtered into quartiles according to *RIMKLA* mRNA levels and Q1 (low) was compared to Q4 (high) for %PFS, showing non-significant poorer outcomes for patients with high *RIMKLA* levels (p = 0.493; HR = 1.787).

4.2.17. *RIMKLA* mRNA levels correlate with worse survival in multiple cancer types

Having examined the prognostic and predictive potential of *RIMKLA*, using publicly available breast cancer datasets, we next asked whether this finding is limited to this cancer type and, if not, which additional cancer types might show a dependent difference in patient prognosis, correlating with *RIMKLA* levels.

Preliminary data from survival analysis of TCGA transcriptomic data for all available cancer types showed that, in total, high *RIMKLA* mRNA levels (Q1 *vs*. Q4 comparison), correlated with significantly worse prognosis (%OS) in patient samples from glioblastoma (GBM), liver intra-hepatic carcinoma (LIHC), thymoma (THYM), uterine carcinosarcoma (UCSC), thyroid and Esophageal carcinomas (ESCA), in addition to breast invasive carcinoma (BRCA) (figure 4.17, A, B, C, D and F).

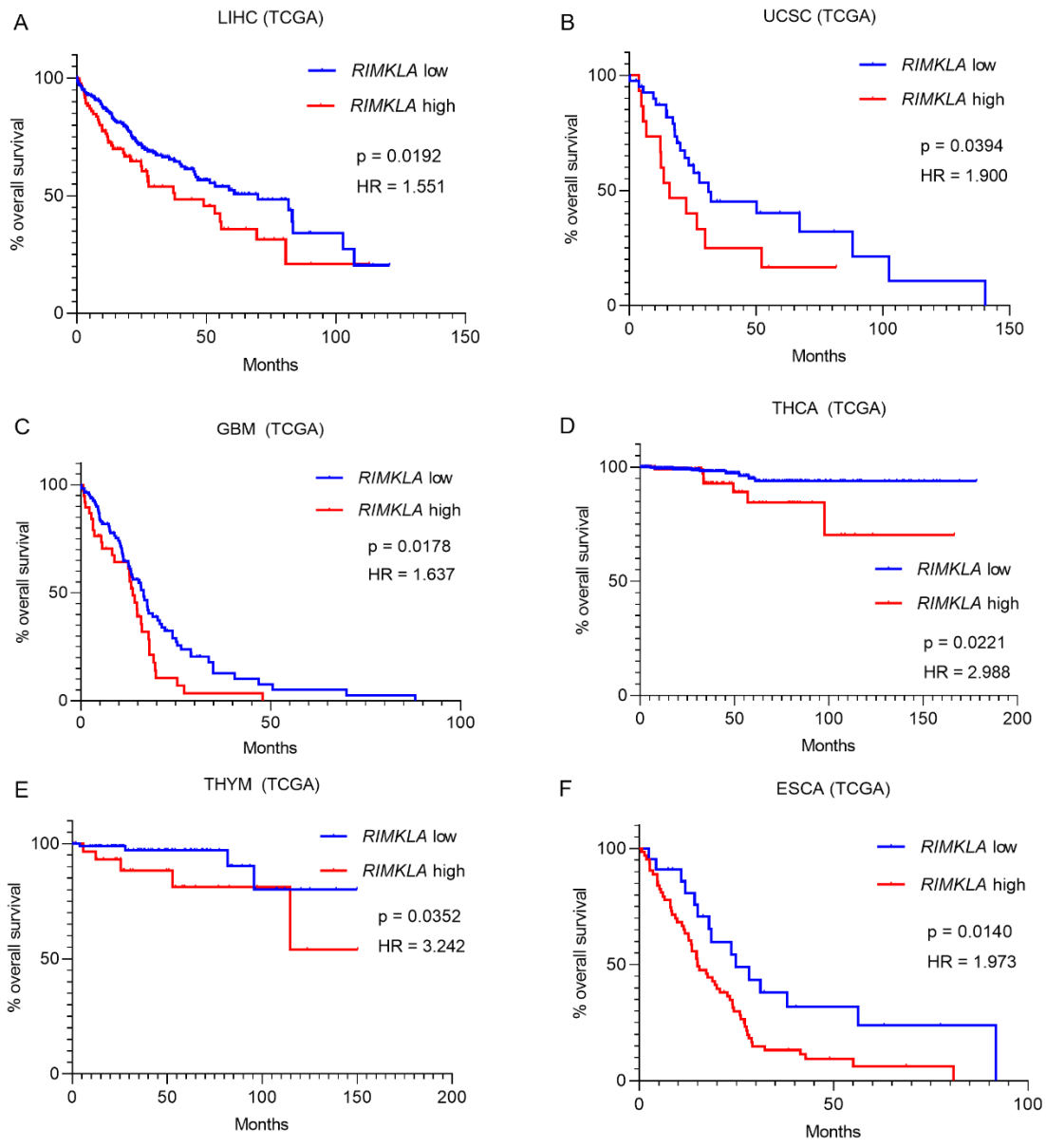

Figure 4.17. Kaplan-Meier curves for tumour types where high expression of *RIMKLA* is associated with significantly decreased overall survival probability. TCGA patient sample data were downloaded from cBioportal. Using mRNA expression levels for *RIMKLA,* lower quartiles (Q1- Q3) (low) and upper quartile (Q4) (high) were identified. Interrogation of clinical data for overall survival indicated that tumours with high *RIMKLA* expression had significantly worse overall survival in patients with: (A) Liver Intra-hepatic carcinoma (LIHC; p = 0.0192; HR = 1.551), (B) Uterine Carcinosarcoma (UCS; p = 0.0394; HR = 1.900), (C) Glioblastoma Multiforme (GBM; p = 0.0178; HR = 1.637), (D) Thyroid Carcinoma (THCA; p = 0.02214; HR = 2.988), (E) Thymoma (THYM; p = 0.0352; HR = 3.242), and (F) Esophageal carcinoma (ESCA: p = 0.0140; HR = 1.973). Statistical significance of $p < 0.05$ was determined by Log-rank (Mentel-Cox) test.

4.2.18. Homology analysis of RIMKLA with RIMKLB active sites

As described (section 1.5.4), the enzymes encoded by *RIMKLA* and its paralogue *RIMKLB,* are both able to catalyse the synthetic reaction of the same acetylated dipeptide, NAAG. Despite previously published evidence regarding the different substrate specificities between RIMKLA and RIMKLB, we wanted to examine the degree of homology between the primary structures of their active sites.

Domain analysis of RIMKLA and RIMKLB showed that, both enzymes share a conserved "ATP-grasp-fold" domain (Collard *et al*. 2010; Lodder-Gadaczek *et al*. 2011). The ATP-grasp fold consists of two α + β domains that "grasp" a molecule of ATP between them. Examples of well-studied enzymes bearing this same domain include, biotin carboxylase, D-alanine-D-alanine ligase and glutathione synthetase, all of which catalysing the ATP-assisted reaction of a carboxylic acid with a nucleophile *via* the formation of an acylphosphate intermediate (Fawaz *et al*. 2011). In the same mechanistic manner, RIMKLA and RIMKLB, catalyse the synthesis of NAAG and NAAG2 (Lodder-Gadaczek *et al*. 2011).

We examined the degree of homology between the amino acids of these two enzyme's active sites: RIMKLA is comprised of a total 391 amino acids, of which amino acid Phenylalanine 115-Methionine 300, form the enzyme's ATP-grasp fold domain, while RIMKLB is composed of 386 amino acids in total and its ATP-grasp fold domain consists of the amino acids Phenylalanine 119 – Alanine 304 (figure 4.18, A, B). The homology analysis between the amino acid sequences of the two enzymes' ATP-grasp fold domains revealed a 69.73% identity (figure 4.18, C), showing that RIMKLA and RIMKLB active sites share a significant amount of homology.

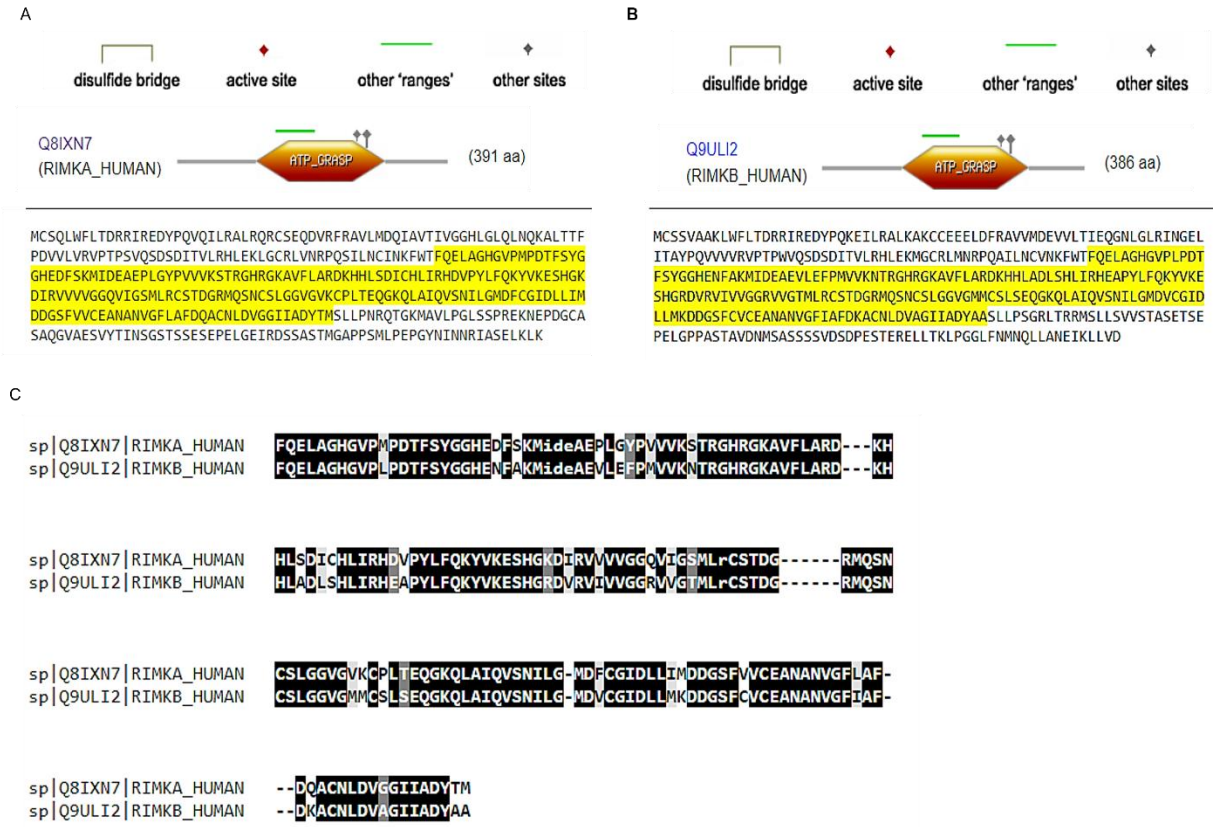

Figure 4.18. Homology analysis of RIMKLA with RIMKLB active sites. Domain analysis of the enzymes was carried out *via* ProSite software (www.prosite.expasy.org). (A) Amino acid (aa) sequence analysis of RIMKLA (391 aa). The amino acids (185 aa) comprising the enzymes ATP-grasp fold domain are highlighted in yellow. (B) Amino acid (aa) sequence analysis of RIMKLB (386 aa). The amino acids (185 aa) comprising the enzymes ATP-grasp fold domain are highlighted in yellow. (C) Homology analysis of RIMKLA and RIMKLB ATP-grasp fold domains (185 aa) for determination of % indentity. Highlighted in black = identical amino acids; Highlighted in grey = amino acids with similar properties; non-highlighted = amino acids that are different between RIMKLA and RIMKLB ATP-grasp fold domain sequences. Non-capital (lowercase**)** letters in alignment outputs indicate regions that have been masked or filtered due to low complexity, repetitive sequences, or compositional bias. These regions are excluded from statistical calculations (e.g., E-values, bit scores) because they can produce misleading alignments with high scores but no biological significance. Homology analysis was carried out using BLASTp (www. blast.ncbi.nlm.nih.gov).

4.2.19. *RIMKLB* is not induced in response to hypoxia

Considering the homology between RIMKLA and RIMKLB, we were interested in investigating the oxygen-dependency of *RIMKLB* and the possibility of its hypoxia-mediated induction. To test this, we analysed our RNA-seq data from MDA-MB-231 cells treated with <0.1% and 2% O_2 for the fold-change of *RIMKLB* compared to its cellular mRNA level at 21% O_2.

We found that the RNA-seq data did not suggested a significant induction of *RIMKLB* in cells exposed to a <0.1% O_2 but did suggest a significant downregulation in cells exposed to 2% O_2 (figure 4.19, A). Furthermore, we validated the RNA-seq data using RT-qPCR mediated analysis of *RIMKLB* mRNA levels in both MDA-MB-231 and CAL-51 cells, exposed to different oxygen levels, using mRNA levels of *CAIX* as a hypoxia control. Similarly, no significant induction was seen in the mRNA levels of *RIMKLB* in response to any of the oxygen levels we tested (figure 4.19, B, C).

Finally, we investigated the correlation of *RIMKLB* mRNA levels with the top-15 genes of both the hypoxia metagene (Buffa) and the pimonidazole-specific (Ragnum) gene signatures, using transcriptomic data from the TCGA BRCA dataset. As expected, a significantly negative correlation of *RIMKLB* with both gene signatures, was found to be the case, suggesting that this gene is downregulated in hypoxic patient tumours (figure 4.19, D and E).

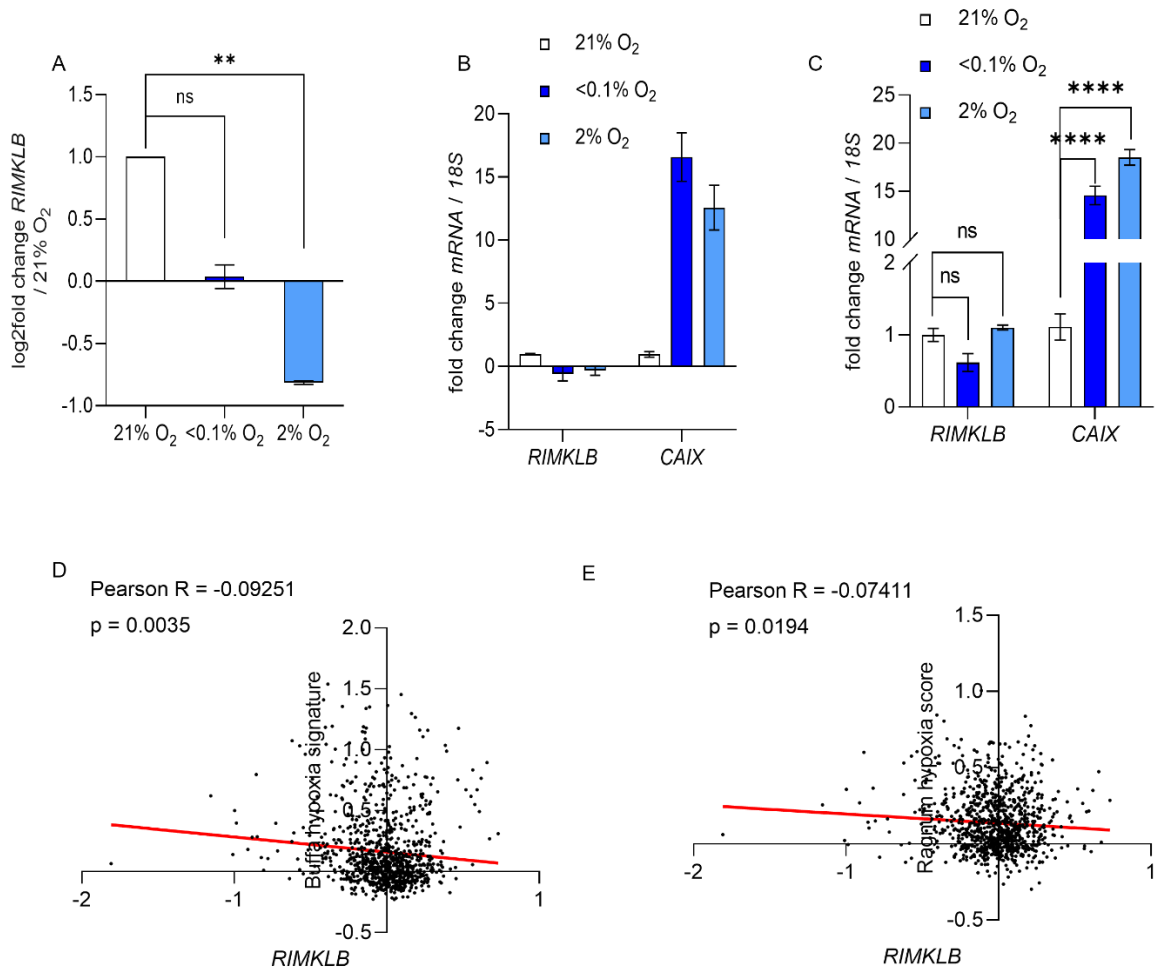

Figure 4.19. *RIMKLB* is not induced in response to hypoxia. Cells were exposed to the indicated oxygen levels for 16 h. (A) RNA-seq data analysis for mRNA levels of *RIMKLB*, represented as log2-fold change, normalised to 21% O_2, in MDA-MB-231 cells. n = 3 (B) RT-qPCR analysis of *RIMKLB* and *CAIX* mRNA levels, normalised to *18S*, in MDA-MB-231 cells. n = 2. *CAIX* mRNA levels analysed as a hypoxia control. (C) RT-qPCR analysis of *RIMKLB* and *CAIX* mRNA levels, normalised to *18S*, in CAL-51 cells. n = 3. *CAIX* mRNA levels analysed as a hypoxia control. (D) Pearson's correlation analysis of *RIMKLB* mRNA levels with mRNA levels of the top-15 genes of the hypoxia metagene (Buffa) signature, in samples from patients of the TCGA BRCA dataset. The log-mean expression of the metagene hypoxia signature top-15 genes for each patient dataset is shown, correlated to the log-mean expression of *RIMKLB* mRNA. (E) Pearson's correlation analysis of *RIMKLB* mRNA levels in patient samples from the TCGA BRCA dataset, with the mRNA levels of the top-15 genes of the pimonidazole-specific (Ragnum) signature, in samples of the same dataset. The log-mean expression of the pimonidazole-specific hypoxia signature top-15 genes for each cancer dataset is shown, correlated to the log-mean expression of *RIMKLB* mRNA.

4.2.20. Published data suggest that *RIMKLA* has an HRE

After validating *RIMKLA*'s induction in response to hypoxia, both on the mRNA and protein levels, we asked what the mechanism of this phenomenon was. A significant fraction of the genes that are induced in response to hypoxia, have been shown by previous works to be under the control of transcription factors of the HIF family (chapter 1). Therefore, we sought to find out, if HIF-responsive elements (HREs) existed, upstream of the *RIMKLA* gene, on the gene's locus in chromosome 1 of the human genome. To do so we analysed a previously published dataset of chromatin immunoprecipitation (ChIP) sequencing for HIF-1α (Zhang *et al.* 2015). Using this dataset and the Integrative genome browser (IGV) for visualisation of the *RIMKLA* gene locus, we identified that, indeed, a HIF-1α binding consensus came up as a peak on the IGV software, -244 base pairs (bp) relative to *RIMKLA*'s transcription initiation site (figure 4.20). This indicates that, indeed HIF-1α could be a transcription factor mediating the induction of *RIMKLA* in response to hypoxia.

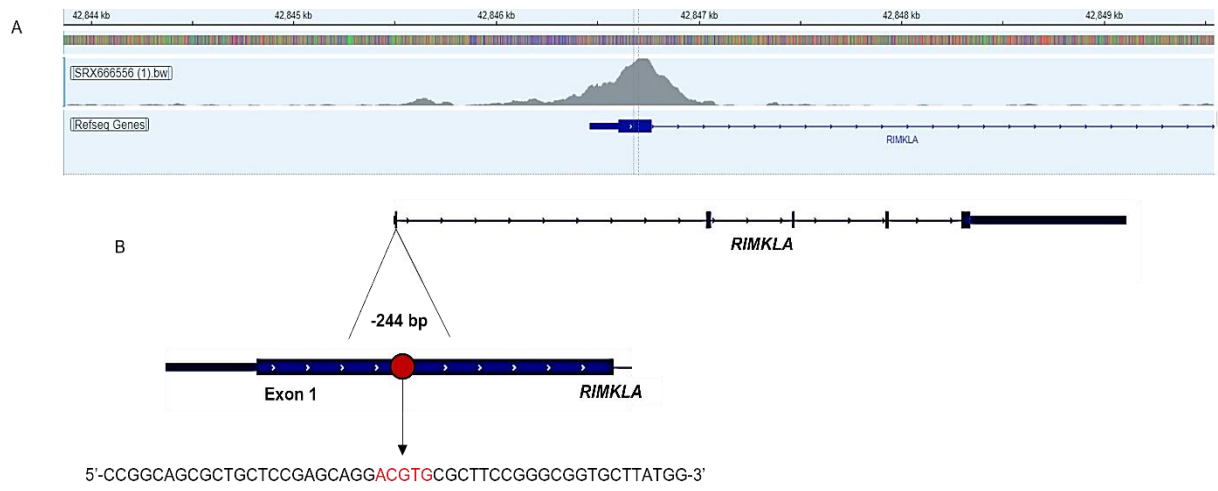

Figure 4.20. Published data suggest that *RIMKLA* has an HRE. (A) Integrative genome viewer (IGV) analysis of *RIMKLA* gene, showing a peak in the gene promoter region. (B) A match to the HIF-1α consensus binding site 5'-(A/G)CGTG-3' was identified in the human *RIMKLA* gene at −244 bp relative to the transcription start site. Data extracted by analysis of GSM1462475: T47D HIF-1α ChIP-seq dataset (Homo sapiens) (ID: SRX666556), *via* the integrative genome viewer (IGV) software.

4.2.21. *RIMKLA* is induced in response to hypoxia mimetics

To examine further if stabilisation of HIFs could increase mRNA levels of *RIMKLA*, we treated CAL-51 cells with chemical compounds that stabilise HIFs, commonly known as “hypoxia mimetics”. In specific, we used Dimethyloxalylglycine (DMOG), an ester of N-oxalylglycine which has a similar structure to 2-Oxoglutarate and acts thereby as a PHD inhibitor. DMOG has been shown to stabilise HIF-1 and HIF-2 in a non-specific manner, both *in vitro* and *in vivo* (Chen *et al*. 2022; Sears *et al*. 2008). Additionally, we used Desferrioxamine (DFO), a compound that stabilises HIF-1α, by chelating iron (Fe^{+}) and thereby inhibiting the function of the iron-dependent PHD enzymes (Wang and Semenza 1993). Finally, we also treated cells with Cobalt Chloride ($CoCl_2$), a chemical known to inhibit HIF-1α degradation, by occupying the iron-binding site of the PHD enzymes, thus inhibiting the interaction between VHL and hydroxylated HIF-1α (Di Mattia *et al*. 2022). CAL-51 cells treated with all three hypoxia mimetics, exhibited increased mRNA levels of *RIMKLA*, assessed by RT-qPCR analysis (figure 4.2, A). A western blot for HIF-1α levels in the hypoxia mimetics-treated cells showed that, even the use of a low concentration of DMOG, which did not significantly stabilise HIF-1α, *RIMKLA* mRNA levels were still upregulated, suggesting that *RIMKLA* might not be under HIF-1α transcriptional control (figure 4.20, A, B).

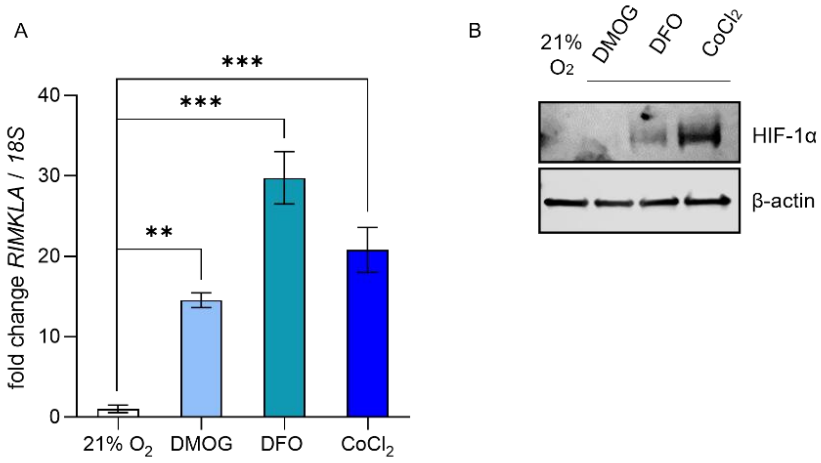

Figure 4.21. Hypoxia mimetics induce *RIMKLA*. (A) RT-qPCR analysis of *RIMKLA* mRNA levels in CAL-51 cells, treated with hypoxia-mimetics for 16 h (DMOG: 1 µmol/L, DFO: 100 µmol/L, CoCl2: 150 µmol/L). n= 3. (B) Western blot analysis of HIF-1α protein levels, as a control for part A. β-actin was used as a loading control. n = 3.

4.2.22. *RIMKLA* is more highly expressed in VHL null RCC

Further into investigating the mechanism of *RIMKLA* induction in hypoxic cells, we tested the levels of its mRNA in pseudohypoxic conditions – i.e., conditions where loss of function mutation or inactivation of the *VHL* gene expression, cause a stabilisation of HIF-1α protein, given the fact that VHL is a critical ubiquitin-ligase which controls the oxygen-dependent degradation of HIF-1α *via* the ubiquitin-proteasome protein degradation system (chapter 1). Hence, conditions of defective function of *VHL* cause the stabilisation and accumulation of HIF-1α protein even in normoxia and, by extension, the induction of transcriptional activity of HIF-1α (Bratslavsky *et al*. 2007; Hayashi *et al*. 2019).

To test the hypothesis of HIF-dependent *RIMKLA* induction in pseudohypoxia, we used a clear-cell renal carcinoma-derived cell line, RCC4 in which, the VHL is inactive and therefore, HIF-1α is permanently stabilised (Perier *et al*. 2011). Normoxic RCC4 $^{VHL-/-}$ samples were analysed for *RIMKLA* mRNA levels compared to samples from RCC4 cells transfected to stably express *VHL* (RCC4 $^{VHL\ +/+}$) and thus exhibit standard oxygen-dependent HIF-1α degradation in normoxia (Maxwell *et al*. 1999). Analysis by means of RT-qPCR showed that, indeed pseudohypoxic RCC4 $^{VHL-/-}$ had higher levels of *RIMKLA* mRNA compared to their RCC4 $^{VHL\ +/+}$ counterparts (figure 4.22, A). Western blot analysis of protein samples from both the cell lines described above for HIF-1α and VHL protein levels, was used to confirm the status of both proteins, in $VHL^{-/-}$ and $VHL^{+/+}$ conditions, respectively (figure 4.22, B).

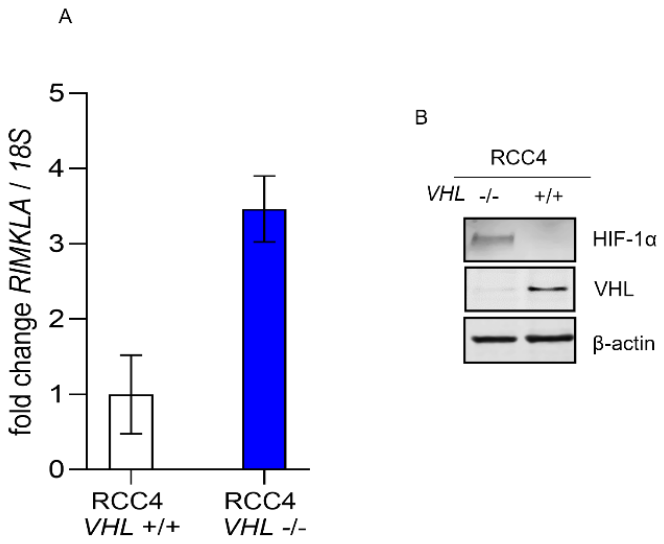

Figure 4.22. *RIMKLA* is more highly expressed, in *VHL* null RRC4 cells. RCC4 $^{VHL+/+}$ and RCC4 $^{VHL-/-}$ cells were used for (A) RT-qPCR analysis of *RIMKLA* mRNA levels normalised to *18S*. (B) Western blot analysis of protein samples from part A, for HIF-1α and VHL protein levels. β-actin used as loading control. n = 2.

4.2.23. *RIMKLA* is not induced in a HIF-2α dependent manner

Despite the differences in HIF-1α and HIF-2α transcription factors regarding their α-subunits, their required coactivators, etc., it has been shown that the two proteins exhibit an overlap in the gene sets whose expression the control, in response to hypoxia (Bartoszewski *et al*. 2019; Downes *et al*. 2018; Loboda *et al*. 2010).

We asked if HIF-2α took part in the hypoxia-dependent induction of *RIMKLA* that we have thus far reported, and if so, to what extent. To test this, we used a cell line derived from a primary tumour of renal adenocarcinoma (RCC), knows as 786-O. These cells lack VHL and HIF-1α but have HIF-2α and therefore served as a good model for investigating our hypothesis. We used 786-O cells transfected to stably express *VHL* (786-$O^{VHL\ +/+}$) to make sure we are looking only at the transcriptional effect of HIF-2α (Maxwell *et al*. 1999; Perier *et al*. 2011; Shinojima *et al*. 2007).

Treating these cells with <0.1% O_2 to stabilise HIF-2α, resulted in no significant increase of the mRNA levels of *RIMKLA*, compared to normoxic control cells, as seen by means of RT-qPCR analysis of cell samples for *RIMKLA* and by means of western blot analysis of protein samples for confirmation of HIF-1α absence and HIF-2α stabilisation by hypoxia (figure 4.23, A and B).

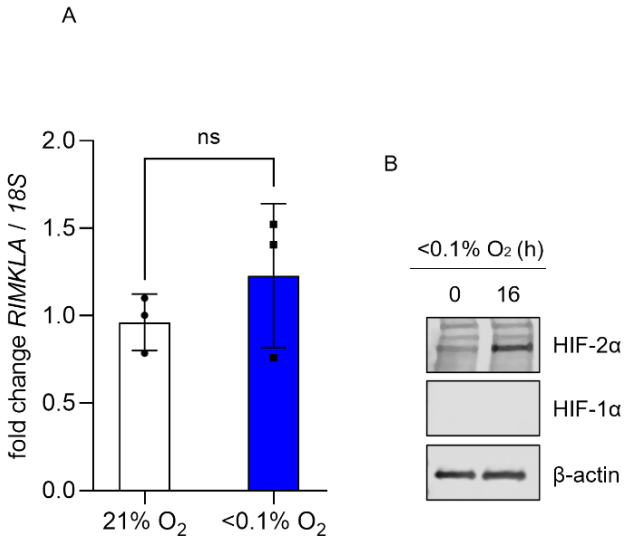

Figure 4.23. Stabilisation of HIF-2α does not induce *RIMKLA*. 786-O$^{VHL+/+}$ cells were treated with <0.1% O_2 for 8 h. (A) RT-qPCR analysis of *RIMKLA* mRNA levels normalised to *18S*. (B) Western blot analysis of protein levels of HIF-1α and HIF-2α, in protein samples from part A. β-actin used as loading control. n = 3.

4.2.24. Loss of HIF-1α abrogates *RIMKLA* induction in hypoxia

Thus far, our data suggested that the upregulation of *RIMKLA* we observed in hypoxic cells could be HIF-1α-dependent. To get a confirmation on the mechanism of induction of *RIMKLA* in hypoxic cells, we examined the mRNA levels of *RIMKLA* in hypoxia-treated RKO cell line models where *HIF-1α* was knocked-out (kindly provided by Dr D. Chan), using their wild-type counterparts as a control.

RT-qPCR analysis of *RIMKLA* mRNA levels, in RKO wild-type and RKO$^{HIF\text{-}1\alpha\ -/-}$ cells, treated with <0.1% O_2, resulted in significant *RIMKLA* induction in wild-type cells compared to a normoxic control, whereas no-significant increase was observed in *HIF-1α* $^{-/-}$ cells, in response to hypoxia (figure 4.24, A). Protein samples of both cell lines were analysed by western blot assay, for HIF-1α status confirmation (figure 4.24, B).

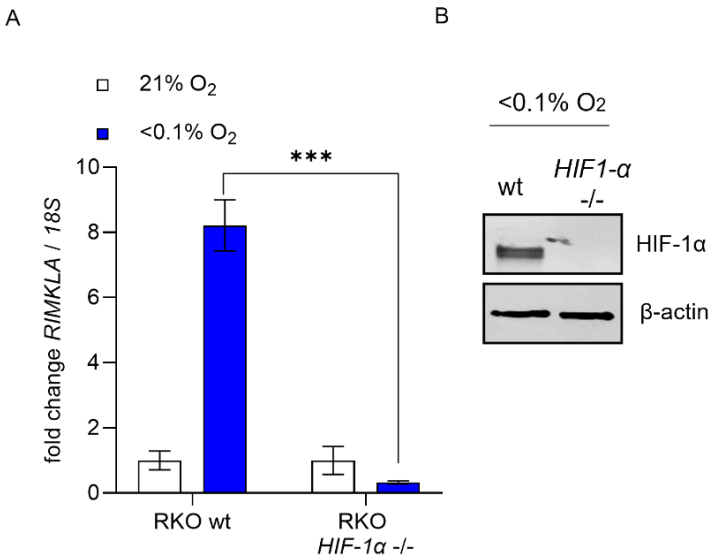

Figure 4.24. Loss of *HIF-1α* abrogates *RIMKLA* induction in hypoxia. Wild-type and *HIF-1α* $^{-/-}$ RKO cells were exposed to <0.1% O_2 for 16 h. (A) Cell samples were used for RT-qPCR analysis of *RIMKLA* mRNA levels in hypoxia. (B) Western blot analysis of HIF-1α protein levels in Wild-type RKO and *HIF-1α* $^{-/-}$ RKO, protein samples from part A. β-actin was used as loading control. n = 3.

4.3. Discussion

In this part of our work, we looked into hypoxia-mediated changes in gene expression of cancer cells, with a focus on their oxygen-dependency and their potential clinical relevance, which we investigated using publicly available data, from cancer patient samples. We examined the expression levels and the oxygen-dependency of four genes, suggested to be upregulated in hypoxia by unpublished RNA-seq data, using breast cancer cells. Whilst all genes demonstrated hypoxia-mediated inductions *in vitro*, their oxygen-dependence, hypoxia specificity, and prognostic potential diverged significantly, underscoring the contextual nature of hypoxia biology, across experimental and clinical settings.

Our identification of *EPHA3* and *EFNA3*, as hypoxia-responsive in breast cancer cells, echoes earlier reports of ephrin signalling modulation by low oxygen conditions (Vihanto *et al*. 2005; Yamashita *et al*. 2008). However, the paradoxical behaviour of *EPHA3* - upregulated at 2% O_2 but not in conditions of <0.1% O_2) in CAL-51 cells yet, negatively correlated with the hypoxia metagene in TCGA-BRCA tumours – suggests that its regulation may be oxygen-threshold dependent or influenced by tumour microenvironmental factors *in vivo*, besides hypoxia. Conversely, *EFNA3* induction under <0.1% O_2/cyclic hypoxia, aligned with its positive hypoxia metagene signature correlation, reinforcing its role in hypoxia-driven signalling pathways, though its preliminary association with disease progression rather than overall survival highlights how individual hypoxia effectors may drive distinct clinical trajectories (Husain *et al*. 2022). *PPFIA4* presented a further conundrum: whilst consistently hypoxia-inducible *in vitro* and positively correlated with Buffa scores, its preliminary association with *improved* survival, albeit not supported by statistics, in TCGA-BRCA hints at potential tumour-suppressive roles or cell-type-specific functionalities not yet fully resolved, particularly given its inconsistent protein induction in hypoxic MDA-MB-231 cells.

RIMKLA emerged as the most biologically and potentially clinically significant candidate. Its consistent induction across diverse hypoxia regimens and breast cancer subtypes *in vitro*, coupled with HIF-1α dependency validated through knockout models, *VHL*-null cells, and hypoxia mimetics, positions it as a *bona fide* hypoxia effector. Preliminary associations of its high expression levels, with poor overall survival, progression-free survival, and chemotherapy resistance across multiple cancer datasets, underscore its translational relevance. However, its negative correlation with the Buffa signature (hypoxia metagene) in breast cancer, contrasting sharply with the positive correlation to the Ragnum (pimonidazole) hypoxia signature in the same cancer type, and to the Winter signature, in tumours like LIHC and UCEC - demands scholarly consideration of how signature construction influences biological interpretation.

The Buffa hypoxia signature employs an unweighted average of its genes, selected *via* PCA for maximal variance capture in hypoxia transcriptomes. Whilst computationally robust, this approach may dilute contributions from genes whose expression variance in bulk tumours may be influenced by non-hypoxic factors or tissue-specific regulation. Conversely, the Ragnum hypoxia signature uses regression weighting, based on direct correlation to pimonidazole staining thus, prioritising genes with stronger links to histological hypoxia. The Winter signature, an unweighted mean of induced minus repressed genes derived from HIF-1α correlations in head and neck cancer, exhibited variable alignment with *RIMKLA*, possibly reflecting tissue-of-origin biases. Such methodological underpinnings of each signature provide a critical lens for interpreting these differential correlations. The Buffa signature was derived by seeding co-expression networks with previously validated hypoxia-inducible genes (e.g., *VEGFA*, *CAIX*), then identifying clusters of tightly co-expressed transcripts across diverse cancers (Buffa *et al*. 2010). This approach prioritises genes embedded in conserved transcriptional networks of hypoxia adaptation but may be biased toward established "hypoxia canon" genes. In stark contrast, both the Ragnum and Winter signatures were built from direct transcriptomic profiling of histologically defined hypoxic tumour regions, yet they employed distinct hypoxia detection methods: Ragnum

used pimonidazole adduct staining (binding covalently to proteins at O_2<1.4%) in prostate cancer, capturing regions of severe oxygen deprivation (Ragnum *et al.* 2015). Winter relied on IHC for HIF-1α and CAIX in head/neck squamous cell carcinomas, detecting regions with active HIF signalling and carbonic anhydrase activity (Winter *et al.* 2007). These foundational differences likely further explain *RIMKLA's* variable associations: Its negative correlation with Buffa hypoxia signature in BRCA may reflect exclusion from "canonical" hypoxia networks or tissue-specific co-expression patterns not captured by the metagene's pan-cancer seeds. Its strong positive correlation with the Ragnum signature in LIHC/BRCA aligns with pimonidazole's detection of acute oxygen scarcity, suggesting *RIMKLA* induction is prominent under pimonidazole-detected hypoxia. Winter's reliance on HIF/CAIX may explain its intermediate correlations, as *RIMKLA's* HIF-1α dependency (validated herein) could be counterbalanced by CAIX-independent regulation in certain tumours.

These discrepancies underscore that hypoxia signatures are not interchangeable; their outputs reflect their derivation methodologies and biological contexts. *RIMKLA*'s signature-specific correlations likely arise from its variable co-regulation with signature genes across tumour types, differential sensitivity to non-hypoxic confounding factors in bulk transcriptomes, or inherent biases in signature training datasets. For instance, the Buffa hypoxia signature was generated using transcriptomic data from multiple cancers and validated for prognostication using both breast and head and neck cancer samples. The presence of other cancer datasets, for example head and neck cancer transcriptomic data might be, thus, "diluting" the correlation analysis results, since analysis of *RIMKLA* levels in tumour *vs.* normal tissues suggests that the gene is not upregulated in head and neck tumours (Buffa *et al.* 2010)(appendix 5). On the contrary, the Ragnum hypoxia-associated gene signature was generated and validated using samples from prostate adenocarcinoma patients, a type of cancer where our tumour *vs.* normal analysis suggests a higher mRNA content of *RIMKLA* in prostate tumours (Ragnum *et al.* 2015)(appendix 5). Thus, as the Buffa hypoxia signature was designed for pan-cancer applicability, it may overlook

genes with more cancer-type specific hypoxia responses. In further support of this hypothesis, stands the cases of genes, previously described as HIF-targets, like *STC2* (Law and Wong 2010), *KLF4* (Mathieu *et al*. 2011), and *SLC38A2* (*SNAT2*) (Morotti *et al*. 2019) which, despite their mechanistically validated HIF-dependence in breast cancer cells, exhibit significantly negative correlation with the Buffa hypoxia signature (appendix 6). Consequently, this might suggest that signature choice must align rigorously with the biological question - Ragnum for direct hypoxia detection, Buffa for pan-cancer prognostic scoring, Winter for HIF-1α-focused studies.

Correlation analysis of *RIMKLA* with the full gene set of all three clinically relevant hypoxia signatures across all TCGA datasets showed that crucially, no cancer type exhibited universally negative correlations across all signatures. Instead, tumours of the liver (LIHC), uterus (UCEC), and paraganglia (PCPG) showed significantly positive correlations between *RIMKLA* and all three hypoxia signatures. This signature-concordant hypoxia association aligns with the known biology of these malignancies: In LIHC, hypoxia is a well-established driver of progression *via* HIF-1α/VEGF pathways, and pimonidazole staining correlates strongly with poor prognosis (Raleigh *et al*. 1998; Tanaka *et al*. 2006). Our preliminary association of high *RIMKLA* expression with prognostication of poorer overall survival in LIHC synergises with this, suggesting *RIMKLA* may amplify hypoxia-mediated aggressiveness - a notion supported by recent work linking HIF-1α to metabolic reprogramming in HCC (Liao *et al*. 2023). In UCEC, HIF-1α overexpression is frequent and associated with advanced stage (Liu *et al*. 2021), while PCPG tumours often harbour pseudohypoxic drivers (e.g., *VHL* mutations) causing constitutive HIF activation (Ohh *et al*. 2022). The concordant signature correlations in these contexts suggest *RIMKLA* induction is integral to hypoxic adaptation.

Despite the name of *RIMKLA* including the “ribosomal modification” component, this name was attributed due to the conserved active site domain of this gene with the RimK protein, identified in *E*. Coli, and identified to modify the bacterial S6 ribosomal subunit. Nonetheless, there is no

previous report associating the eukaryotic *RIMKLA* with ribosomal modification properties. Mechanistically, intriguing questions persist: *RIMKLA*'s nucleolar enrichment - novel for this protein - raises questions about potential roles in ribosomal stress, RNA metabolism, or NAD+ homeostasis beyond its established function in NAAG synthesis. Whilst HIF-1α dependency was clearly demonstrated, the induction of *RIMKLA* by DMOG without concomitant HIF-1α stabilisation hints at ancillary pathways involving oxidative stress or HIF-independent oxygen sensing. Furthermore, *RIMKLA*'s lack of upregulation in TCGA basal-like tumours, despite consistent, *in vitro* induction in TNBC cell lines, suggests subtype-specific post-transcriptional regulation or microenvironmental suppression, not captured in monolayer cultures.

In context with previous research, nucleolar stress is caused by a variety of conditions, including hypoxia. The nucleolus may take part in the response to such stressors, by regulating various stress-related signalling pathways, through abnormal nucleolar sequestration (Weeks *et al*. 2019). The nucleolus, therefore, acts as a unique, stress-sensing cellular compartment and responds to stressors by acquiring morphological and functional changes (Rahane *et al*. 2024). In addition to hypoxia sensing, the nucleolus, has been implicated to be involved in redox stress responses, a fact making the nucleolar localisation and upregulation of RIMKLA which we report here, very interesting, as it suggests that RIMKLA might be part of these biological processes, in hypoxic cells (Hetman and Pietrzak 2012; Ma *et al*. 2023; Rubbi and Milner 2003; Weeks *et al*. 2019; Yang *et al*. 2018). Additionally, taking into account the biological role of the nucleolus in the transcription of ribosomal RNA and the assembly of ribosomes, along with the ability of bacterial RimK proteins to modify bacterial ribosomes, an interesting hypothesis arises on the possibility that mammalian *RIMKLA* might possess the same property (Kresoja-Rakic and Santoro 2019; Melese and Xue 1995; Thomas and Ashcroft 2019; Warner 1990).

While leveraging TCGA, METABRIC and relevant public immunohistochemistry repositories affords some statistical power, the absence of comprehensive metadata - treatment histories,

direct hypoxia measurements and intratumoural heterogeneity metrics - limits causal inference. Our correlations thus remain hypothesis-generating: for example, while *RIMKLA* associates with poorer survival, it may co-vary with unmeasured confounders such as tumour stage, patient age, treatment type/status, aggressive subtype, or tumour/stromal composition, especially in univariate analyses like Kaplan-Meier survival estimation. Similarly, cell line models, though invaluable for mechanistic probing, cannot recapitulate the full spectrum of tumour–stroma interactions or oxygen gradients present *in vivo*. Thus, the limitation of our reports - representing an essentially univariate analysis of public datasets - necessitates viewing public-data-derived associations as hypothesis-generating rather than definitive; experimental validation in prospectively annotated cohorts with spatial resolution is essential, to definitively report such associations.

In sum, this part of our study not only corroborates key paradigms of hypoxia biology but also surfaces unanticipated complexities - gene-specific and oxygen-dependent contexts, signature heterogeneity and mechanistic novelties - which point to a demand for a more nuanced, critically reflective approach to hypoxia biomarker development.

Chapter 5 Investigating the biological role of *RIMKLA* in hypoxic cells

5.1. Introduction

During our investigation of hypoxia-mediated transcriptional upregulations *RIMKLA* emerged as a potential biomarker of clinical relevance, associated to hypoxia and more specifically, induced in a HIF-1α dependent manner in cancer cells (chapter 4).

In this part of our work, we aimed to characterise the biological role of this gene and its enzyme product in hypoxic cancer cells, using breast cancer cells as our *in vitro* model. As a start, we sought to examine the gene's association with the intracellular GSH pool, considering the established functional properties of NAAGS II (the enzyme encoded by *RIMKLA*) (section 1.5.4, figure 1.17), in generating NAAG, a precursor of L-glutamate which is a GSH-component amino acid. As an extension, we investigated any potential impact of *RIMKLA* depletion on the redox status of hypoxic cells, by determining its effect on intracellular ROS levels.

Preliminary data from survival analyses described in the previous chapter, suggested that high levels of *RIMKLA* mRNA, potentially prognosticate a worse outcome for patients with various types of malignancies. Consistently with its hypoxia-mediated inducibility we validated, we aimed to explore if the depletion of this gene has in impact on the viability of hypoxic cancer cells.

5.2. Results

5.2.1. Analysis of the impact of *RIMKLA* on intracellular GSH levels

According to the reported role or NAAGS II, the enzyme encoded by *RIMKLA*, it functions in synthesising NAAG and NAAG2. In context with published data reporting that NAAG can replenish the intracellular pool of L-glutamate in cancer cells (Asaka and Le 2019), we tested the hypothesis that, a part of this L-glutamate pool, might be utilised for the synthesis of GSH, a crucial intracellular antioxidant tripeptide. First, we checked that the gene *FOLH1*, encoding the enzyme (GCP II/PSMA) responsible for the catabolism of NAAG into NAA and L-glutamate, is not reportedly mutated in our cell line model (CAL-51). Indeed, using the cell line encyclopaedia dataset (CCLE; Broad Institute), accessed *via* the cBioportal platform (Ghandi *et al*. 2019), we found that no mutation was reported for this gene. This suggested that downstream, GCP II-mediated catabolism of NAAG should be present in our cell line model.

Next, we assessed the levels of GSH in CAL-51 cells, with or without *RIMKLA*. To do so, we transfected the cells with either siScr or si*RIMKLA* and exposed them to <0.1% O_2 (figure 5.1, A). Using the Mean Fluorescence Intensity (MFI) of the FL-1-GSH probe (figure 2.2), we quantified the levels of intracellular GSH, in response to *RIMKLA* depletion. In normoxic cells (21% O_2) there was no significant change in GSH levels. However, in hypoxic cells loss of *RIMKLA* resulted in decrease of the intracellular GSH levels. Of note, hypoxia treatment (8 h, <0.1% O_2), increased the levels of GSH, consistently with literature describing the HIF-1-mediated upregulation of GSH (section 1.5.5) and with reports from a recent study, describing a hypoxia-mediated increase in GSH (figure 5.1, B) (Twigger *et al*. 2024). The antioxidant N-acetylcysteine (NAC) was used as a positive control, increasing GSH levels by scavenging ROS (Zhang *et al*. 2011). The compound N-ethylmaleimide was used as a negative control, decreasing GSH levels (McLaggan *et al*. 2000). Additionally, samples from the same cells used for GSH measurement, were analysed by means of RT-qPCR for the mRNA levels of *RIMKLA*, for validation of knockdown efficacy (figure 5.1, C).

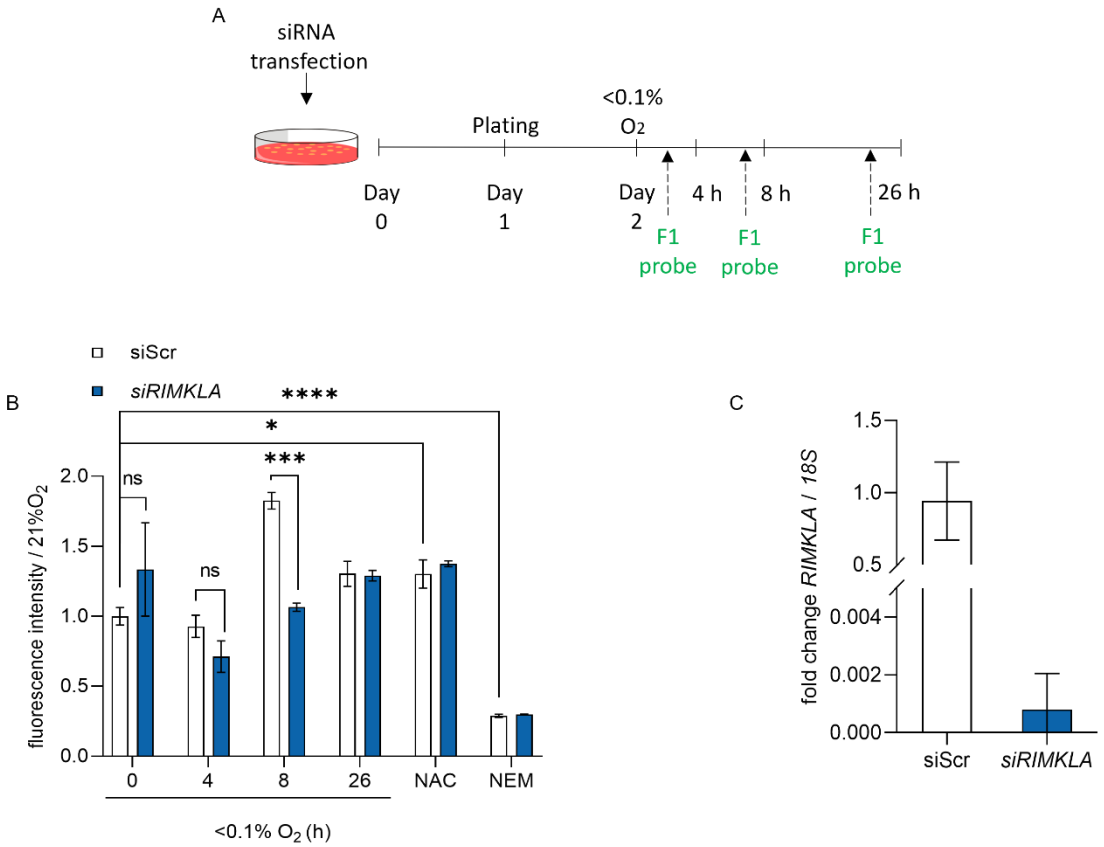

Figure 5.1. Analysis of the impact of *RIMKLA* on intracellular GSH levels. CAL-51 cells were transfected either with siScr or si*RIMKLA*, before treatment with <0.1% O_2 for and FL-1 (F1) probe, for the indicated time points. (A) Schematic representation of the experimental timeline. (B) Quantification of GSH levels in response to hypoxia, in terms of FL-1-probe fluorescence intensity normalised to 21% O_2 control. NAC = N-acetylcysteine, 20 mmol/L for 5 h, used as positive control; NEM = N-ethylmaleimide, µmol/L for 6 h, used as negative control. (C) RT-qPCR analysis of *RIMKLA* mRNA levels for siRNA-mediated knockdown validation. n = 3.

5.2.2. Depletion of *RIMKLA* increases ROS levels in hypoxic and normoxic cells

As a next step we wanted to assess, if and how the cellular redox balance changes, in response to siRNA-mediated depletion of *RIMKLA*. For this purpose, the CellROX Green reagent, a tool that is used for total nuclear ROS quantification, was used on either siScr or si*RIMKLA* transfected CAL-51 cells, exposed to <0.1% O_2 (figure 5.2, A and B). Microscopic analysis of cell samples was applied to quantify ROS levels with or without *RIMKLA*, in normoxic and hypoxic conditions, as function of mean signal intensity of CellROX Green. Results showed that siRNA-mediated *RIMKLA* depletion increased ROS levels in hypoxic cells but surprisingly in normoxic cells as well. This was not anticipated since the GSH levels in normoxic cells were not affected by the presence/absence of *RIMKLA*, according to our previously-described data (figure 5.1, B, C). This finding suggests that the changes of ROS levels in response to *RIMKLA* depletion, might not be GSH-dependent, at least in normoxic conditions. In agreement with our previous data, from ROS level measurements using redox-sensitive plasmids (figure 3.11, B, C, D and E) and with previously published works using CellROX green reagent, hypoxia (<0.1% O_2) increased ROS levels up to 2.5-fold (Ma *et al.* 2023; Twigger *et al.* 2024).

Furthermore, prolonged treatment with <0.1% O_2, resulted in decrease of ROS levels in si*RIMKLA*-transfected CAL-51 cells, suggestive either of a compensatory mechanism taking part, or a time-dependent decrease of siRNA-mediated *RIMKLA* knockdown efficiency. Interestingly, the same kinetics have been reported previously, measuring ROS levels in response to radiation (Terashima *et al.* 2013) (figure 5.2, C and D). Nonetheless, protein samples from the same cells were used for western blot analysis of RIMKLA levels, as a validation of siRNA-mediated *RIMKLA* knockdown efficacy (figure 5.2, E). Finally, treatment with the antioxidant NAC following the manufacturer's instructions, did not reduce basal ROS levels in terms of CellROX mean signal intensity in untreated, siScr-control cells, in agreement with previous descriptions (Arimilli *et al.* 2017; Matta *et al.* 2018; ThermoFisher 2012) (Figure 5.2, C and D).

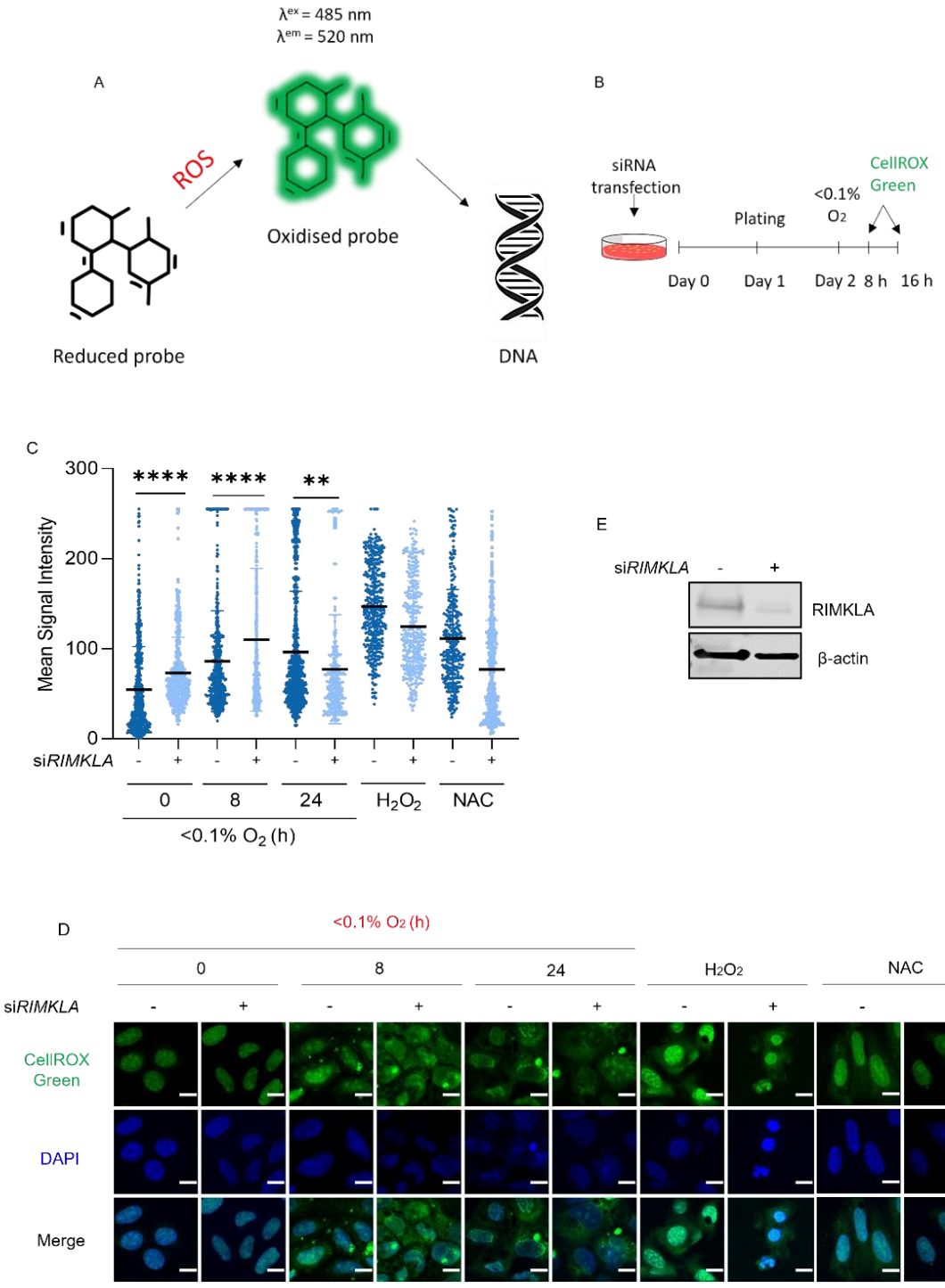

Figure 5.2. Loss of *RIMKLA* increases ROS levels in hypoxic and normoxic cells. CAL-51 cells were transfected with either siScr or si*RIMKLA* before treatment with <0.1% O_2, for the indicated time points. (A) Schematic diagram of CellROX Green reagent for measurement of ROS levels. (B) Schematic representation of the experimental timeline, with time points of treatment with CellROX, indicated. (C) Quantification of ROS levels in CAL-51 cells transfected with siScr or *siRIMKLA* and treated with <0.1% O_2. (H_2O_2 = hydrogen peroxide, 100 µmol/L for 30 min) as positive control and NAC = N-acetylcysteine, 20mmol/L, for 5 h) as a negative control. (D) Representative images from fluorescence analysis of CellROX-treated (green) and DAPI-stained (blue) CAL-51 cells, from part C. (E) Western blot analysis of RIMKLA protein levels for siRNA-mediated knockdown validation and β-actin used as a loading control. n = 3.

5.2.3. Protein levels of *RIMKLA* are upregulated in response to ROS-inducing agents

We hypothesised that *RIMKLA* might be a part of the antioxidant response and thus inducible in response to oxidative stress in addition to its hypoxia-dependent induction (figure 4. 24, A and B).

To investigate a potential ROS-dependency, we treated CAL-51 cells with a broad range of oxidants, i.e., chemical compounds/drugs, known to cause an increase in intracellular ROS levels. Protein samples from these cells were analysed by western blot assay for RIMKLA protein levels. Results of this analysis showed that RIMKLA protein expression was indeed, upregulated in oxidant-treated cells, compared to untreated control. Furthermore, treatment of H_2O_2-treated cells with the antioxidant NAC, managed to rescue the induction of RIMKLA protein levels, significantly (figure 5.3, A and B). Similarly, drugs that are known to exert part of their cytotoxic effects by inducing the formation of ROS (in addition to other mechanisms of cytotoxicity) such as, Doxorubicin (Adriamycin) and Olaparib, also upregulated RIMKLA protein levels (figure 5.3, A).

Somewhat surprisingly, however, the chemical oxidant Menadione (MEN), did not increase RIMKLA protein levels compared to the untreated control, despite its known function of ROS generation (Loor *et al*. 2010). However, as a vitamin K derivative, Menadione has pleiotropic effects – a fact that could potentially explain this unexpected result (figure 5.3, A) (Hirota *et al*. 2013).

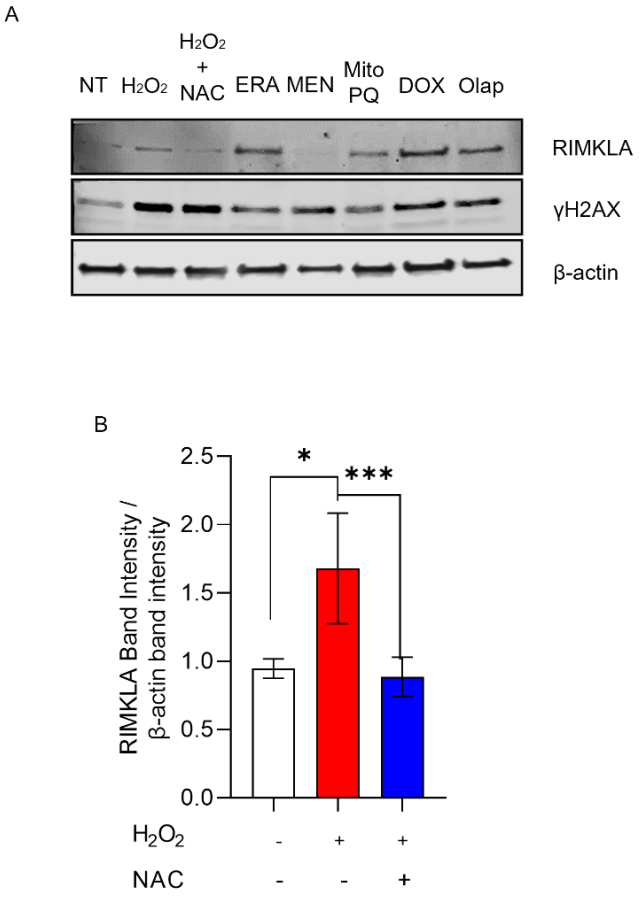

Figure 5.3. Protein levels of RIMKLA are increased, in response to ROS-inducing agents. CAL-51 cells were treated with the indicated ROS-inducing compounds, prior to extraction of protein samples. (A) Western blot analysis of CAL-51 cells for levels of RIMKLA, in response to treatment with ROS-inducers. γH2AX used as a control of induction of DDR signalling, in response to ROS, and β-actin used as a loading control. NT = Untreated control. (B) Quantification of RIMKLA protein levels in terms of band intensity/β-actin band intensity, in control, H_2O_2 and H_2O_2 + NAC treated cells, from part A. n = 3. Treatment with ROS-inducing agents: H_2O_2 = hydrogen peroxide, 100 µmol/L, for 1 h; H_2O_2 + NAC = hydrogen peroxide + N-acetylcysteine, 100 µmol/L + 20 mmol/L, for 5 h; ERA = Erastin = 50 µmol/L, for 24 h; MEN = Menadione, 100 µmol/L, for 6 h; MitoPQ = MitoParaquat, 5 µmol/L, for 6 h. DOX = Doxorubicin, 200 µmol/L for 8 h. Olap = Olaparib, 10 µmol/L, for 4 h.

5.2.4. Loss of *RIMKLA* does not lead to detectable DSBs in hypoxia

Having observed changes in ROS levels of *RIMKLA*-depleted cells, we next sought to investigate if this extended to changes in levels of detectable DSBs. ROS-dependent DNA damage has mainly been studied in the context of anticancer treatments, including drugs (doxorubicin, cisplatin, etc.) and radiation types (e.g., ionising), known to damage the DNA by the formation of ROS. ROS have also been reported to directly induce other forms of DNA damage through oxidising nucleoside bases (e.g. formation of 8-oxoguanine, which can lead to G-T or G-A transversions if unrepaired. Oxidised bases are typically recognised and repaired by the BER pathway, but when they occur simultaneously on opposing strands, attempted BER can lead to the generation of DSBs (Cannan *et al*. 2014; Srinivas *et al*. 2019).

To assess the levels of DSBs in hypoxic *RIMKLA*-depleted cancer cells, we transfected CAL-51 cells with either siScr or si*RIMKLA* and exposed them to <0.1% O_2. Samples were stained with anti-53BP1antibody the for detection and quantification of DSBs, by immunofluorescence for 53BP1 foci (% cells with <5 foci).

Results of this experiment showed that, hypoxia, despite its effect of increasing intracellular ROS levels as described previously herein and by other studies, did not lead to the formation of detectable DSBs. Interestingly, siRNA-mediated *RIMKLA* knockdown, did not lead to the formation of DSBs, in either hypoxic or normoxic cells (figure 5.4, A and B) despite the significant increase in ROS levels which we described in a previous section (figure 5.2, B, C).

Protein samples from the same cells, were analysed for RIMKLA levels by means of western blot, for the purpose of siRNA-mediated knockdown validation, as well as for HIF-1α levels to ensure its stabilisation in the hypoxic conditions we tested (figure 5.4, C).

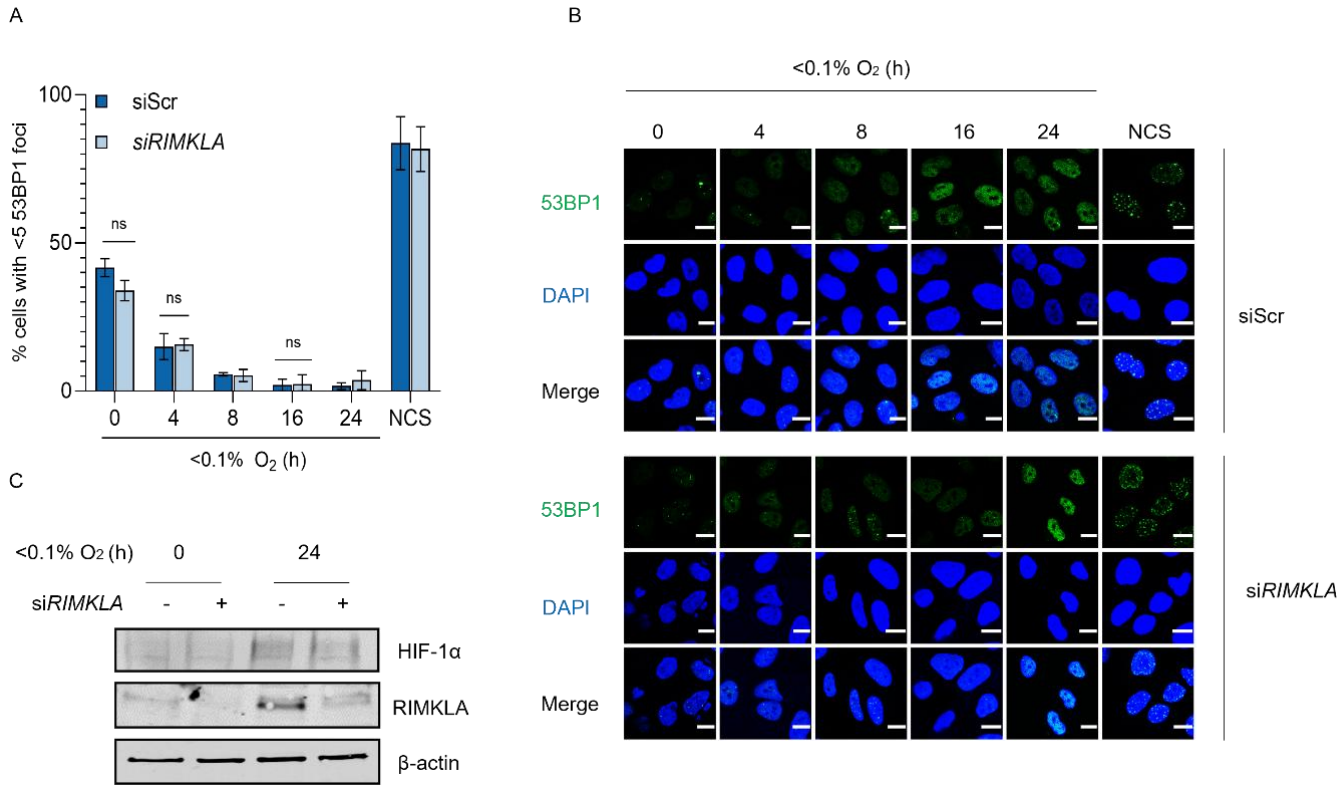

Figure 5.4. Loss of *RIMKLA* does not lead to detectable DNA damage in hypoxia. CAL-51 cells were transfected either with siScr or with si*RIMKLA* before treatment with <0.1% O_2 for the indicated time period. Samples were fixed at the indicated time points. (A) Quantification of % cells with more than 5 (>5) 53BP1 foci. NCS = Neocarzinostatin, 5 µmol/L for 6 h, used as positive control. (B) Representative immunofluorescence images from part A. Scale bar = 10 µm. (C) Western blot analysis of RIMKLA levels for siRNA-mediated knockdown validation. HIF-1α used as hypoxia control and β-actin used as loading control. n = 3.

5.2.5. Loss of *RIMKLA* reduces levels of γH2AX

Since 53BP1 foci analysis can detect and localise only certain types of DNA lesions, we additionally tested the impact of *RIMKLA* depletion on the levels of DNA damage in hypoxic cells, using a more global DNA damage marker, γH2AX. Specifically, histone H2AX is known to be a phosphorylation substrate of all three apical DDR kinases (section 1.1.6), and its phosphorylated form (γH2AX) can, therefore, serve as a marker of a broader range of DNA lesions and active DDR signalling (Mah *et al*. 2010).

Western blot analysis of protein samples from CAL-51 cells, transfected with either siScr or si*RIMKLA*, showed that depletion of this gene resulted in significantly reduced levels of γH2AX in both normoxic and hypoxic cells. Of note, the hypoxia-mediated increase of γH2AX levels, previously reported by relevant studies (Economopoulou *et al*. 2009; Hammond *et al*. 2003a) was observed in this experiment, as well (figure 5.5, A and B)

This finding shows that contrary to what would be anticipated, the increased levels of ROS in response to siRNA-mediated *RIMKLA* knockdown which we demonstrated (figure 5.2, C and D), do not lead to the formation of any detectable DNA damage, regardless of the oxygen levels the cells are exposed to. Instead, despite the increase in ROS levels, the active DDR signalling in cells without *RIMKLA* appears to be reduced.

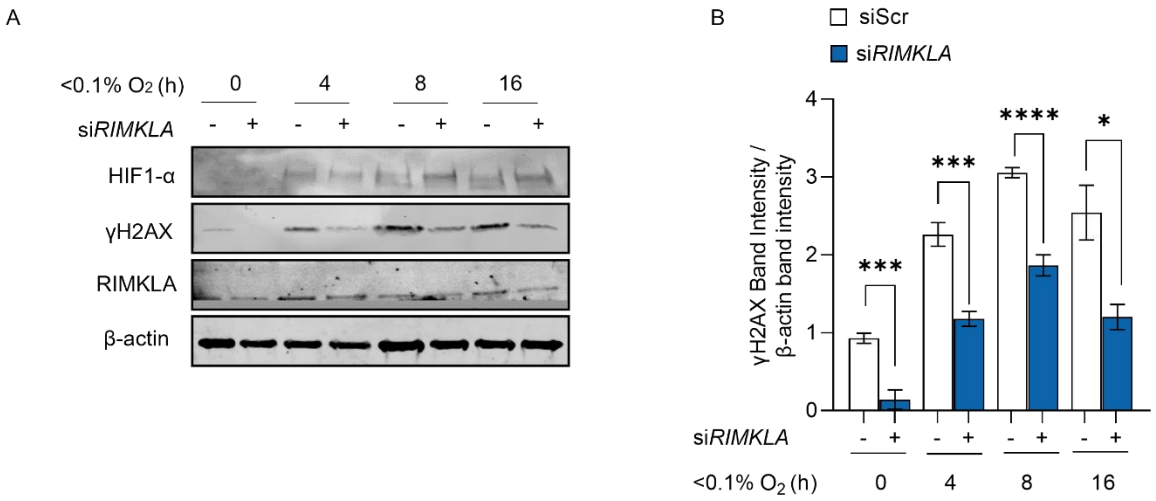

Figure 5.5. Loss of *RIMKLA* reduces levels of γH2AX in hypoxic cells. CAL-51 cells were transfected with either siScr or si*RIMKLA* before treatment with <0.1% O_2 for the indicated time period. Samples were harvested at the indicated timepoints. (A) Protein samples were analysed by western blot assay for levels of γH2AX. HIF-1α levels were analysed as a hypoxia control, and RIMKLA levels, as a control for siRNA-mediated knockdown efficacy. β-actin was used as a loading control. (B) Quantification of γH2AX levels, as band intensity, from part A. n = 3.

5.2.6. Loss of *RIMKLA* decreases the levels of hypoxia-induced replication stress

The findings described in previous sections, collectively indicate the absence of DNA damage in *RIMKLA*-depleted cells, in an oxygen-independent manner, despite increases in ROS levels in response to both hypoxia and to *RIMKLA* knockdown. Apart from DNA lesions, however, excessive ROS and other intracellular free radicals are also associated with the induction of replication stress, i.e., conditions of slowing or stalling of replication fork progression and/or DNA synthesis, independently of DNA damage, a fact previously shown by several studies (Andrs *et al.* 2023; Ma *et al.* 2023; Zeman and Cimprich 2014).

To assess the levels of RPA foci in response to siRNA-mediated *RIMKLA* knockdown, we transfected CAL-51 cells with either siScr or si*RIMKLA* and exposed them to <0.1% O_2. Samples were analysed by means of immunofluorescence. First, the number of cells (%cells) with <5 RPA foci was quantified, for assessment of the cell fraction with an active replication stress response, in each condition. Results of this analysis showed a significant decrease in number of cells with RPA foci accumulation in normoxic cells without *RIMKLA*, suggesting a decrease in levels of endogenous replication stress levels in these cells. Furthermore, depletion of *RIMKLA* in conditions of prolonged hypoxia (24 h <0.1% O_2) also resulted in a decrease of %cells with accumulation of RPA foci (figure 5.6, A and C).

Quantification of RPA foci per cell, was the carried out to assess levels of ongoing replication stress, in response to *RIMKLA* knockdown. This analysis showed a significant reduction in levels of replication stress in response to *RIMKLA* depletion, after 24 h of treatment with <0.1% O_2 (figure 5.6, B and C). Protein samples of the same cells were analysed by western blot assay, for levels of RIMKLA as a validation of siRNA-mediated knockdown efficacy and for levels of HIF-1α, for validation of its stabilisation in hypoxic conditions (figure 5.6, D). Along with our findings that show decreased γH2AX levels (commonly used as a marker of replication stress in hypoxic

conditions), in response to *RIMKLA* depletion, this finding supports that loss of *RIMKLA* reduces levels of replication stress, in an oxygen-independent manner.

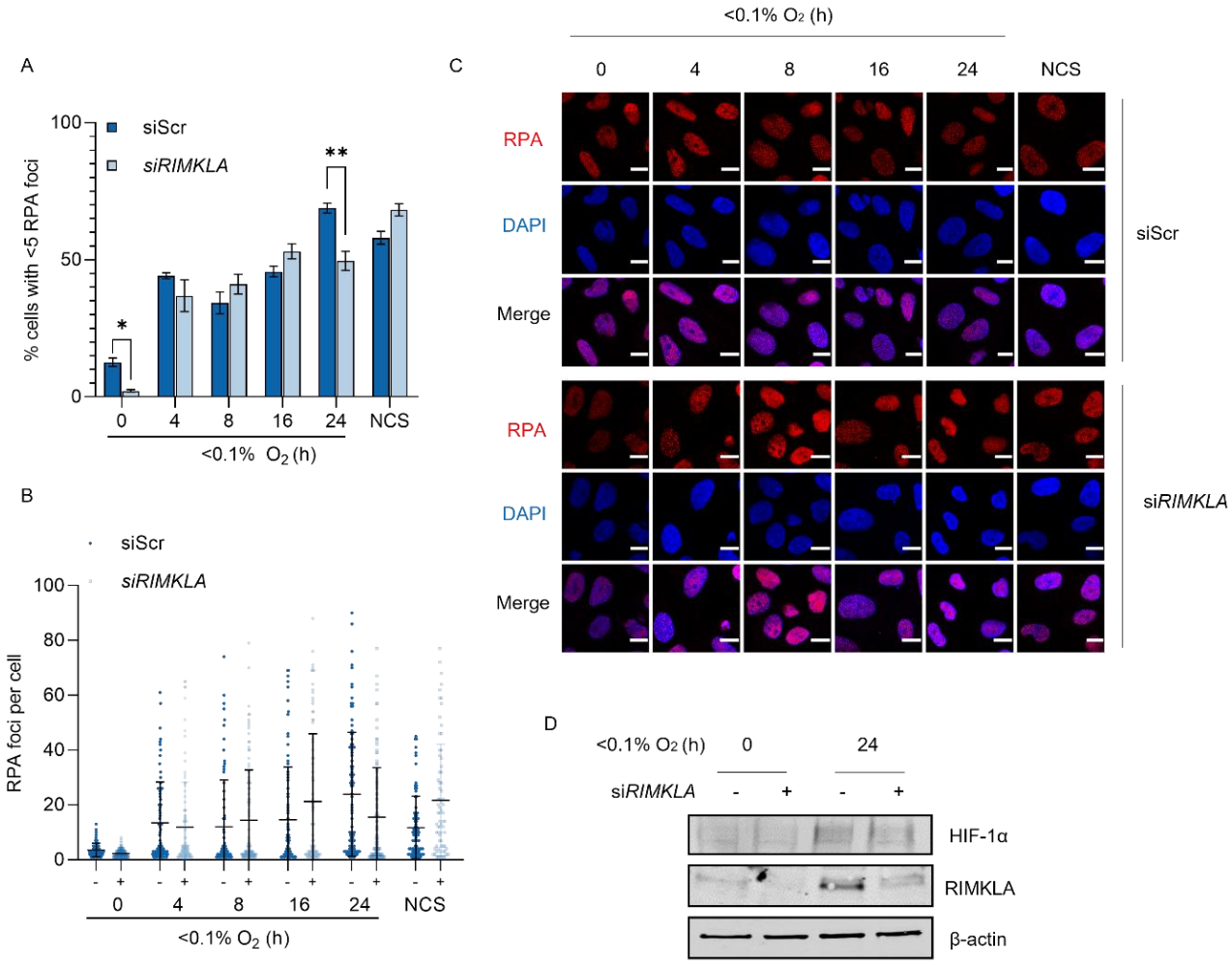

Figure 5.6. Loss of *RIMKLA* decreases the levels of hypoxia-induced replication stress. CAL-51 cells were transfected either with siScr of si*RIMKLA* before treatment with <0.1% O_2 for the indicated time period. Samples were fixed at the indicated timepoints. (A) quantification of cells with >5 RPA foci. (B) Quantification of number of distinct RPA foci per cell. NCS = Neocarzinostatin (5 μmol/L for 6 h), used as positive control. (C) Representative immunofluorescence images from parts A and B. Scale bar = 10 μm. (D) Western blot analysis of RIMKLA levels for siRNA-mediated knockdown validation. HIF-1α used as hypoxia control and β-actin used as loading control (data presented also in figure 5.4, C). n = 3.

5.2.7. Loss of *RIMKLA* reduces cell number in response to hypoxia

During immunofluorescence experiments with *RIMKLA*-depleted hypoxic cells, we observed a significant reduction in cell number per field during microscopic analysis, compared to *Mock*-treated and siScr transfected cells, exposed to the same hypoxic conditions. This phenomenon was not observed in normoxic control cells, nonetheless, as it can be seen in data from a cell-counting experiment with DAPI-stained, either *Mock*-treated or si*RIMKLA* transfected CAL-51 cells, counted using fluorescence microscopy (figure 5.7, A and B). Protein samples of the same cells were used, for western blot analysis of RIMKLA protein levels, as a validation of siRNA-mediated *RIMKLA* knockdown efficacy, before treatment with <0.1% O_2 (figure 5.7, C). Similarly, cells transfected with si*RIMKLA* showed reduced total number when exposed to <0.1% O_2 compared to siScr-transfected counterparts (figure 5.7, D and E). Protein samples of the siScr and *siRIMKLA* transfected cells were used, for western blot analysis of RIMKLA protein levels, as a validation of siRNA-mediated *RIMKLA* knockdown efficacy, before treatment with <0.1% O_2 (figure 5.7, F). These findings are suggestive of either reduced viability, or compromised adherence of hypoxic cells, in response to *RIMKLA* knockdown

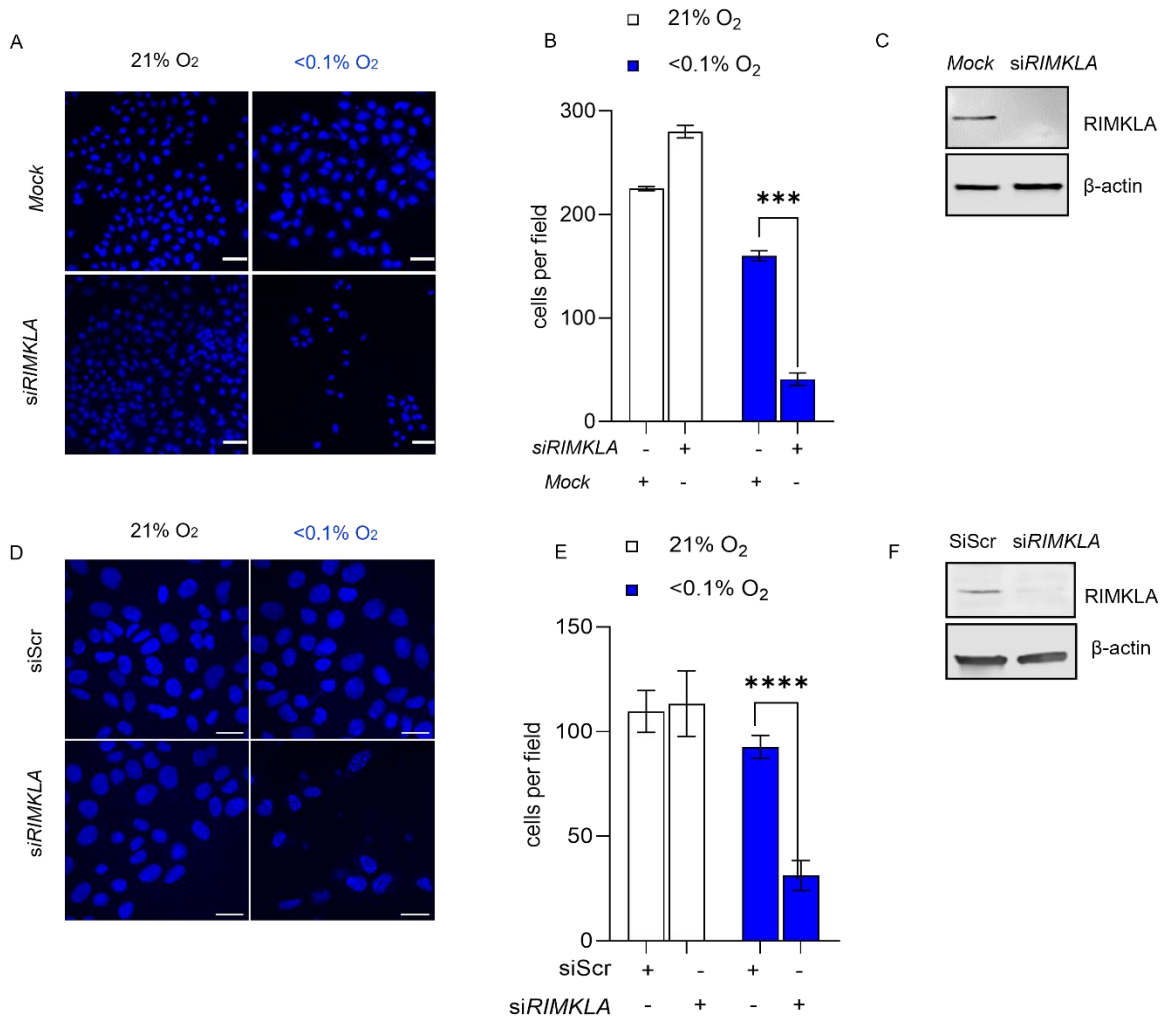

Figure 5.7. Loss of *RIMKLA* reduces cell number in response to hypoxia. CAL-51 cells were either treated with *Mock* or transfected with either siScr or si*RIMKLA*, prior to treatment with <0.1% O_2 for 16 h and then stained with DAPI (blue), for microscopic analysis of cell number. (A) Representative fluorescence microscopy images from DAPI (blue) stained CAL-51 cells, treated with either *Mock* or si*RIMKLA* for cytometry, before and after exposure to <0.1% O_2. Scale bar = 50 µm. (B) Quantification of cell number from part A. n = 3. (C) Western blot analysis of RIMKLA protein levels, for siRNA-mediated knockdown validation. β-actin used as loading control. (D) Representative fluorescence microscopy images from DAPI (blue) stained CAL-51 cells, transfected with either siScr or si*RIMKLA* for cytometry, before and after exposure to <0.1% O_2. Scale bar = 20 µm. (E) Quantification of cell number from part D. n = 3. (F) Western blot analysis of RIMKLA protein levels, for siRNA-mediated knockdown validation. β-actin used as loading control.

5.2.8. Loss of *RIMKLA* in hypoxia decreases survival of cancer cells

Next, we sought to orthogonally test if and how, loss of *RIMKLA* affected the viability of hypoxic cancer cells. To test this hypothesis, we carried out colony survival assays, using CAL-51 cells transfected with either siScr or si*RIMKLA*, exposed to <0.1% or 2% O_2. Additionally, we tested the viability of *Mock*-treated hypoxic CAL-51 cells to make sure we eliminated any potential viability artifact of transfection-associated cytotoxicity.

Results of our experiments demonstrated a significantly decreased clonogenic capacity of *RIMKLA*-depleted CAL-51 cells, specific to hypoxic conditions, independently of transfection toxicity. Of note, *RIMKLA* knockdown resulted in a quantitively higher loss of clonogenicity in response to treatment with <0.1% O_2, compared to treatment with 2% O_2, consistently, perhaps, with the severity of the hypoxic stress (figure 5.8, A, B and C).

RT-qPCR analysis of *RIMKLA* mRNA levels in samples from the *Mock*-treated and si*RIMKLA* transfected cells used for colony formation assays, was applied for validation of siRNA-mediated knockdown efficacy (figure 5.8, D).

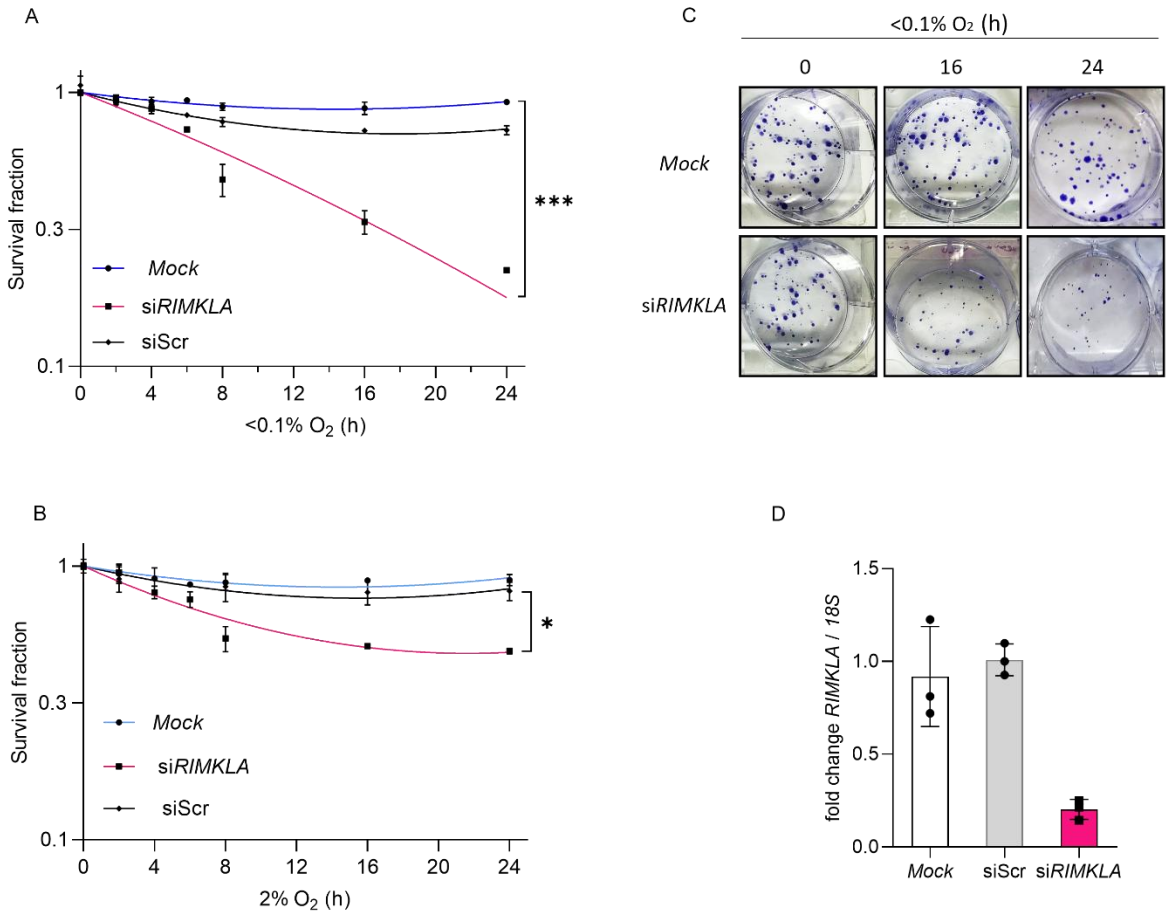

Figure 5.8. Loss of *RIMKLA* sensitises CAL-51 cells to hypoxia. (A) Colony survival assay of CAL-51 cells, either treated with *Mock* or transfected with either siScr or si*RIMKLA* before exposure to <0.1% O_2 for the indicated time-course. n = 3. (B) Colony survival assay of CAL-51 cells treated with *Mock* or transfected with either siScr or si*RIMKLA* before treatment with <2% O_2 for the indicated time-course. n = 3. (C) Representative images of CAL-51 cells, either treated with *Mock* or transfected with si*RIMKLA* and exposed to <0.1% O_2, from colony survival assay in part A. (D) RT-qPCR analysis of *RIMKLA* mRNA levels in CAL-51-cells treated with *Mock*, siScr or si*RIMKLA* transfected, as an siRNA-mediated knockdown validation in cells used for colony survival assays, for parts A and B.

5.2.9. Loss of *RIMKLA* does not induce apoptotic nuclear morphology in hypoxic cells

We then sought to characterise the mechanism of the hypoxia-specific sensitisation of *RIMKLA*-depleted cells. Despite the absence of detectable DNA damage in response to *RIMKLA* depletion, which we reported in previous sections, cell death by apoptosis seemed like a solid hypothesis. Apoptosis is a common form of cell death in response to both excessive ROS and severe hypoxia. Importantly, apoptosis has been reported to occur independently of both genomic damage and active DDR signalling (Korwek *et al*. 2013; Park *et al*. 2017; Yuan *et al*. 2005).

Apoptotic cell nuclear morphology is quite distinctive: nuclei of apoptotic cells appear smaller and brighter upon fluorescent-microscopic examination, due to the chromatin condensation which typically occurs during apoptosis (when there is no DNA fragmentation), while in some cases (where DNA fragmentation does take place) the nuclei of apoptotic cells might even exhibit blebbing, making thus, nuclear morphology an indicative marker, commonly used for determination of apoptosis (Mandelkow *et al*. 2017; Sakahira *et al*. 1999).

Fluorescent microscopy analysis, of DAPI-stained CAL-51 cells, transfected with either siScr or si*RIMKLA*, prior to treatment with <0.1% O_2 for a prolonged time-period (24 h) (to make sure apoptotic signalling had progressed) was used to assess apoptosis. Etoposide, a well-known chemotherapeutic agent specifically targeting the enzyme topoisomerase II, causing thus, DNA-damage and induction of apoptosis, was used as a positive control.

This analysis showed that the hypoxic cells did not exhibit apoptotic nuclear morphology, regardless of *RIMKLA* presence/absence, compared to Etoposide-treated control cells, which exhibited an apoptotic nuclear phenotype (figure 5.9, A and B). Additionally, protein samples of the same cells, were analysed for RIMKLA protein levels as a validation of siRNA-mediated knockdown efficacy, as well as for HIF-1α levels, to validate its stabilisation in hypoxia (figure 5.9, C). Of note, siRNA-mediated *RIMKLA* depletion, did not exhibit an apoptotic nuclear morphology in normoxic cells compared, to siScr-transfected control cells, perhaps unsurprisingly, in

context with our previously-described data, reporting a hypoxia-specific sensitisation in these cells.

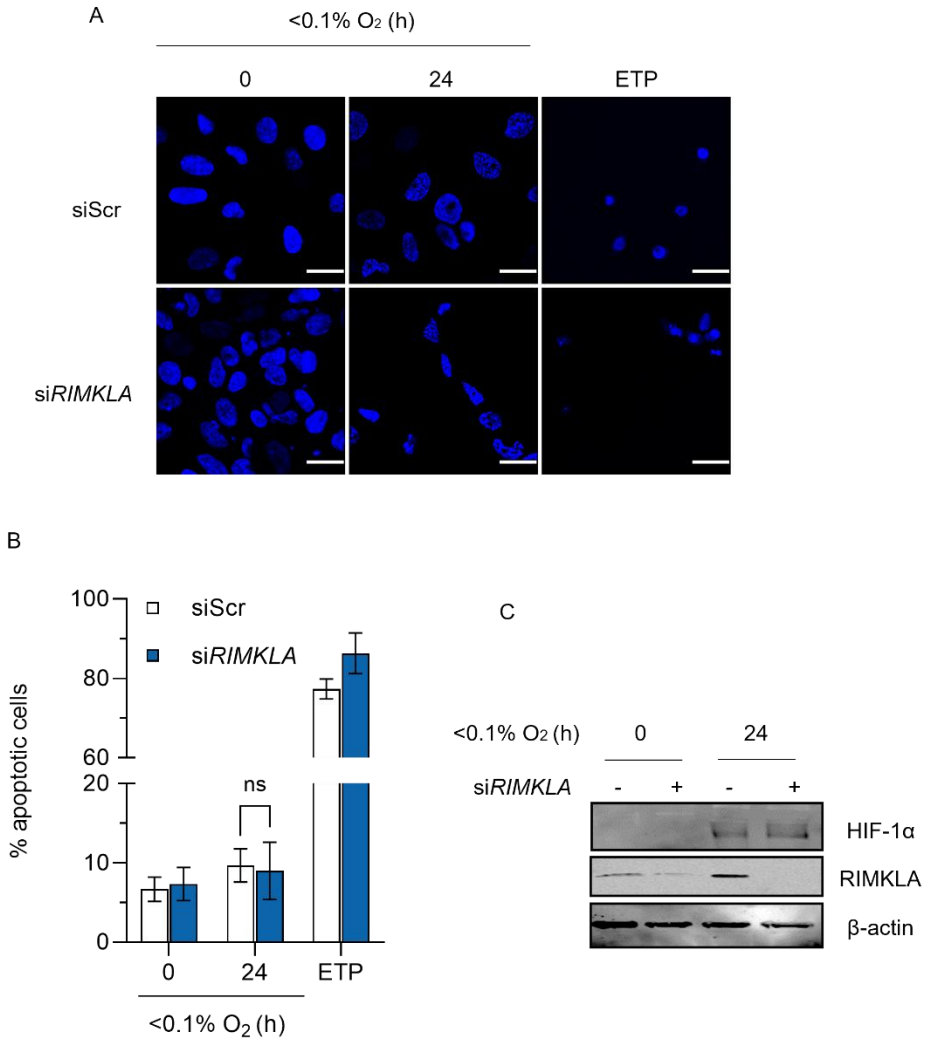

Figure 5.9. Loss of *RIMKLA* does not induce apoptotic nuclear morphology in hypoxic cells. CAL-51 cells were either transfected with either siScr or with *siRIMKLA*, prior to treatment with <0.1% O_2 for 24 h, and then stained with DAPI, for microscopic analysis of cell nuclear morphology. (A) Representative images from DAPI (blue) stained CAL-51 cells, transfected with either siScr or si*RIMKLA*, before and after exposure to <0.1% O_2 for determination of nuclear morphology. ETP = Etoposide used as positive control (2.5 mmol/L, for 24 h). Scale bar = 10 μm. (B) Quantification of apoptotic cell number (as percentage) from part A. n = 3. (C) Western blot analysis of RIMKLA levels, for confirmation of knockdown. HIF-1α used as a hypoxia control. β-actin used as loading control.

5.2.10. Loss of *RIMKLA* does not appear to increase activation of Caspase-3

To reinforce the observation that apoptosis did not mediate cell death in hypoxic *RIMKLA*-depleted cells using a more orthogonal assay, we analysed protein samples of either siScr or si*RIMKLA* transfected CAL-51 cells exposed to <0.1% O_2, by means of western blot assay, for protein levels of Caspase-3/cleaved Caspase-3. We used this assay to determine, if there were any differences in levels of Caspase-3/cleaved Caspase-3 in response to *RIMKLA* depletion.

Preliminary data indicated no difference in the levels of Caspase3/cleaved Caspase-3 in hypoxic cells upon *RIMKLA* siRNA-mediated knockdown, compared to siScr-transfected control hypoxic cells (figure 5.10, A and B).

Surprisingly, the same preliminary data suggested that hypoxia treatment (12 h at <0.1% O_2) led to activation of Caspase-3 (figure 5.10, A). This was unexpected, since data described in the previous section showed that cells exposed to <0.1% O_2 for 24 h did not exhibit apoptotic nuclear morphology (figure 5.9). Nonetheless, several cases have been previously reported, where hypoxia-mediated Caspase-9 and Ccaspase-3 activation, did not lead to apoptosis or DNA fragmentation (Garnier *et al*. 2004; Park *et al*. 2024).

This more orthogonal assay for apoptosis, further hinted that caspase-dependent apoptosis was not the mechanism of cell death, in *RIMKLA*-depleted hypoxic cells, albeit preliminary.

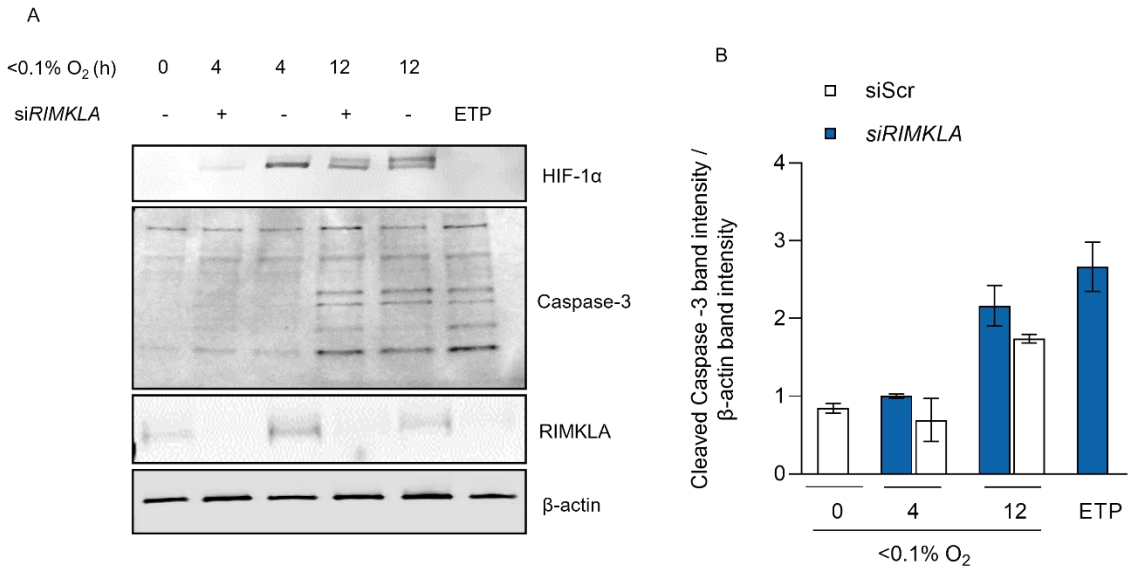

Figure 5.10. Loss of *RIMKLA* does not appear to lead to activation of Caspase-3. CAL-51 cells were transfected with either siScr or s*iRIMKLA*, before treatment with <0.1% O_2 for 0, 4 or and 12 h. Protein samples were analysed by western blot assay, for levels of Caspase-3/cleaved Caspase-3. ETP = Etoposide, used as positive control (2.5 mmol/L, for 24 h) RIMKLA protein levels were also analysed as a knockdown validation. HIF-1α was used as a hypoxia control and β-actin was used a s a loading control. (B) Quantification of cleaved Caspase-3 levels from part A. n = 2.

5.2.11. Depletion of *RIMKLA* drives reoxygenated cells to apoptosis

During our colony formation assays with hypoxic cells, reoxygenation follows after the respective hypoxia and (if any) other additional treatment is completed, for colonies to from during incubation in ambient oxygen conditions. Therefore, we wanted to explore the effect of reoxygenation on the viability *RIMKLA*-depleted cancer cells.

Therefore, we decided to carry out a nuclear morphology analysis of reoxygenated cells either treated with *Mock*, transfected with siScr control or transfected si*RIMKLA*, and exposed to <0.1% O_2 for 16 h, prior to reoxygenation at atmospheric oxygen levels (21% O_2).

We examined the number of cells that exhibited an apoptosis-associated nuclear morphology, after reoxygenation, comparing between *Mock*-treated or si*RIMKLA*-transfected, DAPI-stained CAL-51 cells, using fluorescence microscopy. Results of this quantification, showed that there were significantly more apoptotic *RIMKLA*-depleted reoxygenated cells, compared to *Mock*-treated, reoxygenated controls (figures 5.11, A, B and C, and 5.10, A and B). The nuclear morphology of the *RIMKLA*-depleted reoxygenated cells was identical to the Etoposide-treated apoptotic cell nuclei, described in the previous section. In addition, a reduced total cell number of reoxygenated *RIMKLA*-depleted cells, compared to hypoxic siScr-transfected control cells was observed, using the nuclear morphology analysis assay with the nuclear morphology of apoptotic cells (figure 5.11, E, F, G).

Protein samples from the cells used in this experiments were analysed by western blot assay for RIMKLA protein levels, as a control of the siRNA-mediated knockdown efficacy (figure 5.11, D and H)

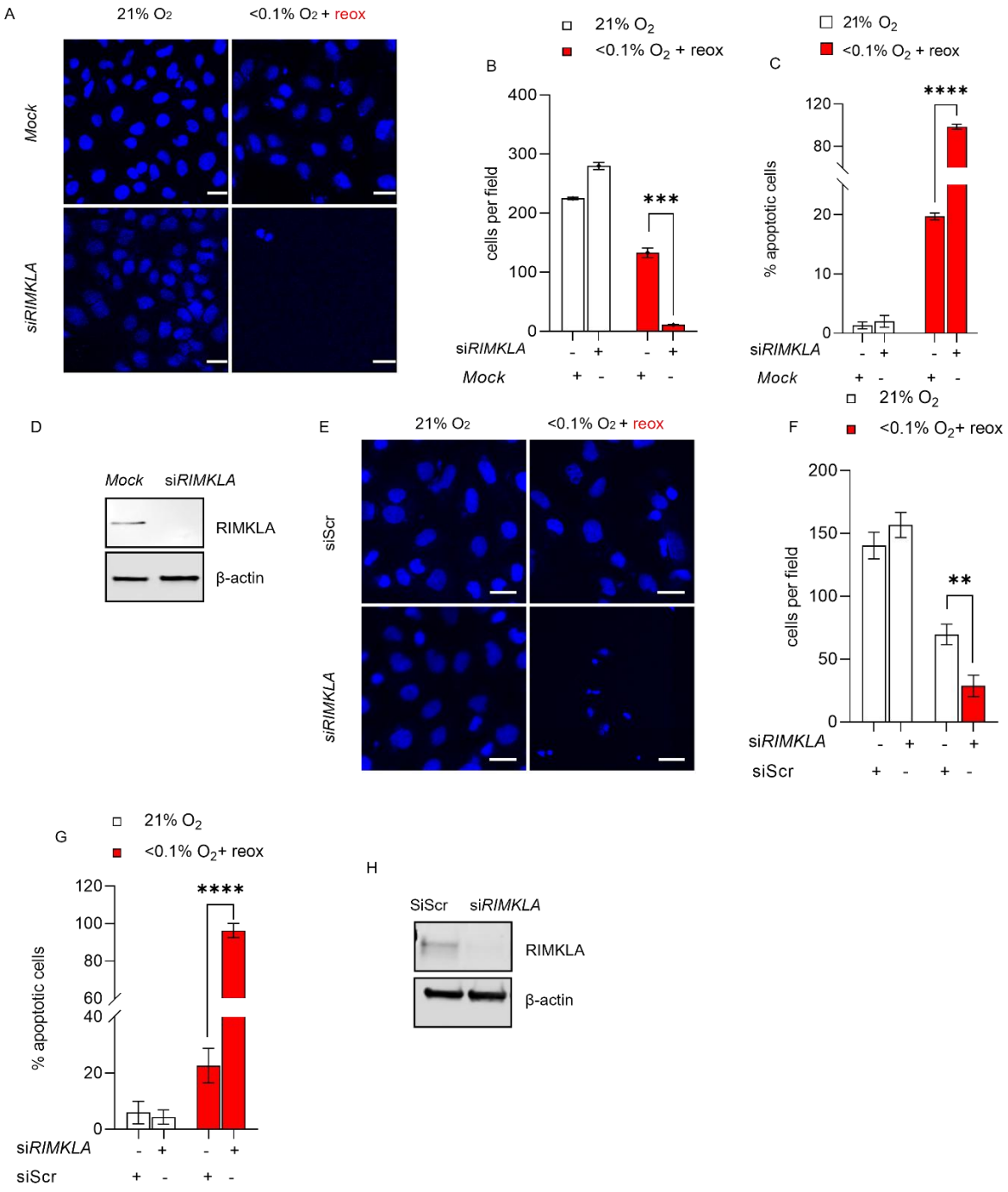

Figure 5.11. The impact of *RIMKLA* loss on nuclear morphology and number of reoxygenated cancer cells. CAL-51 cells were treated with *Mock* or transfected with either an siScr control or with si*RIMKLA* and then treated with <0.1% O_2 for 16 h, before reoxygenation at 21% O_2 for 7 h. (A) Microscopy images from DAPI (blue) stained cells, before and after reoxygenation for cell number analysis. Analysis of *Mock*-treated compared to si*RIMKLA*-transfected cells. Scale bar = 10 µm. (B) Quantification of cell number per microscopic field, from part A. (C) Quantification of %apoptotic cells from part A. (D) Western blot analysis of RIMKLA levels, in protein samples from cells used in part A. n = 3. (E) Microscopy images from DAPI (blue) stained cells, before and after reoxygenation for cell number analysis. Analysis of siScr-transfected compared to si*RIMKLA*-transfected cells. Scale bar = 15 µm. (F) Quantification of cell number per microscopic field, from part E. (G) Quantification of %apoptotic cells from part E. (H) Western blot analysis of RIMKLA levels, in protein samples from cells used in part E. n = 3.

5.2.12. Reoxygenation of *RIMKLA*-depleted cells drives them into apoptosis without p53-stabilisation

We continued on investigating the mechanism of the reoxygenation-induced apoptosis of *RIMKLA*-depleted cells, hypothesising it could be mediated by p53-dependent pro-apoptotic signalling. Preliminary data, however, suggested that the apoptotic phenotype of reoxygenated *RIMKLA*-depleted cells was not p53-dependent.

Specifically, western blot analysis of either siScr or si*RIMKLA* transfected CAL-51 cells and exposed to <0.1% O_2 for 16 h, prior to reoxygenation at atmospheric oxygen levels (figure 5.12, A) suggested that consistently with our previous findings on the apoptosis-mediated sensitisation of reoxygenated *RIMKLA*-depleted cells (figure 5.11, A, B and C), cleaved PARP1 levels were higher in *RIMKLA*-depleted cells in response to reoxygenation, compared to siScr-transfected reoxygenated control cells, a common indication of apoptosis (Cohausz and Althaus 2009; Diamantopoulos *et al*. 2014; Wu *et al*. 2024).

Furthermore, this assay indicated that protein levels of RIMKLA were upregulated in siScr-transfected cells, in response to reoxygenation, as quickly as 30 min after exposure to atmospheric oxygen levels (figure 5.12, B)

However, neither p53 nor its DDR-associated phosphorylated form, known as p53-Ser15, appeared to be stabilised, in *RIMKLA*-depleted reoxygenated cells (Madan *et al*. 2012; Wang *et al*. 2013). Of note, this was the case both at an early time point (30 min) and at a late timepoint (7 h), post-reoxygenation (figure 5.12, B). These findings suggest a p53-independent death by apoptosis of reoxygenated cells, in response to siRNA-mediated *RIMKLA* knockdown.

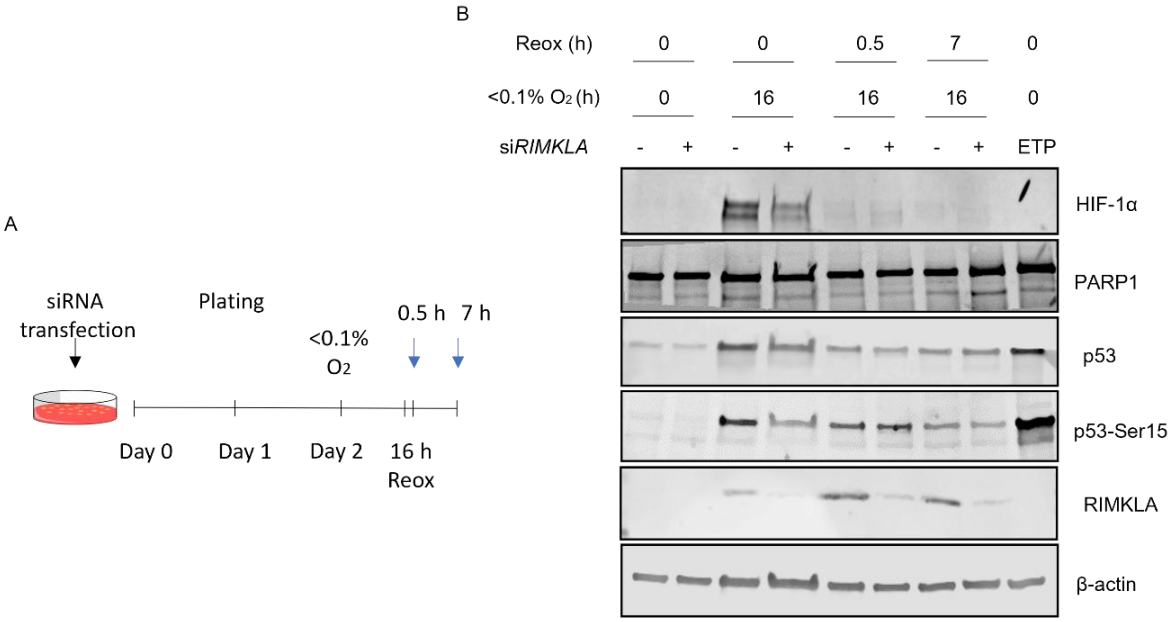

Figure 5.12. Reoxygenation of *RIMKLA*-depleted cells drives them into apoptosis without p53-stabilisation. CAL-51 cells were treated with either siScr or si*RIMKLA* and exposed to <0.1% O_2 for 16 h, prior to reoxygenation at atmospheric oxygen levels. (A) Experimental timeline illustration. Blue arrows indicated timepoints of protein sample harvesting from hypoxic and reoxygenated cells, respectively. (B) Western blot analysis of protein levels of PARP1/cleaved PARP1, p53 and p53-Ser15, RIMKLA for detection of knockdown efficiency, HIF-1α for control of hypoxia/reoxygenation and β-actin, as a loading control. ETP = Etoposide used as a positive control (2.5 mM for 16 h). n = 2.

5.2.13. Reoxygenation of *RIMKLA*-depleted cells leads to higher levels of DSBs

Aiming to further understand the mechanism of sensitisation of reoxygenated cells lacking *RIMKLA*, we tested the impact of reoxygenation on DSB levels in *RIMKLA*-depleted cells.

To do so, we exposed either siScr or si*RIMKLA* transfected CAL-51 cells to <0.1% O_2, for 16 h, before reoxygenating them at ambient oxygen conditions (figure 5.13, A). Samples from these cells were fixed 1 h post-reoxygenation and stained with DAPI and an anti-53BP1 antibody, for immunofluorescent detection and quantification of 53BP1 foci localised at DSB sites. Results of this assay showed that cells lacking *RIMKLA* accumulated significantly more DSBs in response to reoxygenation, compared to their control siScr-transfected counterparts (figure 5.13. B and C). Protein samples of the same cells were analysed by western blot assay, for RIMKLA protein levels, as a validation of siRNA-mediated knockdown efficacy (figure 5.13, D).

These findings suggest that these higher levels of DNA damage (DSBs) drive *RIMKLA*-depleted cells into apoptosis in response to reoxygenation and, in context with the preliminary data described in the previous section (figure 5.12, B), this potentially occurs in a p53-independent manner.

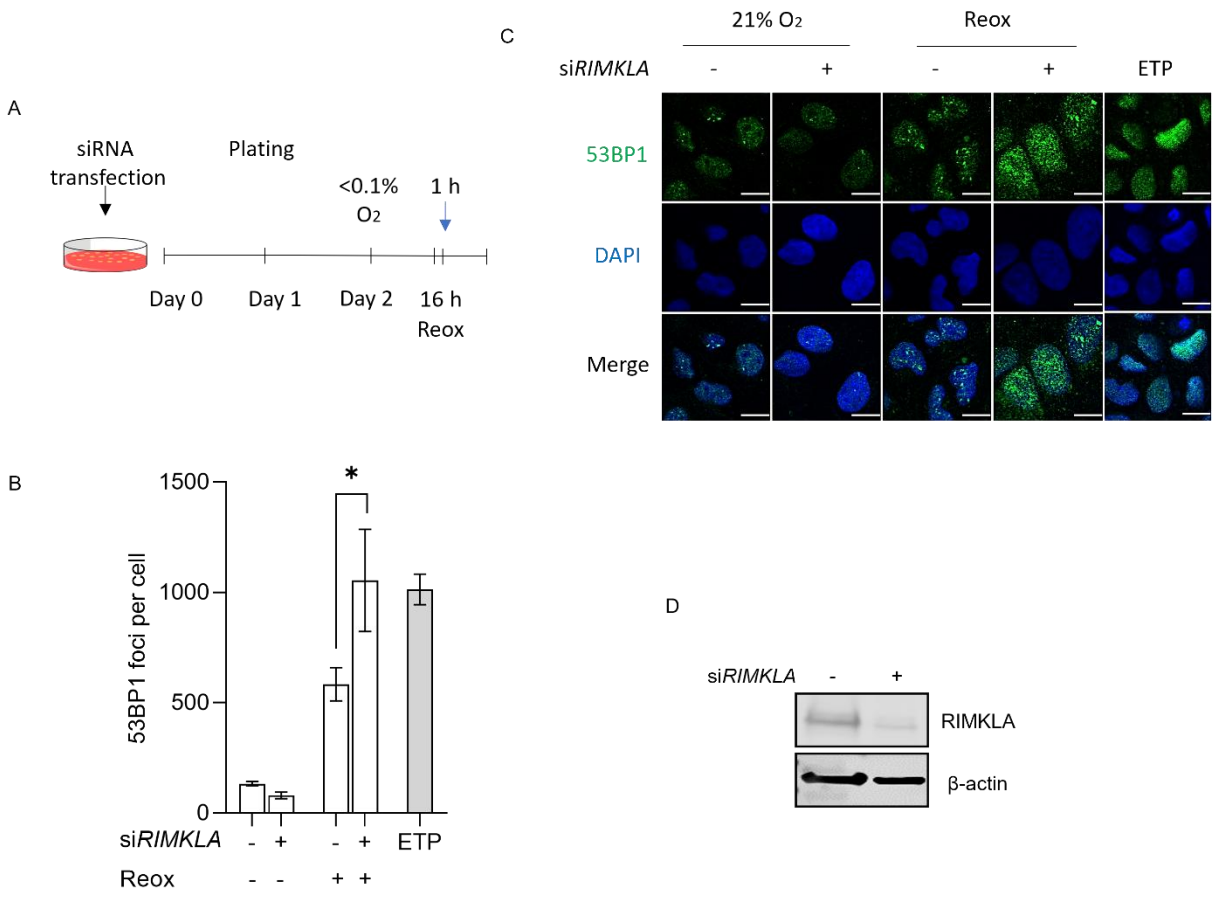

Figure 5.13. Reoxygenation of *RIMKLA*-depleted cells leads to higher levels of DSBs. (A) Experimental timeline: CAL-51 cells were transfected with either siScr or si*RIMKLA* and exposed to <0.1% O_2 for 16 h, before reoxygenation to atmospheric oxygen levels. Samples were fixed for microscopic analysis, 1 h post-reoxygenation. (B) Quantification of 53BP1 (green) foci per cell (in at least 100 cells), in normoxic and reoxygenated siScr/si*RIMKLA* transfected cells, stained with DAPI (blue). ETP = etoposide, used as a positive control (2.5 mmol/L for 2 h). n = 3. (C) Representative immunofluorescence images from part B. Scale bar = 10 µm. (D) Western blot analysis of RIMKLA protein levels in samples from cells used in parts B and C, as a validation of siRNA-mediated knockdown efficacy (data presented also in figure 5.2, E). β-actin was used as a loading control.

5.2.14. Depletion of *RIMKLA* results in induction of apoptosis and decreased cell number in response to treatment with H_2O_2

Next, we asked what happens to *RIMKLA*-depleted cells upon exposure to oxidative stress conditions. In context with the ROS-dependent upregulation of its protein levels we described before (figure 5.3, A and B, and figure 5.13, B), we hypothesised that this gene might play a role in antioxidant cell-responses and redox signalling, independently of oxygen conditions. In addition, since reoxygenation is known to cause an abrupt increase of intracellular ROS levels, among other cellular responses (Marshall *et al.* 1996; Zorov *et al.* 2014), we wanted to test the response of *RIMKLA*-depleted cells to a well-established oxidant, and compare it to the effects of reoxygenation, which we reported in a previous section (figure 5.11 A, B and C).

For this reason, we treated either siScr or si*RIMKLA* transfected CAL-51 cells, with the chemical oxidant H_2O_2, and analysed DAPI-stained samples for cell number and nuclear morphology, as previously described.

Counting of these DAPI-stained cells revealed that depletion of *RIMKLA* lead to significantly decreased cell number in response to H_2O_2 (figure 5.14, A and B). Additionally, the complete fraction of the remaining *RIMKLA*-depleted, reoxygenated cells, displayed an apoptotic nuclear morphology, matching those described previously, in response to prolonged treatment with Etoposide (figure 5.10, A and B) and in response to reoxygenation of RIMKLA-depleted cells (figure 5.11, A and figure 5.14, A and C).

Protein samples of the cells used in this assay were analysed by means of western blot assay, for levels of RIMKLA, as a validation of siRNA-mediated knockdown efficacy (figure 5.14, D)

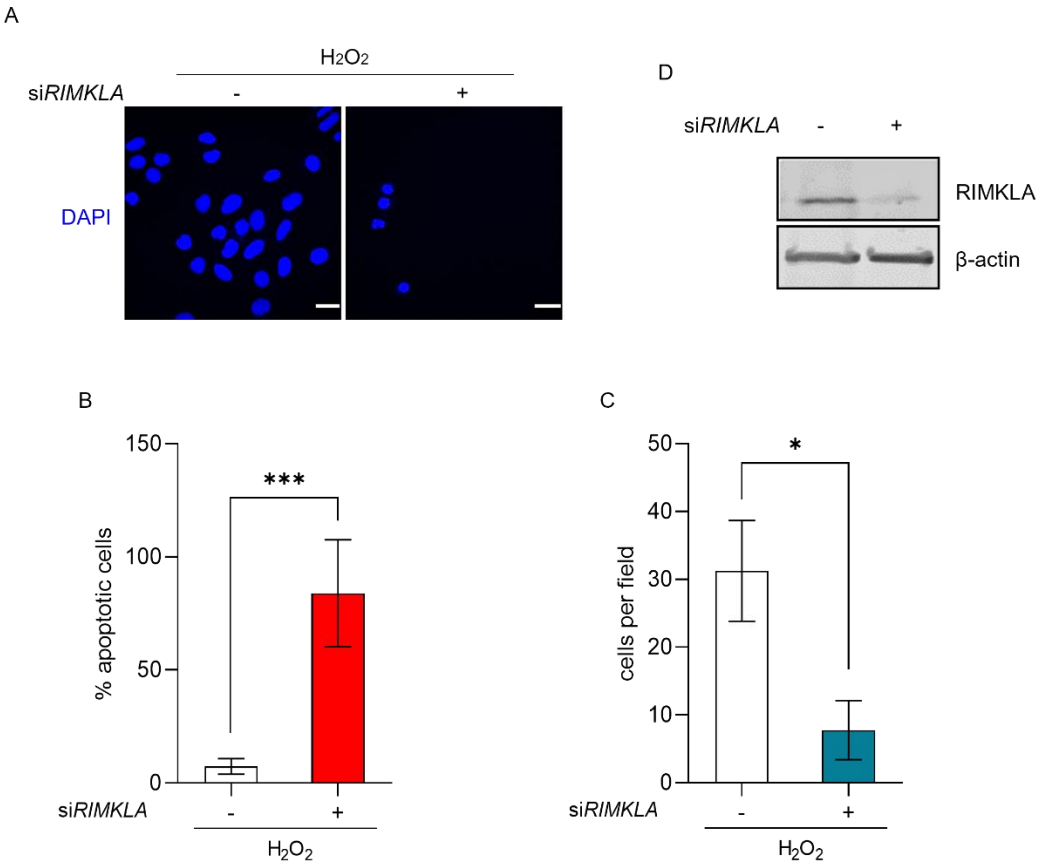

Figure 5.14. Depletion of *RIMKLA* results in induction of apoptosis and decreased cell number in response to treatment with H_2O_2. CAL-51 cells were transfected with either siScr or with si*RIMKLA,* prior to treatment with H_2O_2. (A) Representative images of DAPI-stained cells (blue), for fluorescence-assisted microscopic determination of cell number and nuclear morphology. Scale bar = 20 µm. (B) Quantification of apoptotic cell percentage from part A. (C) quantification of cell number (per microscopic field) from part A. n = 3. H_2O_2 = hydrogen peroxide; 5 mmol/L, for 12 h. (D) Western blot analysis of RIMKLA protein levels, in samples from cells used in parts A, B and C, for siRNA-mediated knockdown validation.

5.2.15. Treatment with ROS scavengers rescues the reduced viability of hypoxic *RIMKLA*-depleted cells

To examine if the reduced viability of hypoxia-treated *RIMKLA*-depleted cells which we previously demonstrated using colony formation assays, was dependent on intracellular ROS level-changes, we tested the clonogenic capacity of these cells by carrying out colony formation assays, with/without treatment with ROS scavengers, prior to hypoxia exposure.

Specifically, CAL-51 cells were transfected with either siScr or si*RIMKLA*, and 24 h later, both untreated transfected cells and transfected cells treated with either N-acetylcysteine (NAC), Vitamin C (Vit C), or Catalase B (CAT B) (1 h pre-treatment) were exposed to <0.1% O_2. Quantification of colony formation assays with these cells showed that pre-treatment with NAC, manged to rescue the viability of the hypoxia-exposed *RIMKLA*-depleted cells, by significantly increasing their clonogenic capacity (figure 5.15, A and B). Preliminary data of colony formation assays with the additional ROS scavengers, Vit C and CAT B, followed the same trend, rescuing the viability of *RIMKLA*-depleted hypoxic cells (figure 5.15, C). Of note, all three chemical compounds have been previously used validated for their ROS-scavenging activities (Bader *et al*. 2021; Ma *et al*. 2023; Twigger *et al*. 2024). Nonetheless, quantification of ROS levels after treatment with the ROS scavengers would further reinforce these data. Protein samples of the cells used for colony formation assays were analysed for RIMKLA levels, as a validation of siRNA-mediated knockdown efficacy (figure 5.15, D)

Collectively, these data support the hypothesis of a ROS-dependent mechanism of sensitisation of *RIMKLA*-depleted cells exposed to hypoxia, consistently with our previously described data, on these cells' sensitive phenotype upon treatment with an established chemical-inducer of oxidative stress (figure 5.14, A and B)

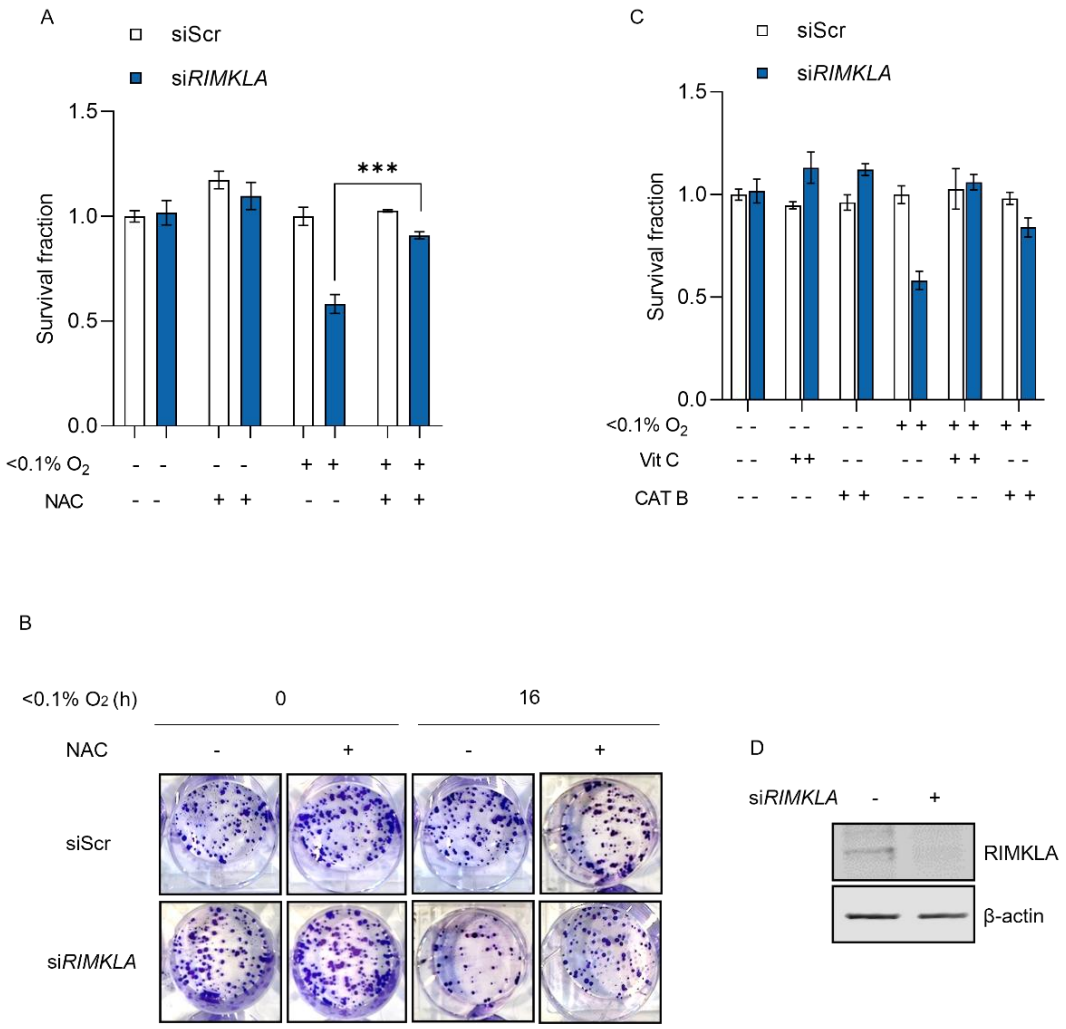

Figure 5.15. Treatment with ROS scavengers rescues the reduced viability of hypoxic *RIMKLA*-depleted cells. CAL-51 cells were transfected with siScr or si*RIMKLA* and 24 h later treated with ROS scavengers and exposed to <0.1% O_2 for 16 h. (A) Quantification of colony formation assays with siScr/si*RIMKLA* transfected cells exposed to hypoxia, with or without the addition of the ROS scavengers NAC. NAC = N-acetylcysteine (20 mmol/L). (B) Representative images from part A. n = 3. (C) Quantification of colony formation assays with siScr/si*RIMKLA* transfected cells exposed to hypoxia, with or without the addition of additional ROS scavengers. Normoxic and hypoxic controls presented also in part A. Vit C = Vitamin C (2 mmol/L); CAT B = Catalase B (2000 units/mg). n = 1. All ROS scavengers were added 1 h prior to hypoxia treatment. (C) Western blot analysis of RIMKLA protein levels, in samples form cells usen in colony formation assays in parts A and B, as a validation of siRNA-mediated knockdown efficacy.

5.2.16. High expression levels of *RIMKLA* correlate with worse survival outcomes in patients with hypoxic breast cancers, *vs*. patients with non-hypoxic breast tumours

Our findings, so far, demonstrate that depletion of *RIMKLA* impacts the viability of cells exposed to hypoxia. We sought to investigate if our findings are reflected in patient survival outcomes, in a hypoxia-specific manner.

As described in previous sections (sections 1.3.2 and 1.3.3), malignant tumours exhibit an oxygen gradients with regions of variable, often fluctuating oxygen levels. To test our hypothesis, we used the publicly available TCGA BRCA transcriptomic dataset. To decipher between breast tumours with higher and those with lower oxygen levels, we filtered the samples according to their Buffa hypoxia score, which is the most commonly used score for assessment of hypoxia-associated changes in breast cancer cases (Iqbal *et al*. 2023; Jacobson *et al*. 2023). The tumour samples were divided into quartiles and samples from Q1 (lowest Buffa hypoxia score, i.e., with higher oxygen levels) and Q4 (highest Buffa hypoxia score, i.e., with the lowest oxygen levels) were filtered down. Then, we used the publicly available transcriptomic data from these selected samples to stratify patient tumours into groups of low/moderate-*RIMKLA* mRNA content (Q1,Q2 and Q3) and high-*RIMKLA* mRNA content (Q4), comparing the survival outcomes of these patient groups.

Results of this preliminary analysis associate higher levels of *RIMKLA* with a significantly negative hypoxia-specific impact on patient survival status, both in terms of %OS and %PFS (figure 5.16, A and B). The hypoxia-specificity is associated with the fact that the unfavourable prognostic impact of high *RIMKLA* levels is seen only in breast tumours with the highest Buffa hypoxia score (i.e., lower oxygen levels) and not in those with the lowest Buffa hypoxia score (i.e., higher oxygen levels) (figure 5.16, C and D). These data, support the potential clinical relevance of the hypoxia-associated effects of *RIMKLA* on cancer cell viability.

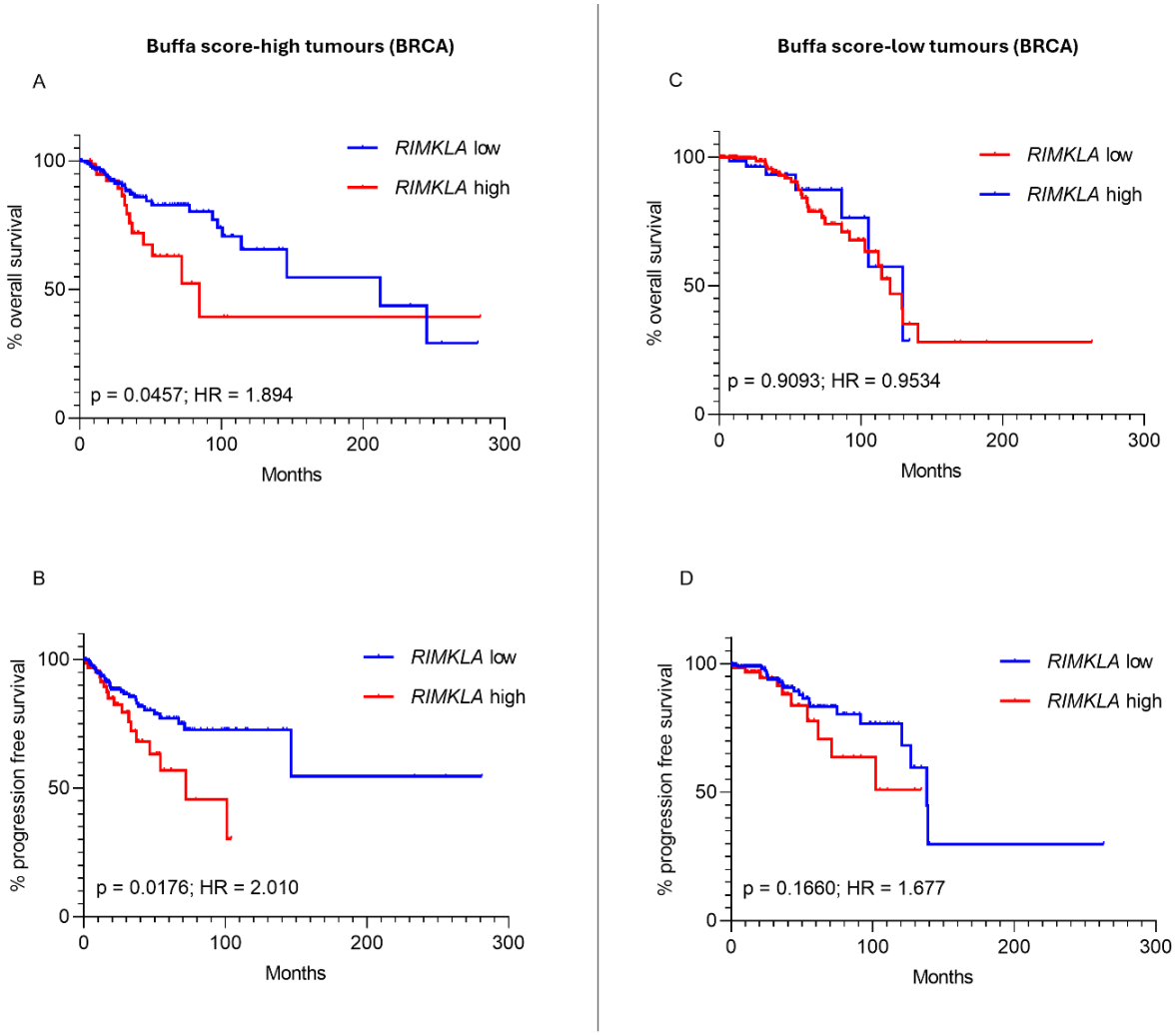

Figure 5.16. High levels of *RIMKLA* correlate with worse survival outcomes in patients with hypoxic breast cancers, vs. patients with non-hypoxic breast tumours. TCGA BRCA publicly available transcriptomic data were accessed and downloaded from cBioportal. Patient samples (n = 1084) from this dataset were divided in quartiles according to Buffa hypoxia score with Q1 (lowest, n = 269) and Q4 (highest, n = 270) samples further filtered down. Transcriptomic data were further used to additionally divide patients samples according to *RIMKLA* mRNA levels in low (Q1, 2 and 3) and high (Q4) groups from comparison of survival outcomes according to buffa score. (A) High levels of *RIMKLA* are associated with significantly poorer %OS in breast cancer patients with high Buffa hypoxia score compared to those with lower *RIMKLA* levels (p = 0.0457; HR = 1.894). (B) High levels of *RIMKLA* are associated with significantly poorer %PFS in breast cancer patients with high Buffa hypoxia score compared to those with lower *RIMKLA* levels (p = 0.0176; HR = 2.010). (C) No significant impact of *RIMKLA* levels is observed on survival outcomes of patients with low Buffa hypoxia score tumours, in terms of %OS (p = 0.9093; HR = 0.9534). (D) No significant impact of *RIMKLA* levels is observed on survival outcomes of patients with low Buffa hypoxia score tumours, in terms of %PFS (p = 0.1660; HR = 1.677).

5.2.17. Depletion of *RIMKLA* leads to radioresistance in normoxic cells without changing the sensitivity of hypoxic cells to ionising radiation

Since our previous data suggested a ROS-dependent sensitisation of *RIMKLA*-depleted cells, exposed to hypoxia, we wanted to characterise their radiation response, in terms of viability. Radiotherapy is known to mainly exert its cytotoxic effects, by mediating the creation of free radicals which, in the intracellular environment, damage macromolecules and cause cell death. Increases in intracellular ROS levels, have been shown to sensitise cells to forms of radiation, by a few previous studies (Bhosle *et al*. 2005; Xu *et al*. 2024a). Radiotherapy is commonly employed as a post-surgical treatment in breast cancer but sometimes it is used as adjuvant to pre-operative chemotherapy, to reduce tumour volume (Li and Barry 2022; Montero and Ciervide 2022). Therefore, we sought to investigate if there were any changes in the viability of irradiated cells, associated with *RIMKLA* levels.

To do so, we carried out colony survival assays with CAL-51 cells, transfected with either siScr or si*RIMKLA*, and treated with increasing doses of ionising radiation, in normoxic (21% O_2) or hypoxic (<0.1% O_2) conditions.

Results from our colony survival assays demonstrated no change in the viability response of hypoxic *RIMKLA*-depleted cells. Specifically, an oxygen enhancement ratio (OER) of 1.7, was seen for both siScr and si*RIMKLA*-transfected cells. Normoxic *RIMKLA*-depleted cells, nonetheless, displayed radioresistance compared to their control-transfected counterparts, with a standard enhancement ratio (SER) of 1.33. Protein samples of the cells used for the radiation colony survival assays were analysed by means of western blot for RIMKLA levels, as a validation of siRNA-mediated knockdown efficacy.

Both these findings were fairly surprising in context with our previous findings. Despite changes increases in ROS levels in both normoxic and hypoxic cells in response to *RIMKLA*-knockdown,

response to the cytotoxic effects of radiation did not change in hypoxia, and even more surprisingly, they were reduced in normoxic conditions, in these *RIMKLA*-depleted cells.

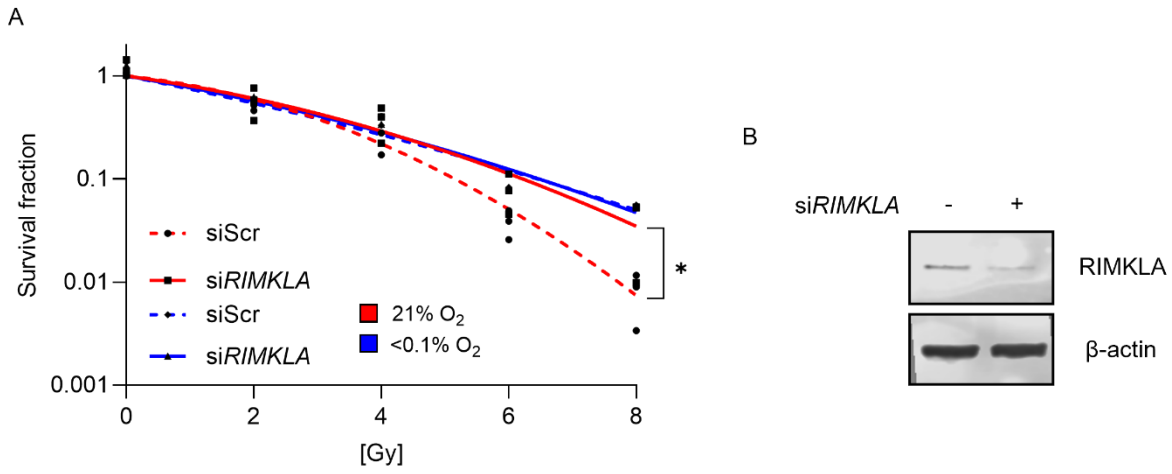

Figure 5.17. Depletion of *RIMKLA* leads to radioresistance in normoxic cells without changing the sensitivity of hypoxic cells to ionising radiation. CAL-51 cells were transfected with either siScr or si*RIMKLA*. Treatment with <0.1% O_2 for 6 h, was followed by irradiation and formation of colonies. Both normoxic and hypoxic cells were irradiated. The OER was calculated from the dose ratio between 21% O_2 and <0.1% O_2. The SER was calculated as dose ratio between siScr and si*RIMKLA* transfected cells.(A) Colony survival assay curves with increasing doses of ionising radiation of normoxic and hypoxic, siScr or si*RIMKLA*-transfected cells. n = 3. (B) Western blot analysis of RIMKLA protein levels, in samples from cells usen in colony formation assays from part A , as a validation of siRNA-mediated knockdown efficacy.

5.2.18. RIMKLA levels appear upregulated and diffusing outside the nucleoli in response to ionising radiation

We previously described the ROS-mediated RIMKLA induction in our cell line model, using a broad range of chemical oxidants and the ROS scavenger, N-acetylcysteine, as well as reoxygenation (figure 5.3, A and B, and figure 5.13, B). Since radiation also has been shown to increase levels of intracellular ROS (Kawamura *et al*. 2018), and considering the surprising findings we encountered during radiation of *RIMKLA*-depleted cancer cells, describe in the previous section, we wanted to examine the cellular localisation and expression of RIMKLA protein, in response to radiation.

To investigate this, we treated CAL-51 cells with a single dose of ionising radiation (8 Gy). Samples of these cells were stained with DAPI and anti-RIMKLA antibody, for immunofluorescent detection of RIMKLA. Results of this preliminary experiment suggested that RIMKLA was upregulated in response to ionising radiation, perhaps non-surprisingly, in context with the ROS-dependent induction of this protein, which we previously reported.

On the contrary, the changes in the intracellular localisation of RIMKLA, suggested by this preliminary data, were unexpected. It appears that, the protein diffuses outside the cell nucleoli, where it is mostly localised in untreated cells, and moves mainly into the perinuclear area of the cell (figure 5.18, A and B)

Importantly, these preliminary observations are reported merely on the benefit of hypothesis generation, rather than as a causality proof: This set of data is significantly underpowered (n = 1) and the additional lack of nucleolar controls like fibrillarin reduce interpretability.

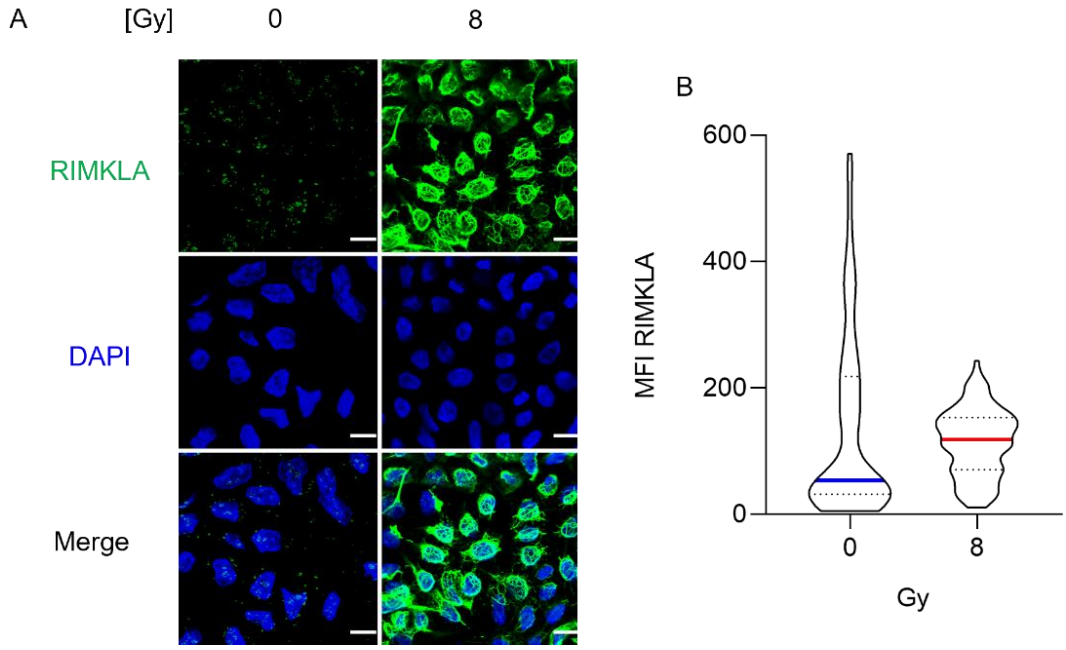

Figure 5.18. RIMKLA levels appear to be upregulated and diffusing outside the nucleoli in response to ionising radiation. CAL-51 cells were treated with 8 Gray (Gy) of ionising radiation. Samples were fixed for microscopic analysis, 3 h post-irradiation. (A) Representative immunofluorescence images of RIMKLA (green) n DAPI-stained (blue) CAL-51 cells, with/without ionising radiation treatment. Scale bar = 10 µm. (B) Quantification of RIMKLA protein levels, in cells from part A (n = 400 cells) as mean fluorescence intensity (MFI). n = 1.

5.2.19. High *RIMKLA* mRNA levels are associated with worse survival in breast cancer patients who received radiotherapy

Hoping to better understand our *in vitro* findings regarding the impact of *RIMKLA* on viability of irradiated cancer cells, we wanted to see how the levels of *RIMKLA* relate to clinical data from patients who received radiotherapy.

To examine this, we used the METABRIC cohort, since it exhibits higher sample numbers and therefore, more tumours that are likely to have received radiotherapy, albeit postoperative for the most part. First, we filtered patients in two groups: those who received radiotherapy and those who did not. On a clinical basis, radiotherapy can be used as a breast cancer treatment at any stage, both before and after mastectomy, as well as in cases of breast-conserving surgery (lumpectomy), but it is more likely to be implemented for larger and/or lymph node invading tumours, as well as in metastatic, locally advanced, and inflammatory breast cancers (Polgar *et al*. 2022). Therefore, we kept in mind that this analysis might reflect the impact of *RIMKLA* levels on survival differences in this patient subsets.

Then we assessed the transcriptomic data from radiotherapy-positive patient samples to distinguish between *RIMKLA* low (Q1) and *RIMKLA* high (Q4) groups. Survival data were used to analyse the %OS and most importantly, the %PFS (since patients had already received treatment), between these two groups. Results of this preliminary analysis indicated the patients with metastatic breast cancer who received radiotherapy, had significantly poorer survival outcomes, both in terms of %OS and %PFS, when their tumour mRNA levels of *RIMKLA* where high (figure 5.19,A and B).

Furthermore, analysis of the same transcriptomic datasets for levels of *RIMKLA* mRNA in radiotherapy-positive tumours *vs*. radiotherapy-negative ones, suggested a significant upregulation of *RIMKLA* mRNA levels in the former group. Using the same filtering method for analysis of chemotherapy-positive *vs*. chemotherapy-negative tumours, we observed that

RIMKLA was not suggested to be induced significantly in chemotherapy-positive samples, suggestive of a radiation-specific induction of *RIMKLA* in tumour samples from this study (figure 5.19, C and D). The lack of detailed metadata, nonetheless, confounds the interpretability of such findings.

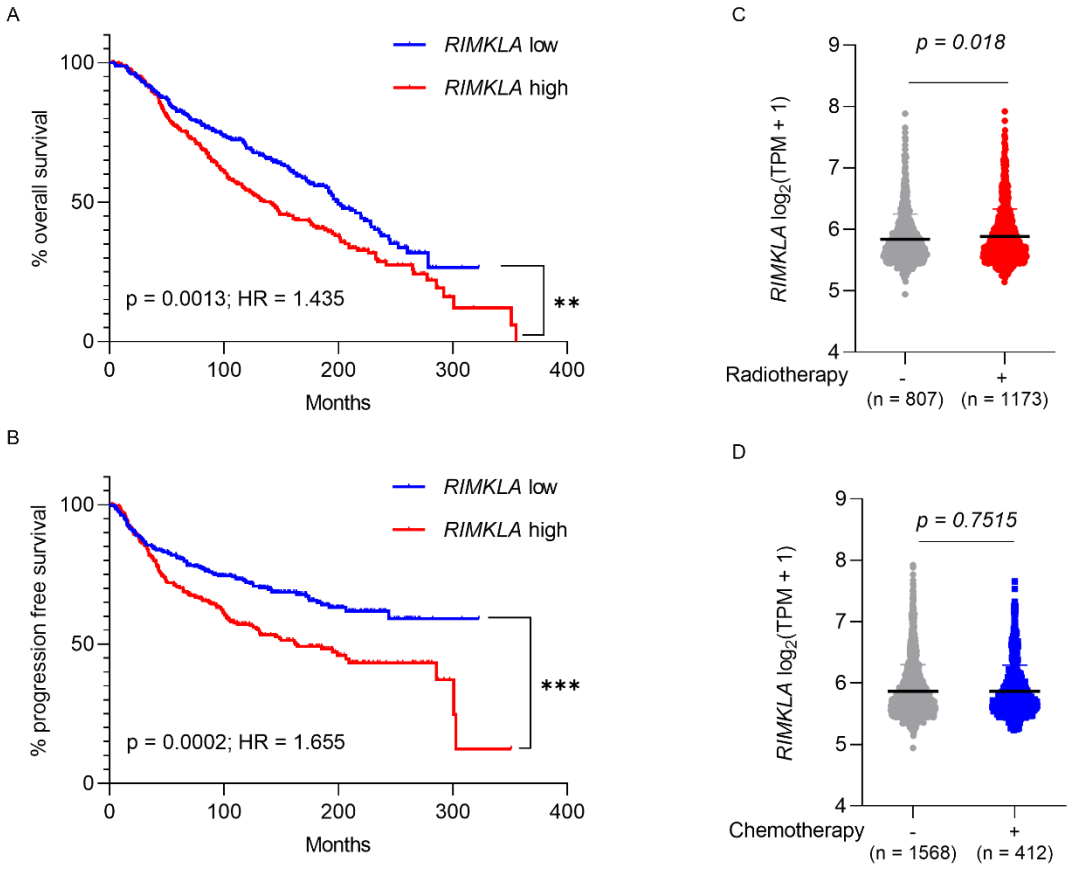

Figure 5.19. High *RIMKLA* mRNA levels are associated with worse survival in breast cancer patients who received radiotherapy. METABRIC patient sample data (n = 2509) were accessed and downloaded from cBioportal. Patients samples were filtered according to radiotherapy status in positive and negative. Transcriptomic data were used to further filter the samples according to *RIMKLA* mRNA levels in low (Q1) and high (Q4) groups. Survival analysis of radiotherapy positive patient samples (n = 1173) showed: (A) significantly worse %OS (p = 0.013; HR = 1.435) and (B) significantly worse %PFS (p= 0.0002; HR = 1.655) in patients with high expression levels of *RIMKLA*. (C) Analysis of the METABRIC transcriptomic data for *RIMKLA* mRNA levels (log_2TPM+1), in radiotherapy-positive (n = 1173) and radiotherapy-negative (n = 807) patient tumour samples. (D) Analysis of the METABRIC transcriptomic data for *RIMKLA* mRNA levels (log_2TPM+1), in chemotherapy-positive (n = 412) and chemotherapy-negative (n = 1568) patient tumour samples.

5.3. Discussion

This part of our study delineates a multifaceted role for *RIMKLA* in the regulation of redox homeostasis, DDR, and cell survival under hypoxic and reoxygenation conditions in breast cancer cells. Our findings both corroborate and extend current understanding of hypoxia-induced metabolic adaptations and reveal unanticipated nuances in how *RIMKLA* influences cellular fate.

Our observation that *RIMKLA* depletion blunts hypoxia-driven GSH accumulation aligns with NAAGS II's established role in NAAG synthesis. However, the paradoxical rise in ROS under normoxia, without a commensurate GSH drop, suggests an alternative antioxidant axis. One possibility is that *RIMKLA* influences cysteine availability *via* transsulfuration: by diverting glutamate away from exchange with extracellular cystine (*via* system Xc^-), its loss could impair thiol homeostasis independently of GSH concentration. This hypothesis could be tested by measuring intracellular cysteine pools or system Xc^- activity after knockdown, in addition to testing alternative thiol pools (e.g., thioredoxin). Such an analysis would move beyond descriptive correlation toward a mechanistic interrogation of *RIMKLA's* metabolic node within the broader redox network. A second possible mechanism for this observation is a potential influence on NADPH availability *via* metabolic shunting, upon *RIMKLA* depletion. This hypothesis is supported by studies indicating that amino acid metabolism can impinge on the pentose phosphate pathway and hence on NADPH-dependent antioxidative capacity (Campbell *et al*. 2016). Testing NADPH levels would be an interesting next step to test this possibility.

Contrary to expectation, *RIMKLA* knockdown reduced RPA and γH2AX signals under hypoxia. Two analytical interpretations of this phenomenon emerge: The first hypothesising a true reduction of fork stalling, where *RIMKLA* loss may slow nucleotide turnover or origin firing, yielding fewer stalled forks. Imbalances in dNTP pools are a potent source of replication stress, and conversely, alterations that slow nucleotide flux can paradoxically reduce fork stalling. Bester et al. showed that oncogene-driven increases in dNTP demand provoke fork collapse, whereas restricting

nucleotide supply can in fact, stabilise forks by reducing origin firing density (Bester *et al*. 2011). Similarly, Koppenhafer and colleagues demonstrated that modulation of ribonucleotide reductase activity alters replication kinetics and stress signalling in leukaemia cells (Koppenhafer *et al*. 2020). By analogy, loss of *RIMKLA* may throttle glutamate-to-α-ketoglutarate flux into nucleotide biosynthesis, thus lowering origin activation and limiting RPA and γH2AX signals, despite elevated ROS. Metabolic profiling of dNTP pools and DNA fibre assays could directly assess replication dynamics, in this case.

The second hypothesis entails impaired DDR: Altered chromatin compaction, *via* changes in histone glutamylation or local pH in *RIMKLA*-deficient cells, might hinder recruitment of ATR/ATM and/or other kinases, underreporting thus DNA lesions. Compact heterochromatin is known to be a refractory to DDR factor access. Kruhlak et al. demonstrated that ATM-dependent chromatin relaxation is required for efficient γH2AX focus formation at DSBs, and failure to decondense chromatin greatly diminishes sensor recruitment (Kruhlak *et al*. 2006). Likewise, Goodarzi and colleagues, reported that the persistence of H3K9me3-rich domains impairs 53BP1 and RPA loading at stalled forks (Goodarzi *et al*. 2008). If *RIMKLA* loss alters lysine glutamylation or local histone modifications - thereby increasing chromatin density - this could blunt RPA/γH2AX readouts without reflecting true reductions in DNA lesions. As a next step towards this hypothesis, ChIP-qPCR for γH2AX at known fragile sites, should effectively discriminate sensor deficits from genuine stress reduction.

Perhaps relatedly to the effects of *RIMKLA*-depletion that we demonstrated, conditions of oxidative stress have been also shown to reduce levels of both γH2AX and total H2AX, mediated by an enhanced interaction of H2AX with the E3-ubiquitin ligase RNF168, which is associated with H2AX poly-ubiquitination and promotes its degradation by the proteasome. Furthermore, this ROS-mediated H2AX decrease, played a crucial role in chemosensitivity, in experiments using TNBC cell lines (Gruosso *et al*. 2016)

Colony assays revealed that *RIMKLA* knockdown selectively compromised survival under severe hypoxia (<0.1% O_2), an effect reversible by ROS scavengers. This underscores ROS as the proximate cytotoxic mediator, but it also raises the question of why normoxic *RIMKLA*-deficient cells remain viable despite elevated ROS. A possible explanation is that hypoxia primes cells to tolerate a defined ROS spectrum, beyond which antioxidant systems become overwhelmed in the absence of *RIMKLA*. Importantly, whereas hypoxic *RIMKLA* depletion did not directly trigger apoptosis (no caspase-3 activation suggested by preliminary data, or nuclear condensation) subsequent reoxygenation induced rapid apoptotic morphology and PARP1 cleavage without p53 stabilisation. This mirrors ischaemia–reperfusion injury paradigms, where sudden oxygen influx generates mitochondrial superoxide bursts and initiates p53-independent apoptosis (Masgras *et al.* 2012; Zorov *et al.* 2000). Our data therefore suggest that *RIMKLA* serves as a buffer during the reoxygenation phase, perhaps by facilitating glutamate provision for mitochondrial GSH import or by modulating mitochondrial permeability transition (figure 5.20). Quantitative ROS kinetics (real-time fluorescent biosensors) and computational modelling of antioxidant flux could validate this threshold concept, allowing prediction of survival outcomes based on dynamic ROS profiles rather than end-point measurements, as those carried out in this study.

Interestingly, another study has shown that RIMKLA's product, NAAG, was crucial in the tumour growth and cancer cell survival, in a specific type of breast cancer. However, metabolomic and transcriptomic data from this study, correlated levels of NAAG in untreated breast cancer cells with higher mRNA levels of *RIMKLA*'s paralogue, *RIMKLB* (Xiao *et al.* 2022). These findings, in context with our data showing a hypoxia-induced upregulation of *RIMKLA* but not of *RIMKLB* expression levels (chapter 4), further support that *RIMKLA* is upregulated to support cancer cell viability, in response to the hypoxic stress.

It is possible that the mechanism of sensitisation of *RIMKLA*-depleted cells in hypoxic conditions, is related to ferroptosis. This mechanism of cell death has been known to occur in an iron-dependent, lipid-peroxidation, GSH- and ROS-dependent and DNA-damage independent

manner (Chen *et al*. 2020b; Kim *et al*. 2023; Lei *et al*. 2021; Sun *et al*. 2018). Supporting this, morphologically, ferroptosis occurs mainly with cells displaying reduced mitochondrial volume, increased bilayer membrane density and reduction or disappearance of mitochondrial cristae, but the cell membrane remaining intact, the nucleus being normal in size, and with no concentration of chromatin (Li *et al*. 2020b; Zhang *et al*. 2024). This might well explain the phenotype which we see with hypoxic cells in the absence of *RIMKLA*, as it correlates with the hypoxia-specific decrease of intracellular GSH, and the increase in hypoxic ROS levels that we report. Unfortunately, the key assay for validation of ferroptosis, involves the use of BODIPY, a lipid-peroxidation marker, which is experimentally challenging to use in hypoxic conditions that are not followed by reoxygenation, since we found that it was not well-compatible with commonly used, cell fixing buffers.

Given ionising radiation's reliance on ROS to inflict DNA damage, we anticipated that *RIMKLA* loss would sensitise cells. Paradoxically, normoxic *RIMKLA* knockdown conferred radioresistance (SER 1.33), whereas hypoxic radiosensitivity remained unchanged. One speculative mechanism is that chronic elevation of basal ROS in *RIMKLA*-deficient cells upregulates adaptive stress responses - such as NRF2 activation or autophagic flux - that protect against acute radiation-induced ROS (Chen *et al*. 2015; Sisakht *et al*. 2020). Conversely, hypoxic cells might already exhibit maximal adaptive pathways, rendering additional *RIMKLA* loss ineffectual. This is further supported by the fact that hypoxic cells are previously reported to exhibit elevated ROS levels (mainly of mitochondrial origin), but nonetheless, they are notorious for being very radioresistant. Furthermore, the mechanisms underpinning this observation might involve the decrease of γH2AX levels in response to *RIMKLA* knockdown, in an oxygen-independent manner, suggesting lower DRR activity. Interestingly, levels of γH2AX have been previously shown to correlate significantly with the radiation response of cancer cells. Studies from Mah *et al* and Taneja *et al* showed that lower levels of this phosphorylated histone variant correlated with radioresistance phenotypes (Mah *et al*. 2010; Taneja *et al*. 2004). Our preliminary observations regarding the

relocalisation of RIMKLA from nucleoli to a perinuclear region post-irradiation, may indicate involvement in ribosomal stress signalling or in trafficking of antioxidant enzymes, hinting at further subcellular fractionation and co-localisation studies.

It would also be interesting to investigate further the effects of *RIMKLA* on DDR signalling and how it might impact the response to radiation and/or chemotherapy. Perhaps starting off by assessing the potential bias created by transfection, using additional controls like *Mock*, or CRISPR-cas9-mediated genome editing in cancer cells. Using the same approaches to investigate further the impact of *RIMKLA* on hypoxic cell viability, e.g., by using CRISPR-Cas9-mediated genome editing to completely abrogate the gene, as well as expanding this dataset by potentially using *in vivo* experimental methods such as xenograft growth and tumorigenicity assessments, would provide significant insight.

Preliminary survival analyses in TCGA BRCA and METABRIC cohorts linked high *RIMKLA* expression with poorer outcomes in hypoxic tumours and in radiotherapy-treated patients (figures 5.16, 5.19). While these associations align with some of our mechanistic data, the risk of confounding by tumour grade, subtype or treatment history necessitates multivariate adjustment. A robust demonstration of independence from such factors would considerably strengthen *RIMKLA's* candidacy as a prognostic biomarker.

Several limitations in this part of our study warrant consideration. First, all *in vitro* experiments were performed exclusively in CAL-51 cells, which may not capture the genetic and phenotypic heterogeneity inherent to breast cancer; thus, validation in additional lines is essential to ensure the generality of our findings. Second, reliance on a single *siRIMKLA* sequence introduces the possibility of off-target effects, underscoring the need for future studies to employ at least one additional siRNA and to perform rescue experiments using an siRNA-resistant *RIMKLA* cDNA. Third, our assessments of GSH and ROS relied on fluorescence-based probes, which provide only indirect measures of antioxidant flux; direct metabolic flux analyses - such as ^13C-tracing of the

NAAG → glutamate → GSH pathway - would more accurately define *RIMKLA's* contribution to cellular redox pools. Fourth, the clinical correlations drawn from publicly available TCGA and METABRIC datasets are inherently constrained by incomplete metadata regarding tumour grade, molecular subtype, and treatment details (for example, specific chemotherapy regimens or radiotherapy dosing); consequently, these survival associations must be interpreted as preliminary and require validation in well-annotated prospective cohorts. Finally, several exploratory assays - most notably Menadione induction and RIMKLA relocalisation imaging - were conducted with only a single biological replicate and should be repeated with at least three independent samples to establish reproducibility.

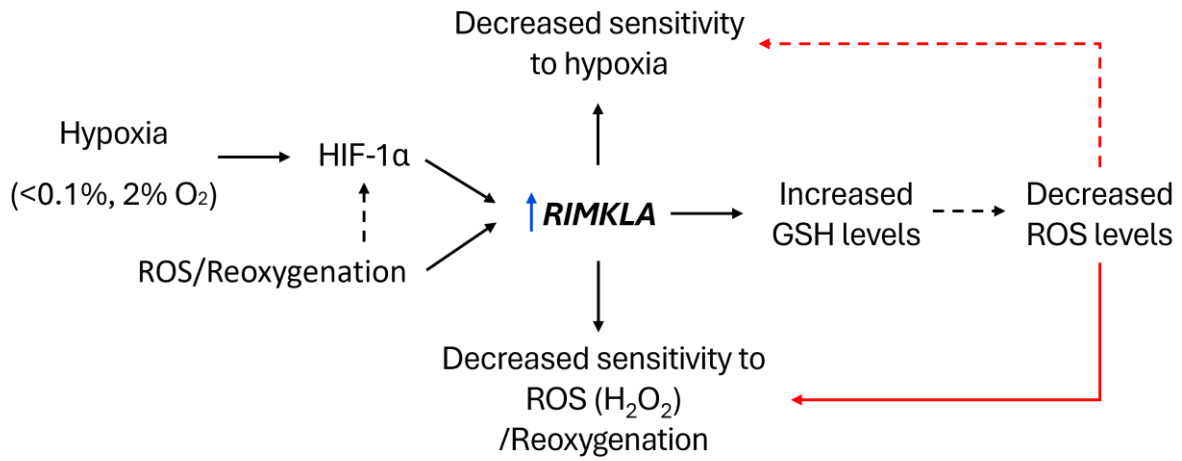

Figure 5.20. Proposed model for the biological role of *RIMKLA* in hypoxic cell viability. Our data show that hypoxia sensitised cancer cells lacking *RIMKLA* by means of siRNA-mediated knockdown, without the accumulation of detectable DNA damage in an apoptosis-independent but likely ferroptosis-related mechanism. Reoxygenation of hypoxic cells induced DNA damage in the form of detectable DSBs, resulting in cell death by apoptosis. The sensitivity of *RIMKLA*-depleted cells that have been exposed to hypoxic conditions, was reversed in response to treatment with ROS scavengers, building the model of a ROS-dependent mechanism of sensitisation.

Chapter 6 Final Discussion

Our research aimed to understand mechanisms that govern the impact of hypoxia, on the therapeutic response in breast cancer. It has been long known that tumour hypoxia is one of the major determinants of prognosis, in virtually all types of cancer, with hypoxic tumours showing typically significantly worse survival outcomes (Vaupel and Mayer 2007). This hypoxia-associated worse prognosis is, in part, stemming from the impact of hypoxia on the tumour response to anticancer therapeutic agents, and the broad range of mechanisms that underlie this impact are the focus of intensive oncological research (Hammond *et al*. 2014).

We specifically investigated the effects of hypoxia on the response to PARPi. The reasons we took special interest in this type of anticancer treatment were multiple. To begin with, PARPi have proven to be useful in the treatment of breast cancers, deficient in DNA repair capacity, what is known as synthetic lethality (Lord and Ashworth 2017). Secondly, PARPi belong to the group of DDRi, a class of drugs which are known to target specific parts of the DDR, thereby disrupting it, causing cancer cells to accumulate excessive genomic damage and eventually senesce or die (Rose *et al*. 2020). Hypoxia is associated with an active DDR signalling, in the absence of detectable DNA damage and therefore, the effects of DDRi in hypoxic cancer cells are bound to be different than those in non-hypoxic ones. Furthermore, what made this research area even more interesting for us, is that this active DDR associated with hypoxia, is shown to be oxygen-dependent, with a robust DDR activation seen in near-anoxic regions of hypoxic tumours (radiobiological hypoxia), while regions of milder hypoxia do not exhibit this phenomenon (Olcina *et al*. 2010). This, by extension, implies that the effects of DDRi in hypoxic tumours are also going to be oxygen-dependent. A significant hypothesis arises when this is put in context with the oxygen gradient that is well-known to exist in the TME, and the dynamic nature of tumour hypoxia, where variable changes in oxygen levels of the TME take place constantly (Bader *et al*. 2020). Much to our surprise, nonetheless, the oxygen-dependency of PARPi has not been adequately

researched: Results of the systematic review which we presented in this work, regarding the published findings on this topic, revealed that only a handful of works adequately assessed the viability of hypoxic cells in response to PARPi, with even less of the relevant studies investigating its oxygen-dependency, and with the respective methodologies used varying significantly an lacking a uniform means of viability assessment.

In our work, we validated the sensitivity of cells exposed to radiobiological hypoxia which has been previously reported and led to the development of the contextual synthetic lethality (Chan *et al.* 2010). However, we also demonstrated that our hypothesis of an oxygen-dependency of the PARPi effects was ture, validating a previously reported PARPi-resistant phenotype of breast cancer cells, exposed to milder hypoxic conditions (2% O_2) (Mehibel *et al.* 2021). Taking it a step further, we showed that, repeated cycles of radiobiological hypoxia and reoxygenation, in non-ambient but instead, in physoxia-like oxygen levels (cyclic hypoxia) - conditions modelling a physiologically relevant type of hypoxia - also led to resistance of breast cancer cells to the cytotoxicity of PARPi. Despite the mechanism of this resistance still being in question, our findings, supported by other studies, show that cells at tissue culture oxygen levers (21% O_2) and cells at radiobiological hypoxic conditions (<0.1% O_2), are the only ones significantly sensitive to the effects of PARPi. However, the former do not actually exist anywhere, in any biological system's tissue, and the latter exist in limited numbers in the hypoxic tumour. This raises the obvious question: why do PARPi then work in oncology? The answer to this question, is what makes our findings notable, whatsoever: PARPi exhibit significant levels of resistance in clinical practice. To begin with, monotherapy with PARPi is exclusively applied in tumours harbouring characteristics of "*BRCA*ness." However, even in these cases where synthetic lethality takes place, emerging data have demonstrated the clinical challenge of PARPi resistance: Despite the enthusiasm for the addition of PARPi, to the anticancer treatment landscape of HR-deficient malignant tumours, not all patients actually benefit and when they do, in most cases, the durability of treatment responses is limited. In fact, more than 40% of patients with *BRCA1/2*-

deficient tumours, fail to respond to PARPi treatment, and most of the patients acquire PARPi resistance with prolonged administration (Li *et al.* 2020a; Pham *et al.* 2021). In terms of clinical outcome, PARPi are significantly more effective when administered in combination with other treatments, such as radiation or chemotherapy, where they act as sensitisers – an area of active research currently (Hill *et al.* 2022; Minchom *et al.* 2018; Pham *et al.* 2021).

Based on our findings, we propose that the potential clinical benefit of PARPi as monotherapy in cancer, has not been fully reaped. It is logical to hypothesise that one of the causes of the prominent resistance to PARPi, described in clinical oncology practice, might well be the reflection of the model which we described: the PARPi-sensitive tumour cells experiencing near-anoxic conditions are eliminated rapidly in response to the drug (assuming it manages to reach them), leaving behind the resistant cells which reside in better oxygenated regions of the malignancy. The active hypoxic signalling in these resistant cells, nonetheless, is known to activate EMT, and other pro-metastatic processes which might, in addition, underlie the high relapse rates, encountered with PARPi monotherapy (Bredow *et al.* 2022; Gadducci *et al.* 2022; Ji *et al.* 2022; Takatani-Nakase *et al.* 2022). Therefore, we suggest that the contextual synthetic lethality concept should be expanded to address the oxygen-dependency of PARPi effects, and ideally, include considerations of additional, established elements of the TME, such as dynamic hypoxia and reoxygenation at physiologically relevant oxygen levels.

Future directions on this topic should be focused on two key areas: further *in vitro* studies, should investigate the mechanism of this hypoxia-mediated resistance to PARPi. For instance, it would be interesting to see how levels of replication stress, known to be largely reduced or even absent in mild/moderate hypoxic conditions, can affect the response to PARPi. Specifically, RPA exhaustion has been shown to be a major sensitiser to PARPi (VanderVere-Carozza *et al.* 2022). This phenomenon, however, is very likely to be absent in conditions of milder hypoxia or, based on our findings, even in cyclic hypoxic conditions, due to absence of excessive replication stress

(Pires *et al*. 2010). Therefore, it would be interesting to see how depletion of RPA, in these hypoxic conditions might impact the response to PARPi. ATR-signalling has already been shown to protect from RPA exhaustion by preventing replication origin firing and ATRi have been reported to drive RPA exhaustion-mediated sensitisation to PARPi (Toledo *et al*. 2013; VanderVere-Carozza *et al*. 2022). Even more interestingly, the use of ATRi in addition to orally administered PARPi has shown a positive preliminary efficacy outcome in data from a recent Phase I clinical trial evaluation, with this combination being characterised suitable for further evaluation (Yap *et al*. 2024). On this basis, it would be extremely interesting to see how the combination of the recently developed hypoxia-responsive prodrug of ATRi, AZD6738, which is hypoxia-activated and specifically releases AZD6738 only in hypoxic conditions *in vitro*, impacts the sensitivity to PARPi, in an HR-independent study model (Barnieh *et al*. 2024). Lastly the combination of PARPi with other hypoxia-activated cytotoxins, seems like an interesting research question as well, as it has already been suggested by preliminary evidence (Mehibel *et al*. 2021). A second, interesting mechanistic hypothesis involves the characterisation of transcriptional changes that occur in hypoxic cancer cells, in response to treatment with PARPi. For instance, RNA-seq analysis of hypoxic cells, exposed to different oxygen levels, in the presence/absence of PARPi, might reveal intrinsic, hypoxia-mediated transcriptional changes, unrelated to the status of DDR/replications stress, which might underlie the hypoxia-driven PARPi-resistant phenotypes.

The second area of focus which we suggest, becomes evident when one considers the added challenge of assessing tumour hypoxia *in vivo*. It seems that, in order to optimise delivery of context synthetic lethal agents like PARPi, it is necessary to effectively and accurately determine the intratumoural levels of oxygen. Nonetheless, imaging and measuring tumour hypoxia have been areas of intense scrutiny (Olcina *et al*. 2010). Potential avenues involve advancing/confirming hypoxia-associated biomarkers that can be measured in bodily fluids, imaging hypoxic areas in tumours with nitroimidazole derivatives, or directly measuring tumour oxygenation with an Eppendorf electrode. A recently published study reported the synthesis,

chemical analysis, and biological validation of a range of indolequinone-based, bioreductive fluorescent probes, which are activated in different levels of oxygen below 4% O_2, and when combined they can give a "clearer" picture of different oxygen levels in 3D-cancer cell culture models (Wallabregue *et al.* 2023). It might be interesting to examine, how using this and other similar systems might aid in targeted delivery of PARPi to resistant hypoxic tumour fractions, and evaluate, thence, the response to PARPi monotherapy, starting off with xenografts or PDX models.

In our effort of further characterising the influence of hypoxic conditions to the therapeutic response of breast cancer cells, we investigated transcriptional changes in response to hypoxia and their oxygen-dependency. Additionally, we explored their potential clinical relevance, using publicly available breast cancer datasets, aiming to identify a prognostic and ideally predictive, hypoxia-associated biomarker for further investigation. This part of our work, helped us identify a hypoxia-inducible gene, *RIMKLA*, as candidate prognostic and predictive biomarker, according to the relevant guidelines, set by Cancer Research UK (CRUK), collectively referred to as biomarker roadmaps (Lioumi and Newell 2014). At this point, however, a logical question might arise: do we need another hypoxia biomarker? Indeed, the prominent and widely acknowledged implication of hypoxia in anticancer treatment failure and cancer recurrence, along with its omnipresence in most TMEs, have led to a significant number of studies identifying a number of hypoxia-associated biomarkers, including molecules like HIF, VEGF, CAIX, BNIP3, GLUT-1, LDH-5 and PDK-1, some of which have additionally exhibited prognostic significance (Kim *et al.* 2015; Rademakers *et al.* 2011). Adding in this equation, the development of hypoxia-associated gene signatures, with clinically-validated prognostic significance in some types of cancer, which have been extensively used throughout our work as well, leads to the hypothesis that oncology has achieved all the tools necessary for successful cancer patient risk-stratification in terms of hypoxia and treatment response (e.g., for radiotherapy protocols). Unfortunately, this is not always the case: For example, in recent randomised trials, the use of hypoxia-associated gene signatures, failed to stratify patients with locally advanced HNSCC by hypoxia and to

prognosticate loco -regional control (Hassan Metwally *et al*. 2015; Thomson *et al*. 2024). Another relevant study, additionally, showed that none of the previously published hypoxia signatures exhibited prognostic value in bladder cancer, using transcriptomic data, available from public datasets and generated from 152 tumour samples from the BCON phase III trial of radiotherapy (RT) alone, or RT with carbogen and nicotinamide (CON), nor predicted benefit from hypoxia modification in the BCON patients (Choudhury *et al*.). A potential reason for this could be the fact that, gene signatures are typically created using cell lines subjected to low oxygen levels, subsequently selecting genes *via* enrichment methods, from pathways associated with hypoxia. Following an initial phase of statistical exploration, such gene signatures are frequently filtered down to include a smaller group of potential candidates. Both the examination and eventual filtering process may, thus, oversimplify the extensive biology of tumour hypoxia. Although this simplification can aid with translating findings to clinical practice, it might lead to inadequate representation of the diverse nature of hypoxia in the TME setting (Bitto *et al*. 2024).

Despite all the extensive research, on developing prognostic and predictive biomarkers for tumour hypoxia, such as the above-mentioned endogenous markers which are commonly used to identify hypoxia and/or prognosticate survival/predict treatment responses, they all demonstrate significant shortcomings. For instance, HIF-1α and CAIX are traditionally assessed through immunohistochemistry (IHC) and serve as indicators of hypoxia. Nonetheless, despite hypoxia-mediated stabilisation of HIF-1α and induction of *CAIX* in experimental settings, it's important to acknowledge that, the expression of HIF-1α and its downstream targets may also occur independently of hypoxia (Pugh and Ratcliffe 2017; Sorensen *et al*. 2010; Vaupel and Mayer 2016). Indeed, supporting this fact, it has been reported that, direct comparison of the differences in staining patterns, between endogenous and injectable hypoxia-associated markers (e.g. pimonidazole), indicated varied induction and activation methods at different oxygen levels, with endogenous markers generally showing a more diffuse staining near blood vessels. Furthermore, there appears to be insignificant correlation between endogenous marker

staining intensity and tumour pO_2 levels. Specifically, no correlation was found between IHC staining parameters of HIF-1α, CAIX, and GLUT-1 and measured pO_2 in rigorous studies, in which tumour biopsies were analysed along with the concomitant use of polarographic electrodes (Le and Courter 2008). It is therefore obvious that, despite the significant benefit of such endogenous, hypoxia-associated biomarkers of being identifiable with minimal invasiveness, (apart from that of the necessary tumour biopsy), they are far from being adequately accurate.

Lastly, other endogenous tissue makers that have been studied in relation to hypoxia, including VEGF, BNIP3, LOX, and LDH-5, have shown conflicting or limited clinical potential, with either contradicting results, such as those with VEG,F or the need for better, more rigorous clinical validation, such as the data regarding LOX and LDH-5 (De Paola *et al*. 2002; Kyzas *et al*. 2005; Le and Courter 2008).

Setting a somewhat utopic standard, the ideal clinical biomarker for evaluating tumour hypoxia should have the following attributes: capable of distinguishing different physiologically-relevant oxygen levels, while at the same time, differentiating between perfusion- and diffusion-limited hypoxia; reflecting cellular rather than vascular oxygenation status; being minimally-invasive; suitable for all tumour locations; usable in pre-clinical models and patients; easy and safe to use; enabling repeated measurements in long-term studies; monitoring treatment effects; prognostic and predictive of outcomes. Despite extensive research on creating and validating ideal hypoxia biomarkers, it must be acknowledged that such a tool has not been found, yet.

On this basis, we advocate that the gaps and limitations of each individual hypoxia-associated biomarker, could be bridged and compensated for by the combined used of multiple biomarkers, each relevant to a specific feature of the vast biology of tumour hypoxia, and to the scientific question to be addressed. Such an approach, seems the most efficient avenue to efficiently stratify cancer patients according to tumour hypoxic status, evaluate prognosis and guide treatment regimens.

Our research hints that *RIMKLA*, could be a hypoxia-specific prognostic, and neoadjuvant chemotherapy predictive biomarker, inducible in response to tested physiologically-relevant oxygen levels, downstream HIF-1α. We report *in vitro* viability data with *RIMKLA*-depleted cancer cells, supporting the prognostic associations of *RIMKLA*, in the context of hypoxic breast cancer. It would be interesting to further investigate the loss-of-*RIMKLA* phenotype, with the aid of CRISPR-Cas9 mediated knockout of *RIMKLA* in cancer cells and potentially, animal models. Additionally, it will be very intriguing to further characterise the mechanism of sensitivity of *RIMKLA*-depleted hypoxic cells, potentially expanding to testing its biological role in cyclic hypoxic conditions, accounting thus, for the dynamic nature of tumour hypoxia.

The fate of reoxygenated *RIMKLA*-depleted cancer cells which we report, reinforces the physiological relevance of this gene's impact on cancer cell survival. Reoxygenation is a typical phenomenon of hypoxic tumours, occurring both due to the aberrant nature of their vasculature, as well as due to reductions in the tumour volume which are often post anticancer treatment and which can lead to re-established supply of tumour cells with oxygen and nutrients from vessels, which were previously inaccessible. It would be therefore, interesting to further investigate what this mechanism looks like, after reoxygenation at physoxic conditions and what are the relevant effects on cancer cell viability.

Another interesting point for future research would be the characterisation of *RIMKLA*'s potential in sensitising cancer cells to ROS-induced genomic damage. Despite our data from radiation colony survival not suggesting any sensitisation of *RIMKLA*-depleted cancer cells to the effects of ionising radiation, it would be interesting to find out, how inactivating other antioxidant cell systems or reducing the cell's antioxidant capacity, thereby increasing endogenous oxidative stress could affect cancer cell viability. This could be achieved by investigating potential epistatic mechanisms between loss of *RIMKLA* and other genes like, *NRF2*, *TRX4*, etc., or by combining depletion of *RIMKLA* with inhibitors of the UPR pathway, responsible for antioxidant gene

expression, such as PERKi or ISRIB (Amodio *et al*. 2018; Mahameed *et al*. 2019; Morales-Gonzalez *et al*. 2017; Olcina *et al*. 2010; Sidrauski *et al*. 2015; Surma *et al*. 2014).

The overlap of *RIMKLA* and *RIMKLB* should also be more thoroughly investigated. We found no upregulation of *RIMKLB* in hypoxia, however, that is not a validation that enzyme encoded by *RIMKLB* does not have a function, even at baseline levels, in hypoxic cells. A good next step would be the combined knockout of *RIMKLA* and *RIMKLB*, in hypoxic cancer cells, to further evaluate the potential contribution of each gene in the redox balance and viability of cancer cells.

One of the crucial advantages of NAAGS II, the enzyme encoded by *RIMKLA*, is exactly the fact that it is an enzyme. This means that it is a viable pharmacological target and therefore, a NAAGS II inhibitor would be more than interesting to investigate further. Notably, inhibitors of GCP II/PSMA, have been recently reported to reduce tumour weight in ovarian cancer *in vivo* models, in a NAAG- and L-glutamate-dependent manner (Nguyen *et al*. 2019). It would be interesting to characterise the potential synergy between clinically-validated, potent and selective GCP II/PSMA inhibitors, such as 2-PMPA, with a small molecule selective inhibitor of the upstream enzyme encoded by *RIMKLA* (Guo *et al*. 2015; Jackson *et al*. 1996; Nguyen *et al*. 2019). Additionally, while increased NAAG concentrations have been correlated with multiple higher-grade malignancies, the enzyme GCP II is not ubiquitously expressed in all cancer types and, when present, it might not effectively catalyse the hydrolysis of NAAG to its catabolic products (Asaka and Le 2019; Mhawech-Fauceglia *et al*. 2007). It would be, therefore, interesting to see, how reducing the intracellular pool of NAAG might affect these types of tumours, in terms of growth and progression, and what alternative pathways (if any), are employed for the metabolism of NAAG in these tumour cells. The production of NAAG from L-glutamate and NAA, mediated by NAAGS II activity has been established, however, little is known about the regulation or mechanism of this enzyme, and no isolated NAAGS II activity has been found in preparations without cells. NAAGS II activity is somewhat unique since post-translational processing is used

to synthesise practically all vertebrate peptides and other neuropeptides (Arun *et al.* 2006; Gehl *et al.* 2004). Further research into the regulatory mechanisms of this enzyme, might also provide insight into the design of a potent, safe, and effective small molecule inhibitor of NAAGS II.

Limitations inherent to our work are acknowledged in chapter discussions and warrant consideration upon interpretation of our findings. On a more general basis, while our discoveries set promising insights, the use of 2D *in vitro* models to simulate hypoxic conditions cannot fully replicate the complex and heterogeneous oxygen gradients that are commonly present within solid tumours *in vivo*. Consequently, the physiological relevance of our findings may be constrained. Furthermore, our experimental design primarily relied on a limited set of breast cancer cell lines, which restricts the generalisability of the conclusions to other breast cancer subtypes or malignancies of different tissue origin. Mechanistically, although *RIMKLA* knockdown demonstrated an effect on cell viability under hypoxic conditions, the downstream signalling pathways, and molecular interactions responsible for this phenotype remain uncharacterised. Finally, the potential of *RIMKLA* as a prognostic or predictive biomarker is based on analyses of retrospective, heterogenous transcriptomic datasets. Prospective studies, ideally in multi-centre cohorts, are necessary to validate these associations and determine the clinical utility of *RIMKLA* expression in stratifying patients for hypoxia-targeted or other types of targeted anticancer therapies.

In conclusion, based on our data which are described in this work and in context with previously reported findings, we suggest that *RIMKLA* and its enzyme product NAAGS II, are good candidates for targeted sensitisation of hypoxic cancer cells and we support that further research should be carried out in order to deeply understand their biological role and hopefully, reap their full potential.

Chapter 7 References

Abbott, E. M., Falzone, N., Lenzo, N., and Vallis, K. A. (2021), 'Combining External Beam Radiation and Radionuclide Therapies: Rationale, Radiobiology, Results and Roadblocks', *Clin Oncol (R Coll Radiol),* 33 (11), 735-43.

Abd El-Rehim, D. M., Pinder, S. E., Paish, C. E., Bell, J., Blamey, R. W., Robertson, J. F., Nicholson, R. I., and Ellis, I. O. (2004), 'Expression of luminal and basal cytokeratins in human breast carcinoma', *J Pathol,* 203 (2), 661-71.

Abel, M. L., Takahashi, N., Peer, C., Redon, C. E., Nichols, S., Vilimas, R., Lee, M. J., Lee, S., Shelat, M., Kattappuram, R., Sciuto, L., Pinkiert, D., Graham, C., Butcher, D., Karim, B., Sharma, A. K., Malin, J., Kumar, R., Schultz, C. W., Goyal, S., Del Rivero, J., Krishnamurthy, M., Upadhyay, D., Schroeder, B., Sissung, T., Tyagi, M., Kim, J., Pommier, Y., Aladjem, M., Raffeld, M., Figg, W. D., Trepel, J., Xi, L., Desai, P., and Thomas, A. (2023), 'Targeting Replication Stress and Chemotherapy Resistance with a Combination of Sacituzumab Govitecan and Berzosertib: A Phase I Clinical Trial', *Clin Cancer Res,* 29 (18), 3603-11.

Abramov, A. Y., Scorziello, A., and Duchen, M. R. (2007), 'Three distinct mechanisms generate oxygen free radicals in neurons and contribute to cell death during anoxia and reoxygenation', *J Neurosci,* 27 (5), 1129-38.

Aggarwal, V., Tuli, H. S., Varol, A., Thakral, F., Yerer, M. B., Sak, K., Varol, M., Jain, A., Khan, M. A., and Sethi, G. (2019), 'Role of Reactive Oxygen Species in Cancer Progression: Molecular Mechanisms and Recent Advancements', *Biomolecules,* 9 (11).

Ahrabi, S., Sarkar, S., Pfister, S. X., Pirovano, G., Higgins, G. S., Porter, A. C., and Humphrey, T. C. (2016), 'A role for human homologous recombination factors in suppressing microhomology-mediated end joining', *Nucleic Acids Res,* 44 (12), 5743-57.

Ahuja, A. K., Barber, R. C., Hardwick, R. J., Weil, M. M., Genik, P. C., Brenner, D. J., and Dubrova, Y. E. (2008), 'The effects of Atm haploinsufficiency on mutation rate in the mouse germ line and somatic tissue', *Mutagenesis,* 23 (5), 367-70.

Alhmoud, J. F., Woolley, J. F., Al Moustafa, A. E., and Malki, M. I. (2020), 'DNA Damage/Repair Management in Cancers', *Cancers (Basel),* 12 (4).

Ali, A. A., Timinszky, G., Arribas-Bosacoma, R., Kozlowski, M., Hassa, P. O., Hassler, M., Ladurner, A. G., Pearl, L. H., and Oliver, A. W. (2015), 'Corrigendum: The zinc-finger domains of PARP1 cooperate to recognize DNA strand breaks', *Nat Struct Mol Biol,* 22 (8), 645.

Ali, A. A. E., Timinszky, G., Arribas-Bosacoma, R., Kozlowski, M., Hassa, P. O., Hassler, M., Ladurner, A. G., Pearl, L. H., and Oliver, A. W. (2012), 'The zinc-finger domains of PARP1 cooperate to recognize DNA strand breaks', *Nat Struct Mol Biol,* 19 (7), 685-92.

Ali, R. M. M., McIntosh, S. A., and Savage, K. I. (2021), 'Homologous recombination deficiency in breast cancer: Implications for risk, cancer development, and therapy', *Genes Chromosomes Cancer,* 60 (5), 358-72.

Ali, S. O., Khan, F. A., Galindo-Campos, M. A., and Yelamos, J. (2016), 'Understanding specific functions of PARP-2: new lessons for cancer therapy', *Am J Cancer Res,* 6 (9), 1842-63.

Allison, K. H. (2012), 'Molecular pathology of breast cancer: what a pathologist needs to know', *Am J Clin Pathol,* 138 (6), 770-80.

Amelio, I., Cutruzzola, F., Antonov, A., Agostini, M., and Melino, G. (2014), 'Serine and glycine metabolism in cancer', *Trends Biochem Sci,* 39 (4), 191-8.

Amodio, G., Moltedo, O., Faraonio, R., and Remondelli, P. (2018), 'Targeting the Endoplasmic Reticulum Unfolded Protein Response to Counteract the Oxidative Stress-Induced Endothelial Dysfunction', *Oxid Med Cell Longev,* 2018, 4946289.

Anbalagan, S., Biasoli, D., Leszczynska, K. B., Mukherjee, S., and Hammond, E. M. (2015), 'In Vitro Radiosensitization of Esophageal Cancer Cells with the Aminopeptidase Inhibitor CHR-2797', *Radiat Res,* 184 (3), 259-65.

Andreassen, P. R., D'Andrea, A. D., and Taniguchi, T. (2004), 'ATR couples FANCD2 monoubiquitination to the DNA-damage response', *Genes Dev,* 18 (16), 1958-63.

Andrs, M., Stoy, H., Boleslavska, B., Chappidi, N., Kanagaraj, R., Nascakova, Z., Menon, S., Rao, S., Oravetzova, A., Dobrovolna, J., Surendranath, K., Lopes, M., and Janscak, P. (2023), 'Excessive reactive oxygen species induce transcription-dependent replication stress', *Nat Commun,* 14 (1), 1791.

Antoniou, A. C., Foulkes, W. D., and Tischkowitz, M. (2014), 'Breast-cancer risk in families with mutations in PALB2', *N Engl J Med,* 371 (17), 1651-2.

Arimilli, S., Schmidt, E., Damratoski, B. E., and Prasad, G. L. (2017), 'Role of Oxidative Stress in the Suppression of Immune Responses in Peripheral Blood Mononuclear Cells Exposed to Combustible Tobacco Product Preparation', *Inflammation,* 40 (5), 1622-30.

Arun, P., Madhavarao, C. N., Moffett, J. R., and Namboodiri, M. A. (2006), 'Regulation of N-acetylaspartate and N-acetylaspartylglutamate biosynthesis by protein kinase activators', *J Neurochem,* 98 (6), 2034-42.

Asaka, R. and Le, A. (2019), 'Dual role of N-acetyl-aspartyl-glutamate metabolism in cancer monitor and therapy', *Mol Cell Oncol,* 6 (5), e1627273.

Asgari, R., Mehran, Y. Z., Weber, H. M., Weber, M., Golestanha, S. A., Hosseini Kazerouni, S. M., Panahi, F., Mohammadi, P., and Mansouri, K. (2024), 'Management of oxidative stress for cell therapy through combinational approaches of stem cells, antioxidants, and photobiomodulation', *Eur J Pharm Sci,* 196, 106715.

Babar, Q., Saeed, A., Tabish, T. A., Sarwar, M., and Thorat, N. D. (2023), 'Targeting the tumor microenvironment: Potential strategy for cancer therapeutics', *Biochim Biophys Acta Mol Basis Dis,* 1869 (6), 166746.

Bader, S. B., Dewhirst, M. W., and Hammond, E. M. (2020), 'Cyclic Hypoxia: An Update on Its Characteristics, Methods to Measure It and Biological Implications in Cancer', *Cancers (Basel),* 13 (1).

Bader, S. B., Ma, T. S., Simpson, C. J., Liang, J., Maezono, S. E. B., Olcina, M. M., Buffa, F. M., and Hammond, E. M. (2021), 'Replication catastrophe induced by cyclic hypoxia leads to increased APOBEC3B activity', *Nucleic Acids Res,* 49 (13), 7492-506.

Baliakas, P., Munters, A. R., Kampe, A., Tesi, B., Bondeson, M. L., Ladenvall, C., and Eriksson, D. (2024), 'Integrating a Polygenic Risk Score into a clinical setting would impact risk predictions in familial breast cancer', *J Med Genet,* 61 (2), 150-54.

Bannik, K., Madas, B., Jarke, S., Sutter, A., Siemeister, G., Schatz, C., Mumberg, D., and Zitzmann-Kolbe, S. (2021), 'DNA repair inhibitors sensitize cells differently to high and low LET radiation', *Sci Rep,* 11 (1), 23257.

Barinka, C., Rojas, C., Slusher, B., and Pomper, M. (2012), 'Glutamate carboxypeptidase II in diagnosis and treatment of neurologic disorders and prostate cancer', *Curr Med Chem,* 19 (6), 856-70.

Barnieh, F. M., Morais, G. R., Loadman, P. M., Falconer, R. A., and El-Khamisy, S. F. (2024), 'Hypoxia-Responsive Prodrug of ATR Inhibitor, AZD6738, Selectively Eradicates Treatment-Resistant Cancer Cells', *Adv Sci (Weinh),* 11 (34), e2403831.

Bartek, J., Lukas, C., and Lukas, J. (2004), 'Checking on DNA damage in S phase', *Nat Rev Mol Cell Biol,* 5 (10), 792-804.

Bartoszewski, R., Moszynska, A., Serocki, M., Cabaj, A., Polten, A., Ochocka, R., Dell'Italia, L., Bartoszewska, S., Kroliczewski, J., Dabrowski, M., and Collawn, J. F. (2019), 'Primary endothelial cell-specific regulation of hypoxia-inducible factor (HIF)-1 and HIF-2 and their target gene expression profiles during hypoxia', *FASEB J,* 33 (7), 7929-41.

Basheeruddin, M. and Qausain, S. (2024), 'Hypoxia-Inducible Factor 1-Alpha (HIF-1alpha): An Essential Regulator in Cellular Metabolic Control', *Cureus,* 16 (7), e63852.

Baumann, R., Depping, R., Delaperriere, M., and Dunst, J. (2016), 'Targeting hypoxia to overcome radiation resistance in head & neck cancers: real challenge or clinical fairytale?', *Expert Rev Anticancer Ther,* 16 (7), 751-8.

Beck, C., Robert, I., Reina-San-Martin, B., Schreiber, V., and Dantzer, F. (2014), 'Poly(ADP-ribose) polymerases in double-strand break repair: focus on PARP1, PARP2 and PARP3', *Exp Cell Res,* 329 (1), 18-25.

Beckmann, M. P., Cerretti, D. P., Baum, P., Vanden Bos, T., James, L., Farrah, T., Kozlosky, C., Hollingsworth, T., Shilling, H., Maraskovsky, E., and et al. (1994), 'Molecular characterization of a family of ligands for eph-related tyrosine kinase receptors', *EMBO J,* 13 (16), 3757-62.

Bedard, K. and Krause, K. H. (2007), 'The NOX family of ROS-generating NADPH oxidases: physiology and pathophysiology', *Physiol Rev,* 87 (1), 245-313.

Befani, C., Mylonis, I., Gkotinakou, I. M., Georgoulias, P., Hu, C. J., Simos, G., and Liakos, P. (2013), 'Cobalt stimulates HIF-1-dependent but inhibits HIF-2-dependent gene expression in liver cancer cells', *Int J Biochem Cell Biol,* 45 (11), 2359-68.

Begg, K. and Tavassoli, M. (2020), 'Inside the hypoxic tumour: reprogramming of the DDR and radioresistance', *Cell Death Discov,* 6, 77.

Beitner-Johnson, D. and Millhorn, D. E. (1998), 'Hypoxia induces phosphorylation of the cyclic AMP response element-binding protein by a novel signaling mechanism', *J Biol Chem,* 273 (31), 19834-9.

Belli, C., Duso, B. A., Ferraro, E., and Curigliano, G. (2019), 'Homologous recombination deficiency in triple negative breast cancer', *Breast,* 45, 15-21.

Bencokova, Z., Kaufmann, M. R., Pires, I. M., Lecane, P. S., Giaccia, A. J., and Hammond, E. M. (2009), 'ATM activation and signaling under hypoxic conditions', *Mol Cell Biol,* 29 (2), 526-37.

Benhar, M. (2020), 'Oxidants, Antioxidants and Thiol Redox Switches in the Control of Regulated Cell Death Pathways', *Antioxidants (Basel),* 9 (4).

Bernardi, R. and Gianni, L. (2014), 'Hallmarks of triple negative breast cancer emerging at last?', *Cell Res,* 24 (8), 904-5.

Bester, A. C., Roniger, M., Oren, Y. S., Im, M. M., Sarni, D., Chaoat, M., Bensimon, A., Zamir, G., Shewach, D. S., and Kerem, B. (2011), 'Nucleotide deficiency promotes genomic instability in early stages of cancer development', *Cell,* 145 (3), 435-46.

Bhattacharyya, A., Chattopadhyay, R., Mitra, S., and Crowe, S. E. (2014), 'Oxidative stress: an essential factor in the pathogenesis of gastrointestinal mucosal diseases', *Physiol Rev,* 94 (2), 329-54.

Bhosle, S. M., Huilgol, N. G., and Mishra, K. P. (2005), 'Enhancement of radiation-induced oxidative stress and cytotoxicity in tumor cells by ellagic acid', *Clin Chim Acta,* 359 (1-2), 89-100.

Bigos, K. J., Quiles, C. G., Lunj, S., Smith, D. J., Krause, M., Troost, E. G., West, C. M., Hoskin, P., and Choudhury, A. (2024), 'Tumour response to hypoxia: understanding the hypoxic tumour microenvironment to improve treatment outcome in solid tumours', *Front Oncol,* 14, 1331355.

Bindra, R. S. and Glazer, P. M. (2007a), 'Repression of RAD51 gene expression by E2F4/p130 complexes in hypoxia', *Oncogene,* 26 (14), 2048-57.

--- (2007b), 'Co-repression of mismatch repair gene expression by hypoxia in cancer cells: role of the Myc/Max network', *Cancer Lett,* 252 (1), 93-103.

Bindra, R. S., Gibson, S. L., Meng, A., Westermark, U., Jasin, M., Pierce, A. J., Bristow, R. G., Classon, M. K., and Glazer, P. M. (2005), 'Hypoxia-induced down-regulation of BRCA1 expression by E2Fs', *Cancer Res,* 65 (24), 11597-604.

Bitto, V., Honscheid, P., Besso, M. J., Sperling, C., Kurth, I., Baumann, M., and Brors, B. (2024), 'Enhancing mass spectrometry imaging accessibility using convolutional autoencoders for deriving hypoxia-associated peptides from tumors', *NPJ Syst Biol Appl,* 10 (1), 57.

Blackford, A. N. and Jackson, S. P. (2017), 'ATM, ATR, and DNA-PK: The Trinity at the Heart of the DNA Damage Response', *Mol Cell,* 66 (6), 801-17.

Bolland, H., Ma, T. S., Ramlee, S., Ramadan, K., and Hammond, E. M. (2021), 'Links between the unfolded protein response and the DNA damage response in hypoxia: a systematic review', *Biochem Soc Trans,* 49 (3), 1251-63.

Borresen, A. L., Andersen, T. I., Tretli, S., Heiberg, A., and Moller, P. (1990), 'Breast cancer and other cancers in Norwegian families with ataxia-telangiectasia', *Genes Chromosomes Cancer,* 2 (4), 339-40.

Borst, G. R., Kumareswaran, R., Yucel, H., Telli, S., Do, T., McKee, T., Zafarana, G., Jonkers, J., Verheij, M., O'Connor, M. J., Rottenberg, S., and Bristow, R. G. (2017), 'Neoadjuvant olaparib targets hypoxia to improve radioresponse in a homologous recombination-proficient breast cancer model', *Oncotarget,* 8 (50), 87638-46.

Bouwman, P., Aly, A., Escandell, J. M., Pieterse, M., Bartkova, J., van der Gulden, H., Hiddingh, S., Thanasoula, M., Kulkarni, A., Yang, Q., Haffty, B. G., Tommiska, J., Blomqvist, C., Drapkin, R., Adams, D. J., Nevanlinna, H., Bartek, J., Tarsounas, M., Ganesan, S., and Jonkers, J. (2010), '53BP1 loss rescues BRCA1 deficiency and is associated with triple-negative and BRCA-mutated breast cancers', *Nat Struct Mol Biol,* 17 (6), 688-95.

Brahimi-Horn, M. C. and Pouyssegur, J. (2009), 'HIF at a glance', *J Cell Sci,* 122 (Pt 8), 1055-7.

Brandsma, I., Fleuren, E. D. G., Williamson, C. T., and Lord, C. J. (2017), 'Directing the use of DDR kinase inhibitors in cancer treatment', *Expert Opin Investig Drugs,* 26 (12), 1341-55.

Bratek, E., Ziembowicz, A., and Salinska, E. (2020), 'N-Acetylaspartylglutamate (NAAG) Pretreatment Reduces Hypoxic-Ischemic Brain Damage and Oxidative Stress in Neonatal Rats', *Antioxidants (Basel),* 9 (9).

Bratslavsky, G., Sudarshan, S., Neckers, L., and Linehan, W. M. (2007), 'Pseudohypoxic pathways in renal cell carcinoma', *Clin Cancer Res,* 13 (16), 4667-71.

Bredow, K., Blumcke, B., Schneider, S., Pusken, M., Schmutzler, R., and Rhiem, K. (2022), 'Long-term survival of a BRCA2 mutation carrier following second ovarian cancer relapse using PARPi therapy: A case report', *Mol Clin Oncol,* 17 (3), 137.

Brigelius-Flohe, R. (1999), 'Tissue-specific functions of individual glutathione peroxidases', *Free Radic Biol Med,* 27 (9-10), 951-65.

Brown, J. M. and Wilson, W. R. (2004), 'Exploiting tumour hypoxia in cancer treatment', *Nat Rev Cancer,* 4 (6), 437-47.

Bruin, M. A. C., Sonke, G. S., Beijnen, J. H., and Huitema, A. D. R. (2022), 'Pharmacokinetics and Pharmacodynamics of PARP Inhibitors in Oncology', *Clin Pharmacokinet,* 61 (12), 1649-75.

Brunelle, J. K., Bell, E. L., Quesada, N. M., Vercauteren, K., Tiranti, V., Zeviani, M., Scarpulla, R. C., and Chandel, N. S. (2005), 'Oxygen sensing requires mitochondrial ROS but not oxidative phosphorylation', *Cell Metab,* 1 (6), 409-14.

Buffa, F. M., Harris, A. L., West, C. M., and Miller, C. J. (2010), 'Large meta-analysis of multiple cancers reveals a common, compact and highly prognostic hypoxia metagene', *Br J Cancer,* 102 (2), 428-35.

Buisson, R., Dion-Cote, A. M., Coulombe, Y., Launay, H., Cai, H., Stasiak, A. Z., Stasiak, A., Xia, B., and Masson, J. Y. (2010), 'Cooperation of breast cancer proteins PALB2 and piccolo BRCA2 in stimulating homologous recombination', *Nat Struct Mol Biol,* 17 (10), 1247-54.

Cai, Y., Han, M., Luo, L., Song, W., and Zhou, X. (1996), 'Increased expression of PDGF and c-myc genes in lungs and pulmonary arteries of pulmonary hypertensive rats induced by hypoxia', *Chin Med Sci J,* 11 (3), 152-6.

Campbell, K., Vowinckel, J., Keller, M. A., and Ralser, M. (2016), 'Methionine Metabolism Alters Oxidative Stress Resistance via the Pentose Phosphate Pathway', *Antioxid Redox Signal,* 24 (10), 543-7.

Cancer Genome Atlas, Network (2012), 'Comprehensive molecular portraits of human breast tumours', *Nature,* 490 (7418), 61-70.

Cancer Genome Atlas Research, Network, Weinstein, J. N., Collisson, E. A., Mills, G. B., Shaw, K. R., Ozenberger, B. A., Ellrott, K., Shmulevich, I., Sander, C., and Stuart, J. M. (2013), 'The Cancer Genome Atlas Pan-Cancer analysis project', *Nat Genet,* 45 (10), 1113-20.

Cancer Genome Atlas Research Network. Electronic address, wheeler bcm edu and Cancer Genome Atlas Research, Network (2017), 'Comprehensive and Integrative Genomic Characterization of Hepatocellular Carcinoma', *Cell,* 169 (7), 1327-41 e23.

Cannan, W. J., Tsang, B. P., Wallace, S. S., and Pederson, D. S. (2014), 'Nucleosomes suppress the formation of double-strand DNA breaks during attempted base excision repair of clustered oxidative damages', *J Biol Chem,* 289 (29), 19881-93.

Cao, S., Sun, Y., Wang, W., Wang, B., Zhang, Q., Pan, C., Yuan, Q., Xu, F., Wei, S., and Chen, Y. (2019), 'Poly (ADP-ribose) polymerase inhibition protects against myocardial ischaemia/reperfusion injury via suppressing mitophagy', *J Cell Mol Med,* 23 (10), 6897-906.

Carreau, A., El Hafny-Rahbi, B., Matejuk, A., Grillon, C., and Kieda, C. (2011), 'Why is the partial oxygen pressure of human tissues a crucial parameter? Small molecules and hypoxia', *J Cell Mol Med,* 15 (6), 1239-53.

Carusillo, A. and Mussolino, C. (2020), 'DNA Damage: From Threat to Treatment', *Cells,* 9 (7).

Cassier-Chauvat, C., Marceau, F., Farci, S., Ouchane, S., and Chauvat, F. (2023), 'The Glutathione System: A Journey from Cyanobacteria to Higher Eukaryotes', *Antioxidants (Basel),* 12 (6).

Ceccaldi, R., Liu, J. C., Amunugama, R., Hajdu, I., Primack, B., Petalcorin, M. I., O'Connor, K. W., Konstantinopoulos, P. A., Elledge, S. J., Boulton, S. J., Yusufzai, T., and D'Andrea, A. D. (2015), 'Homologous-recombination-deficient tumours are dependent on Poltheta-mediated repair', *Nature,* 518 (7538), 258-62.

Ceccaldi, Raphael, Rondinelli, Beatrice, and D'Andrea, Alan D. (2016), 'Repair Pathway Choices and Consequences at the Double-Strand Break', *Trends in Cell Biology,* 26 (1), 52-64.

Cecchini, M. J., Amiri, M., and Dick, F. A. (2012), 'Analysis of cell cycle position in mammalian cells', *J Vis Exp,* (59).

Cecconi, F. (2020), 'Autophagy, replication stress and DNA synthesis, an intricate relationship', *Cell Death Differ,* 27 (2), 829-30.

Cerami, E., Gao, J., Dogrusoz, U., Gross, B. E., Sumer, S. O., Aksoy, B. A., Jacobsen, A., Byrne, C. J., Heuer, M. L., Larsson, E., Antipin, Y., Reva, B., Goldberg, A. P., Sander, C., and Schultz, N. (2012), 'The cBio cancer genomics portal: an open platform for exploring multidimensional cancer genomics data', *Cancer Discov,* 2 (5), 401-4.

Cerrato, A., Morra, F., and Celetti, A. (2016), 'Use of poly ADP-ribose polymerase [PARP] inhibitors in cancer cells bearing DDR defects: the rationale for their inclusion in the clinic', *J Exp Clin Cancer Res,* 35 (1), 179.

Chakraborty, A. A. (2020), 'Coalescing lessons from oxygen sensing, tumor metabolism, and epigenetics to target VHL loss in kidney cancer', *Semin Cancer Biol,* 67 (Pt 2), 34-42.

Chan, N., Ali, M., McCallum, G. P., Kumareswaran, R., Koritzinsky, M., Wouters, B. G., Wells, P. G., Gallinger, S., and Bristow, R. G. (2014), 'Hypoxia provokes base excision repair changes and a repair-deficient, mutator phenotype in colorectal cancer cells', *Mol Cancer Res,* 12 (10), 1407-15.

Chan, N., Pires, I. M., Bencokova, Z., Coackley, C., Luoto, K. R., Bhogal, N., Lakshman, M., Gottipati, P., Oliver, F. J., Helleday, T., Hammond, E. M., and Bristow, R. G. (2010), 'Contextual synthetic lethality of cancer cell kill based on the tumor microenvironment', *Cancer Res,* 70 (20), 8045-54.

Chandel, N. S., McClintock, D. S., Feliciano, C. E., Wood, T. M., Melendez, J. A., Rodriguez, A. M., and Schumacker, P. T. (2000), 'Reactive oxygen species generated at mitochondrial complex III stabilize hypoxia-inducible factor-1alpha during hypoxia: a mechanism of O2 sensing', *J Biol Chem,* 275 (33), 25130-8.

Chang, H. H. Y., Pannunzio, N. R., Adachi, N., and Lieber, M. R. (2017), 'Non-homologous DNA end joining and alternative pathways to double-strand break repair', *Nat Rev Mol Cell Biol,* 18 (8), 495-506.

Chatterjee, Nimrat and Walker, Graham C. (2017), 'Mechanisms of DNA damage, repair, and mutagenesis', *Environmental and Molecular Mutagenesis,* 58 (5), 235-63.

Chen, C., Liu, Y., Lu, C., Cross, J. R., Morris, J. P. th, Shroff, A. S., Ward, P. S., Bradner, J. E., Thompson, C., and Lowe, S. W. (2013a), 'Cancer-associated IDH2 mutants drive an acute myeloid leukemia that is susceptible to Brd4 inhibition', *Genes Dev,* 27 (18), 1974-85.

Chen, D., Tavana, O., Chu, B., Erber, L., Chen, Y., Baer, R., and Gu, W. (2017), 'NRF2 Is a Major Target of ARF in p53-Independent Tumor Suppression', *Mol Cell,* 68 (1), 224-32 e4.

Chen, E. Y., Tan, C. M., Kou, Y., Duan, Q., Wang, Z., Meirelles, G. V., Clark, N. R., and Ma'ayan, A. (2013b), 'Enrichr: interactive and collaborative HTML5 gene list enrichment analysis tool', *BMC Bioinformatics,* 14, 128.

Chen, J., Li, P., Song, L., Bai, L., Huen, M. S. Y., Liu, Y., and Lu, L. Y. (2020a), '53BP1 loss rescues embryonic lethality but not genomic instability of BRCA1 total knockout mice', *Cell Death Differ,* 27 (9), 2552-67.

Chen, J., Ding, Z., Peng, Y., Pan, F., Li, J., Zou, L., Zhang, Y., and Liang, H. (2014), 'HIF-1alpha inhibition reverses multidrug resistance in colon cancer cells via downregulation of MDR1/P-glycoprotein', *PLoS One,* 9 (6), e98882.

Chen, J., Qiao, W., Xue, X., Li, D., Zhang, Y., Xie, D., Wang, J., Sun, Y., Yang, S., and Yang, Z. (2024a), 'Amelioration of Oxidative Stress in Rats with Chronic Obstructive Pulmonary Disease through Shenqi Huatan Decoction Activation of Peroxisome Proliferator-Activated Receptor Gamma-Mediated Activated Protein Kinase/Forkhead Transcription Factor O3a Signaling Pathway', *Can Respir J,* 2024, 5647813.

Chen, M., Lei, N., Guo, R., Han, L., Zhao, Q., Zhao, Y., Qiu, L., Wu, F., Jiang, S., Tong, N., Wang, K., Li, S., and Chang, L. (2024b), 'Genetic landscape of homologous recombination repair

and practical outcomes of PARPi therapy in ovarian cancer management', *Ther Adv Med Oncol,* 16, 17588359241271845.

Chen, N., Wu, L., Yuan, H., and Wang, J. (2015), 'ROS/Autophagy/Nrf2 Pathway Mediated Low-Dose Radiation Induced Radio-Resistance in Human Lung Adenocarcinoma A549 Cell', *Int J Biol Sci,* 11 (7), 833-44.

Chen, P. H., Tseng, W. H., and Chi, J. T. (2020b), 'The Intersection of DNA Damage Response and Ferroptosis-A Rationale for Combination Therapeutics', *Biology (Basel),* 9 (8).

Chen, R., Ahmed, M. A., and Forsyth, N. R. (2022), 'Dimethyloxalylglycine (DMOG), a Hypoxia Mimetic Agent, Does Not Replicate a Rat Pheochromocytoma (PC12) Cell Biological Response to Reduced Oxygen Culture', *Biomolecules,* 12 (4).

Cheng, Binbin, Pan, Wei, Xing, Yi, Xiao, Yao, Chen, Jianjun, and Xu, Zheng (2022), 'Recent advances in DDR (DNA damage response) inhibitors for cancer therapy', *European Journal of Medicinal Chemistry,* 230, 114109.

Chiappa, M., Guffanti, F., Bertoni, F., Colombo, I., and Damia, G. (2021), 'Overcoming PARPi resistance: Preclinical and clinical evidence in ovarian cancer', *Drug Resist Updat,* 55, 100744.

Choudhury, Ananya, Yang, Lingjian, Irlam, Joely J., Williamson, Amanda, Denley, Helen, Hoskin, Peter, and West, Catharine 'A hypoxia transcriptomic signature to predict benefit from hypoxia-modifying treatment for muscle-invasive bladder cancer patients', *Journal of Clinical Oncology,* 35 (6_suppl), 301-01.

Ciccia, A. and Elledge, S. J. (2010), 'The DNA damage response: making it safe to play with knives', *Mol Cell,* 40 (2), 179-204.

Cohausz, O. and Althaus, F. R. (2009), 'Role of PARP-1 and PARP-2 in the expression of apoptosis-regulating genes in HeLa cells', *Cell Biol Toxicol,* 25 (4), 379-91.

Colditz, G. A., Kaphingst, K. A., Hankinson, S. E., and Rosner, B. (2012), 'Family history and risk of breast cancer: nurses' health study', *Breast Cancer Res Treat,* 133 (3), 1097-104.

Collard, F., Stroobant, V., Lamosa, P., Kapanda, C. N., Lambert, D. M., Muccioli, G. G., Poupaert, J. H., Opperdoes, F., and Van Schaftingen, E. (2010), 'Molecular identification of N-acetylaspartylglutamate synthase and beta-citrylglutamate synthase', *J Biol Chem,* 285 (39), 29826-33.

Cooper, J. A. (1987), 'Effects of cytochalasin and phalloidin on actin', *J Cell Biol,* 105 (4), 1473-8.

Cortes-Ibanez, F. O., Johnson, T., Mascalchi, M., Katzke, V., Delorme, S., and Kaaks, R. (2023), 'Serum-based biomarkers associated with lung cancer risk and cause-specific mortality in the German randomized Lung Cancer Screening Intervention (LUSI) trial', *Transl Lung Cancer Res,* 12 (12), 2460-75.

Cousineau, I. and Belmaaza, A. (2007), 'BRCA1 haploinsufficiency, but not heterozygosity for a BRCA1-truncating mutation, deregulates homologous recombination', *Cell Cycle,* 6 (8), 962-71.

Couve, S., Ishchenko, A. A., Fedorova, O. S., Ramanculov, E. M., Laval, J., and Saparbaev, M. (2013), 'Direct DNA Lesion Reversal and Excision Repair in Escherichia coli', *EcoSal Plus,* 5 (2).

Crosby, M. E., Kulshreshtha, R., Ivan, M., and Glazer, P. M. (2009), 'MicroRNA regulation of DNA repair gene expression in hypoxic stress', *Cancer Res,* 69 (3), 1221-9.

Cullen, J. J., Weydert, C., Hinkhouse, M. M., Ritchie, J., Domann, F. E., Spitz, D., and Oberley, L. W. (2003), 'The role of manganese superoxide dismutase in the growth of pancreatic adenocarcinoma', *Cancer Res,* 63 (6), 1297-303.

Curtis, C., Shah, S. P., Chin, S. F., Turashvili, G., Rueda, O. M., Dunning, M. J., Speed, D., Lynch, A. G., Samarajiwa, S., Yuan, Y., Graf, S., Ha, G., Haffari, G., Bashashati, A., Russell, R., McKinney, S., Group, Metabric, Langerod, A., Green, A., Provenzano, E., Wishart, G., Pinder, S., Watson, P., Markowetz, F., Murphy, L., Ellis, I., Purushotham, A., Borresen-Dale, A. L., Brenton, J. D., Tavare, S., Caldas, C., and Aparicio, S. (2012), 'The genomic and

transcriptomic architecture of 2,000 breast tumours reveals novel subgroups', *Nature,* 486 (7403), 346-52.

Dai, C. H., Chen, P., Li, J., Lan, T., Chen, Y. C., Qian, H., Chen, K., and Li, M. Y. (2016), 'Co-inhibition of pol theta and HR genes efficiently synergize with cisplatin to suppress cisplatin-resistant lung cancer cells survival', *Oncotarget,* 7 (40), 65157-70.

Dana, H., Chalbatani, G. M., Mahmoodzadeh, H., Karimloo, R., Rezaiean, O., Moradzadeh, A., Mehmandoost, N., Moazzen, F., Mazraeh, A., Marmari, V., Ebrahimi, M., Rashno, M. M., Abadi, S. J., and Gharagouzlo, E. (2017), 'Molecular Mechanisms and Biological Functions of siRNA', *Int J Biomed Sci,* 13 (2), 48-57.

Davis, S., Gale, N. W., Aldrich, T. H., Maisonpierre, P. C., Lhotak, V., Pawson, T., Goldfarb, M., and Yancopoulos, G. D. (1994), 'Ligands for EPH-related receptor tyrosine kinases that require membrane attachment or clustering for activity', *Science,* 266 (5186), 816-9.

de Almeida, Ajpo, de Oliveira, Jcpl, da Silva Pontes, L. V., de Souza Junior, J. F., Goncalves, T. A. F., Dantas, S. H., de Almeida Feitosa, M. S., Silva, A. O., and de Medeiros, I. A. (2022), 'ROS: Basic Concepts, Sources, Cellular Signaling, and its Implications in Aging Pathways', *Oxid Med Cell Longev,* 2022, 1225578.

de Baat, A., Meier, D. T., Fontana, A., Boni-Schnetzler, M., and Donath, M. Y. (2023), 'Cystine/Glutamate antiporter system xc- deficiency impairs macrophage glutathione metabolism and cytokine production', *PLoS One,* 18 (10), e0291950.

de Bastos, D. R., Longatto-Filho, A., Conceicao, M. P. F., and Termini, L. (2024), 'High Levels of Superoxide Dismutase 2 Are Associated With Worse Prognosis in Patients With Breast Cancer', *Eur J Breast Health,* 20 (3), 185-93.

De Paola, F., Granato, A. M., Scarpi, E., Monti, F., Medri, L., Bianchi, S., Amadori, D., and Volpi, A. (2002), 'Vascular endothelial growth factor and prognosis in patients with node-negative breast cancer', *Int J Cancer,* 98 (2), 228-33.

De Soto, J. A., Wang, X., Tominaga, Y., Wang, R. H., Cao, L., Qiao, W., Li, C., Xu, X., Skoumbourdis, A. P., Prindiville, S. A., Thomas, C. J., and Deng, C. X. (2006), 'The inhibition and treatment of breast cancer with poly (ADP-ribose) polymerase (PARP-1) inhibitors', *Int J Biol Sci,* 2 (4), 179-85.

Delacroix, S., Wagner, J. M., Kobayashi, M., Yamamoto, K., and Karnitz, L. M. (2007), 'The Rad9-Hus1-Rad1 (9-1-1) clamp activates checkpoint signaling via TopBP1', *Genes Dev,* 21 (12), 1472-7.

Deng, M., Tong, R., Zhang, Z., Wang, T., Liang, C., Zhou, X., and Hou, G. (2021), 'EFNA3 as a predictor of clinical prognosis and immune checkpoint therapy efficacy in patients with lung adenocarcinoma', *Cancer Cell Int,* 21 (1), 535.

Di Mattia, M., Mauro, A., Delle Monache, S., Pulcini, F., Russo, V., Berardinelli, P., Citeroni, M. R., Turriani, M., Peserico, A., and Barboni, B. (2022), 'Hypoxia-Mimetic CoCl(2) Agent Enhances Pro-Angiogenic Activities in Ovine Amniotic Epithelial Cells-Derived Conditioned Medium', *Cells,* 11 (3).

Diamantopoulos, P. T., Sofotasiou, M., Papadopoulou, V., Polonyfi, K., Iliakis, T., and Viniou, N. A. (2014), 'PARP1-driven apoptosis in chronic lymphocytic leukemia', *Biomed Res Int,* 2014, 106713.

Dianov, G. L. and Hubscher, U. (2013), 'Mammalian base excision repair: the forgotten archangel', *Nucleic Acids Res,* 41 (6), 3483-90.

Dias, Mariana Paes, Moser, Sarah C., Ganesan, Shridar, and Jonkers, Jos (2021), 'Understanding and overcoming resistance to PARP inhibitors in cancer therapy', *Nature Reviews Clinical Oncology,* 18 (12), 773-91.

Dixon, S. J., Lemberg, K. M., Lamprecht, M. R., Skouta, R., Zaitsev, E. M., Gleason, C. E., Patel, D. N., Bauer, A. J., Cantley, A. M., Yang, W. S., Morrison, B., 3rd, and Stockwell, B. R. (2012), 'Ferroptosis: an iron-dependent form of nonapoptotic cell death', *Cell,* 149 (5), 1060-72.

Djuzenova, C. S., Zimmermann, M., Katzer, A., Fiedler, V., Distel, L. V., Gasser, M., Waaga-Gasser, A. M., Flentje, M., and Polat, B. (2015), 'A prospective study on histone gamma-H2AX and 53BP1 foci expression in rectal carcinoma patients: correlation with radiation therapy-induced outcome', *BMC Cancer,* 15, 856.

Downes, N. L., Laham-Karam, N., Kaikkonen, M. U., and Yla-Herttuala, S. (2018), 'Differential but Complementary HIF1alpha and HIF2alpha Transcriptional Regulation', *Mol Ther,* 26 (7), 1735-45.

Duranteau, J., Chandel, N. S., Kulisz, A., Shao, Z., and Schumacker, P. T. (1998), 'Intracellular signaling by reactive oxygen species during hypoxia in cardiomyocytes', *J Biol Chem,* 273 (19), 11619-24.

Durinikova, E., Reilly, N. M., Buzo, K., Mariella, E., Chila, R., Lorenzato, A., Dias, J. M. L., Grasso, G., Pisati, F., Lamba, S., Corti, G., Degasperi, A., Cancelliere, C., Mauri, G., Andrei, P., Linnebacher, M., Marsoni, S., Siena, S., Sartore-Bianchi, A., Nik-Zainal, S., Di Nicolantonio, F., Bardelli, A., and Arena, S. (2022), 'Targeting the DNA Damage Response Pathways and Replication Stress in Colorectal Cancer', *Clin Cancer Res,* 28 (17), 3874-89.

Economopoulou, M., Langer, H. F., Celeste, A., Orlova, V. V., Choi, E. Y., Ma, M., Vassilopoulos, A., Callen, E., Deng, C., Bassing, C. H., Boehm, M., Nussenzweig, A., and Chavakis, T. (2009), 'Histone H2AX is integral to hypoxia-driven neovascularization', *Nat Med,* 15 (5), 553-8.

Eker, A. P., Quayle, C., Chaves, I., and van der Horst, G. T. (2009), 'DNA repair in mammalian cells: Direct DNA damage reversal: elegant solutions for nasty problems', *Cell Mol Life Sci,* 66 (6), 968-80.

Fang, M., Zhu, L., Li, H., Li, X., Wu, Y., Wu, K., Lin, J., Sheng, Y., and Yu, Y. (2018), 'Characterization of mutations in BRCA1/2 and the relationship with clinic-pathological features of breast cancer in a hereditarily high-risk sample of chinese population', *Oncol Lett,* 15 (3), 3068-74.

Fang, P., De Souza, C., Minn, K., and Chien, J. (2019), 'Genome-scale CRISPR knockout screen identifies TIGAR as a modifier of PARP inhibitor sensitivity', *Commun Biol,* 2, 335.

Farmer, H., McCabe, N., Lord, C. J., Tutt, A. N., Johnson, D. A., Richardson, T. B., Santarosa, M., Dillon, K. J., Hickson, I., Knights, C., Martin, N. M., Jackson, S. P., Smith, G. C., and Ashworth, A. (2005), 'Targeting the DNA repair defect in BRCA mutant cells as a therapeutic strategy', *Nature,* 434 (7035), 917-21.

Fawaz, M. V., Topper, M. E., and Firestine, S. M. (2011), 'The ATP-grasp enzymes', *Bioorg Chem,* 39 (5-6), 185-91.

Felty, Q., Singh, K. P., and Roy, D. (2005), 'Estrogen-induced G1/S transition of G0-arrested estrogen-dependent breast cancer cells is regulated by mitochondrial oxidant signaling', *Oncogene,* 24 (31), 4883-93.

Feng, Y., Spezia, M., Huang, S., Yuan, C., Zeng, Z., Zhang, L., Ji, X., Liu, W., Huang, B., Luo, W., Liu, B., Lei, Y., Du, S., Vuppalapati, A., Luu, H. H., Haydon, R. C., He, T. C., and Ren, G. (2018), 'Breast cancer development and progression: Risk factors, cancer stem cells, signaling pathways, genomics, and molecular pathogenesis', *Genes Dis,* 5 (2), 77-106.

Fenor de la Maza, M. D., Perez Gracia, J. L., Minana, B., and Castro, E. (2024), 'PARP inhibitors alone or in combination for prostate cancer', *Ther Adv Urol,* 16, 17562872241272929.

Fischer-Fantuzzi, L. and Vesco, C. (1988), 'Cell-dependent efficiency of reiterated nuclear signals in a mutant simian virus 40 oncoprotein targeted to the nucleus', *Mol Cell Biol,* 8 (12), 5495-503.

Flanagan, J. G. and Vanderhaeghen, P. (1998), 'The ephrins and Eph receptors in neural development', *Annu Rev Neurosci,* 21, 309-45.

Foskolou, I. P. and Hammond, E. M. (2017), 'RRM2B: An oxygen-requiring protein with a role in hypoxia', *Mol Cell Oncol,* 4 (5), e1335272.

Foskolou, I. P., Biasoli, D., Olcina, M. M., and Hammond, E. M. (2016), 'Measuring DNA Replication in Hypoxic Conditions', *Adv Exp Med Biol,* 899, 11-25.

Foskolou, I. P., Jorgensen, C., Leszczynska, K. B., Olcina, M. M., Tarhonskaya, H., Haisma, B., D'Angiolella, V., Myers, W. K., Domene, C., Flashman, E., and Hammond, E. M. (2017), 'Ribonucleotide Reductase Requires Subunit Switching in Hypoxia to Maintain DNA Replication', *Mol Cell,* 66 (2), 206-20 e9.

Frankenberg-Schwager, M. (1990), 'Induction, repair and biological relevance of radiation-induced DNA lesions in eukaryotic cells', *Radiation and Environmental Biophysics,* 29 (4), 273-92.

Freedman, S. J., Sun, Z. Y., Poy, F., Kung, A. L., Livingston, D. M., Wagner, G., and Eck, M. J. (2002), 'Structural basis for recruitment of CBP/p300 by hypoxia-inducible factor-1 alpha', *Proc Natl Acad Sci U S A,* 99 (8), 5367-72.

Freiberg, R. A., Hammond, E. M., Dorie, M. J., Welford, S. M., and Giaccia, A. J. (2006), 'DNA damage during reoxygenation elicits a Chk2-dependent checkpoint response', *Mol Cell Biol,* 26 (5), 1598-609.

Frezzini, S., Tasca, G., Borgato, L., Sartor, L., Ferrero, A., Artioli, G., Modena, A., and Baldoni, A. (2024), 'PARP Inhibitors in Brain Metastases from Epithelial Ovarian Cancer through a Multimodal Patient Journey: Case Reports and Literature Review', *Int J Mol Sci,* 25 (14).

Fried, William, Tyagi, Mrityunjay, Minakhin, Leonid, Chandramouly, Gurushankar, Tredinnick, Taylor, Ramanjulu, Mercy, Auerbacher, William, Calbert, Marissa, Rusanov, Timur, Hoang, Trung, Borisonnik, Nikita, Betsch, Robert, Krais, John J., Wang, Yifan, Vekariya, Umeshkumar M., Gordon, John, Morton, George, Kent, Tatiana, Skorski, Tomasz, Johnson, Neil, Childers, Wayne, Chen, Xiaojiang S., and Pomerantz, Richard T. (2024), 'Discovery of a small-molecule inhibitor that traps Polθ on DNA and synergizes with PARP inhibitors', *Nature Communications,* 15 (1), 2862.

Fu, X., Li, P., Zhou, Q., He, R., Wang, G., Zhu, S., Bagheri, A., Kupfer, G., Pei, H., and Li, J. (2024a), 'Mechanism of PARP inhibitor resistance and potential overcoming strategies', *Genes Dis,* 11 (1), 306-20.

Fu, Xiaoyu, Li, Ping, Zhou, Qi, He, Ruyuan, Wang, Guannan, Zhu, Shiya, Bagheri, Amir, Kupfer, Gary, Pei, Huadong, and Li, Juanjuan (2024b), 'Mechanism of PARP inhibitor resistance and potential overcoming strategies', *Genes & Diseases,* 11 (1), 306-20.

Fukuda, R., Zhang, H., Kim, J. W., Shimoda, L., Dang, C. V., and Semenza, G. L. (2007), 'HIF-1 regulates cytochrome oxidase subunits to optimize efficiency of respiration in hypoxic cells', *Cell,* 129 (1), 111-22.

Gadducci, A., Cosio, S., Landoni, F., Lissoni, A. A., Zola, P., Laudani, M. E., Ardizzoia, A., Gambino, A., and Sartori, E. (2022), 'Response to Chemotherapy and Clinical Outcome of Patients With Recurrent Epithelial Ovarian Cancer After PARP Inhibitor Maintenance Treatment: A Multicenter Retrospective Italian Study', *Anticancer Res,* 42 (4), 2017-22.

Gagou, M. E., Zuazua-Villar, P., and Meuth, M. (2010), 'Enhanced H2AX phosphorylation, DNA replication fork arrest, and cell death in the absence of Chk1', *Mol Biol Cell,* 21 (5), 739-52.

Galadari, S., Rahman, A., Pallichankandy, S., and Thayyullathil, F. (2017), 'Reactive oxygen species and cancer paradox: To promote or to suppress?', *Free Radic Biol Med,* 104, 144-64.

Gambino, V., De Michele, G., Venezia, O., Migliaccio, P., Dall'Olio, V., Bernard, L., Minardi, S. P., Della Fazia, M. A., Bartoli, D., Servillo, G., Alcalay, M., Luzi, L., Giorgio, M., Scrable, H., Pelicci, P. G., and Migliaccio, E. (2013), 'Oxidative stress activates a specific p53 transcriptional response that regulates cellular senescence and aging', *Aging Cell,* 12 (3), 435-45.

Ganguin, Aymar Abel, Aleandri, Simone, and Luciani, Paola (2023), 'Chapter 2 - The cell: cell microenvironment and cell handling', in Gerardo Perozziello, Ulrich Krühne, and Paola Luciani (eds.), *Microfluidics for Cellular Applications* (Elsevier), 5-26.

Gao, Y. H., Li, C. X., Shen, S. M., Li, H., Chen, G. Q., Wei, Q., and Wang, L. S. (2013), 'Hypoxia-inducible factor 1alpha mediates the down-regulation of superoxide dismutase 2 in von

Hippel-Lindau deficient renal clear cell carcinoma', *Biochem Biophys Res Commun,* 435 (1), 46-51.

Gardner, Lawrence B., Li, Qing, Park, Michele S., Flanagan, W. Michael, Semenza, Gregg L., and Dang, Chi V. (2001), 'Hypoxia Inhibits G1/S Transition through Regulation of p27 Expression*', *Journal of Biological Chemistry,* 276 (11), 7919-26.

Garnier, P., Prigent-Tessier, A., Van Hoecke, M., Bertrand, N., Demougeot, C., Sordet, O., Swanson, R. A., Marie, C., and Beley, A. (2004), 'Hypoxia induces caspase-9 and caspase-3 activation without neuronal death in gerbil brains', *Eur J Neurosci,* 20 (4), 937-46.

Ge, R., Wang, Z., and Cheng, L. (2022), 'Tumor microenvironment heterogeneity an important mediator of prostate cancer progression and therapeutic resistance', *NPJ Precis Oncol,* 6 (1), 31.

Gehl, L. M., Saab, O. H., Bzdega, T., Wroblewska, B., and Neale, J. H. (2004), 'Biosynthesis of NAAG by an enzyme-mediated process in rat central nervous system neurons and glia', *J Neurochem,* 90 (4), 989-97.

Geng, H., Su, Y., Huang, R., Fan, M., Li, X., Lu, X., and Sheng, H. (2021), 'Specific protein 1 inhibitor mithramycin A protects cardiomyocytes from myocardial infarction via interacting with PARP', *In Vitro Cell Dev Biol Anim,* 57 (3), 315-23.

Ghandi, M., Huang, F. W., Jane-Valbuena, J., Kryukov, G. V., Lo, C. C., McDonald, E. R., 3rd, Barretina, J., Gelfand, E. T., Bielski, C. M., Li, H., Hu, K., Andreev-Drakhlin, A. Y., Kim, J., Hess, J. M., Haas, B. J., Aguet, F., Weir, B. A., Rothberg, M. V., Paolella, B. R., Lawrence, M. S., Akbani, R., Lu, Y., Tiv, H. L., Gokhale, P. C., de Weck, A., Mansour, A. A., Oh, C., Shih, J., Hadi, K., Rosen, Y., Bistline, J., Venkatesan, K., Reddy, A., Sonkin, D., Liu, M., Lehar, J., Korn, J. M., Porter, D. A., Jones, M. D., Golji, J., Caponigro, G., Taylor, J. E., Dunning, C. M., Creech, A. L., Warren, A. C., McFarland, J. M., Zamanighomi, M., Kauffmann, A., Stransky, N., Imielinski, M., Maruvka, Y. E., Cherniack, A. D., Tsherniak, A., Vazquez, F., Jaffe, J. D., Lane, A. A., Weinstock, D. M., Johannessen, C. M., Morrissey, M. P., Stegmeier, F.,

Schlegel, R., Hahn, W. C., Getz, G., Mills, G. B., Boehm, J. S., Golub, T. R., Garraway, L. A., and Sellers, W. R. (2019), 'Next-generation characterization of the Cancer Cell Line Encyclopedia', *Nature,* 569 (7757), 503-08.

Giaccia, A. J., Simon, M. C., and Johnson, R. (2004), 'The biology of hypoxia: the role of oxygen sensing in development, normal function, and disease', *Genes Dev,* 18 (18), 2183-94.

Giovannini, Sara, Weller, Marie-Christine, Repmann, Simone, Moch, Holger, and Jiricny, Josef (2019), 'Synthetic lethality between BRCA1 deficiency and poly(ADP-ribose) polymerase inhibition is modulated by processing of endogenous oxidative DNA damage', *Nucleic Acids Research,* 47 (17), 9132-43.

Gogola, E., Duarte, A. A., de Ruiter, J. R., Wiegant, W. W., Schmid, J. A., de Bruijn, R., James, D. I., Llobet, S. G., Vis, D. J., Annunziato, S., van den Broek, B., Barazas, M., Kersbergen, A., van de Ven, M., Tarsounas, M., Ogilvie, D. J., van Vugt, M., Wessels, L. F. A., Bartkova, J., Gromova, I., Andujar-Sanchez, M., Bartek, J., Lopes, M., van Attikum, H., Borst, P., Jonkers, J., and Rottenberg, S. (2019), 'Selective Loss of PARG Restores PARylation and Counteracts PARP Inhibitor-Mediated Synthetic Lethality', *Cancer Cell,* 35 (6), 950-52.

Gomes, B. C., Silva, S. N., Azevedo, A. P., Manita, I., Gil, O. M., Ferreira, T. C., Limbert, E., Rueff, J., and Gaspar, J. F. (2010), 'The role of common variants of non-homologous end-joining repair genes XRCC4, LIG4 and Ku80 in thyroid cancer risk', *Oncol Rep,* 24 (4), 1079-85.

Gonzalez-Flores, A., Aguilar-Quesada, R., Siles, E., Pozo, S., Rodríguez-Lara, M. I., López – Jiménez, L., López-Rodríguez, M., Peralta-Leal, A., Villar, D., Martín-Oliva, D., del Peso, L., Berra, E., and Oliver, F. J. (2013), 'Interaction between PARP-1 and HIF-2α in the hypoxic response', *Oncogene,* 33 (7), 891-98.

Goodarzi, A. A., Noon, A. T., Deckbar, D., Ziv, Y., Shiloh, Y., Lobrich, M., and Jeggo, P. A. (2008), 'ATM signaling facilitates repair of DNA double-strand breaks associated with heterochromatin', *Mol Cell,* 31 (2), 167-77.

Gorman, C. M., Lane, D. P., and Rigby, P. W. (1984), 'High efficiency gene transfer into mammalian cells', *Philos Trans R Soc Lond B Biol Sci,* 307 (1132), 343-6.

Graeser, M., McCarthy, A., Lord, C. J., Savage, K., Hills, M., Salter, J., Orr, N., Parton, M., Smith, I. E., Reis-Filho, J. S., Dowsett, M., Ashworth, A., and Turner, N. C. (2010), 'A marker of homologous recombination predicts pathologic complete response to neoadjuvant chemotherapy in primary breast cancer', *Clin Cancer Res,* 16 (24), 6159-68.

Gray, M. J., Zhang, J., Ellis, L. M., Semenza, G. L., Evans, D. B., Watowich, S. S., and Gallick, G. E. (2005), 'HIF-1alpha, STAT3, CBP/p300 and Ref-1/APE are components of a transcriptional complex that regulates Src-dependent hypoxia-induced expression of VEGF in pancreatic and prostate carcinomas', *Oncogene,* 24 (19), 3110-20.

Greenwald, P. and Dunn, B. K. (2009), 'Landmarks in the history of cancer epidemiology', *Cancer Res,* 69 (6), 2151-62.

Gruosso, T., Mieulet, V., Cardon, M., Bourachot, B., Kieffer, Y., Devun, F., Dubois, T., Dutreix, M., Vincent-Salomon, A., Miller, K. M., and Mechta-Grigoriou, F. (2016), 'Chronic oxidative stress promotes H2AX protein degradation and enhances chemosensitivity in breast cancer patients', *EMBO Mol Med,* 8 (5), 527-49.

Gu, W., Zhuang, W., Zhuang, M., He, M., and Li, Z. (2023), 'DNA damage response and repair gene mutations are associated with tumor mutational burden and outcomes to platinum-based chemotherapy/immunotherapy in advanced NSCLC patients', *Diagn Pathol,* 18 (1), 119.

Guo, H., Liu, J., Van Shura, K., Chen, H., Flora, M. N., Myers, T. M., McDonough, J. H., and McCabe, J. T. (2015), 'N-acetyl-aspartyl-glutamate and inhibition of glutamate carboxypeptidases protects against soman-induced neuropathology', *Neurotoxicology,* 48, 180-91.

Gurley, L. R., D'Anna, J. A., Barham, S. S., Deaven, L. L., and Tobey, R. A. (1978), 'Histone phosphorylation and chromatin structure during mitosis in Chinese hamster cells', *Eur J Biochem,* 84 (1), 1-15.

Haas, J., Park, E. C., and Seed, B. (1996), 'Codon usage limitation in the expression of HIV-1 envelope glycoprotein', *Curr Biol,* 6 (3), 315-24.

Haller, B., Ulm, K., and Hapfelmeier, A. (2019), 'A Simulation Study Comparing Different Statistical Approaches for the Identification of Predictive Biomarkers', *Comput Math Methods Med,* 2019, 7037230.

Halliwell, B. and J, M. C. Gutteridge (2022), 'Reprint of: Oxygen Free Radicals and Iron in Relation to Biology and Medicine: Some Problems and Concepts', *Arch Biochem Biophys,* 726, 109246.

Hammond, E. M. and Giaccia, A. J. (2005), 'The role of p53 in hypoxia-induced apoptosis', *Biochem Biophys Res Commun,* 331 (3), 718-25.

--- (2006), 'Hypoxia-inducible factor-1 and p53: friends, acquaintances, or strangers?', *Clin Cancer Res,* 12 (17), 5007-9.

Hammond, E. M., Dorie, M. J., and Giaccia, A. J. (2003a), 'ATR/ATM targets are phosphorylated by ATR in response to hypoxia and ATM in response to reoxygenation', *J Biol Chem,* 278 (14), 12207-13.

Hammond, E. M., Green, S. L., and Giaccia, A. J. (2003b), 'Comparison of hypoxia-induced replication arrest with hydroxyurea and aphidicolin-induced arrest', *Mutat Res,* 532 (1-2), 205-13.

Hammond, E. M., Dorie, M. J., and Giaccia, A. J. (2004), 'Inhibition of ATR leads to increased sensitivity to hypoxia/reoxygenation', *Cancer Res,* 64 (18), 6556-62.

Hammond, E. M., Freiberg, R. A., and Giaccia, A. J. (2006a), 'The roles of Chk 1 and Chk 2 in hypoxia and reoxygenation', *Cancer Lett,* 238 (2), 161-7.

Hammond, E. M., Denko, N. C., Dorie, M. J., Abraham, R. T., and Giaccia, A. J. (2002), 'Hypoxia links ATR and p53 through replication arrest', *Mol Cell Biol,* 22 (6), 1834-43.

Hammond, E. M., Asselin, M. C., Forster, D., O'Connor, J. P., Senra, J. M., and Williams, K. J. (2014), 'The meaning, measurement and modification of hypoxia in the laboratory and the clinic', *Clin Oncol (R Coll Radiol),* 26 (5), 277-88.

Hammond, E. M., Mandell, D. J., Salim, A., Krieg, A. J., Johnson, T. M., Shirazi, H. A., Attardi, L. D., and Giaccia, A. J. (2006b), 'Genome-wide analysis of p53 under hypoxic conditions', *Mol Cell Biol,* 26 (9), 3492-504.

Hampton-Smith, R. J., Davenport, B. A., Nagarajan, Y., and Peet, D. J. (2019), 'The conservation and functionality of the oxygen-sensing enzyme Factor Inhibiting HIF (FIH) in non-vertebrates', *PLoS One,* 14 (4), e0216134.

Han, D., Williams, E., and Cadenas, E. (2001), 'Mitochondrial respiratory chain-dependent generation of superoxide anion and its release into the intermembrane space', *Biochem J,* 353 (Pt 2), 411-6.

Hanahan, D. (2022), 'Hallmarks of Cancer: New Dimensions', *Cancer Discov,* 12 (1), 31-46.

Hanahan, D. and Weinberg, R. A. (2000), 'The hallmarks of cancer', *Cell,* 100 (1), 57-70.

--- (2011), 'Hallmarks of cancer: the next generation', *Cell,* 144 (5), 646-74.

Hans, F. and Dimitrov, S. (2001), 'Histone H3 phosphorylation and cell division', *Oncogene,* 20 (24), 3021-7.

Hanzlikova, H., Gittens, W., Krejcikova, K., Zeng, Z., and Caldecott, K. W. (2017), 'Overlapping roles for PARP1 and PARP2 in the recruitment of endogenous XRCC1 and PNKP into oxidized chromatin', *Nucleic Acids Res,* 45 (5), 2546-57.

Harbeck, N., Penault-Llorca, F., Cortes, J., Gnant, M., Houssami, N., Poortmans, P., Ruddy, K., Tsang, J., and Cardoso, F. (2019), 'Breast cancer', *Nat Rev Dis Primers,* 5 (1), 66.

Hassan Metwally, M. A., Ali, R., Kuddu, M., Shouman, T., Strojan, P., Iqbal, K., Prasad, R., Grau, C., and Overgaard, J. (2015), 'IAEA-HypoX. A randomized multicenter study of the hypoxic radiosensitizer nimorazole concomitant with accelerated radiotherapy in head and neck squamous cell carcinoma', *Radiother Oncol,* 116 (1), 15-20.

Hayashi, Y., Yokota, A., Harada, H., and Huang, G. (2019), 'Hypoxia/pseudohypoxia-mediated activation of hypoxia-inducible factor-1alpha in cancer', *Cancer Sci,* 110 (5), 1510-17.

Hayes, J. D., Dinkova-Kostova, A. T., and Tew, K. D. (2020), 'Oxidative Stress in Cancer', *Cancer Cell,* 38 (2), 167-97.

He, Y., Lu, D., Cheng, H., Zhang, Y., Wu, F., and Chen, Z. (2023), 'PPFIA4 Promotes Proliferation, Migration and Glycolysis of Esophageal Cancer Cells', *Ann Clin Lab Sci,* 53 (6), 840-46.

Heffernan, A. L., Aylward, L. L., Toms, L. M., Sly, P. D., Macleod, M., and Mueller, J. F. (2014), 'Pooled biological specimens for human biomonitoring of environmental chemicals: opportunities and limitations', *J Expo Sci Environ Epidemiol,* 24 (3), 225-32.

Hegan, Denise Campisi, Lu, Yuhong, Stachelek, Gregory C., Crosby, Meredith E., Bindra, Ranjit S., and Glazer, Peter M. (2010), 'Inhibition of poly(ADP-ribose) polymerase down-regulates BRCA1 and RAD51 in a pathway mediated by E2F4 and p130', *Proceedings of the National Academy of Sciences,* 107 (5), 2201-06.

Herceg, Z. and Wang, Z. Q. (2001), 'Functions of poly(ADP-ribose) polymerase (PARP) in DNA repair, genomic integrity and cell death', *Mutat Res,* 477 (1-2), 97-110.

Hetman, M. and Pietrzak, M. (2012), 'Emerging roles of the neuronal nucleolus', *Trends Neurosci,* 35 (5), 305-14.

Hill, R. M., Rocha, S., and Parsons, J. L. (2022), 'Overcoming the Impact of Hypoxia in Driving Radiotherapy Resistance in Head and Neck Squamous Cell Carcinoma', *Cancers (Basel),* 14 (17).

Hirota, Y., Tsugawa, N., Nakagawa, K., Suhara, Y., Tanaka, K., Uchino, Y., Takeuchi, A., Sawada, N., Kamao, M., Wada, A., Okitsu, T., and Okano, T. (2013), 'Menadione (vitamin K3) is a catabolic product of oral phylloquinone (vitamin K1) in the intestine and a circulating precursor of tissue menaquinone-4 (vitamin K2) in rats', *J Biol Chem,* 288 (46), 33071-80.

Ho, K. V., Tatum, D. S., Watkinson, L., Carmack, T., Jia, F., Mascioni, A., Maitz, C. A., Magda, D., and Anderson, C. J. (2024), 'Single Chelator-Minibody Theranostic Agents for (89)Zr PET

Imaging and (177)Lu Radiopharmaceutical Therapy of PSMA-Expressing Prostate Cancer', *J Nucl Med,* 65 (9), 1435-42.

Ho, Y. J., Thao, D. T., and Yeh, C. K. (2022), 'Overcoming Hypoxia-Induced Drug Resistance via Promotion of Drug Uptake and Reoxygenation by Acousto-Mechanical Oxygen Delivery', *Pharmaceutics,* 14 (5).

Hogbom, M., Galander, M., Andersson, M., Kolberg, M., Hofbauer, W., Lassmann, G., Nordlund, P., and Lendzian, F. (2003), 'Displacement of the tyrosyl radical cofactor in ribonucleotide reductase obtained by single-crystal high-field EPR and 1.4-A x-ray data', *Proc Natl Acad Sci U S A,* 100 (6), 3209-14.

Hoidy, W. H., Esaa, S. M., and Al-Saadi, M. H. (2022), 'Association of the Manganese Superoxide Dismutase (Mn-SOD) Gene C47T Polymorphism with Lung Cancer: A Case-Control Study', *Asian Pac J Cancer Prev,* 23 (8), 2617-21.

Horsman, M. R. and Overgaard, J. (1992), 'Overcoming tumour radiation resistance resulting from acute hypoxia', *Eur J Cancer,* 28A (4-5), 717-8.

Horsman, M. R., Mortensen, L. S., Petersen, J. B., Busk, M., and Overgaard, J. (2012), 'Imaging hypoxia to improve radiotherapy outcome', *Nat Rev Clin Oncol,* 9 (12), 674-87.

Hossain, M. A., Lin, Y., and Yan, S. (2018), 'Single-Strand Break End Resection in Genome Integrity: Mechanism and Regulation by APE2', *Int J Mol Sci,* 19 (8).

Hu, C. J., Wang, L. Y., Chodosh, L. A., Keith, B., and Simon, M. C. (2003), 'Differential roles of hypoxia-inducible factor 1alpha (HIF-1alpha) and HIF-2alpha in hypoxic gene regulation', *Mol Cell Biol,* 23 (24), 9361-74.

Huang, J., Zhang, L., Wan, D., Zhou, L., Zheng, S., Lin, S., and Qiao, Y. (2021a), 'Extracellular matrix and its therapeutic potential for cancer treatment', *Signal Transduct Target Ther,* 6 (1), 153.

Huang, J., Yang, M., Liu, Z., Li, X., Wang, J., Fu, N., Cao, T., and Yang, X. (2021b), 'PPFIA4 Promotes Colon Cancer Cell Proliferation and Migration by Enhancing Tumor Glycolysis', *Front Oncol,* 11, 653200.

Huang, Ruixue and Zhou, Ping-Kun (2021), 'DNA damage repair: historical perspectives, mechanistic pathways and clinical translation for targeted cancer therapy', *Signal Transduction and Targeted Therapy,* 6 (1), 254.

Huang, Ruixue, Yu, Ting, Li, Ying, and Hu, Jianan (2018), 'Upregulated has-miR-4516 as a potential biomarker for early diagnosis of dust-induced pulmonary fibrosis in patients with pneumoconiosis', *Toxicology Research,* 7 (3), 415-22.

Huang, Y., He, H., Liang, L., Zhang, Y., Peng, K., Wang, Y., Wu, J., Long, X., Kairemo, K., Goldberg, H., Mendez, L. C., and Gu, D. (2024), 'Efficacy and safety of PARP inhibitors in the treatment of prostatic cancer: a systematic review and network meta-analysis', *Chin Clin Oncol,* 13 (4), 64.

Hulka, B. S. (1996), 'Epidemiology of susceptibility to breast cancer', *Prog Clin Biol Res,* 395, 159-74.

Husain, A., Chiu, Y. T., Sze, K. M., Ho, D. W., Tsui, Y. M., Suarez, E. M. S., Zhang, V. X., Chan, L. K., Lee, E., Lee, J. M., Cheung, T. T., Wong, C. C., Chung, C. Y., and Ng, I. O. (2022), 'Ephrin-A3/EphA2 axis regulates cellular metabolic plasticity to enhance cancer stemness in hypoxic hepatocellular carcinoma', *J Hepatol,* 77 (2), 383-96.

Ingebriktsen, L. M., Finne, K., Akslen, L. A., and Wik, E. (2022), 'A novel age-related gene expression signature associates with proliferation and disease progression in breast cancer', *Br J Cancer,* 127 (10), 1865-75.

Iqbal, M. A., Siddiqui, S., Smith, K., Singh, P., Kumar, B., Chouaib, S., and Chandrasekaran, S. (2023), 'Metabolic stratification of human breast tumors reveal subtypes of clinical and therapeutic relevance', *iScience,* 26 (10), 108059.

Jackson, Lindsey M. and Moldovan, George-Lucian (2022), 'Mechanisms of PARP1 inhibitor resistance and their implications for cancer treatment', *NAR Cancer,* 4 (4), zcac042.

Jackson, P. F., Cole, D. C., Slusher, B. S., Stetz, S. L., Ross, L. E., Donzanti, B. A., and Trainor, D. A. (1996), 'Design, synthesis, and biological activity of a potent inhibitor of the

neuropeptidase N-acetylated alpha-linked acidic dipeptidase', *J Med Chem,* 39 (2), 619-22.

Jackson, S. P. and Bartek, J. (2009), 'The DNA-damage response in human biology and disease', *Nature,* 461 (7267), 1071-8.

Jacobson, D. H., Pan, S., Fisher, J., and Secrier, M. (2023), 'Multi-scale characterisation of homologous recombination deficiency in breast cancer', *Genome Med,* 15 (1), 90.

Jang, H. R., Lee, K., Jeon, J., Kim, J. R., Lee, J. E., Kwon, G. Y., Kim, Y. G., Kim, D. J., Ko, J. W., and Huh, W. (2020), 'Poly (ADP-Ribose) Polymerase Inhibitor Treatment as a Novel Therapy Attenuating Renal Ischemia-Reperfusion Injury', *Front Immunol,* 11, 564288.

Jaspers, J. E., Kersbergen, A., Boon, U., Sol, W., van Deemter, L., Zander, S. A., Drost, R., Wientjens, E., Ji, J., Aly, A., Doroshow, J. H., Cranston, A., Martin, N. M., Lau, A., O'Connor, M. J., Ganesan, S., Borst, P., Jonkers, J., and Rottenberg, S. (2013), 'Loss of 53BP1 causes PARP inhibitor resistance in Brca1-mutated mouse mammary tumors', *Cancer Discov,* 3 (1), 68-81.

Javed, S. R., Lord, S., El Badri, S., Harman, R., Holmes, J., Kamzi, F., Maughan, T., McIntosh, D., Mukherjee, S., Ooms, A., Radhakrishna, G., Shaw, P., and Hawkins, M. A. (2024), 'CHARIOT: a phase I study of berzosertib with chemoradiotherapy in oesophageal and other solid cancers using time to event continual reassessment method', *Br J Cancer,* 130 (3), 467-75.

Ji, Z., Bao, S., Li, L., Wang, D., Shi, M., and Liu, X. (2022), 'Hypoxia-inducible factor-2alpha promotes EMT in esophageal squamous cell carcinoma through the Notch pathway', *Adv Clin Exp Med,* 31 (7), 795-805.

Jiang, X., Stockwell, B. R., and Conrad, M. (2021), 'Ferroptosis: mechanisms, biology and role in disease', *Nat Rev Mol Cell Biol,* 22 (4), 266-82.

Jiang, Y., Verbiest, T., Devery, A. M., Bokobza, S. M., Weber, A. M., Leszczynska, K. B., Hammond, E. M., and Ryan, A. J. (2016), 'Hypoxia Potentiates the Radiation-Sensitizing Effect of

Olaparib in Human Non-Small Cell Lung Cancer Xenografts by Contextual Synthetic Lethality', *Int J Radiat Oncol Biol Phys,* 95 (2), 772-81.

Jin, G., Liu, K., Guo, Z., and Dong, Z. (2024), 'Precision therapy for cancer prevention by targeting carcinogenesis', *Mol Carcinog*.

Jin, W. S., Kong, Z. L., Shen, Z. F., Jin, Y. Z., Zhang, W. K., and Chen, G. F. (2011), 'Regulation of hypoxia inducible factor-1alpha expression by the alteration of redox status in HepG2 cells', *J Exp Clin Cancer Res,* 30 (1), 61.

Jing, X., Yang, F., Shao, C., Wei, K., Xie, M., Shen, H., and Shu, Y. (2019), 'Role of hypoxia in cancer therapy by regulating the tumor microenvironment', *Mol Cancer,* 18 (1), 157.

Johnson, S. F., Cruz, C., Greifenberg, A. K., Dust, S., Stover, D. G., Chi, D., Primack, B., Cao, S., Bernhardy, A. J., Coulson, R., Lazaro, J. B., Kochupurakkal, B., Sun, H., Unitt, C., Moreau, L. A., Sarosiek, K. A., Scaltriti, M., Juric, D., Baselga, J., Richardson, A. L., Rodig, S. J., D'Andrea, A. D., Balmana, J., Johnson, N., Geyer, M., Serra, V., Lim, E., and Shapiro, G. I. (2016), 'CDK12 Inhibition Reverses De Novo and Acquired PARP Inhibitor Resistance in BRCA Wild-Type and Mutated Models of Triple-Negative Breast Cancer', *Cell Rep,* 17 (9), 2367-81.

Jongen, J. M. J., van der Waals, L. M., Trumpi, K., Laoukili, J., Peters, N. A., Schenning-van Schelven, S. J., Govaert, K. M., Borel Rinkes, I. H. M., and Kranenburg, O. (2017), 'Downregulation of DNA repair proteins and increased DNA damage in hypoxic colon cancer cells is a therapeutically exploitable vulnerability', *Oncotarget,* 8 (49), 86296-311.

Juan, C. A., Perez de la Lastra, J. M., Plou, F. J., and Perez-Lebena, E. (2021), 'The Chemistry of Reactive Oxygen Species (ROS) Revisited: Outlining Their Role in Biological Macromolecules (DNA, Lipids and Proteins) and Induced Pathologies', *Int J Mol Sci,* 22 (9).

Jurkovicova, D., Neophytou, C. M., Gasparovic, A. C., and Goncalves, A. C. (2022), 'DNA Damage Response in Cancer Therapy and Resistance: Challenges and Opportunities', *Int J Mol Sci,* 23 (23).

Kaluz, S., Kaluzova, M., Chrastina, A., Olive, P. L., Pastorekova, S., Pastorek, J., Lerman, M. I., and Stanbridge, E. J. (2002), 'Lowered oxygen tension induces expression of the hypoxia marker MN/carbonic anhydrase IX in the absence of hypoxia-inducible factor 1 alpha stabilization: a role for phosphatidylinositol 3'-kinase', *Cancer Res,* 62 (15), 4469-77.

Kang, W. K., Icho, T., Isono, S., Kitakawa, M., and Isono, K. (1989), 'Characterization of the gene rimK responsible for the addition of glutamic acid residues to the C-terminus of ribosomal protein S6 in Escherichia coli K12', *Mol Gen Genet,* 217 (2-3), 281-8.

Kaplan, E. L. and and Meier, Paul (1958), 'Nonparametric Estimation from Incomplete Observations', *Journal of the American Statistical Association,* 53 (282), 457-81.

Kast, K., Rhiem, K., Larsen, M., Wappenschmidt, B., and Schmutzler, R. (2024), 'Phenotype analysis of families with TP53 germline variants at the Center for Familial Breast and Ovarian Cancer, Cologne', *Cancer Med,* 13 (3), e6920.

Katsura, C., Ogunmwonyi, I., Kankam, H. K., and Saha, S. (2022), 'Breast cancer: presentation, investigation and management', *Br J Hosp Med (Lond),* 83 (2), 1-7.

Kawamura, K., Qi, F., and Kobayashi, J. (2018), 'Potential relationship between the biological effects of low-dose irradiation and mitochondrial ROS production', *J Radiat Res,* 59 (suppl_2), ii91-ii97.

Keulers, T. G., Koch, A., van Gisbergen, M. W., Barbeau, L. M. O., Zonneveld, M. I., de Jong, M. C., Savelkouls, K. G. M., Wanders, R. G., Bussink, J., Melotte, V., and Rouschop, K. M. A. (2022), 'ATG12 deficiency results in intracellular glutamine depletion, abrogation of tumor hypoxia and a favorable prognosis in cancer', *Autophagy,* 18 (8), 1898-914.

Kim, D. and Nam, H. J. (2022), 'PARP Inhibitors: Clinical Limitations and Recent Attempts to Overcome Them', *Int J Mol Sci,* 23 (15).

Kim, J. I., Choi, K. U., Lee, I. S., Choi, Y. J., Kim, W. T., Shin, D. H., Kim, K., Lee, J. H., Kim, J. Y., and Sol, M. Y. (2015), 'Expression of hypoxic markers and their prognostic significance in soft tissue sarcoma', *Oncol Lett,* 9 (4), 1699-706.

Kim, J. W., Min, D. W., Kim, D., Kim, J., Kim, M. J., Lim, H., and Lee, J. Y. (2023), 'GPX4 overexpressed non-small cell lung cancer cells are sensitive to RSL3-induced ferroptosis', *Sci Rep,* 13 (1), 8872.

Klaunig, J. E., Kamendulis, L. M., and Hocevar, B. A. (2010), 'Oxidative stress and oxidative damage in carcinogenesis', *Toxicol Pathol,* 38 (1), 96-109.

Koppenhafer, S. L., Goss, K. L., Terry, W. W., and Gordon, D. J. (2020), 'Inhibition of the ATR-CHK1 Pathway in Ewing Sarcoma Cells Causes DNA Damage and Apoptosis via the CDK2-Mediated Degradation of RRM2', *Mol Cancer Res,* 18 (1), 91-104.

Korwek, Z., Bielak-Zmijewska, A., Mosieniak, G., Alster, O., Moreno-Villanueva, M., Burkle, A., and Sikora, E. (2013), 'DNA damage-independent apoptosis induced by curcumin in normal resting human T cells and leukaemic Jurkat cells', *Mutagenesis,* 28 (4), 411-6.

Kostos, L., Tran, B., and Azad, A. A. (2024), 'Combination of PARP Inhibitors and Androgen Receptor Pathway Inhibitors in Metastatic Castration-Resistant Prostate Cancer', *Drugs*.

Kotsopoulos, J., Chen, Z., Vallis, K. A., Poll, A., Ainsworth, P., and Narod, S. A. (2007), 'DNA repair capacity as a possible biomarker of breast cancer risk in female BRCA1 mutation carriers', *Br J Cancer,* 96 (1), 118-25.

Kresoja-Rakic, J. and Santoro, R. (2019), 'Nucleolus and rRNA Gene Chromatin in Early Embryo Development', *Trends Genet,* 35 (11), 868-79.

Krop, I., Ismaila, N., Andre, F., Bast, R. C., Barlow, W., Collyar, D. E., Hammond, M. E., Kuderer, N. M., Liu, M. C., Mennel, R. G., Van Poznak, C., Wolff, A. C., and Stearns, V. (2017), 'Use of Biomarkers to Guide Decisions on Adjuvant Systemic Therapy for Women With Early-Stage Invasive Breast Cancer: American Society of Clinical Oncology Clinical Practice Guideline Focused Update', *J Clin Oncol,* 35 (24), 2838-47.

Kruhlak, M. J., Celeste, A., Dellaire, G., Fernandez-Capetillo, O., Muller, W. G., McNally, J. G., Bazett-Jones, D. P., and Nussenzweig, A. (2006), 'Changes in chromatin structure and mobility in living cells at sites of DNA double-strand breaks', *J Cell Biol,* 172 (6), 823-34.

Kuleshov, M. V., Jones, M. R., Rouillard, A. D., Fernandez, N. F., Duan, Q., Wang, Z., Koplev, S., Jenkins, S. L., Jagodnik, K. M., Lachmann, A., McDermott, M. G., Monteiro, C. D., Gundersen, G. W., and Ma'ayan, A. (2016), 'Enrichr: a comprehensive gene set enrichment analysis web server 2016 update', *Nucleic Acids Res,* 44 (W1), W90-7.

Kumar, A., Purohit, S., and Sharma, N. K. (2016), 'Aberrant DNA Double-strand Break Repair Threads in Breast Carcinoma: Orchestrating Genomic Insult Survival', *J Cancer Prev,* 21 (4), 227-34.

Kumar, N., Gann, P. H., McGregor, S. M., and Sethi, A. (2023), 'Quantification of subtype purity in Luminal A breast cancer predicts clinical characteristics and survival', *Breast Cancer Res Treat,* 200 (2), 225-35.

Kumareswaran, R., Chaudary, N., Jaluba, K., Meng, A., Sykes, J., Borhan, A., Hill, R. P., and Bristow, R. G. (2015), 'Cyclic hypoxia does not alter RAD51 expression or PARP inhibitor cell kill in tumor cells', *Radiother Oncol,* 116 (3), 388-91.

Kun, E. and Bauer, P. I. (2001), 'Cell biological functions of PARP I: an overview', *Ital J Biochem,* 50 (1-2), 15-8.

Kung-Chun Chiu, D., Pui-Wah Tse, A., Law, C. T., Ming-Jing Xu, I., Lee, D., Chen, M., Kit-Ho Lai, R., Wai-Hin Yuen, V., Wing-Sum Cheu, J., Wai-Hung Ho, D., Wong, C. M., Zhang, H., Oi-Lin Ng, I., and Chak-Lui Wong, C. (2019), 'Hypoxia regulates the mitochondrial activity of hepatocellular carcinoma cells through HIF/HEY1/PINK1 pathway', *Cell Death Dis,* 10 (12), 934.

Kuo, L. J. and Yang, L. X. (2008), 'Gamma-H2AX - a novel biomarker for DNA double-strand breaks', *In Vivo,* 22 (3), 305-9.

Kurian, A. W. (2010), 'BRCA1 and BRCA2 mutations across race and ethnicity: distribution and clinical implications', *Curr Opin Obstet Gynecol,* 22 (1), 72-8.

Kuwahara, K. (2023), 'DNA Damage, DNA Repair, and Cancer: Second Edition', *Int J Mol Sci,* 24 (23).

Kyzas, P. A., Cunha, I. W., and Ioannidis, J. P. (2005), 'Prognostic significance of vascular endothelial growth factor immunohistochemical expression in head and neck squamous cell carcinoma: a meta-analysis', *Clin Cancer Res,* 11 (4), 1434-40.

Laenkholm, A. V., Jensen, M. B., Eriksen, J. O., Rasmussen, B. B., Knoop, A. S., Buckingham, W., Ferree, S., Schaper, C., Nielsen, T. O., Haffner, T., Kibol, T., Moller Talman, M. L., Bak Jylling, A. M., Tabor, T. P., and Ejlertsen, B. (2018), 'PAM50 Risk of Recurrence Score Predicts 10-Year Distant Recurrence in a Comprehensive Danish Cohort of Postmenopausal Women Allocated to 5 Years of Endocrine Therapy for Hormone Receptor-Positive Early Breast Cancer', *J Clin Oncol,* 36 (8), 735-40.

Lalloo, F. and Evans, D. G. (2012a), 'Familial Breast Cancer', *Clinical Genetics,* 82 (2), 105-14.

--- (2012b), 'Familial breast cancer', *Clin Genet,* 82 (2), 105-14.

Landry, W. D. and Cotter, T. G. (2014), 'ROS signalling, NADPH oxidases and cancer', *Biochem Soc Trans,* 42 (4), 934-8.

Lappin, K. M., Barros, E. M., Jhujh, S. S., Irwin, G. W., McMillan, H., Liberante, F. G., Latimer, C., La Bonte, M. J., Mills, K. I., Harkin, D. P., Stewart, G. S., and Savage, K. I. (2022), 'Cancer-Associated SF3B1 Mutations Confer a BRCA-Like Cellular Phenotype and Synthetic Lethality to PARP Inhibitors', *Cancer Res,* 82 (5), 819-30.

Law, A. Y. and Wong, C. K. (2010), 'Stanniocalcin-2 is a HIF-1 target gene that promotes cell proliferation in hypoxia', *Exp Cell Res,* 316 (3), 466-76.

Lawrenson, I. D., Wimmer-Kleikamp, S. H., Lock, P., Schoenwaelder, S. M., Down, M., Boyd, A. W., Alewood, P. F., and Lackmann, M. (2002), 'Ephrin-A5 induces rounding, blebbing and de-adhesion of EphA3-expressing 293T and melanoma cells by CrkII and Rho-mediated signalling', *J Cell Sci,* 115 (Pt 5), 1059-72.

Le, B. V., Podszywalow-Bartnicka, P., Maifrede, S., Sullivan-Reed, K., Nieborowska-Skorska, M., Golovine, K., Yao, J. C., Nejati, R., Cai, K. Q., Caruso, L. B., Swatler, J., Dabrowski, M., Lian, Z., Valent, P., Paietta, E. M., Levine, R. L., Fernandez, H. F., Tallman, M. S., Litzow, M. R.,

Huang, J., Challen, G. A., Link, D., Tempera, I., Wasik, M. A., Piwocka, K., and Skorski, T. (2020), 'TGFbetaR-SMAD3 Signaling Induces Resistance to PARP Inhibitors in the Bone Marrow Microenvironment', *Cell Rep,* 33 (1), 108221.

Le, Q. T. and Courter, D. (2008), 'Clinical biomarkers for hypoxia targeting', *Cancer Metastasis Rev,* 27 (3), 351-62.

Lee, F. S. (2019), 'At the crossroads of oxygen and iron sensing: hepcidin control of HIF-2alpha', *J Clin Invest,* 129 (1), 72-74.

Lee, J. H. and Paull, T. T. (2004), 'Direct activation of the ATM protein kinase by the Mre11/Rad50/Nbs1 complex', *Science,* 304 (5667), 93-6.

--- (2005), 'ATM activation by DNA double-strand breaks through the Mre11-Rad50-Nbs1 complex', *Science,* 308 (5721), 551-4.

Lee, T. W., Wong, W. W., Dickson, B. D., Lipert, B., Cheng, G. J., Hunter, F. W., Hay, M. P., and Wilson, W. R. (2019), 'Radiosensitization of head and neck squamous cell carcinoma lines by DNA-PK inhibitors is more effective than PARP-1 inhibition and is enhanced by SLFN11 and hypoxia', *Int J Radiat Biol,* 95 (12), 1597-612.

Lei, G., Mao, C., Yan, Y., Zhuang, L., and Gan, B. (2021), 'Ferroptosis, radiotherapy, and combination therapeutic strategies', *Protein Cell,* 12 (11), 836-57.

Leszczynska, K. B., Gottgens, E. L., Biasoli, D., Olcina, M. M., Ient, J., Anbalagan, S., Bernhardt, S., Giaccia, A. J., and Hammond, E. M. (2016), 'Mechanisms and consequences of ATMIN repression in hypoxic conditions: roles for p53 and HIF-1', *Sci Rep,* 6, 21698.

Levitz, S. M. and Diamond, R. D. (1985), 'A rapid colorimetric assay of fungal viability with the tetrazolium salt MTT', *J Infect Dis,* 152 (5), 938-45.

Li, H., Liu, Z. Y., Wu, N., Chen, Y. C., Cheng, Q., and Wang, J. (2020a), 'PARP inhibitor resistance: the underlying mechanisms and clinical implications', *Mol Cancer,* 19 (1), 107.

Li, J., Cao, F., Yin, H. L., Huang, Z. J., Lin, Z. T., Mao, N., Sun, B., and Wang, G. (2020b), 'Ferroptosis: past, present and future', *Cell Death Dis,* 11 (2), 88.

Li, S., Tabar, S. S., Malec, V., Eul, B. G., Klepetko, W., Weissmann, N., Grimminger, F., Seeger, W., Rose, F., and Hanze, J. (2008), 'NOX4 regulates ROS levels under normoxic and hypoxic conditions, triggers proliferation, and inhibits apoptosis in pulmonary artery adventitial fibroblasts', *Antioxid Redox Signal,* 10 (10), 1687-98.

Li, Y. R. and Barry, P. N. (2022), 'Pre-operative partial breast irradiation: revolutionizing radiation treatment for women with early stage breast cancer', *Ann Breast Surg,* 6.

Li, Z., You, Q., and Zhang, X. (2019), 'Small-Molecule Modulators of the Hypoxia-Inducible Factor Pathway: Development and Therapeutic Applications', *J Med Chem,* 62 (12), 5725-49.

Liao, C., Liu, X., Zhang, C., and Zhang, Q. (2023), 'Tumor hypoxia: From basic knowledge to therapeutic implications', *Semin Cancer Biol,* 88, 172-86.

Lieber, M. R. (2008), 'The mechanism of human nonhomologous DNA end joining', *J Biol Chem,* 283 (1), 1-5.

Liou, Geou-Yarh and Storz, Peter (2010), 'Reactive oxygen species in cancer', *Free Radical Research,* 44 (5), 479-96.

Lioumi, Maria and Newell, David (2014), 'CR-UK biomarker roadmaps', *Clinical Cancer Research,* 16 (19_Supplement), B33-B33.

Liu, C., Vyas, A., Kassab, M. A., Singh, A. K., and Yu, X. (2017), 'The role of poly ADP-ribosylation in the first wave of DNA damage response', *Nucleic Acids Res,* 45 (14), 8129-41.

Liu, D. and Xu, Y. (2011), 'p53, oxidative stress, and aging', *Antioxid Redox Signal,* 15 (6), 1669-78.

Liu, H., Wang, Q., Liu, D., Li, Z., Fu, Y., Tse, G., Li, G., Liu, T., and Xu, G. (2022a), 'Manganese Superoxide Dismutase as a Novel Oxidative Stress Biomarker for Predicting Paroxysmal Atrial Fibrillation', *J Clin Med,* 11 (17).

Liu, J., Chen, T., Yang, M., Zhong, Z., Ni, S., Yang, S., Shao, F., Cai, L., Bai, J., and Yu, H. (2021), 'Development of an Oxidative Phosphorylation-Related and Immune Microenvironment Prognostic Signature in Uterine Corpus Endometrial Carcinoma', *Front Cell Dev Biol,* 9, 753004.

Liu, Q., Guntuku, S., Cui, X. S., Matsuoka, S., Cortez, D., Tamai, K., Luo, G., Carattini-Rivera, S., DeMayo, F., Bradley, A., Donehower, L. A., and Elledge, S. J. (2000), 'Chk1 is an essential kinase that is regulated by Atr and required for the G(2)/M DNA damage checkpoint', *Genes Dev,* 14 (12), 1448-59.

Liu, X., Ge, Z., Yang, F., Contreras, A., Lee, S., White, J. B., Lu, Y., Labrie, M., Arun, B. K., Moulder, S. L., Mills, G. B., Piwnica-Worms, H., Litton, J. K., and Chang, J. T. (2022b), 'Identification of biomarkers of response to preoperative talazoparib monotherapy in treatment naive gBRCA+ breast cancers', *NPJ Breast Cancer,* 8 (1), 64.

Liu, Y., Bernauer, A. M., Yingling, C. M., and Belinsky, S. A. (2012), 'HIF1alpha regulated expression of XPA contributes to cisplatin resistance in lung cancer', *Carcinogenesis,* 33 (6), 1187-92.

Liu, Y., Mao, J., Xiang, L., Zhang, X., and Qu, Z. (2024), 'Clinical characteristics and genetic analysis of a case of a patient with familial hereditary breast cancer: a case report', *J Med Case Rep,* 18 (1), 368.

Lloyd, Rebecca L., Wijnhoven, Paul W. G., Ramos-Montoya, Antonio, Wilson, Zena, Illuzzi, Giuditta, Falenta, Katarzyna, Jones, Gemma N., James, Neil, Chabbert, Christophe D., Stott, Jonathan, Dean, Emma, Lau, Alan, and Young, Lucy A. (2020), 'Combined PARP and ATR inhibition potentiates genome instability and cell death in ATM-deficient cancer cells', *Oncogene,* 39 (25), 4869-83.

Loboda, A., Jozkowicz, A., and Dulak, J. (2010), 'HIF-1 and HIF-2 transcription factors--similar but not identical', *Mol Cells,* 29 (5), 435-42.

Lodder-Gadaczek, J., Becker, I., Gieselmann, V., Wang-Eckhardt, L., and Eckhardt, M. (2011), 'N-acetylaspartylglutamate synthetase II synthesizes N-acetylaspartylglutamylglutamate', *J Biol Chem,* 286 (19), 16693-706.

Long, P. M., Moffett, J. R., Namboodiri, A. M. A., Viapiano, M. S., Lawler, S. E., and Jaworski, D. M. (2013), 'N-acetylaspartate (NAA) and N-acetylaspartylglutamate (NAAG) promote growth and inhibit differentiation of glioma stem-like cells', *J Biol Chem,* 288 (36), 26188-200.

Loor, G., Kondapalli, J., Schriewer, J. M., Chandel, N. S., Vanden Hoek, T. L., and Schumacker, P. T. (2010), 'Menadione triggers cell death through ROS-dependent mechanisms involving PARP activation without requiring apoptosis', *Free Radic Biol Med,* 49 (12), 1925-36.

Lord, C. J. and Ashworth, A. (2017), 'PARP inhibitors: Synthetic lethality in the clinic', *Science,* 355 (6330), 1152-58.

Lord, Christopher J. and Ashworth, Alan (2012), 'The DNA damage response and cancer therapy', *Nature,* 481 (7381), 287-94.

Lu, B., Chen, X. B., Ying, M. D., He, Q. J., Cao, J., and Yang, B. (2017), 'The Role of Ferroptosis in Cancer Development and Treatment Response', *Front Pharmacol,* 8, 992.

Lu, H., Samanta, D., Xiang, L., Zhang, H., Hu, H., Chen, I., Bullen, J. W., and Semenza, G. L. (2015), 'Chemotherapy triggers HIF-1-dependent glutathione synthesis and copper chelation that induces the breast cancer stem cell phenotype', *Proc Natl Acad Sci U S A,* 112 (33), E4600-9.

Lu, Q., Long, Y., Gai, Y., Liu, Q., Jiang, D., and Lan, X. (2023), '[(177)Lu]Lu-PSMA-617 theranostic probe for hepatocellular carcinoma imaging and therapy', *Eur J Nucl Med Mol Imaging,* 50 (8), 2342-52.

Lu, Y., Chu, A., Turker, M. S., and Glazer, P. M. (2011), 'Hypoxia-induced epigenetic regulation and silencing of the BRCA1 promoter', *Mol Cell Biol,* 31 (16), 3339-50.

Ma, T. S., Worth, K. R., Maher, C., Ng, N., Beghe, C., Gromak, N., Rose, A. M., and Hammond, E. M. (2023), 'Hypoxia-induced transcriptional stress is mediated by ROS-induced R-loops', *Nucleic Acids Res,* 51 (21), 11584-99.

Madan, E., Gogna, R., and Pati, U. (2012), 'p53 Ser15 phosphorylation disrupts the p53-RPA70 complex and induces RPA70-mediated DNA repair in hypoxia', *Biochem J,* 443 (3), 811-20.

Mah, L. J., El-Osta, A., and Karagiannis, T. C. (2010), 'gammaH2AX: a sensitive molecular marker of DNA damage and repair', *Leukemia,* 24 (4), 679-86.

Mahameed, M., Wilhelm, T., Darawshi, O., Obiedat, A., Tommy, W. S., Chintha, C., Schubert, T., Samali, A., Chevet, E., Eriksson, L. A., Huber, M., and Tirosh, B. (2019), 'The unfolded protein response modulators GSK2606414 and KIRA6 are potent KIT inhibitors', *Cell Death Dis,* 10 (4), 300.

Mahdavi, M., Nassiri, M., Kooshyar, M. M., Vakili-Azghandi, M., Avan, A., Sandry, R., Pillai, S., Lam, A. K., and Gopalan, V. (2019), 'Hereditary breast cancer; Genetic penetrance and current status with BRCA', *J Cell Physiol,* 234 (5), 5741-50.

Makino, Y., Kanopka, A., Wilson, W. J., Tanaka, H., and Poellinger, L. (2002), 'Inhibitory PAS domain protein (IPAS) is a hypoxia-inducible splicing variant of the hypoxia-inducible factor-3alpha locus', *J Biol Chem,* 277 (36), 32405-8.

Malec, V., Gottschald, O. R., Li, S., Rose, F., Seeger, W., and Hanze, J. (2010), 'HIF-1 alpha signaling is augmented during intermittent hypoxia by induction of the Nrf2 pathway in NOX1-expressing adenocarcinoma A549 cells', *Free Radic Biol Med,* 48 (12), 1626-35.

Mandelkow, R., Gumbel, D., Ahrend, H., Kaul, A., Zimmermann, U., Burchardt, M., and Stope, M. B. (2017), 'Detection and Quantification of Nuclear Morphology Changes in Apoptotic Cells by Fluorescence Microscopy and Subsequent Analysis of Visualized Fluorescent Signals', *Anticancer Res,* 37 (5), 2239-44.

Mao, H., Lockyer, P., Townley-Tilson, W. H., Xie, L., and Pi, X. (2016), 'LRP1 Regulates Retinal Angiogenesis by Inhibiting PARP-1 Activity and Endothelial Cell Proliferation', *Arterioscler Thromb Vasc Biol,* 36 (2), 350-60.

Marcus, J. M., Hossain, M. I., Gagne, J. P., Poirier, G. G., McMahon, L. L., Cowell, R. M., and Andrabi, S. A. (2021), 'PARP-1 activation leads to cytosolic accumulation of TDP-43 in neurons', *Neurochem Int,* 148, 105077.

Maremonti, Erica, Brede, Dag Anders, Olsen, Ann-Karin, Eide, Dag M., and Berg, Einar S. (2020), 'Ionizing radiation, genotoxic stress, and mitochondrial DNA copy-number variation in Caenorhabditis elegans: droplet digital PCR analysis', *Mutation Research/Genetic Toxicology and Environmental Mutagenesis,* 858-860, 503277.

Marshall, C., Mamary, A. J., Verhoeven, A. J., and Marshall, B. E. (1996), 'Pulmonary artery NADPH-oxidase is activated in hypoxic pulmonary vasoconstriction', *Am J Respir Cell Mol Biol,* 15 (5), 633-44.

Marti, J. M., Garcia-Diaz, A., Delgado-Bellido, D., O'Valle, F., Gonzalez-Flores, A., Carlevaris, O., Rodriguez-Vargas, J. M., Ame, J. C., Dantzer, F., King, G. L., Dziedzic, K., Berra, E., de Alava, E., Amaral, A. T., Hammond, E. M., and Oliver, F. J. (2021), 'Selective modulation by PARP-1 of HIF-1alpha-recruitment to chromatin during hypoxia is required for tumor adaptation to hypoxic conditions', *Redox Biol,* 41, 101885.

Martin-Puig, S., Tello, D., and Aragones, J. (2015), 'Novel perspectives on the PHD-HIF oxygen sensing pathway in cardioprotection mediated by IPC and RIPC', *Front Physiol,* 6, 137.

Martinez-Zamudio, R. and Ha, H. C. (2012), 'Histone ADP-ribosylation facilitates gene transcription by directly remodeling nucleosomes', *Mol Cell Biol,* 32 (13), 2490-502.

Masgras, I., Carrera, S., de Verdier, P. J., Brennan, P., Majid, A., Makhtar, W., Tulchinsky, E., Jones, G. D. D., Roninson, I. B., and Macip, S. (2012), 'Reactive oxygen species and mitochondrial sensitivity to oxidative stress determine induction of cancer cell death by p21', *J Biol Chem,* 287 (13), 9845-54.

Mateos-Gomez, P. A., Kent, T., Deng, S. K., McDevitt, S., Kashkina, E., Hoang, T. M., Pomerantz, R. T., and Sfeir, A. (2017), 'The helicase domain of Poltheta counteracts RPA to promote alt-NHEJ', *Nat Struct Mol Biol,* 24 (12), 1116-23.

Mathieu, J., Zhang, Z., Zhou, W., Wang, A. J., Heddleston, J. M., Pinna, C. M., Hubaud, A., Stadler, B., Choi, M., Bar, M., Tewari, M., Liu, A., Vessella, R., Rostomily, R., Born, D., Horwitz, M.,

Ware, C., Blau, C. A., Cleary, M. A., Rich, J. N., and Ruohola-Baker, H. (2011), 'HIF induces human embryonic stem cell markers in cancer cells', *Cancer Res,* 71 (13), 4640-52.

Matsuoka, S., Rotman, G., Ogawa, A., Shiloh, Y., Tamai, K., and Elledge, S. J. (2000), 'Ataxia telangiectasia-mutated phosphorylates Chk2 in vivo and in vitro', *Proc Natl Acad Sci U S A,* 97 (19), 10389-94.

Matsuoka, S., Ballif, B. A., Smogorzewska, A., McDonald, E. R., 3rd, Hurov, K. E., Luo, J., Bakalarski, C. E., Zhao, Z., Solimini, N., Lerenthal, Y., Shiloh, Y., Gygi, S. P., and Elledge, S. J. (2007), 'ATM and ATR substrate analysis reveals extensive protein networks responsive to DNA damage', *Science,* 316 (5828), 1160-6.

Matta, S. K., Patten, K., Wang, Q., Kim, B. H., MacMicking, J. D., and Sibley, L. D. (2018), 'NADPH Oxidase and Guanylate Binding Protein 5 Restrict Survival of Avirulent Type III Strains of Toxoplasma gondii in Naive Macrophages', *mBio,* 9 (4).

Maxwell, P. H., Wiesener, M. S., Chang, G. W., Clifford, S. C., Vaux, E. C., Cockman, M. E., Wykoff, C. C., Pugh, C. W., Maher, E. R., and Ratcliffe, P. J. (1999), 'The tumour suppressor protein VHL targets hypoxia-inducible factors for oxygen-dependent proteolysis', *Nature,* 399 (6733), 271-5.

McAleese, C. E., Choudhury, C., Butcher, N. J., and Minchin, R. F. (2021), 'Hypoxia-mediated drug resistance in breast cancers', *Cancer Lett,* 502, 189-99.

McCabe, N., Turner, N. C., Lord, C. J., Kluzek, K., Bialkowska, A., Swift, S., Giavara, S., O'Connor, M. J., Tutt, A. N., Zdzienicka, M. Z., Smith, G. C., and Ashworth, A. (2006), 'Deficiency in the repair of DNA damage by homologous recombination and sensitivity to poly(ADP-ribose) polymerase inhibition', *Cancer Res,* 66 (16), 8109-15.

McKeown, S. R. (2014), 'Defining normoxia, physoxia and hypoxia in tumours-implications for treatment response', *Br J Radiol,* 87 (1035), 20130676.

McKinnell RG, Parchment RE, Perantoni AO, Pierce GB. (1998), *The biological basis of cancer* (New York:: Cambridge University Press).

McLaggan, D., Rufino, H., Jaspars, M., and Booth, I. R. (2000), 'Glutathione-dependent conversion of N-ethylmaleimide to the maleamic acid by Escherichia coli: an intracellular detoxification process', *Appl Environ Microbiol,* 66 (4), 1393-9.

Meena, J. K., Wang, J. H., Neill, N. J., Keough, D., Putluri, N., Katsonis, P., Koire, A. M., Lee, H., Bowling, E. A., Tyagi, S., Orellana, M., Dominguez-Vidana, R., Li, H., Eagle, K., Danan, C., Chung, H. C., Yang, A. D., Wu, W., Kurley, S. J., Ho, B. M., Zoeller, J. R., Olson, C. M., Meerbrey, K. L., Lichtarge, O., Sreekumar, A., Dacso, C. C., Guddat, L. W., Rejman, D., Hockova, D., Janeba, Z., Simon, L. M., Lin, C. Y., Pillon, M. C., and Westbrook, T. F. (2024), 'MYC Induces Oncogenic Stress through RNA Decay and Ribonucleotide Catabolism in Breast Cancer', *Cancer Discov,* 14 (9), 1699-716.

Mehibel, M., Xu, Y., Li, C. G., Moon, E. J., Thakkar, K. N., Diep, A. N., Kim, R. K., Bloomstein, J. D., Xiao, Y., Bacal, J., Saldivar, J. C., Le, Q. T., Cimprich, K. A., Rankin, E. B., and Giaccia, A. J. (2021), 'Eliminating hypoxic tumor cells improves response to PARP inhibitors in homologous recombination-deficient cancer models', *J Clin Invest,* 131 (11).

Melese, T. and Xue, Z. (1995), 'The nucleolus: an organelle formed by the act of building a ribosome', *Curr Opin Cell Biol,* 7 (3), 319-24.

Mesters, J. R., Barinka, C., Li, W., Tsukamoto, T., Majer, P., Slusher, B. S., Konvalinka, J., and Hilgenfeld, R. (2006), 'Structure of glutamate carboxypeptidase II, a drug target in neuronal damage and prostate cancer', *EMBO J,* 25 (6), 1375-84.

Metsalu, T. and Vilo, J. (2015), 'ClustVis: a web tool for visualizing clustering of multivariate data using Principal Component Analysis and heatmap', *Nucleic Acids Res,* 43 (W1), W566-70.

Mhawech-Fauceglia, P., Zhang, S., Terracciano, L., Sauter, G., Chadhuri, A., Herrmann, F. R., and Penetrante, R. (2007), 'Prostate-specific membrane antigen (PSMA) protein expression in normal and neoplastic tissues and its sensitivity and specificity in prostate adenocarcinoma: an immunohistochemical study using mutiple tumour tissue microarray technique', *Histopathology,* 50 (4), 472-83.

Michailidou, K. andLindstrom, S. andDennis, J. andBeesley, J. andHui, S. andKar, S. andLemacon, A. andSoucy, P. andGlubb, D. andRostamianfar, A. andBolla, M. K. andWang, Q. andTyrer, J. andDicks, E. andLee, A. andWang, Z. andAllen, J. andKeeman, R. andEilber, U. andFrench, J. D. andQing Chen, X. andFachal, L. andMcCue, K. andMcCart Reed, A. E. andGhoussaini, M. andCarroll, J. S. andJiang, X. andFinucane, H. andAdams, M. andAdank, M. A. andAhsan, H. andAittomaki, K. andAnton-Culver, H. andAntonenkova, N. N. andArndt, V. andAronson, K. J. andArun, B. andAuer, P. L. andBacot, F. andBarrdahl, M. andBaynes, C. andBeckmann, M. W. andBehrens, S. andBenitez, J. andBermisheva, M. andBernstein, L. andBlomqvist, C. andBogdanova, N. V. andBojesen, S. E. andBonanni, B. andBorresen-Dale, A. L. andBrand, J. S. andBrauch, H. andBrennan, P. andBrenner, H. andBrinton, L. andBroberg, P. andBrock, I. W. andBroeks, A. andBrooks-Wilson, A. andBrucker, S. Y. andBruning, T. andBurwinkel, B. andButterbach, K. andCai, Q. andCai, H. andCaldes, T. andCanzian, F. andCarracedo, A. andCarter, B. D. andCastelao, J. E. andChan, T. L. andDavid Cheng, T. Y. andSeng Chia, K. andChoi, J. Y. andChristiansen, H. andClarke, C. L. andCollaborators, Nbcs andCollee, M. andConroy, D. M. andCordina-Duverger, E. andCornelissen, S. andCox, D. G. andCox, A. andCross, S. S. andCunningham, J. M. andCzene, K. andDaly, M. B. andDevilee, P. andDoheny, K. F. andDork, T. andDos-Santos-Silva, I. andDumont, M. andDurcan, L. andDwek, M. andEccles, D. M. andEkici, A. B. andEliassen, A. H. andEllberg, C. andElvira, M. andEngel, C. andEriksson, M. andFasching, P. A. andFigueroa, J. andFlesch-Janys, D. andFletcher, O. andFlyger, H. andFritschi, L. andGaborieau, V. andGabrielson, M. andGago-Dominguez, M. andGao, Y. T. andGapstur, S. M. andGarcia-Saenz, J. A. andGaudet, M. M. andGeorgoulias, V. andGiles, G. G. andGlendon, G. andGoldberg, M. S. andGoldgar, D. E. andGonzalez-Neira, A. andGrenaker Alnaes, G. I. andGrip, M. andGronwald, J. andGrundy, A. andGuenel, P. andHaeberle, L. andHahnen, E. andHaiman, C. A. andHakansson, N. andHamann, U. andHamel, N. andHankinson, S. andHarrington, P.

andHart, S. N. andHartikainen, J. M. andHartman, M. andHein, A. andHeyworth, J. andHicks, B. andHillemanns, P. andHo, D. N. andHollestelle, A. andHooning, M. J. andHoover, R. N. andHopper, J. L. andHou, M. F. andHsiung, C. N. andHuang, G. andHumphreys, K. andIshiguro, J. andIto, H. andIwasaki, M. andIwata, H. andJakubowska, A. andJanni, W. andJohn, E. M. andJohnson, N. andJones, K. andJones, M. andJukkola-Vuorinen, A. andKaaks, R. andKabisch, M. andKaczmarek, K. andKang, D. andKasuga, Y. andKerin, M. J. andKhan, S. andKhusnutdinova, E. andKiiski, J. I. andKim, S. W. andKnight, J. A. andKosma, V. M. andKristensen, V. N. andKruger, U. andKwong, A. andLambrechts, D. andLe Marchand, L. andLee, E. andLee, M. H. andLee, J. W. andNeng Lee, C. andLejbkowicz, F. andLi, J. andLilyquist, J. andLindblom, A. andLissowska, J. andLo, W. Y. andLoibl, S. andLong, J. andLophatananon, A. andLubinski, J. andLuccarini, C. andLux, M. P. andMa, E. S. K. andMacInnis, R. J. andMaishman, T. andMakalic, E. andMalone, K. E. andKostovska, I. M. andMannermaa, A. andManoukian, S. andManson, J. E. andMargolin, S. andMariapun, S. andMartinez, M. E. andMatsuo, K. andMavroudis, D. andMcKay, J. andMcLean, C. andMeijers-Heijboer, H. andMeindl, A. andMenendez, P. andMenon, U. andMeyer, J. andMiao, H. andMiller, N. andTaib, N. A. M. andMuir, K. andMulligan, A. M. andMulot, C. andNeuhausen, S. L. andNevanlinna, H. andNeven, P. andNielsen, S. F. andNoh, D. Y. andNordestgaard, B. G. andNorman, A. andOlopade, O. I. andOlson, J. E. andOlsson, H. andOlswold, C. andOrr, N. andPankratz, V. S. andPark, S. K. andPark-Simon, T. W. andLloyd, R. andPerez, J. I. A. andPeterlongo, P. andPeto, J. andPhillips, K. A. andPinchev, M. andPlaseska-Karanfilska, D. andPrentice, R. andPresneau, N. andProkofyeva, D. andPugh, E. andPylkas, K. andRack, B. andRadice, P. andRahman, N. andRennert, G. andRennert, H. S. andRhenius, V. andRomero, A. andRomm, J. andRuddy, K. J. andRudiger, T. andRudolph, A. andRuebner, M. andRutgers, E. J. T. andSaloustros, E. andSandler, D. P. andSangrajrang, S. andSawyer, E. J. andSchmidt, D. F. andSchmutzler, R. K. andSchneeweiss, A. andSchoemaker, M. J.

andSchumacher, F. andSchurmann, P. andScott, R. J. andScott, C. andSeal, S. andSeynaeve, C. andShah, M. andSharma, P. andShen, C. Y. andSheng, G. andSherman, M. E. andShrubsole, M. J. andShu, X. O. andSmeets, A. andSohn, C. andSouthey, M. C. andSpinelli, J. J. andStegmaier, C. andStewart-Brown, S. andStone, J. andStram, D. O. andSurowy, H. andSwerdlow, A. andTamimi, R. andTaylor, J. A. andTengstrom, M. andTeo, S. H. andBeth Terry, M. andTessier, D. C. andThanasitthichai, S. andThone, K. andTollenaar, Raem andTomlinson, I. andTong, L. andTorres, D. andTruong, T. andTseng, C. C. andTsugane, S. andUlmer, H. U. andUrsin, G. andUntch, M. andVachon, C. andvan Asperen, C. J. andVan Den Berg, D. andvan den Ouweland, A. M. W. andvan der Kolk, L. andvan der Luijt, R. B. andVincent, D. andVollenweider, J. andWaisfisz, Q. andWang-Gohrke, S. andWeinberg, C. R. andWendt, C. andWhittemore, A. S. andWildiers, H. andWillett, W. andWinqvist, R. andWolk, A. andWu, A. H. andXia, L. andYamaji, T. andYang, X. R. andHar Yip, C. andYoo, K. Y. andYu, J. C. andZheng, W. andZheng, Y. andZhu, B. andZiogas, A. andZiv, E. andInvestigators, Abctb andConFab, Aocs Investigators andLakhani, S. R. andAntoniou, A. C. andDroit, A. andAndrulis, I. L. andAmos, C. I. andCouch, F. J. andPharoah, P. D. P. andChang-Claude, J. andHall, P. andHunter, D. J. andMilne, R. L. andGarcia-Closas, M. andSchmidt, M. K. andChanock, S. J. andDunning, A. M. andEdwards, S. L. andBader, G. D. andChenevix-Trench, G. andSimard, J. andKraft, P. and Easton, D. F. (2017), 'Association analysis identifies 65 new breast cancer risk loci', *Nature,* 551 (7678), 92-94.

Michiels, C., Tellier, C., and Feron, O. (2016), 'Cycling hypoxia: A key feature of the tumor microenvironment', *Biochim Biophys Acta,* 1866 (1), 76-86.

Mihaylova, V. T., Bindra, R. S., Yuan, J., Campisi, D., Narayanan, L., Jensen, R., Giordano, F., Johnson, R. S., Rockwell, S., and Glazer, P. M. (2003), 'Decreased expression of the DNA mismatch repair gene Mlh1 under hypoxic stress in mammalian cells', *Mol Cell Biol,* 23 (9), 3265-73.

Min, A., Im, S. A., Yoon, Y. K., Song, S. H., Nam, H. J., Hur, H. S., Kim, H. P., Lee, K. H., Han, S. W., Oh, D. Y., Kim, T. Y., O'Connor, M. J., Kim, W. H., and Bang, Y. J. (2013), 'RAD51C-deficient cancer cells are highly sensitive to the PARP inhibitor olaparib', *Mol Cancer Ther,* 12 (6), 865-77.

Minchom, A., Aversa, C., and Lopez, J. (2018), 'Dancing with the DNA damage response: next-generation anti-cancer therapeutic strategies', *Ther Adv Med Oncol,* 10, 1758835918786658.

Minello, A. and Carreira, A. (2024), 'BRCA1/2 Haploinsufficiency: Exploring the Impact of Losing one Allele', *J Mol Biol,* 436 (1), 168277.

Mirza-Aghazadeh-Attari, Mohammad, Darband, Saber Ghazizadeh, Kaviani, Mojtaba, Mihanfar, Ainaz, Aghazadeh Attari, Javad, Yousefi, Bahman, and Majidinia, Maryam (2018), 'DNA damage response and repair in colorectal cancer: Defects, regulation and therapeutic implications', *DNA Repair,* 69, 34-52.

Moller, M. N., Orrico, F., Villar, S. F., Lopez, A. C., Silva, N., Donze, M., Thomson, L., and Denicola, A. (2023), 'Oxidants and Antioxidants in the Redox Biochemistry of Human Red Blood Cells', *ACS Omega,* 8 (1), 147-68.

Montero, A. and Ciervide, R. (2022), 'Preoperative Radio(Chemo)Therapy in Breast Cancer: Time to Switch the Perspective?', *Curr Oncol,* 29 (12), 9767-87.

Morales-Gonzalez, A., Bautista, M., Madrigal-Santillan, E., Posadas-Mondragon, A., Anguiano-Robledo, L., Madrigal-Bujaidar, E., Alvarez-Gonzalez, I., Fregoso-Aguilar, T., Gayosso-Islas, E., Sanchez-Moreno, C., and Morales-Gonzalez, J. A. (2017), 'Nrf2 modulates cell proliferation and antioxidants defenses during liver regeneration induced by partial hepatectomy', *Int J Clin Exp Pathol,* 10 (7), 7801-11.

Morotti, M., Bridges, E., Valli, A., Choudhry, H., Sheldon, H., Wigfield, S., Gray, N., Zois, C. E., Grimm, F., Jones, D., Teoh, E. J., Cheng, W. C., Lord, S., Anastasiou, D., Haider, S., McIntyre, A., Goberdhan, D. C. I., Buffa, F., and Harris, A. L. (2019), 'Hypoxia-induced

switch in SNAT2/SLC38A2 regulation generates endocrine resistance in breast cancer', *Proc Natl Acad Sci U S A,* 116 (25), 12452-61.

Mucino-Hernandez, G., Acevo-Rodriguez, P. S., Cabrera-Benitez, S., Guerrero, A. O., Merchant-Larios, H., and Castro-Obregon, S. (2023), 'Nucleophagy contributes to genome stability through degradation of type II topoisomerases A and B and nucleolar components', *J Cell Sci,* 136 (1).

Muoio, D., Laspata, N., Dannenberg, R. L., Curry, C., Darkoa-Larbi, S., Hedglin, M., Uttam, S., and Fouquerel, E. (2024), 'PARP2 promotes Break Induced Replication-mediated telomere fragility in response to replication stress', *Nat Commun,* 15 (1), 2857.

Muvaffak, A. and Coleman, K. G. (2024), 'PARP inhibitor synthetic lethality in ATM biallelic mutant cancer cell lines is associated with BRCA1/2 and RAD51 downregulation', *Front Oncol,* 14, 1380633.

Nagy, J. A. and Dvorak, H. F. (2012), 'Heterogeneity of the tumor vasculature: the need for new tumor blood vessel type-specific targets', *Clin Exp Metastasis,* 29 (7), 657-62.

Nagy, J. A., Chang, S. H., Shih, S. C., Dvorak, A. M., and Dvorak, H. F. (2010), 'Heterogeneity of the tumor vasculature', *Semin Thromb Hemost,* 36 (3), 321-31.

Nakamura, H., Sekine, H., Kato, H., Masai, H., Gradin, K., and Poellinger, L. (2022), 'Hypoxia-inducible factor-1alpha and poly [ADP ribose] polymerase 1 cooperatively regulate Notch3 expression under hypoxia via a noncanonical mechanism', *J Biol Chem,* 298 (7), 102137.

Nakamura, H., Tanimoto, K., Hiyama, K., Yunokawa, M., Kawamoto, T., Kato, Y., Yoshiga, K., Poellinger, L., Hiyama, E., and Nishiyama, M. (2008), 'Human mismatch repair gene, MLH1, is transcriptionally repressed by the hypoxia-inducible transcription factors, DEC1 and DEC2', *Oncogene,* 27 (30), 4200-9.

Nakamura, S., Kojima, Y., and Takeuchi, S. (2025), 'Causative Genes of Homologous Recombination Deficiency (HRD)-Related Breast Cancer and Specific Strategies at Present', *Curr Oncol,* 32 (2).

Nakayama, K. and Kataoka, N. (2019), 'Regulation of Gene Expression under Hypoxic Conditions', *Int J Mol Sci,* 20 (13).

Nasioudis, D., George, E. M., Xu, H., Kim, H., and Simpkins, F. (2023), 'Combination DNA Damage Response (DDR) Inhibitors to Overcome Drug Resistance in Ovarian Cancer', *Cancer Treat Res,* 186, 189-206.

Negrini, S., Gorgoulis, V. G., and Halazonetis, T. D. (2010), 'Genomic instability--an evolving hallmark of cancer', *Nat Rev Mol Cell Biol,* 11 (3), 220-8.

Nesic, K., Kondrashova, O., Hurley, R. M., McGehee, C. D., Vandenberg, C. J., Ho, G. Y., Lieschke, E., Dall, G., Bound, N., Shield-Artin, K., Radke, M., Musafer, A., Chai, Z. Q., Ghamsari, M. R. E., Harrell, M. I., Kee, D., Olesen, I., McNally, O., Traficante, N., Australian Ovarian Cancer, Study, DeFazio, A., Bowtell, D. D. L., Swisher, E. M., Weroha, S. J., Nones, K., Waddell, N., Kaufmann, S. H., Dobrovic, A., Wakefield, M. J., and Scott, C. L. (2021), 'Acquired RAD51C Promoter Methylation Loss Causes PARP Inhibitor Resistance in High-Grade Serous Ovarian Carcinoma', *Cancer Res,* 81 (18), 4709-22.

Nguyen, T., Kirsch, B. J., Asaka, R., Nabi, K., Quinones, A., Tan, J., Antonio, M. J., Camelo, F., Li, T., Nguyen, S., Hoang, G., Nguyen, K., Udupa, S., Sazeides, C., Shen, Y. A., Elgogary, A., Reyes, J., Zhao, L., Kleensang, A., Chaichana, K. L., Hartung, T., Betenbaugh, M. J., Marie, S. K., Jung, J. G., Wang, T. L., Gabrielson, E., and Le, A. (2019), 'Uncovering the Role of N-Acetyl-Aspartyl-Glutamate as a Glutamate Reservoir in Cancer', *Cell Rep,* 27 (2), 491-501 e6.

Nguyen, T. T., Wei, S., Nguyen, T. H., Jo, Y., Zhang, Y., Park, W., Gariani, K., Oh, C. M., Kim, H. H., Ha, K. T., Park, K. S., Park, R., Lee, I. K., Shong, M., Houtkooper, R. H., and Ryu, D. (2023),

'Mitochondria-associated programmed cell death as a therapeutic target for age-related disease', *Exp Mol Med,* 55 (8), 1595-619.

Nicum, S., McGregor, N., Austin, R., Collins, L., Dutton, S., McNeish, I., Glasspool, R., Hall, M., Roux, R., Michael, A., Clamp, A., Jayson, G., Kristeleit, R., Banerjee, S., and Mansouri, A. (2024), 'Results of a randomised Phase II trial of olaparib, chemotherapy or olaparib and cediranib in patients with platinum-resistant ovarian cancer', *Br J Cancer,* 130 (6), 941-50.

Nielsen, T. O., Parker, J. S., Leung, S., Voduc, D., Ebbert, M., Vickery, T., Davies, S. R., Snider, J., Stijleman, I. J., Reed, J., Cheang, M. C., Mardis, E. R., Perou, C. M., Bernard, P. S., and Ellis, M. J. (2010), 'A comparison of PAM50 intrinsic subtyping with immunohistochemistry and clinical prognostic factors in tamoxifen-treated estrogen receptor-positive breast cancer', *Clin Cancer Res,* 16 (21), 5222-32.

NIH, National Institutes of Health (2007) *Understanding cancer* [online text], <https://www.ncbi.nlm.nih.gov/books/NBK20362/>

Nir, D., Ribarski-Chorev, I., Shimoni, C., Strauss, C., Frank, J., and Schlesinger, S. (2022), 'Antioxidants Attenuate Heat Shock Induced Premature Senescence of Bovine Mesenchymal Stem Cells', *Int J Mol Sci,* 23 (10).

Nogueras Pérez, Raquel, Heredia-Nicolás, Noelia, de Lara-Peña, Laura, López de Andrés, Julia, Marchal, Juan Antonio, Jiménez, Gema, and Griñán-Lisón, Carmen (2023), 'Unraveling the Potential of miRNAs from CSCs as an Emerging Clinical Tool for Breast Cancer Diagnosis and Prognosis', *International Journal of Molecular Sciences,* 24 (21), 16010.

Noordermeer, S. M. and van Attikum, H. (2019), 'PARP Inhibitor Resistance: A Tug-of-War in BRCA-Mutated Cells', *Trends Cell Biol,* 29 (10), 820-34.

O'Connor, M. J. and Forment, J. V. (2023), 'Mechanisms of PARP Inhibitor Resistance', *Cancer Treat Res,* 186, 25-42.

Ochi, T., Blackford, A. N., Coates, J., Jhujh, S., Mehmood, S., Tamura, N., Travers, J., Wu, Q., Draviam, V. M., Robinson, C. V., Blundell, T. L., and Jackson, S. P. (2015), 'DNA repair.

PAXX, a paralog of XRCC4 and XLF, interacts with Ku to promote DNA double-strand break repair', *Science,* 347 (6218), 185-88.

Oh, C., Dong, Y., Harman, C., Mighty, H. E., Kopelman, J., and Thompson, L. P. (2008), 'Chronic hypoxia differentially increases glutathione content and gamma-glutamyl cysteine synthetase expression in fetal guinea pig organs', *Early Hum Dev,* 84 (2), 121-7.

Ohh, M., Taber, C. C., Ferens, F. G., and Tarade, D. (2022), 'Hypoxia-inducible factor underlies von Hippel-Lindau disease stigmata', *Elife,* 11.

Okamoto, Y., Iwasaki, W. M., Kugou, K., Takahashi, K. K., Oda, A., Sato, K., Kobayashi, W., Kawai, H., Sakasai, R., Takaori-Kondo, A., Yamamoto, T., Kanemaki, M. T., Taoka, M., Isobe, T., Kurumizaka, H., Innan, H., Ohta, K., Ishiai, M., and Takata, M. (2018), 'Replication stress induces accumulation of FANCD2 at central region of large fragile genes', *Nucleic Acids Res,* 46 (6), 2932-44.

Olcina, M., Lecane, P. S., and Hammond, E. M. (2010), 'Targeting hypoxic cells through the DNA damage response', *Clin Cancer Res,* 16 (23), 5624-9.

Olcina, M. M., Grand, R. J., and Hammond, E. M. (2014), 'ATM activation in hypoxia - causes and consequences', *Mol Cell Oncol,* 1 (1), e29903.

Olcina, M. M., Foskolou, I. P., Anbalagan, S., Senra, J. M., Pires, I. M., Jiang, Y., Ryan, A. J., and Hammond, E. M. (2013), 'Replication stress and chromatin context link ATM activation to a role in DNA replication', *Mol Cell,* 52 (5), 758-66.

Olcina, Monica M. and Hammond, Ester M. (2014), 'Hypoxia and the DNA Damage Response', in Giovanni Melillo (ed.), *Hypoxia and Cancer: Biological Implications and Therapeutic Opportunities* (New York, NY: Springer New York), 21-41.

Olivieri, M., Cho, T., Alvarez-Quilon, A., Li, K., Schellenberg, M. J., Zimmermann, M., Hustedt, N., Rossi, S. E., Adam, S., Melo, H., Heijink, A. M., Sastre-Moreno, G., Moatti, N., Szilard, R. K., McEwan, A., Ling, A. K., Serrano-Benitez, A., Ubhi, T., Feng, S., Pawling, J., Delgado-Sainz, I., Ferguson, M. W., Dennis, J. W., Brown, G. W., Cortes-Ledesma, F., Williams, R.

S., Martin, A., Xu, D., and Durocher, D. (2020), 'A Genetic Map of the Response to DNA Damage in Human Cells', *Cell,* 182 (2), 481-96 e21.

Omar, M., Harrell, J. C., Tamimi, R., Marchionni, L., Erdogan, C., Nakshatri, H., and Ince, T. A. (2024), 'A triple hormone receptor ER, AR, and VDR signature is a robust prognosis predictor in breast cancer', *Breast Cancer Res,* 26 (1), 132.

Oren, Y., Tsabar, M., Cuoco, M. S., Amir-Zilberstein, L., Cabanos, H. F., Hutter, J. C., Hu, B., Thakore, P. I., Tabaka, M., Fulco, C. P., Colgan, W., Cuevas, B. M., Hurvitz, S. A., Slamon, D. J., Deik, A., Pierce, K. A., Clish, C., Hata, A. N., Zaganjor, E., Lahav, G., Politi, K., Brugge, J. S., and Regev, A. (2021), 'Cycling cancer persister cells arise from lineages with distinct programs', *Nature*.

Orrantia-Borunda, E., Anchondo-Nunez, P., Acuna-Aguilar, L. E., Gomez-Valles, F. O., and Ramirez-Valdespino, C. A. (2022), 'Subtypes of Breast Cancer', in H. N. Mayrovitz (ed.), *Breast Cancer* (Brisbane (AU)).

Page, M. J., McKenzie, J. E., Bossuyt, P. M., Boutron, I., Hoffmann, T. C., Mulrow, C. D., Shamseer, L., Tetzlaff, J. M., Akl, E. A., Brennan, S. E., Chou, R., Glanville, J., Grimshaw, J. M., Hrobjartsson, A., Lalu, M. M., Li, T., Loder, E. W., Mayo-Wilson, E., McDonald, S., McGuinness, L. A., Stewart, L. A., Thomas, J., Tricco, A. C., Welch, V. A., Whiting, P., and Moher, D. (2021), 'The PRISMA 2020 statement: an updated guideline for reporting systematic reviews', *BMJ,* 372, n71.

Pan, M., Zorbas, C., Sugaya, M., Ishiguro, K., Kato, M., Nishida, M., Zhang, H. F., Candeias, M. M., Okamoto, A., Ishikawa, T., Soga, T., Aburatani, H., Sakai, J., Matsumura, Y., Suzuki, T., Proud, C. G., Lafontaine, D. L. J., and Osawa, T. (2022), 'Glutamine deficiency in solid tumor cells confers resistance to ribosomal RNA synthesis inhibitors', *Nat Commun,* 13 (1), 3706.

Panier, S. and Boulton, S. J. (2014), 'Double-strand break repair: 53BP1 comes into focus', *Nat Rev Mol Cell Biol,* 15 (1), 7-18.

Park, C. H., Park, J. Y., and Cho, W. G. (2024), 'Chemical Hypoxia Induces Pyroptosis in Neuronal Cells by Caspase-Dependent Gasdermin Activation', *Int J Mol Sci,* 25 (4).

Park, H. Y., Park, S. H., Jeong, J. W., Yoon, D., Han, M. H., Lee, D. S., Choi, G., Yim, M. J., Lee, J. M., Kim, D. H., Kim, G. Y., Choi, I. W., Kim, S., Kim, H. S., Cha, H. J., and Choi, Y. H. (2017), 'Induction of p53-Independent Apoptosis and G1 Cell Cycle Arrest by Fucoidan in HCT116 Human Colorectal Carcinoma Cells', *Mar Drugs,* 15 (6).

Parker, J. S., Mullins, M., Cheang, M. C., Leung, S., Voduc, D., Vickery, T., Davies, S., Fauron, C., He, X., Hu, Z., Quackenbush, J. F., Stijleman, I. J., Palazzo, J., Marron, J. S., Nobel, A. B., Mardis, E., Nielsen, T. O., Ellis, M. J., Perou, C. M., and Bernard, P. S. (2009), 'Supervised risk predictor of breast cancer based on intrinsic subtypes', *J Clin Oncol,* 27 (8), 1160-7.

Parsels, L. A., Parsels, J. D., Tanska, D. M., Maybaum, J., Lawrence, T. S., and Morgan, M. A. (2018), 'The contribution of DNA replication stress marked by high-intensity, pan-nuclear gammaH2AX staining to chemosensitization by CHK1 and WEE1 inhibitors', *Cell Cycle,* 17 (9), 1076-86.

Parsons, J. L. and Dianov, G. L. (2013), 'Co-ordination of base excision repair and genome stability', *DNA Repair (Amst),* 12 (5), 326-33.

Pasanen, A., Heikkila, M., Rautavuoma, K., Hirsila, M., Kivirikko, K. I., and Myllyharju, J. (2010), 'Hypoxia-inducible factor (HIF)-3alpha is subject to extensive alternative splicing in human tissues and cancer cells and is regulated by HIF-1 but not HIF-2', *Int J Biochem Cell Biol,* 42 (7), 1189-200.

Patel, N., Harris, A. L., Gleeson, F. V., and Vallis, K. A. (2012), 'Clinical imaging of tumor angiogenesis', *Future Oncol,* 8 (11), 1443-59.

Peng, X., Na, R., Zhou, W., Meng, X., Yang, Y., Amini, S., and Song, L. (2022), 'Nuclear translocation of Gasdermin D sensitizes colorectal cancer to chemotherapy in a pyroptosis-independent manner', *Oncogene,* 41 (47), 5092-106.

Peng, Y. J., Yuan, G., Khan, S., Nanduri, J., Makarenko, V. V., Reddy, V. D., Vasavda, C., Kumar, G. K., Semenza, G. L., and Prabhakar, N. R. (2014), 'Regulation of hypoxia-inducible factor-alpha isoforms and redox state by carotid body neural activity in rats', *J Physiol,* 592 (17), 3841-58.

Pereira, K. M., Chaves, F. N., Viana, T. S., Carvalho, F. S., Costa, F. W., Alves, A. P., and Sousa, F. B. (2013), 'Oxygen metabolism in oral cancer: HIF and GLUTs (Review)', *Oncol Lett,* 6 (2), 311-16.

Perier, A., Fregni, G., Wittnebel, S., Gad, S., Allard, M., Gervois, N., Escudier, B., Azzarone, B., and Caignard, A. (2011), 'Mutations of the von Hippel-Lindau gene confer increased susceptibility to natural killer cells of clear-cell renal cell carcinoma', *Oncogene,* 30 (23), 2622-32.

Peripolli, S., Meneguello, L., Perrod, C., Singh, T., Patel, H., Rahman, S. T., Kiso, K., Thorpe, P., Calvanese, V., Bertoli, C., and de Bruin, R. A. M. (2024), 'Oncogenic c-Myc induces replication stress by increasing cohesins chromatin occupancy in a CTCF-dependent manner', *Nat Commun,* 15 (1), 1579.

Perou, C. M., Sorlie, T., Eisen, M. B., van de Rijn, M., Jeffrey, S. S., Rees, C. A., Pollack, J. R., Ross, D. T., Johnsen, H., Akslen, L. A., Fluge, O., Pergamenschikov, A., Williams, C., Zhu, S. X., Lonning, P. E., Borresen-Dale, A. L., Brown, P. O., and Botstein, D. (2000), 'Molecular portraits of human breast tumours', *Nature,* 406 (6797), 747-52.

Pettitt, S. J., Krastev, D. B., Brandsma, I., Drean, A., Song, F., Aleksandrov, R., Harrell, M. I., Menon, M., Brough, R., Campbell, J., Frankum, J., Ranes, M., Pemberton, H. N., Rafiq, R., Fenwick, K., Swain, A., Guettler, S., Lee, J. M., Swisher, E. M., Stoynov, S., Yusa, K., Ashworth, A., and Lord, C. J. (2018), 'Genome-wide and high-density CRISPR-Cas9 screens identify point mutations in PARP1 causing PARP inhibitor resistance', *Nat Commun,* 9 (1), 1849.

Pham, M. M., Hinchcliff, E., Avila, M., and Westin, S. N. (2021), 'The Clinical Challenges, Trials, and Errors of Combatting Poly(ADP-Ribose) Polymerase Inhibitors Resistance', *Cancer J,* 27 (6), 491-500.

Pires, I. M., Bencokova, Z., Milani, M., Folkes, L. K., Li, J. L., Stratford, M. R., Harris, A. L., and Hammond, E. M. (2010), 'Effects of acute versus chronic hypoxia on DNA damage responses and genomic instability', *Cancer Res,* 70 (3), 925-35.

Pires, I. M., Olcina, M. M., Anbalagan, S., Pollard, J. R., Reaper, P. M., Charlton, P. A., McKenna, W. G., and Hammond, E. M. (2012), 'Targeting radiation-resistant hypoxic tumour cells through ATR inhibition', *Br J Cancer,* 107 (2), 291-9.

Polgar, C., Kahan, Z., Ivanov, O., Chorvath, M., Ligacova, A., Csejtei, A., Gabor, G., Landherr, L., Mangel, L., Mayer, A., and Fodor, J. (2022), 'Radiotherapy of Breast Cancer-Professional Guideline 1st Central-Eastern European Professional Consensus Statement on Breast Cancer', *Pathol Oncol Res,* 28, 1610378.

Polo, S. E., Blackford, A. N., Chapman, J. R., Baskcomb, L., Gravel, S., Rusch, A., Thomas, A., Blundred, R., Smith, P., Kzhyshkowska, J., Dobner, T., Taylor, A. M., Turnell, A. S., Stewart, G. S., Grand, R. J., and Jackson, S. P. (2012), 'Regulation of DNA-end resection by hnRNPU-like proteins promotes DNA double-strand break signaling and repair', *Mol Cell,* 45 (4), 505-16.

Polyak, K. (2007), 'Breast cancer: origins and evolution', *J Clin Invest,* 117 (11), 3155-63.

Possenti, L., Vitullo, P., Cicchetti, A., Zunino, P., and Rancati, T. (2024), 'Modeling hypoxia-induced radiation resistance and the impact of radiation sources', *Comput Biol Med,* 173, 108334.

Pothuri, V. S., Hogg, G. D., Conant, L., Borcherding, N., James, C. A., Mudd, J., Williams, G., Seo, Y. D., Hawkins, W. G., Pillarisetty, V. G., DeNardo, D. G., and Fields, R. C. (2024), 'Intratumoral T-cell receptor repertoire composition predicts overall survival in patients with pancreatic ductal adenocarcinoma', *Oncoimmunology,* 13 (1), 2320411.

Pouyssegur, J. and Mechta-Grigoriou, F. (2006), 'Redox regulation of the hypoxia-inducible factor', *Biol Chem,* 387 (10-11), 1337-46.

Pugh, C. W. and Ratcliffe, P. J. (2003), 'Regulation of angiogenesis by hypoxia: role of the HIF system', *Nat Med,* 9 (6), 677-84.

--- (2017), 'New horizons in hypoxia signaling pathways', *Exp Cell Res,* 356 (2), 116-21.

Quinlan, C. L., Goncalves, R. L., Hey-Mogensen, M., Yadava, N., Bunik, V. I., and Brand, M. D. (2014), 'The 2-oxoacid dehydrogenase complexes in mitochondria can produce superoxide/hydrogen peroxide at much higher rates than complex I', *J Biol Chem,* 289 (12), 8312-25.

Qutub, A. A. and Popel, A. S. (2008), 'Reactive oxygen species regulate hypoxia-inducible factor 1alpha differentially in cancer and ischemia', *Mol Cell Biol,* 28 (16), 5106-19.

Rademakers, S. E., Lok, J., van der Kogel, A. J., Bussink, J., and Kaanders, J. H. (2011), 'Metabolic markers in relation to hypoxia; staining patterns and colocalization of pimonidazole, HIF-1alpha, CAIX, LDH-5, GLUT-1, MCT1 and MCT4', *BMC Cancer,* 11, 167.

Ragnum, H. B., Vlatkovic, L., Lie, A. K., Axcrona, K., Julin, C. H., Frikstad, K. M., Hole, K. H., Seierstad, T., and Lyng, H. (2015), 'The tumour hypoxia marker pimonidazole reflects a transcriptional programme associated with aggressive prostate cancer', *Br J Cancer,* 112 (2), 382-90.

Rahane, D., Dhingra, T., Chalavady, G., Datta, A., Ghosh, B., Rana, N., Borah, A., Saraf, S., and Bhattacharya, P. (2024), 'Hypoxia and its effect on the cellular system', *Cell Biochem Funct,* 42 (2), e3940.

Raleigh, J. A., Calkins-Adams, D. P., Rinker, L. H., Ballenger, C. A., Weissler, M. C., Fowler, W. C., Jr., Novotny, D. B., and Varia, M. A. (1998), 'Hypoxia and vascular endothelial growth factor expression in human squamous cell carcinomas using pimonidazole as a hypoxia marker', *Cancer Res,* 58 (17), 3765-8.

Ramachandran, S., Ma, T. S., Griffin, J., Ng, N., Foskolou, I. P., Hwang, M. S., Victori, P., Cheng, W. C., Buffa, F. M., Leszczynska, K. B., El-Khamisy, S. F., Gromak, N., and Hammond, E. M. (2021), 'Hypoxia-induced SETX links replication stress with the unfolded protein response', *Nat Commun,* 12 (1), 3686.

Rauf, A., Khalil, A. A., Awadallah, S., Khan, S. A., Abu-Izneid, T., Kamran, M., Hemeg, H. A., Mubarak, M. S., Khalid, A., and Wilairatana, P. (2024), 'Reactive oxygen species in biological systems: Pathways, associated diseases, and potential inhibitors-A review', *Food Sci Nutr,* 12 (2), 675-93.

Reed, E. (2010), 'DNA damage and repair in translational oncology: an overview', *Clin Cancer Res,* 16 (18), 4511-6.

Reinfeld, B. I., Madden, M. Z., Wolf, M. M., Chytil, A., Bader, J. E., Patterson, A. R., Sugiura, A., Cohen, A. S., Ali, A., Do, B. T., Muir, A., Lewis, C. A., Hongo, R. A., Young, K. L., Brown, R. E., Todd, V. M., Huffstater, T., Abraham, A., O'Neil, R. T., Wilson, M. H., Xin, F., Tantawy, M. N., Merryman, W. D., Johnson, R. W., Williams, C. S., Mason, E. F., Mason, F. M., Beckermann, K. E., Vander Heiden, M. G., Manning, H. C., Rathmell, J. C., and Rathmell, W. K. (2021), 'Cell-programmed nutrient partitioning in the tumour microenvironment', *Nature,* 593 (7858), 282-88.

Reuter, S., Gupta, S. C., Chaturvedi, M. M., and Aggarwal, B. B. (2010), 'Oxidative stress, inflammation, and cancer: how are they linked?', *Free Radic Biol Med,* 49 (11), 1603-16.

Rodriguez-Berriguete, G., Ranzani, M., Prevo, R., Puliyadi, R., Machado, N., Bolland, H. R., Millar, V., Ebner, D., Boursier, M., Cerutti, A., Cicconi, A., Galbiati, A., Grande, D., Grinkevich, V., Majithiya, J. B., Piscitello, D., Rajendra, E., Stockley, M. L., Boulton, S. J., Hammond, E. M., Heald, R. A., Smith, G. C. M., Robinson, H. M. R., and Higgins, G. S. (2023), 'Small-Molecule Poltheta Inhibitors Provide Safe and Effective Tumor Radiosensitization in Preclinical Models', *Clin Cancer Res,* 29 (8), 1631-42.

Rofstad, E. K., Gaustad, J. V., Egeland, T. A., Mathiesen, B., and Galappathi, K. (2010), 'Tumors exposed to acute cyclic hypoxic stress show enhanced angiogenesis, perfusion and metastatic dissemination', *Int J Cancer,* 127 (7), 1535-46.

Rose, Maddison, Burgess, Joshua T., O'Byrne, Kenneth, Richard, Derek J., and Bolderson, Emma (2020), 'PARP Inhibitors: Clinical Relevance, Mechanisms of Action and Tumor Resistance', *Frontiers in Cell and Developmental Biology,* 8.

Rouschop, K. M., Dubois, L. J., Keulers, T. G., van den Beucken, T., Lambin, P., Bussink, J., van der Kogel, A. J., Koritzinsky, M., and Wouters, B. G. (2013), 'PERK/eIF2alpha signaling protects therapy resistant hypoxic cells through induction of glutathione synthesis and protection against ROS', *Proc Natl Acad Sci U S A,* 110 (12), 4622-7.

Rubbi, C. P. and Milner, J. (2003), 'Disruption of the nucleolus mediates stabilization of p53 in response to DNA damage and other stresses', *EMBO J,* 22 (22), 6068-77.

Rudenko, N. N., Vetoshkina, D. V., Marenkova, T. V., and Borisova-Mubarakshina, M. M. (2023), 'Antioxidants of Non-Enzymatic Nature: Their Function in Higher Plant Cells and the Ways of Boosting Their Biosynthesis', *Antioxidants (Basel),* 12 (11).

Ruiz, S., Mayor-Ruiz, C., Lafarga, V., Murga, M., Vega-Sendino, M., Ortega, S., and Fernandez-Capetillo, O. (2016), 'A Genome-wide CRISPR Screen Identifies CDC25A as a Determinant of Sensitivity to ATR Inhibitors', *Mol Cell,* 62 (2), 307-13.

Rulten, S. L., Fisher, A. E., Robert, I., Zuma, M. C., Rouleau, M., Ju, L., Poirier, G., Reina-San-Martin, B., and Caldecott, K. W. (2011), 'PARP-3 and APLF function together to accelerate nonhomologous end-joining', *Mol Cell,* 41 (1), 33-45.

Saha, S., Rundle, S., Kotsopoulos, I. C., Begbie, J., Howarth, R., Pappworth, I. Y., Mukhopadhyay, A., Kucukmetin, A., Marchbank, K. J., and Curtin, N. (2022), 'Determining the Potential of DNA Damage Response (DDR) Inhibitors in Cervical Cancer Therapy', *Cancers (Basel),* 14 (17).

Sahgal, P., Patil, D. T., Bala, P., Sztupinszki, Z. M., Tisza, V., Spisak, S., Luong, A. G., Huffman, B., Prosz, A., Singh, H., Lazaro, J. B., Szallasi, Z., Cleary, J. M., and Sethi, N. S. (2023), 'Replicative stress in gastroesophageal cancer is associated with chromosomal instability and sensitivity to DNA damage response inhibitors', *iScience,* 26 (11), 108169.

Sakahira, Hideki, Enari, Masato, Ohsawa, Yoshiyuki, Uchiyama, Yasuo, and Nagata, Shigekazu (1999), 'Apoptotic nuclear morphological change without DNA fragmentation', *Current Biology,* 9 (10), 543-46.

Sallmyr, A. and Tomkinson, A. E. (2018), 'Repair of DNA double-strand breaks by mammalian alternative end-joining pathways', *J Biol Chem,* 293 (27), 10536-46.

Samanta, D., Park, Y., Andrabi, S. A., Shelton, L. M., Gilkes, D. M., and Semenza, G. L. (2022), 'Correction: PHGDH Expression Is Required for Mitochondrial Redox Homeostasis, Breast Cancer Stem Cell Maintenance, and Lung Metastasis', *Cancer Res,* 82 (6), 1153.

Samstein, R. M., Krishna, C., Ma, X., Pei, X., Lee, K. W., Makarov, V., Kuo, F., Chung, J., Srivastava, R. M., Purohit, T. A., Hoen, D. R., Mandal, R., Setton, J., Wu, W., Shah, R., Qeriqi, B., Chang, Q., Kendall, S., Braunstein, L., Weigelt, B., Carrillo Albornoz, P. B., Morris, L. G. T., Mandelker, D. L., Reis-Filho, J. S., de Stanchina, E., Powell, S. N., Chan, T. A., and Riaz, N. (2021), 'Mutations in BRCA1 and BRCA2 differentially affect the tumor microenvironment and response to checkpoint blockade immunotherapy', *Nat Cancer,* 1 (12), 1188-203.

Sarada, S., Himadri, P., Mishra, C., Geetali, P., Ram, M. S., and Ilavazhagan, G. (2008), 'Role of oxidative stress and NFkB in hypoxia-induced pulmonary edema', *Exp Biol Med (Maywood),* 233 (9), 1088-98.

Sarmiento-Salinas, F. L., Perez-Gonzalez, A., Acosta-Casique, A., Ix-Ballote, A., Diaz, A., Trevino, S., Rosas-Murrieta, N. H., Millan-Perez-Pena, L., and Maycotte, P. (2021), 'Reactive oxygen species: Role in carcinogenesis, cancer cell signaling and tumor progression', *Life Sci,* 284, 119942.

Savage, K. I. and Harkin, D. P. (2015), 'BRCA1, a 'complex' protein involved in the maintenance of genomic stability', *FEBS J,* 282 (4), 630-46.

Saxena, K. and Jolly, M. K. (2019), 'Acute vs. Chronic vs. Cyclic Hypoxia: Their Differential Dynamics, Molecular Mechanisms, and Effects on Tumor Progression', *Biomolecules,* 9 (8).

Scanlon, S. E., Hegan, D. C., Sulkowski, P. L., and Glazer, P. M. (2018), 'Suppression of homology-dependent DNA double-strand break repair induces PARP inhibitor sensitivity in VHL-deficient human renal cell carcinoma', *Oncotarget,* 9 (4), 4647-60.

Scearce, L. M., Laz, T. M., Hazel, T. G., Lau, L. F., and Taub, R. (1993), 'RNR-1, a nuclear receptor in the NGFI-B/Nur77 family that is rapidly induced in regenerating liver', *J Biol Chem,* 268 (12), 8855-61.

Schonlau, F., Maibucher, A., Kohnlein, W., and Garnett, M. C. (1997), 'Mechanism of free and conjugated neocarzinostatin activity: studies on chromophore and protein uptake using a transferrin-neocarzinostatin conjugate', *Z Naturforsch C J Biosci,* 52 (3-4), 245-54.

Scortegagna, M., Ding, K., Oktay, Y., Gaur, A., Thurmond, F., Yan, L. J., Marck, B. T., Matsumoto, A. M., Shelton, J. M., Richardson, J. A., Bennett, M. J., and Garcia, J. A. (2003), 'Multiple organ pathology, metabolic abnormalities and impaired homeostasis of reactive oxygen species in Epas1-/- mice', *Nat Genet,* 35 (4), 331-40.

Scott, M. C., Temiz, N. A., Sarver, A. E., LaRue, R. S., Rathe, S. K., Varshney, J., Wolf, N. K., Moriarity, B. S., O'Brien, T. D., Spector, L. G., Largaespada, D. A., Modiano, J. F., Subramanian, S., and Sarver, A. L. (2018), 'Comparative Transcriptome Analysis Quantifies Immune Cell Transcript Levels, Metastatic Progression, and Survival in Osteosarcoma', *Cancer Res,* 78 (2), 326-37.

Seal, S., Thompson, D., Renwick, A., Elliott, A., Kelly, P., Barfoot, R., Chagtai, T., Jayatilake, H., Ahmed, M., Spanova, K., North, B., McGuffog, L., Evans, D. G., Eccles, D., Breast Cancer Susceptibility, Collaboration, Easton, D. F., Stratton, M. R., and Rahman, N. (2006),

'Truncating mutations in the Fanconi anemia J gene BRIP1 are low-penetrance breast cancer susceptibility alleles', *Nat Genet,* 38 (11), 1239-41.

Sears, J. E., Hoppe, G., Ebrahem, Q., and Anand-Apte, B. (2008), 'Prolyl hydroxylase inhibition during hyperoxia prevents oxygen-induced retinopathy', *Proc Natl Acad Sci U S A,* 105 (50), 19898-903.

Semenza, G. L. (2011), 'Regulation of metabolism by hypoxia-inducible factor 1', *Cold Spring Harb Symp Quant Biol,* 76, 347-53.

--- (2012), 'Hypoxia-inducible factors in physiology and medicine', *Cell,* 148 (3), 399-408.

Serra-Pages, C., Medley, Q. G., Tang, M., Hart, A., and Streuli, M. (1998), 'Liprins, a family of LAR transmembrane protein-tyrosine phosphatase-interacting proteins', *J Biol Chem,* 273 (25), 15611-20.

Serra-Pages, C., Kedersha, N. L., Fazikas, L., Medley, Q., Debant, A., and Streuli, M. (1995), 'The LAR transmembrane protein tyrosine phosphatase and a coiled-coil LAR-interacting protein co-localize at focal adhesions', *EMBO J,* 14 (12), 2827-38.

Sgarbi, G., Gorini, G., Costanzini, A., Barbato, S., Solaini, G., and Baracca, A. (2017), 'Hypoxia decreases ROS level in human fibroblasts', *Int J Biochem Cell Biol,* 88, 133-44.

Shahini, A. and Riazalhosseini, Y. (2024), 'Combination of PARP and DNA methylation inhibitors as a potential personalized therapy for SETD2-mutated clear-cell renal cancers', *Transl Androl Urol,* 13 (7), 1315-18.

Shen, Z. (2011), 'Genomic instability and cancer: an introduction', *J Mol Cell Biol,* 3 (1), 1-3.

Shinojima, T., Oya, M., Takayanagi, A., Mizuno, R., Shimizu, N., and Murai, M. (2007), 'Renal cancer cells lacking hypoxia inducible factor (HIF)-1alpha expression maintain vascular endothelial growth factor expression through HIF-2alpha', *Carcinogenesis,* 28 (3), 529-36.

Shiota, M., Ushijima, M., Tsukahara, S., Nagakawa, S., Okada, T., Tanegashima, T., Kobayashi, S., Matsumoto, T., and Eto, M. (2024), 'Oxidative stress in peroxisomes induced by androgen

receptor inhibition through peroxisome proliferator-activated receptor promotes enzalutamide resistance in prostate cancer', *Free Radic Biol Med,* 221, 81-88.

Shweiki, D., Itin, A., Soffer, D., and Keshet, E. (1992), 'Vascular endothelial growth factor induced by hypoxia may mediate hypoxia-initiated angiogenesis', *Nature,* 359 (6398), 843-5.

Sidrauski, C., McGeachy, A. M., Ingolia, N. T., and Walter, P. (2015), 'The small molecule ISRIB reverses the effects of eIF2alpha phosphorylation on translation and stress granule assembly', *Elife,* 4.

Simon, H. U., Haj-Yehia, A., and Levi-Schaffer, F. (2000), 'Role of reactive oxygen species (ROS) in apoptosis induction', *Apoptosis,* 5 (5), 415-8.

Sisakht, M., Darabian, M., Mahmoodzadeh, A., Bazi, A., Shafiee, S. M., Mokarram, P., and Khoshdel, Z. (2020), 'The role of radiation induced oxidative stress as a regulator of radio-adaptive responses', *Int J Radiat Biol,* 96 (5), 561-76.

Slade, D. (2020), 'PARP and PARG inhibitors in cancer treatment', *Genes Dev,* 34 (5-6), 360-94.

Smith, E. S., Da Cruz Paula, A., Cadoo, K. A., Abu-Rustum, N. R., Pei, X., Brown, D. N., Ferrando, L., Sebastiao, A. P. M., Riaz, N., Robson, M. E., Soslow, R. A., Reis-Filho, J. S., Mandelker, D., and Weigelt, B. (2019), 'Endometrial Cancers in BRCA1 or BRCA2 Germline Mutation Carriers: Assessment of Homologous Recombination DNA Repair Defects', *JCO Precis Oncol,* 3.

Snezhkina, A. V., Kudryavtseva, A. V., Kardymon, O. L., Savvateeva, M. V., Melnikova, N. V., Krasnov, G. S., and Dmitriev, A. A. (2019), 'ROS Generation and Antioxidant Defense Systems in Normal and Malignant Cells', *Oxid Med Cell Longev,* 2019, 6175804.

Sorensen, B. S., Toustrup, K., Horsman, M. R., Overgaard, J., and Alsner, J. (2010), 'Identifying pH independent hypoxia induced genes in human squamous cell carcinomas in vitro', *Acta Oncol,* 49 (7), 895-905.

Sotiriou, C., Neo, S. Y., McShane, L. M., Korn, E. L., Long, P. M., Jazaeri, A., Martiat, P., Fox, S. B., Harris, A. L., and Liu, E. T. (2003), 'Breast cancer classification and prognosis based on

gene expression profiles from a population-based study', *Proc Natl Acad Sci U S A,* 100 (18), 10393-8.

Srinivas, U. S., Tan, B. W. Q., Vellayappan, B. A., and Jeyasekharan, A. D. (2019), 'ROS and the DNA damage response in cancer', *Redox Biol,* 25, 101084.

Srivastava, N., Usmani, S. S., Subbarayan, R., Saini, R., and Pandey, P. K. (2023), 'Hypoxia: syndicating triple negative breast cancer against various therapeutic regimens', *Front Oncol,* 13, 1199105.

Statz-Geary, K., Elliott, A., Bialick, S., Serrano, C., von Mehren, M., Oberley, M., Espejo-Freire, A. P., Barreto Coelho, P., Costa, P. A., D'Amato, G. Z., Jonczak, E., Trent, J. C., Montgomery, E., Lombard, D., Rosenberg, A., and Dhir, A. (2025), 'DNA Damage Repair Pathway Alterations and Immune Landscape Differences in Pediatric/Adolescent, Young Adult (AYA) and Adult Sarcomas', *Cancers (Basel),* 17 (12).

Stegen, S., van Gastel, N., Eelen, G., Ghesquiere, B., D'Anna, F., Thienpont, B., Goveia, J., Torrekens, S., Van Looveren, R., Luyten, F. P., Maxwell, P. H., Wielockx, B., Lambrechts, D., Fendt, S. M., Carmeliet, P., and Carmeliet, G. (2016), 'HIF-1alpha Promotes Glutamine-Mediated Redox Homeostasis and Glycogen-Dependent Bioenergetics to Support Postimplantation Bone Cell Survival', *Cell Metab,* 23 (2), 265-79.

Stewart-Ornstein, J. and Lahav, G. (2017), 'p53 dynamics in response to DNA damage vary across cell lines and are shaped by efficiency of DNA repair and activity of the kinase ATM', *Sci Signal,* 10 (476).

Storz, P. (2005), 'Reactive oxygen species in tumor progression', *Front Biosci,* 10, 1881-96.

--- (2006), 'Reactive oxygen species-mediated mitochondria-to-nucleus signaling: a key to aging and radical-caused diseases', *Sci STKE,* 2006 (332), re3.

Sun, Y., Zheng, Y., Wang, C., and Liu, Y. (2018), 'Glutathione depletion induces ferroptosis, autophagy, and premature cell senescence in retinal pigment epithelial cells', *Cell Death Dis,* 9 (7), 753.

Surma, M., Handy, C., Chang, J., Kapur, R., Wei, L., and Shi, J. (2014), 'ROCK1 deficiency enhances protective effects of antioxidants against apoptosis and cell detachment', *PLoS One,* 9 (3), e90758.

Swanton, C., Bernard, E., Abbosh, C., Andre, F., Auwerx, J., Balmain, A., Bar-Sagi, D., Bernards, R., Bullman, S., DeGregori, J., Elliott, C., Erez, A., Evan, G., Febbraio, M. A., Hidalgo, A., Jamal-Hanjani, M., Joyce, J. A., Kaiser, M., Lamia, K., Locasale, J. W., Loi, S., Malanchi, I., Merad, M., Musgrave, K., Patel, K. J., Quezada, S., Wargo, J. A., Weeraratna, A., White, E., Winkler, F., Wood, J. N., Vousden, K. H., and Hanahan, D. (2024), 'Embracing cancer complexity: Hallmarks of systemic disease', *Cell,* 187 (7), 1589-616.

Swift, M., Reitnauer, P. J., Morrell, D., and Chase, C. L. (1987), 'Breast and other cancers in families with ataxia-telangiectasia', *N Engl J Med,* 316 (21), 1289-94.

Tafani, M., Sansone, L., Limana, F., Arcangeli, T., De Santis, E., Polese, M., Fini, M., and Russo, M. A. (2016), 'The Interplay of Reactive Oxygen Species, Hypoxia, Inflammation, and Sirtuins in Cancer Initiation and Progression', *Oxid Med Cell Longev,* 2016, 3907147.

Takatani-Nakase, T., Matsui, C., Hosotani, M., Omura, M., Takahashi, K., and Nakase, I. (2022), 'Hypoxia enhances motility and EMT through the Na(+)/H(+) exchanger NHE-1 in MDA-MB-231 breast cancer cells', *Exp Cell Res,* 412 (1), 113006.

Talia, M., Cirillo, F., Spinelli, A., Zicarelli, A., Scordamaglia, D., Muglia, L., De Rosis, S., Rigiracciolo, D. C., Filippelli, G., Perrotta, I. D., Davoli, M., De Rosa, R., Macirella, R., Brunelli, E., Miglietta, A. M., Nardo, B., Tosoni, D., Pece, S., De Francesco, E. M., Belfiore, A., Maggiolini, M., and Lappano, R. (2023), 'The Ephrin tyrosine kinase a3 (EphA3) is a novel mediator of RAGE-prompted motility of breast cancer cells', *J Exp Clin Cancer Res,* 42 (1), 164.

Tan, D., Miao, D., Zhao, C., Shi, J., Lv, Q., Xiong, Z., Yang, H., and Zhang, X. (2023a), 'Comprehensive analyses of A 12-metabolism-associated gene signature and its

connection with tumor metastases in clear cell renal cell carcinoma', *BMC Cancer,* 23 (1), 264.

Tan, S., Yu, H., Xu, Y., Zhao, Y., and Lou, G. (2023b), 'Hypoxia-induced PPFIA4 accelerates the progression of ovarian cancer through glucose metabolic reprogramming', *Med Oncol,* 40 (9), 272.

Tanaka, H., Yamamoto, M., Hashimoto, N., Miyakoshi, M., Tamakawa, S., Yoshie, M., Tokusashi, Y., Yokoyama, K., Yaginuma, Y., and Ogawa, K. (2006), 'Hypoxia-independent overexpression of hypoxia-inducible factor 1alpha as an early change in mouse hepatocarcinogenesis', *Cancer Res,* 66 (23), 11263-70.

Taneja, Neelam, Davis, Mandel, Choy, John S., Beckett, Michael A., Singh, Rachana, Kron, Stephen J., and Weichselbaum, Ralph R. (2004), 'Histone H2AX Phosphorylation as a Predictor of Radiosensitivity and Target for Radiotherapy *', *Journal of Biological Chemistry,* 279 (3), 2273-80.

Tanoue, S., Karino, A., Nayuki, Y., and Ohtsuki, K. (1998), 'Neocarzinostatin-chromophore: a potent inhibitor of casein kinase II in vitro', *J Antibiot (Tokyo),* 51 (1), 95-8.

Tattersall, A., Ryan, N., Wiggans, A. J., Rogozinska, E., and Morrison, J. (2022), 'Poly(ADP-ribose) polymerase (PARP) inhibitors for the treatment of ovarian cancer', *Cochrane Database Syst Rev,* 2 (2), CD007929.

Telli, M. L., Hellyer, J., Audeh, W., Jensen, K. C., Bose, S., Timms, K. M., Gutin, A., Abkevich, V., Peterson, R. N., Neff, C., Hughes, E., Sangale, Z., Jones, J., Hartman, A. R., Chang, P. J., Vinayak, S., Wenstrup, R., and Ford, J. M. (2018), 'Homologous recombination deficiency (HRD) status predicts response to standard neoadjuvant chemotherapy in patients with triple-negative or BRCA1/2 mutation-associated breast cancer', *Breast Cancer Res Treat,* 168 (3), 625-30.

Telli, M. L., Timms, K. M., Reid, J., Hennessy, B., Mills, G. B., Jensen, K. C., Szallasi, Z., Barry, W. T., Winer, E. P., Tung, N. M., Isakoff, S. J., Ryan, P. D., Greene-Colozzi, A., Gutin, A., Sangale,

Z., Iliev, D., Neff, C., Abkevich, V., Jones, J. T., Lanchbury, J. S., Hartman, A. R., Garber, J. E., Ford, J. M., Silver, D. P., and Richardson, A. L. (2016), 'Homologous Recombination Deficiency (HRD) Score Predicts Response to Platinum-Containing Neoadjuvant Chemotherapy in Patients with Triple-Negative Breast Cancer', *Clin Cancer Res,* 22 (15), 3764-73.

Tello, D., Balsa, E., Acosta-Iborra, B., Fuertes-Yebra, E., Elorza, A., Ordonez, A., Corral-Escariz, M., Soro, I., Lopez-Bernardo, E., Perales-Clemente, E., Martinez-Ruiz, A., Enriquez, J. A., Aragones, J., Cadenas, S., and Landazuri, M. O. (2011), 'Induction of the mitochondrial NDUFA4L2 protein by HIF-1alpha decreases oxygen consumption by inhibiting Complex I activity', *Cell Metab,* 14 (6), 768-79.

Terashima, S., Hosokawa, Y., Yoshino, H., Yamaguchi, M., and Nakamura, T. (2013), 'Effect of ascorbic acid and X-irradiation on HL-60 human leukemia cells: the kinetics of reactive oxygen species', *Oncol Rep,* 30 (6), 2653-8.

Tew, B. Y., Kalfa, A. J., Yang, Z., Hurth, K. M., Simon, T., Abnoosian, E., Durant, S. T., Hamerlik, P., and Salhia, B. (2023), 'ATM-Inhibitor AZD1390 Is a Radiosensitizer for Breast Cancer CNS Metastasis', *Clin Cancer Res,* 29 (21), 4492-503.

ThermoFisher (2012), 'CellROX® Oxidative Stress Reagents '.

Thomas, Luke W. and Ashcroft, Margaret (2019), 'Exploring the molecular interface between hypoxia-inducible factor signalling and mitochondria', *Cellular and Molecular Life Sciences,* 76 (9), 1759-77.

Thomson, D. J., Slevin, N. J., Baines, H., Betts, G., Bolton, S., Evans, M., Garcez, K., Irlam, J., Lee, L., Melillo, N., Mistry, H., More, E., Nutting, C., Price, J. M., Schipani, S., Sen, M., Yang, H., West, C. M., and Group, Nimrad Trial (2024), 'Randomized Phase 3 Trial of the Hypoxia Modifier Nimorazole Added to Radiation Therapy With Benefit Assessed in Hypoxic Head and Neck Cancers Determined Using a Gene Signature (NIMRAD)', *Int J Radiat Oncol Biol Phys,* 119 (3), 771-82.

Thul, P. J., Akesson, L., Wiking, M., Mahdessian, D., Geladaki, A., Ait Blal, H., Alm, T., Asplund, A., Bjork, L., Breckels, L. M., Backstrom, A., Danielsson, F., Fagerberg, L., Fall, J., Gatto, L., Gnann, C., Hober, S., Hjelmare, M., Johansson, F., Lee, S., Lindskog, C., Mulder, J., Mulvey, C. M., Nilsson, P., Oksvold, P., Rockberg, J., Schutten, R., Schwenk, J. M., Sivertsson, A., Sjostedt, E., Skogs, M., Stadler, C., Sullivan, D. P., Tegel, H., Winsnes, C., Zhang, C., Zwahlen, M., Mardinoglu, A., Ponten, F., von Feilitzen, K., Lilley, K. S., Uhlen, M., and Lundberg, E. (2017), 'A subcellular map of the human proteome', *Science,* 356 (6340).

Timms, K. M., Abkevich, V., Hughes, E., Neff, C., Reid, J., Morris, B., Kalva, S., Potter, J., Tran, T. V., Chen, J., Iliev, D., Sangale, Z., Tikishvili, E., Perry, M., Zharkikh, A., Gutin, A., and Lanchbury, J. S. (2014), 'Association of BRCA1/2 defects with genomic scores predictive of DNA damage repair deficiency among breast cancer subtypes', *Breast Cancer Res,* 16 (6), 475.

Toledo, L. I., Altmeyer, M., Rask, M. B., Lukas, C., Larsen, D. H., Povlsen, L. K., Bekker-Jensen, S., Mailand, N., Bartek, J., and Lukas, J. (2013), 'ATR prohibits replication catastrophe by preventing global exhaustion of RPA', *Cell,* 155 (5), 1088-103.

Townsend, D. M. and Tew, K. D. (2003), 'The role of glutathione-S-transferase in anti-cancer drug resistance', *Oncogene,* 22 (47), 7369-75.

Trenner, A. and Sartori, A. A. (2019), 'Harnessing DNA Double-Strand Break Repair for Cancer Treatment', *Front Oncol,* 9, 1388.

Trichopoulos, D., Li, F. P., and Hunter, D. J. (1996), 'What causes cancer?', *Sci Am,* 275 (3), 80-7.

Tsang, E. S., Dhawan, M. S., Pacaud, R., Thomas, S., Grabowsky, J., Wilch, L., Karipineni, S., Kelley, R. K., Ko, A. H., Collisson, E., Chapman, J. S., Ueda, S., Bergsland, E. K., and Munster, P. (2024), 'Synthetic Lethality Beyond BRCA: A Phase I Study of Rucaparib and Irinotecan in Metastatic Solid Tumors With Homologous Recombination-Deficiency Mutations Beyond BRCA1/2', *JCO Precis Oncol,* 8, e2300494.

Tubbs, Anthony and Nussenzweig, André (2017), 'Endogenous DNA Damage as a Source of Genomic Instability in Cancer', *Cell,* 168 (4), 644-56.

Turnbull, C., Ahmed, S., Morrison, J., Pernet, D., Renwick, A., Maranian, M., Seal, S., Ghoussaini, M., Hines, S., Healey, C. S., Hughes, D., Warren-Perry, M., Tapper, W., Eccles, D., Evans, D. G., Breast Cancer Susceptibility, Collaboration, Hooning, M., Schutte, M., van den Ouweland, A., Houlston, R., Ross, G., Langford, C., Pharoah, P. D., Stratton, M. R., Dunning, A. M., Rahman, N., and Easton, D. F. (2010), 'Genome-wide association study identifies five new breast cancer susceptibility loci', *Nat Genet,* 42 (6), 504-7.

Turner, N., Tutt, A., and Ashworth, A. (2004), 'Hallmarks of 'BRCAness' in sporadic cancers', *Nat Rev Cancer,* 4 (10), 814-9.

Tuttle, S. W., Maity, A., Oprysko, P. R., Kachur, A. V., Ayene, I. S., Biaglow, J. E., and Koch, C. J. (2007), 'Detection of reactive oxygen species via endogenous oxidative pentose phosphate cycle activity in response to oxygen concentration: implications for the mechanism of HIF-1alpha stabilization under moderate hypoxia', *J Biol Chem,* 282 (51), 36790-6.

Twigger, S. A., Dominguez, B., Porto, V., Hacker, L., Chalmers, A. J., Breckenridge, R., Treder, M., Sedgwick, A. C., Dominguez, F., and Hammond, E. M. (2024), 'The activity of therapeutic molecular cluster Ag5 is dependent on oxygen level and HIF-1 mediated signalling', *Redox Biol,* 76, 103326.

Ursini, F., Maiorino, M., Brigelius-Flohe, R., Aumann, K. D., Roveri, A., Schomburg, D., and Flohe, L. (1995), 'Diversity of glutathione peroxidases', *Methods Enzymol,* 252, 38-53.

Van Allen, E. M., Miao, D., Schilling, B., Shukla, S. A., Blank, C., Zimmer, L., Sucker, A., Hillen, U., Foppen, M. H. G., Goldinger, S. M., Utikal, J., Hassel, J. C., Weide, B., Kaehler, K. C., Loquai, C., Mohr, P., Gutzmer, R., Dummer, R., Gabriel, S., Wu, C. J., Schadendorf, D., and Garraway, L. A. (2015), 'Genomic correlates of response to CTLA-4 blockade in metastatic melanoma', *Science,* 350 (6257), 207-11.

van Beek, L., McClay, E., Patel, S., Schimpl, M., Spagnolo, L., and Maia de Oliveira, T. (2021), 'PARP Power: A Structural Perspective on PARP1, PARP2, and PARP3 in DNA Damage Repair and Nucleosome Remodelling', *Int J Mol Sci,* 22 (10).

VanderVere-Carozza, P. S., Gavande, N. S., Jalal, S. I., Pollok, K. E., Ekinci, E., Heyza, J., Patrick, S. M., Masters, A., Turchi, J. J., and Pawelczak, K. S. (2022), 'In Vivo Targeting Replication Protein A for Cancer Therapy', *Front Oncol,* 12, 826655.

Vassin, V. M., Anantha, R. W., Sokolova, E., Kanner, S., and Borowiec, J. A. (2009), 'Human RPA phosphorylation by ATR stimulates DNA synthesis and prevents ssDNA accumulation during DNA-replication stress', *J Cell Sci,* 122 (Pt 22), 4070-80.

Vaupel, P. and Mayer, A. (2007), 'Hypoxia in cancer: significance and impact on clinical outcome', *Cancer Metastasis Rev,* 26 (2), 225-39.

--- (2016), 'Tumor Hypoxia: Causative Mechanisms, Microregional Heterogeneities, and the Role of Tissue-Based Hypoxia Markers', *Adv Exp Med Biol,* 923, 77-86.

Vaupel, P., Fortmeyer, H. P., Runkel, S., and Kallinowski, F. (1987), 'Blood flow, oxygen consumption, and tissue oxygenation of human breast cancer xenografts in nude rats', *Cancer Res,* 47 (13), 3496-503.

Vaupel, P., Schlenger, K., Knoop, C., and Hockel, M. (1991), 'Oxygenation of human tumors: evaluation of tissue oxygen distribution in breast cancers by computerized O2 tension measurements', *Cancer Res,* 51 (12), 3316-22.

Vihanto, M. M., Plock, J., Erni, D., Frey, B. M., Frey, F. J., and Huynh-Do, U. (2005), 'Hypoxia up-regulates expression of Eph receptors and ephrins in mouse skin', *FASEB J,* 19 (12), 1689-91.

Vogelstein, B., Papadopoulos, N., Velculescu, V. E., Zhou, S., Diaz, L. A., Jr., and Kinzler, K. W. (2013), 'Cancer genome landscapes', *Science,* 339 (6127), 1546-58.

Vorlova, B., Knedlik, T., Tykvart, J., and Konvalinka, J. (2019), 'GCPII and its close homolog GCPIII: from a neuropeptidase to a cancer marker and beyond', *Front Biosci (Landmark Ed),* 24 (4), 648-87.

Vyas, S., Chesarone-Cataldo, M., Todorova, T., Huang, Y. H., and Chang, P. (2013), 'A systematic analysis of the PARP protein family identifies new functions critical for cell physiology', *Nat Commun,* 4, 2240.

Wachsberger, P., Burd, R., and Dicker, A. P. (2004), 'Improving tumor response to radiotherapy by targeting angiogenesis signaling pathways', *Hematol Oncol Clin North Am,* 18 (5), 1039-57, viii.

Wallabregue, A. L. D., Bolland, H., Faulkner, S., Hammond, E. M., and Conway, S. J. (2023), 'Two Color Imaging of Different Hypoxia Levels in Cancer Cells', *J Am Chem Soc,* 145 (4), 2572-83.

Wang, B., Li, D., and Kovalchuk, O. (2013), 'p53 Ser15 phosphorylation and histone modifications contribute to IR-induced miR-34a transcription in mammary epithelial cells', *Cell Cycle,* 12 (13), 2073-83.

Wang, D. Y., Jiang, Z., Ben-David, Y., Woodgett, J. R., and Zacksenhaus, E. (2019), 'Molecular stratification within triple-negative breast cancer subtypes', *Sci Rep,* 9 (1), 19107.

Wang, G. L. and Semenza, G. L. (1993), 'Desferrioxamine induces erythropoietin gene expression and hypoxia-inducible factor 1 DNA-binding activity: implications for models of hypoxia signal transduction', *Blood,* 82 (12), 3610-5.

Wang, J., Zhang, H., and Zhang, R. (2024), 'BRCA2 germline mutation in familial leukaemia with familial breast cancer: a case report', *Ann Hematol,* 103 (2), 685-87.

Wang, L., Chen, X., and Yan, C. (2022), 'Ferroptosis: An emerging therapeutic opportunity for cancer', *Genes Dis,* 9 (2), 334-46.

Warburg, O. (1956), 'On the origin of cancer cells', *Science,* 123 (3191), 309-14.

Warner, J. R. (1990), 'The nucleolus and ribosome formation', *Curr Opin Cell Biol,* 2 (3), 521-7.

Warren, M., Lord, C. J., Masabanda, J., Griffin, D., and Ashworth, A. (2003), 'Phenotypic effects of heterozygosity for a BRCA2 mutation', *Hum Mol Genet,* 12 (20), 2645-56.

Weaver, A. N. and Yang, E. S. (2013), 'Beyond DNA Repair: Additional Functions of PARP-1 in Cancer', *Front Oncol,* 3, 290.

Webb, J. D., Coleman, M. L., and Pugh, C. W. (2009), 'Hypoxia, hypoxia-inducible factors (HIF), HIF hydroxylases and oxygen sensing', *Cell Mol Life Sci,* 66 (22), 3539-54.

Weeks, S. E., Metge, B. J., and Samant, R. S. (2019), 'The nucleolus: a central response hub for the stressors that drive cancer progression', *Cell Mol Life Sci,* 76 (22), 4511-24.

Whitaker, A. M. and Freudenthal, B. D. (2018), 'APE1: A skilled nucleic acid surgeon', *DNA Repair (Amst),* 71, 93-100.

Wicker, C. A., Petery, T., Dubey, P., Wise-Draper, T. M., and Takiar, V. (2022), 'Improving Radiotherapy Response in the Treatment of Head and Neck Cancer', *Crit Rev Oncog,* 27 (2), 73-84.

Winter, S. C., Buffa, F. M., Silva, P., Miller, C., Valentine, H. R., Turley, H., Shah, K. A., Cox, G. J., Corbridge, R. J., Homer, J. J., Musgrove, B., Slevin, N., Sloan, P., Price, P., West, C. M., and Harris, A. L. (2007), 'Relation of a hypoxia metagene derived from head and neck cancer to prognosis of multiple cancers', *Cancer Res,* 67 (7), 3441-9.

Wong, W. W., O'Brien-Gortner, S. F., Anderson, R. F., Wilson, W. R., Hay, M. P., and Dickson, B. D. (2023), 'Hypoxia-activated prodrugs of phenolic olaparib analogues for tumour-selective chemosensitisation', *RSC Med Chem,* 14 (7), 1309-30.

Wouters, B. G. and Koritzinsky, M. (2008), 'Hypoxia signalling through mTOR and the unfolded protein response in cancer', *Nat Rev Cancer,* 8 (11), 851-64.

Wu, H., Tang, H., Zou, X., Huang, Q., Wang, S., Sun, M., Ye, Z., Wang, H., Wu, Y., Sun, L., Chen, Y., and Tang, H. (2024), 'Role of the PARP1/NF-kappaB Pathway in DNA Damage and Apoptosis of TK6 Cells Induced by Hydroquinone', *Chem Res Toxicol,* 37 (7), 1187-98.

Wu, Rongrong, Högberg, Johan, Adner, Mikael, Ramos-Ramírez, Patricia, Stenius, Ulla, and Zheng, Huiyuan (2020), 'Crystalline silica particles cause rapid NLRP3-dependent mitochondrial depolarization and DNA damage in airway epithelial cells', *Particle and Fibre Toxicology,* 17 (1), 39.

Xiao, F., Wang, Z., Qiao, L., Zhang, X., Wu, N., Wang, J., and Yu, X. (2024), 'Application of PARP inhibitors combined with immune checkpoint inhibitors in ovarian cancer', *J Transl Med,* 22 (1), 778.

Xiao, Y., Ma, D., Yang, Y. S., Yang, F., Ding, J. H., Gong, Y., Jiang, L., Ge, L. P., Wu, S. Y., Yu, Q., Zhang, Q., Bertucci, F., Sun, Q., Hu, X., Li, D. Q., Shao, Z. M., and Jiang, Y. Z. (2022), 'Comprehensive metabolomics expands precision medicine for triple-negative breast cancer', *Cell Res,* 32 (5), 477-90.

Xie, Y., Xiao, D., Li, D., Peng, M., Peng, W., Duan, H., and Yang, X. (2024), 'Combined strategies with PARP inhibitors for the treatment of BRCA wide type cancer', *Front Oncol,* 14, 1441222.

Xie, Z., Bailey, A., Kuleshov, M. V., Clarke, D. J. B., Evangelista, J. E., Jenkins, S. L., Lachmann, A., Wojciechowicz, M. L., Kropiwnicki, E., Jagodnik, K. M., Jeon, M., and Ma'ayan, A. (2021), 'Gene Set Knowledge Discovery with Enrichr', *Curr Protoc,* 1 (3), e90.

Xing, F., Hu, Q., Qin, Y., Xu, J., Zhang, B., Yu, X., and Wang, W. (2022), 'The Relationship of Redox With Hallmarks of Cancer: The Importance of Homeostasis and Context', *Front Oncol,* 12, 862743.

Xu, Q., Zhang, H., Qin, H., Wang, H., and Wang, H. (2024a), 'Norcantharidin Sensitizes Colorectal Cancer Cells to Radiotherapy via Reactive Oxygen Species-DRP1-Mediated Mitochondrial Damage', *Antioxidants (Basel),* 13 (3).

Xu, Z., Zhang, N., and Shi, L. (2024b), 'Potential roles of UCH family deubiquitinases in tumorigenesis and chemical inhibitors developed against them', *Am J Cancer Res,* 14 (6), 2666-94.

Yagoda, N., von Rechenberg, M., Zaganjor, E., Bauer, A. J., Yang, W. S., Fridman, D. J., Wolpaw, A. J., Smukste, I., Peltier, J. M., Boniface, J. J., Smith, R., Lessnick, S. L., Sahasrabudhe, S., and Stockwell, B. R. (2007), 'RAS-RAF-MEK-dependent oxidative cell death involving voltage-dependent anion channels', *Nature,* 447 (7146), 864-8.

Yamamoto, H. and Hirasawa, A. (2021), 'Homologous Recombination Deficiencies and Hereditary Tumors', *Int J Mol Sci,* 23 (1).

Yamashita, T., Ohneda, K., Nagano, M., Miyoshi, C., Kaneko, N., Miwa, Y., Yamamoto, M., Ohneda, O., and Fujii-Kuriyama, Y. (2008), 'Hypoxia-inducible transcription factor-2alpha in endothelial cells regulates tumor neovascularization through activation of ephrin A1', *J Biol Chem,* 283 (27), 18926-36.

Yan, H., Liu, W., Xiang, R., Li, X., Hou, S., Xu, L., Wang, L., Zhao, D., Liu, X., Wang, G., Chi, Y., and Yang, J. (2024), 'Ribosomal modification protein rimK-like family member A activates betaine-homocysteine S-methyltransferase 1 to ameliorate hepatic steatosis', *Signal Transduct Target Ther,* 9 (1), 214.

Yan, X., Qu, X., Liu, B., Zhao, Y., Xu, L., Yu, S., Wang, J., Wang, L., and Su, J. (2021), 'Autophagy-Induced HDAC6 Activity During Hypoxia Regulates Mitochondrial Energy Metabolism Through the beta-Catenin/COUP-TFII Axis in Hepatocellular Carcinoma Cells', *Front Oncol,* 11, 742460.

Yang, K., Yang, J., and Yi, J. (2018), 'Nucleolar Stress: hallmarks, sensing mechanism and diseases', *Cell Stress,* 2 (6), 125-40.

Yang, S. L., Wu, C., Xiong, Z. F., and Fang, X. (2015), 'Progress on hypoxia-inducible factor-3: Its structure, gene regulation and biological function (Review)', *Mol Med Rep,* 12 (2), 2411-6.

Yang, W., Wei, J., Sun, T., and Liu, F. (2013), 'Effects of knockdown of miR-210 in combination with ionizing radiation on human hepatoma xenograft in nude mice', *Radiat Oncol,* 8, 102.

Yang, X., Zhang, Z. C., Lu, Y. N., Chen, H. L., Wang, H. S., Lin, T., Chen, Q. Q., Chen, J. S., and He, W. B. (2024), 'Identification and experimental validation of programmed cell death- and

mitochondria-associated biomarkers in osteoporosis and immune microenvironment', *Front Genet,* 15, 1439171.

Yang, Yuting, Wu, Jihong, Lu, Wei, Dai, Yiqin, Zhang, Youjia, and Sun, Xinghuai (2022), 'Olaparib, a PARP-1 inhibitor, protects retinal cells from ocular hypertension-associated oxidative damage', *Frontiers in Cell and Developmental Biology,* 10.

Yap, Timothy A., Plummer, Elizabeth Ruth, Tolcher, Anthony W., Szucs, Zoltan, Gounaris, Ioannis, Locatelli, Giuseppe, Enderlin, Marta, Hicking, Christine, Kaur Mukker, Jatinder, and De Bono, Johann S. (2024), 'A phase I study of highly potent oral ATR inhibitor (ATRi) tuvusertib plus oral PARP inhibitor (PARPi) niraparib in patients with solid tumors', *Journal of Clinical Oncology,* 42 (16_suppl), 3018-18.

Yazinski, S. A., Comaills, V., Buisson, R., Genois, M. M., Nguyen, H. D., Ho, C. K., Todorova Kwan, T., Morris, R., Lauffer, S., Nussenzweig, A., Ramaswamy, S., Benes, C. H., Haber, D. A., Maheswaran, S., Birrer, M. J., and Zou, L. (2017), 'ATR inhibition disrupts rewired homologous recombination and fork protection pathways in PARP inhibitor-resistant BRCA-deficient cancer cells', *Genes Dev,* 31 (3), 318-32.

Ye, J., Fan, J., Venneti, S., Wan, Y. W., Pawel, B. R., Zhang, J., Finley, L. W., Lu, C., Lindsten, T., Cross, J. R., Qing, G., Liu, Z., Simon, M. C., Rabinowitz, J. D., and Thompson, C. B. (2014), 'Serine catabolism regulates mitochondrial redox control during hypoxia', *Cancer Discov,* 4 (12), 1406-17.

Yersal, O. and Barutca, S. (2014), 'Biological subtypes of breast cancer: Prognostic and therapeutic implications', *World J Clin Oncol,* 5 (3), 412-24.

Yiminniyaze, R., Zhang, X., Zhu, N., Wang, J., Li, C., Wumaier, G., Zhou, D., Li, J., Xia, J., Zhang, Y., Dong, L., Zhang, Y., and Li, S. (2023), 'EphrinA3 is a key regulator of malignant behaviors and a potential prognostic factor in lung adenocarcinoma', *Cancer Med,* 12 (2), 1630-42.

Yin, Z. X., Hang, W., Liu, G., Wang, Y. S., Shen, X. F., Sun, Q. H., Li, D. D., Jian, Y. P., Zhang, Y. H., Quan, C. S., Zeng, Q., Li, Y. L., Zhao, R. X., Ding, Q., and Xu, Z. X. (2018), 'PARP-1 inhibitors

sensitize HNSCC cells to APR-246 by inactivation of thioredoxin reductase 1 (TrxR1) and promotion of ROS accumulation', *Oncotarget,* 9 (2), 1885-97.

Yoo, Hee Chan, Park, Seung Joon, Nam, Miso, Kang, Juwon, Kim, Kibum, Yeo, Joo Hye, Kim, Joon-Ki, Heo, Yunkyung, Lee, Hee Seung, and Lee, Myeong Youl (2020), 'A variant of SLC1A5 is a mitochondrial glutamine transporter for metabolic reprogramming in cancer cells', *Cell metabolism,* 31 (2), 267-83. e12.

Yuan, J., Narayanan, L., Rockwell, S., and Glazer, P. M. (2000), 'Diminished DNA repair and elevated mutagenesis in mammalian cells exposed to hypoxia and low pH', *Cancer Res,* 60 (16), 4372-6.

Yuan, X., Zhou, Y., Casanova, E., Chai, M., Kiss, E., Grone, H. J., Schutz, G., and Grummt, I. (2005), 'Genetic inactivation of the transcription factor TIF-IA leads to nucleolar disruption, cell cycle arrest, and p53-mediated apoptosis', *Mol Cell,* 19 (1), 77-87.

Zatreanu, D., Robinson, H. M. R., Alkhatib, O., Boursier, M., Finch, H., Geo, L., Grande, D., Grinkevich, V., Heald, R. A., Langdon, S., Majithiya, J., McWhirter, C., Martin, N. M. B., Moore, S., Neves, J., Rajendra, E., Ranzani, M., Schaedler, T., Stockley, M., Wiggins, K., Brough, R., Sridhar, S., Gulati, A., Shao, N., Badder, L. M., Novo, D., Knight, E. G., Marlow, R., Haider, S., Callen, E., Hewitt, G., Schimmel, J., Prevo, R., Alli, C., Ferdinand, A., Bell, C., Blencowe, P., Bot, C., Calder, M., Charles, M., Curry, J., Ekwuru, T., Ewings, K., Krajewski, W., MacDonald, E., McCarron, H., Pang, L., Pedder, C., Rigoreau, L., Swarbrick, M., Wheatley, E., Willis, S., Wong, A. C., Nussenzweig, A., Tijsterman, M., Tutt, A., Boulton, S. J., Higgins, G. S., Pettitt, S. J., Smith, G. C. M., and Lord, C. J. (2021), 'Poltheta inhibitors elicit BRCA-gene synthetic lethality and target PARP inhibitor resistance', *Nat Commun,* 12 (1), 3636.

Zeman, M. K. and Cimprich, K. A. (2014), 'Causes and consequences of replication stress', *Nat Cell Biol,* 16 (1), 2-9.

Zeng, Z., Lei, S., Wang, J., Yang, Y., Lan, J., Tian, Q., Chen, T., and Hao, X. (2022), 'A novel hypoxia-driven gene signature that can predict the prognosis of hepatocellular carcinoma', *Bioengineered,* 13 (5), 12193-210.

Zhang, D., Ni, Y., Wang, Y., Feng, J., Zhuang, N., Li, J., Liu, L., Shen, W., Zheng, J., Zheng, W., Qian, C., Shan, J., and Zhou, Z. (2023), 'Spatial heterogeneity of tumor microenvironment influences the prognosis of clear cell renal cell carcinoma', *J Transl Med,* 21 (1), 489.

Zhang, F., Lau, S. S., and Monks, T. J. (2011), 'The cytoprotective effect of N-acetyl-L-cysteine against ROS-induced cytotoxicity is independent of its ability to enhance glutathione synthesis', *Toxicol Sci,* 120 (1), 87-97.

Zhang, F., Lin, J., Zhu, D., Tang, Y., Lu, Y., Liu, Z., and Wang, X. (2022), 'Identification of an amino acid metabolism-associated gene signature predicting the prognosis and immune therapy response of clear cell renal cell carcinoma', *Front Oncol,* 12, 970208.

Zhang, F., Wang, X., Bai, Y., Hu, H., Yang, Y., Wang, J., Tang, Y., Ma, H., Feng, D., Li, D., and Han, P. (2021), 'Development and Validation of a Hypoxia-Related Signature for Predicting Survival Outcomes in Patients With Bladder Cancer', *Front Genet,* 12, 670384.

Zhang, J., Wang, C., Chen, X., Takada, M., Fan, C., Zheng, X., Wen, H., Liu, Y., Wang, C., Pestell, R. G., Aird, K. M., Kaelin, W. G., Jr., Liu, X. S., and Zhang, Q. (2015), 'EglN2 associates with the NRF1-PGC1alpha complex and controls mitochondrial function in breast cancer', *EMBO J,* 34 (23), 2953-70.

Zhang, L., Luo, Y. L., Xiang, Y., Bai, X. Y., Qiang, R. R., Zhang, X., Yang, Y. L., and Liu, X. L. (2024), 'Ferroptosis inhibitors: past, present and future', *Front Pharmacol,* 15, 1407335.

Zhang, Q., Huang, R., Hu, H., Yu, L., Tang, Q., Tao, Y., Liu, Z., Li, J., and Wang, G. (2020), 'Integrative Analysis of Hypoxia-Associated Signature in Pan-Cancer', *iScience,* 23 (9), 101460.

Zhang, Y. W., Otterness, D. M., Chiang, G. G., Xie, W., Liu, Y. C., Mercurio, F., and Abraham, R. T. (2005), 'Genotoxic stress targets human Chk1 for degradation by the ubiquitin-proteasome pathway', *Mol Cell,* 19 (5), 607-18.

Zhao, H., Yang, Q., Hu, Y., and Zhang, J. (2018), 'Antitumor effects and mechanisms of olaparib in combination with carboplatin and BKM120 on human triple-negative breast cancer cells', *Oncol Rep,* 40 (6), 3223-34.

Zhao, R., Feng, T., Gao, L., Sun, F., Zhou, Q., Wang, X., Liu, J., Zhang, W., Wang, M., Xiong, X., Jia, W., Chen, W., Wang, L., and Han, B. (2022), 'PPFIA4 promotes castration-resistant prostate cancer by enhancing mitochondrial metabolism through MTHFD2', *J Exp Clin Cancer Res,* 41 (1), 125.

Zhao, Y., Xing, C., Deng, Y., Ye, C., and Peng, H. (2024), 'HIF-1alpha signaling: Essential roles in tumorigenesis and implications in targeted therapies', *Genes Dis,* 11 (1), 234-51.

Zheng, P., Liu, X., Li, H., Gao, L., Yu, Y., Wang, N., and Chen, H. (2021), 'EFNA3 Is a Prognostic Biomarker Correlated With Immune Cell Infiltration and Immune Checkpoints in Gastric Cancer', *Front Genet,* 12, 796592.

Zheng, S., Zou, Y., Liang, J. Y., Xiao, W., Yang, A., Meng, T., Lu, S., Luo, Z., and Xie, X. (2020), 'Identification and validation of a combined hypoxia and immune index for triple-negative breast cancer', *Mol Oncol,* 14 (11), 2814-33.

Zhou, J., Gelot, C., Pantelidou, C., Li, A., Yucel, H., Davis, R. E., Farkkila, A., Kochupurakkal, B., Syed, A., Shapiro, G. I., Tainer, J. A., Blagg, B. S. J., Ceccaldi, R., and D'Andrea, A. D. (2021), 'A first-in-class Polymerase Theta Inhibitor selectively targets Homologous-Recombination-Deficient Tumors', *Nat Cancer,* 2 (6), 598-610.

Zhou, R. (1998), 'The Eph family receptors and ligands', *Pharmacol Ther,* 77 (3), 151-81.

Zhou, X., Patel, D., Sen, S., Shanmugam, V., Sidawy, A., Mishra, L., and Nguyen, B. N. (2017), 'Poly-ADP-ribose polymerase inhibition enhances ischemic and diabetic wound healing by promoting angiogenesis', *J Vasc Surg,* 65 (4), 1161-69.

Zhu, W., Kato, Y., and Artemov, D. (2014), 'Heterogeneity of tumor vasculature and antiangiogenic intervention: insights from MR angiography and DCE-MRI', *PLoS One,* 9 (1), e86583.

Zorov, D. B., Juhaszova, M., and Sollott, S. J. (2014), 'Mitochondrial reactive oxygen species (ROS) and ROS-induced ROS release', *Physiol Rev,* 94 (3), 909-50.

Zorov, D. B., Filburn, C. R., Klotz, L. O., Zweier, J. L., and Sollott, S. J. (2000), 'Reactive oxygen species (ROS)-induced ROS release: a new phenomenon accompanying induction of the mitochondrial permeability transition in cardiac myocytes', *J Exp Med,* 192 (7), 1001-14.

Appendix 1 Thematic grouping of papers filtered from our systematic review screen

Study themes	Title	Author	Journal	Year
Viability tested with PARPi + hypoxia	Inhibition of poly (ADP-ribose) Polymerase-1 (PARP-1) improves endothelial function in pulmonary hypertension	Shafiq M	Pulm Pharmacol Ther	2023
	Hypoxia-activated prodrugs of phenolic Olaparib analogues for tumour-selective chemosensitisation	Wong WW	RSC Med Chem	2023
	Nuclear translocation of Gasdermin D sensitizes colorectal cancer to chemotherapy in a pyroptosis-independent manner	Peng X	Oncogene	2022
	Olaparib, a PARP-1 inhibitor, protects retinal cells from ocular hypertension-associated oxidative damage	Yang Y	Front Cell Dev Biol	2022

	Identification of biomarkers of response to preoperative talazoparib monotherapy in treatment naïve gBRCA+ breast cancers	Liu X	NPJ Breast Cancer	2022
	PARP-1 activation leads to cytosolic accumulation of TDP-43 in neurons	Marcus JM	Neurochem Int	2021
	Eliminating hypoxic tumor cells improves response to PARP inhibitors in homologous recombination-deficient cancer models	Mehibel M	J Clin Invest	2021
	Poly (ADP-Ribose) Polymerase Inhibitor Treatment as a Novel Therapy Attenuating Renal Ischemia-Reperfusion Injury	Jang HR	Front Immunol	2020
	Synthetic lethality between BRCA1 deficiency and poly(ADP-ribose) polymerase inhibition is modulated by processing	Giovannini S	Nucleic Acids Res	2019

	endogenous oxidative DNA damage			
	Contextual synthetic lethality of cancer cell kill based on the tumor microenvironment	Chan N	Cancer Res	2010
	Inhibition of poly(ADP-ribose) polymerase down-regulates BRCA1 and RAD51 in a pathway mediated by E2F4 and p130	Hegan DC	Proc Natl Acad Sci U S A	2010
	Cyclic hypoxia does not alter RAD51 expression or PARP inhibitor cell kill in tumor cells	Kumareswaran R	Radiother Oncol	2015
	Neuroprotective effects of a novel poly (ADP-ribose) polymerase-1 inhibitor, JPI-289, in hypoxic rat cortical neurons	Kim Y	Clin Exp Pharmacol Physiol	2017
	EGFR Mutations Compromise Hypoxia-Associated Radiation Resistance through Impaired Replication Fork-	Saki M	Mol Cancer Res	2017

	Associated DNA Damage Repair			
Viability tested with PARPi + hypoxia + only with treatment combination	Specific protein 1 inhibitor mithramycin A protects cardiomyocytes from myocardial infarction via interacting with PARP	Geng H	In Vitro Cell Dev Biol Anim	2021
	TGFβR-SMAD3 Signaling Induces Resistance to PARP Inhibitors in the Bone Marrow Microenvironment	Le BV	Cell Rep	2020
	Radiosensitisation of head and neck squamous cell carcinoma lines by DNA-PK inhibitors is more effective than PARP-1 inhibition and is enhanced by SLFN11 and hypoxia	Lee TW	Int J Radiat Biol	2019
	Neoadjuvant Olaparib targets hypoxia to improve radiation response in a homologous recombination-proficient breast cancer model	Borst GR	Oncotarget	2017
	Hypoxia Potentiates the	Jiang Y	Int J Radiat	2016

	Radiation-Sensitizing Effect of Olaparib in Human Non-Small Cell Lung Cancer Xenografts by Contextual Synthetic Lethality		Oncol Biol Phys	
	Novel poly (ADP-ribose) polymerase inhibitor, AZD2281, enhances radiosensitivity of both normoxic and hypoxic esophageal squamous cancer cells	Zhan L	Dis Esophagus	2016
	Role of poly(ADP-ribosyl)ation in a 'two-hit' model of hypoxia and oxidative stress in human A549 epithelial cells in vitro	Erdélyi K	Int J Mol Med	2013
	Zinc promotes the death of hypoxic astrocytes by upregulating hypoxia-induced hypoxia-inducible factor-1alpha expression via poly(ADP-ribose) polymerase-1	Pan R	CNS Neurosci Ther	2013
	In vivo studies of the PARP	Gani C	Radiother	2015

	inhibitor, AZD-2281, in combination with fractionated radiotherapy: An exploration of the therapeutic ratio		Oncol	
Viability tested with PARPi + hypoxia / reoxygenation	Poly(ADP-ribose) Polymerase (PARP) is Critically Involved in Liver Ischemia/Reperfusion-injury	Haga S	J Surg Res	2022
	Poly (ADP-ribose) polymerase inhibition protects against myocardial ischemia/reperfusion injury via suppressing mitophagy	Cao S	J Cell Mol Med	2019
PARPi and HIF relationship	CaMKII Inhibitor KN-62 Blunts Tumor Response to Hypoxia by Inhibiting HIF-1α in Hepatoma Cells	Lee KH	Korean J Physiol Pharmacol	2010
	Selective modulation by PARP-1 of HIF-1α-recruitment to chromatin during hypoxia is required for tumor adaptation to hypoxic conditions	Martí JM	Redox Biol	2021

	Interaction between PARP-1 and HIF-2α in the hypoxic response	Gonzalez-Flores A	Oncogene	2014
viability with PARPi in hypoxia not tested	PARP inhibition promotes endothelial-like traits in melanoma cells and modulates pericyte coverage dynamics during vasculogenic mimicry	Fernández-Cortés M	J Pathol	2023
	Hypoxia-inducible factor-1α and poly [ADP ribose] polymerase 1 cooperatively regulate Notch3 expression under hypoxia via a noncanonical mechanism	Nakamura H	J Biol Chem	2022
	Suppression of homology-dependent DNA double-strand break repair induces PARP inhibitor sensitivity in VHL-deficient human renal cell carcinoma	Scanlon SE	Oncotarget	2017
	Poly-ADP-ribose polymerase inhibition enhances ischemic and diabetic wound healing by	Zhou X	J Vasc Surg	2017

	promoting angiogenesis			
	LRP1 Regulates Retinal Angiogenesis by Inhibiting PARP-1 Activity and Endothelial Cell Proliferation	Mao H	Arterioscler Thromb Vasc Biol	2016
	Gemcitabine induces poly (ADP-ribose) polymerase-1 (PARP-1) degradation through autophagy in pancreatic cancer	Wang Y	PLoS One	2014
	Hypoxia-induced epigenetic regulation and silencing of the BRCA1 promoter	Lu Y	Mol Cell Biol	2011

Appendix 2 Data from CCLE for status of key HR protein encoding genes - oncoprint diagrams

CAL-51 (TNBC)

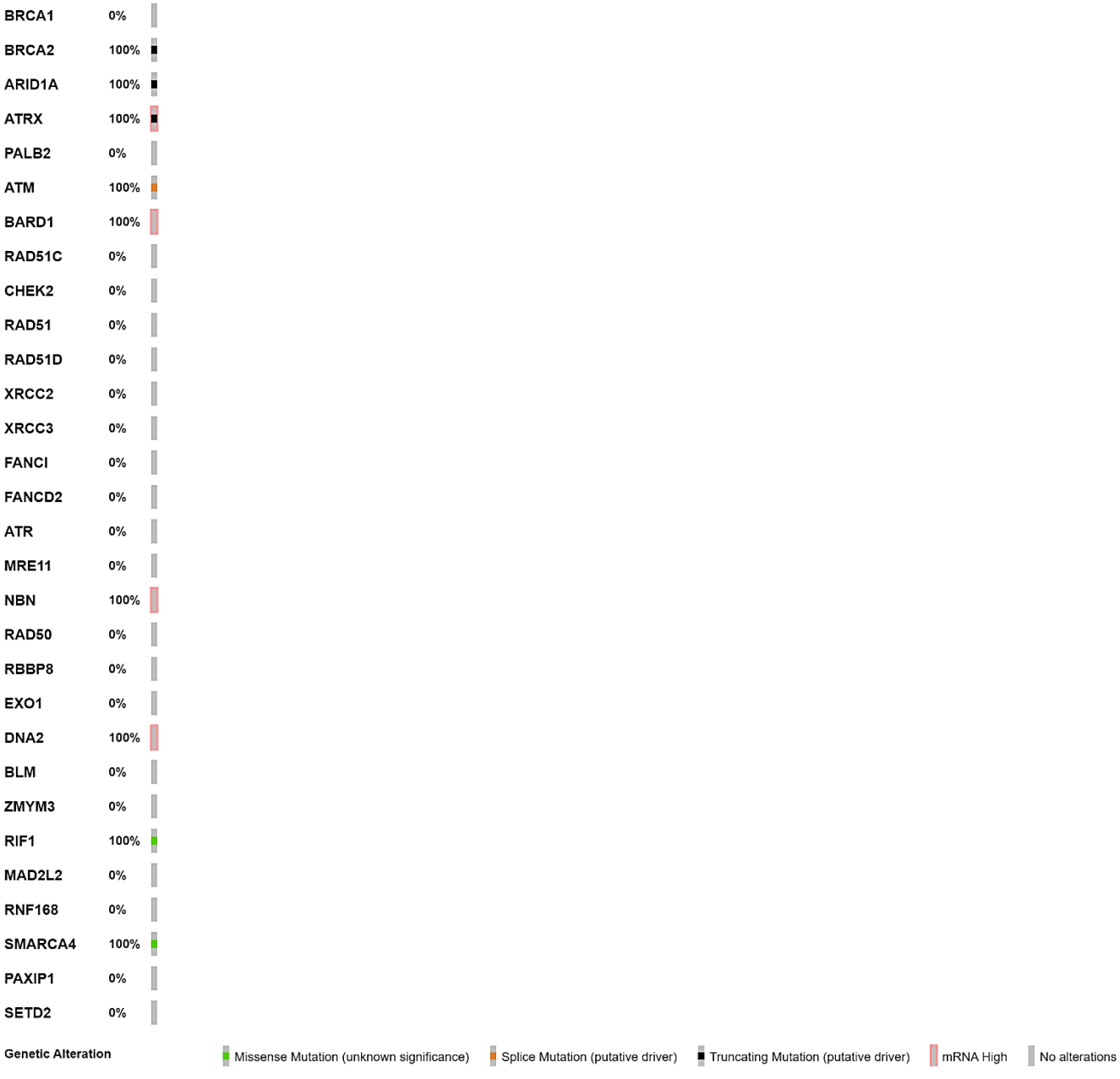

MDA-MB-231 (TNBC)

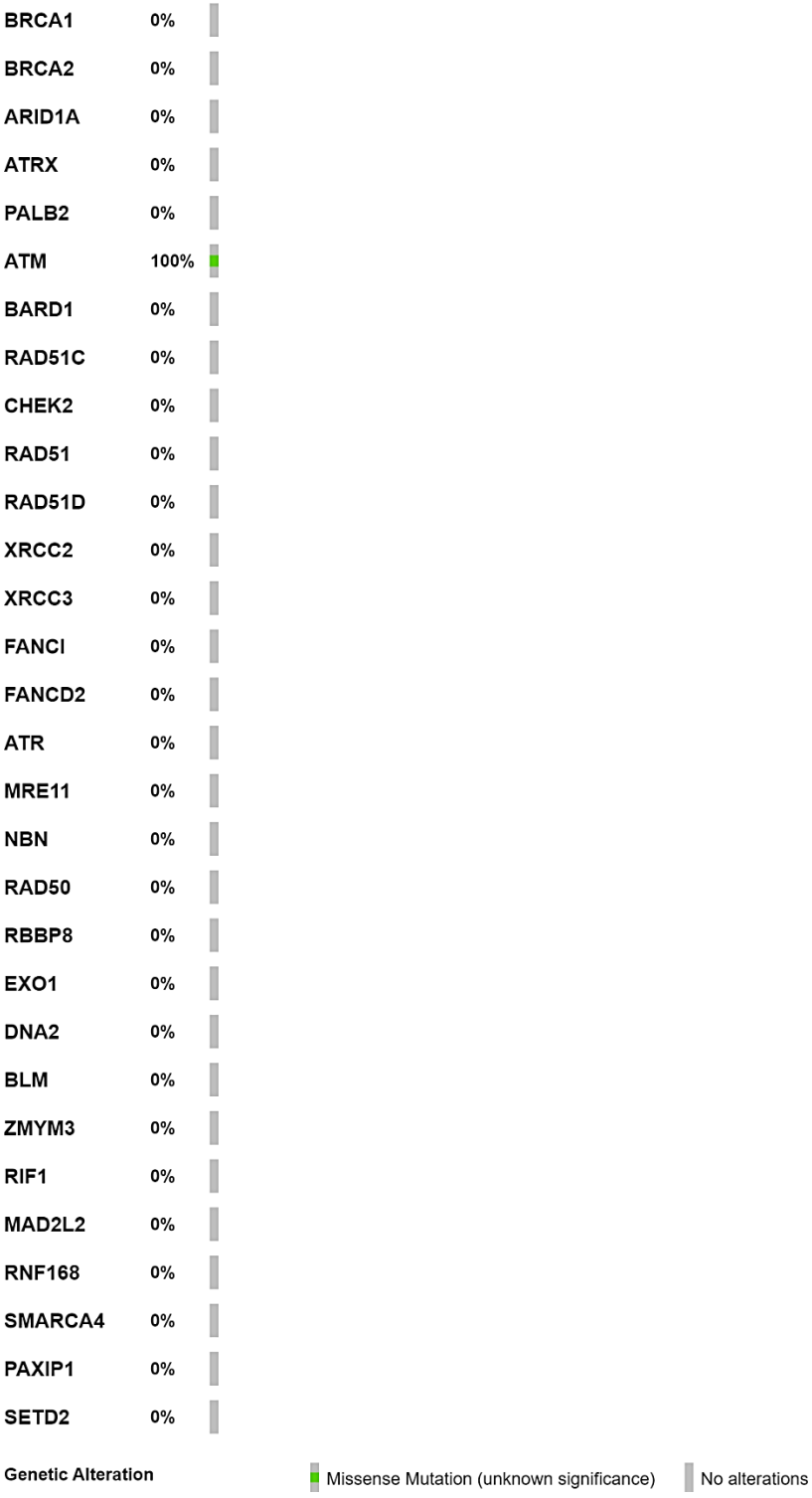

Appendix 3 Genes mostly upregulated in cyclic hypoxic conditions – RNAseq data (Hammond EM, 2020, unpublished)

Gene name	log2 fold change
RIMKLA	3.762510391
MIR1915	3.290993222
EFNA3	2.478841251
EPHA3	2.02186341
PPFIA4	2.02096354
MISP3	1.716420888
AC090114.1	1.612459693
SNORD12B	1.605000783
ZSWIM5	1.592545519
RPS10P3	1.564056792
HLA-Z	1.525191764
CSPG5	1.429222196
ESPN	1.40008303
LINC00705	1.329941372
AC117422.1	1.30177527
SEMA3F	1.279995913
AC110285.3	1.254013394
RNU6-387P	1.16748783
RF00019	1.164729548
AC004656.1	1.092077361
AC005586.1	1.051987014
CLPSL2	1.051613116

SLC2A13	1.004085864
AC069234.5	1.000597531
FEZF1-AS1	0.999025587
BANF1P3	0.970300214
KIAA1958	0.962905923
GAREM1	0.930675768
LINC01389	0.901871723
THSD4	0.894327253
CYTH4	0.880306064
LMO7-AS1	0.867366976
SNORD19	0.855482947
FBXL7	0.797836292
RF00019	0.796889335
TRPV4	0.782906164
AC009549.1	0.768502887
PLD5	0.754250241
TLR2	0.734249478
PASK	0.726603435
AC090587.2	0.67981801
SREBF2-AS1	0.668543297
RNU6-415P	0.648042237
RFX2	0.645388993
RF00410	0.636480458
GFAP	0.623665083
NFIA	0.620403653
AC004877.2	0.614580421
ZKSCAN2	0.611673984
AC005000.1	0.589705786
AL354892.2	0.56160246
AC116345.1	0.559368786
FKBP1C	0.55470066
YWHAZP3	0.55415617
AC018904.1	0.519859468
IFNLR1	0.495961339
POLQ	0.495909429
DMTN	0.485010989
AC145343.1	0.483640974
RECK	0.481836478
ACOT4	0.477118922
TMEM191B	0.474030623

SFXN5	0.471919505
RF00019	0.471897296
DOCK2	0.438301862
ALMS1	0.383168421
PRELID2	0.375817882
GASAL1	0.373910818
ANKRD36C	0.366598332
PTPRE	0.335555187
AL359091.5	0.321000217
ZNF804A	0.319677033
MYORG	0.28659294
RALGDS	0.281847615
SNRPGP2	0.26757673
SPATA13	0.238787231
RNU7-171P	0.204252049
PSTPIP2	0.189553147
PIAS2	0.174379951
SUCLG2-AS1	0.168119911
AC004918.3	0.15262589
MIR641	0.138732835
SNORD12C	0.104298365
D2HGDH	0.090705695
MELTF-AS1	0.08539676
TRPV2	0.081642468
LHFPL4	0.051938883
GAL	0.022211821

Appendix 4 Analyses of the correlative power of top-15 genes from hypoxia-associated signatures used in the study

A. Pathway enrichment analyses of top-15 genes *vs*. full gene sets of hypoxia-associated signatures

- Top-15 *vs*. full gene set from Buffa hypoxia signature:

Top-15 genes (Buffa) MSigDB Hallmark 2020 enrichment analysis

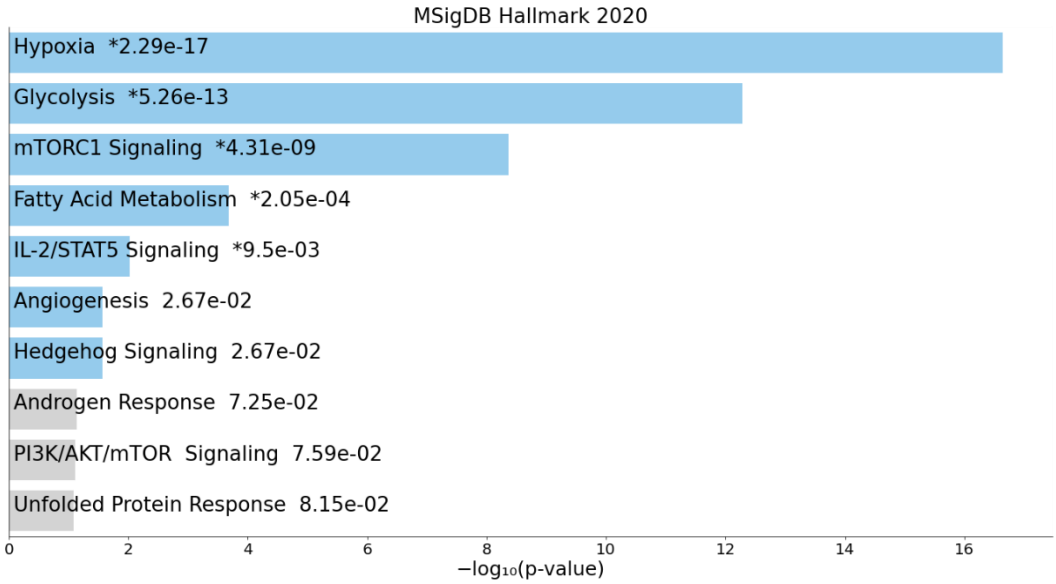

Full gene set (Buffa) MSigDB Hallmark 2020 enrichment analysis

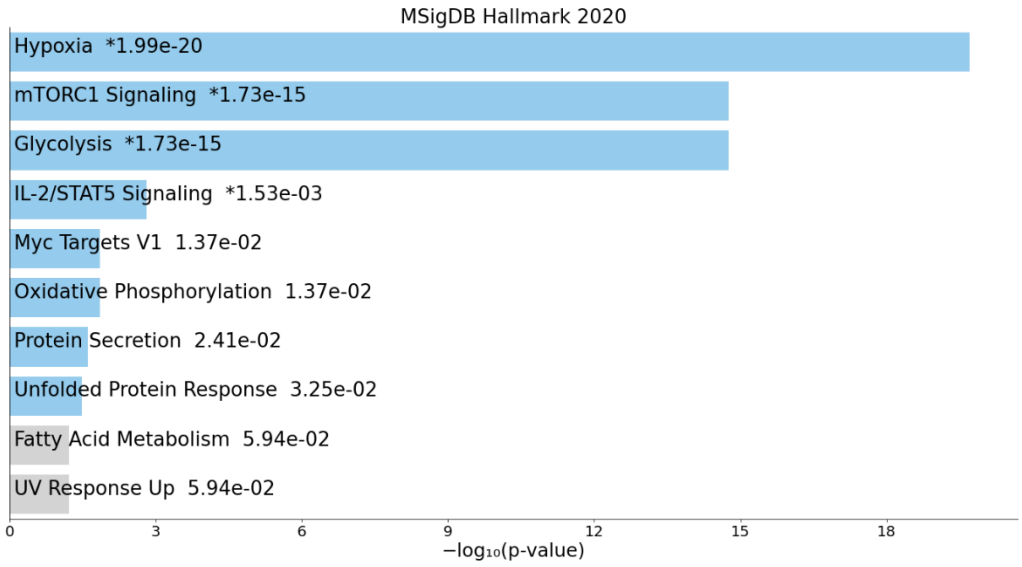

- Top-15 *vs*. full gene set from Ragnum (pimonidazole) hypoxia signature:

Top-15 genes (Ragnum) MSigDB Hallmark 2020 enrichment analysis

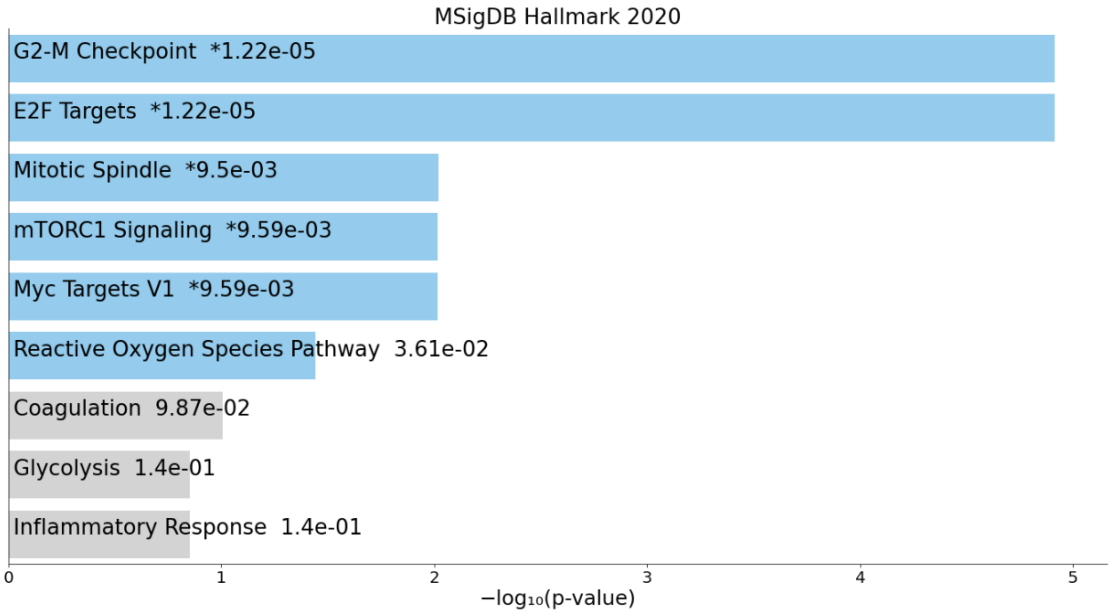

Full gene set (Ragnum) MSigDB Hallmark 2020 enrichment analysis

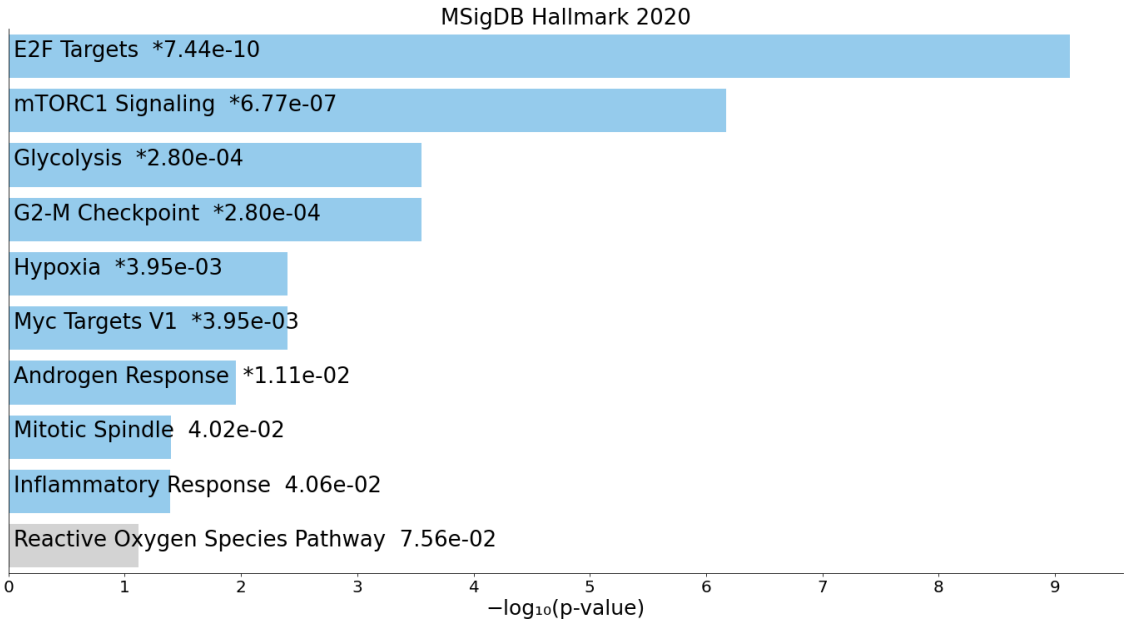

B. PCA analyses of top-15 genes *vs*. full gene sets of hypoxia-associated signatures using TCGA BRCA samples transcriptomic data

Top-15 genes from Buffa hypoxia signature PCA plot: *(PC1+PC2 = 64.6%)*

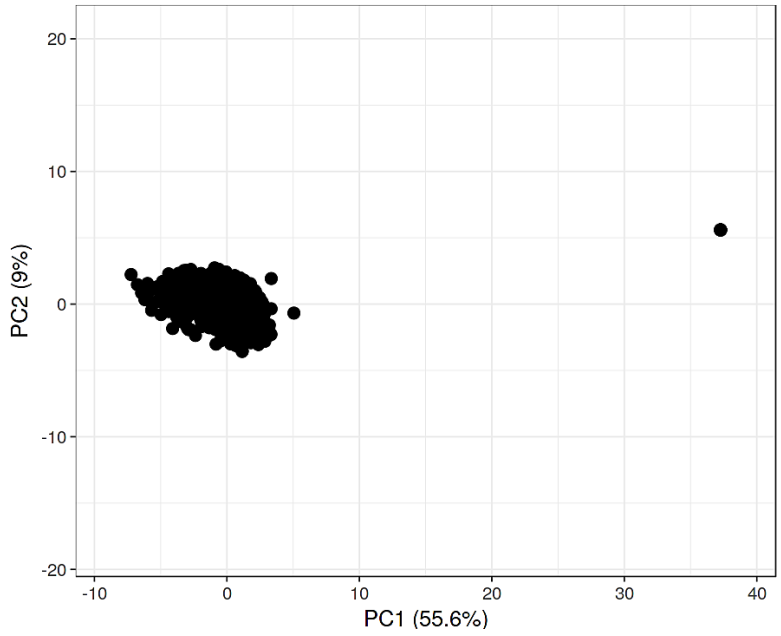

Full gene set from Buffa hypoxia signature PCA plot: *(PC1+PC2 = 60.4%)*

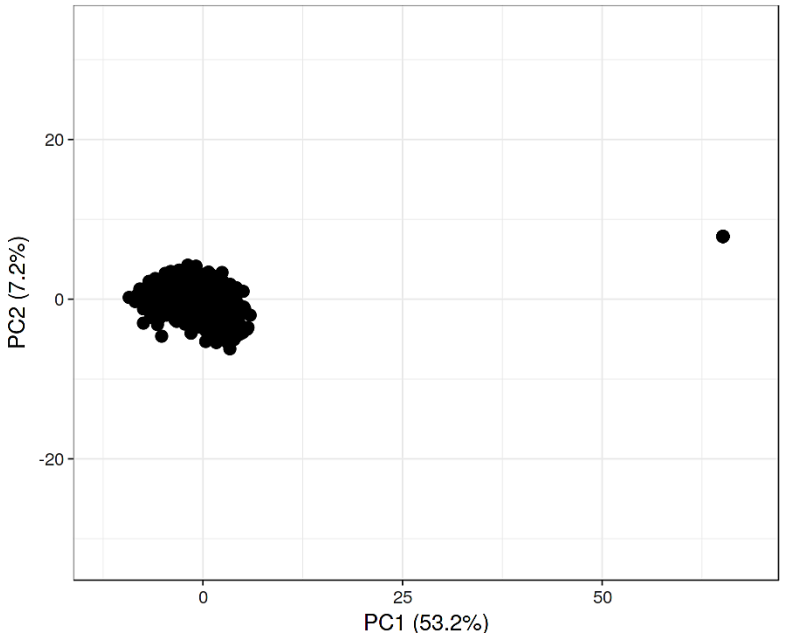

Top-15 genes from Ragnum hypoxia signature PCA plot: *(PC1+PC2 = 69.3%)*

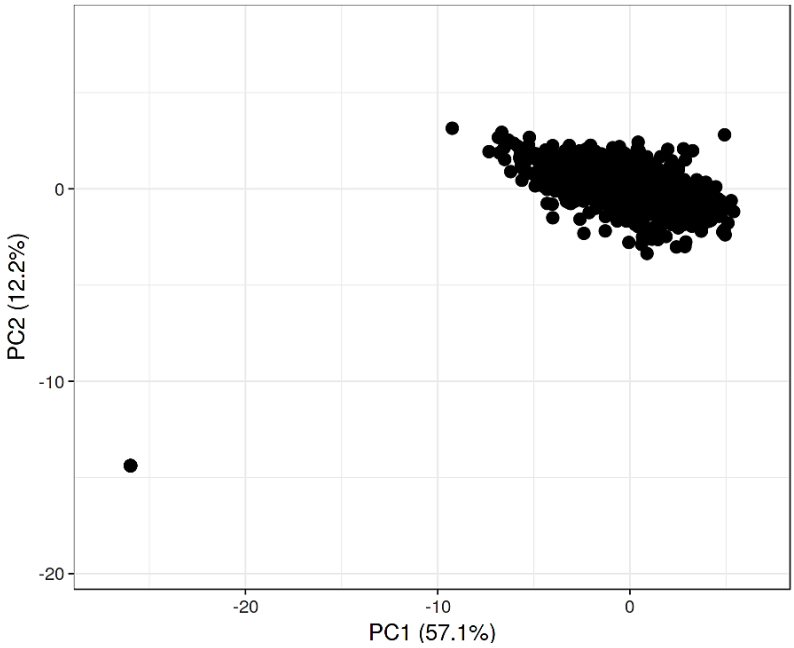

Full gene set from Ragnum hypoxia signature PCA plot: *(PC1+PC2 = 54.4%)*

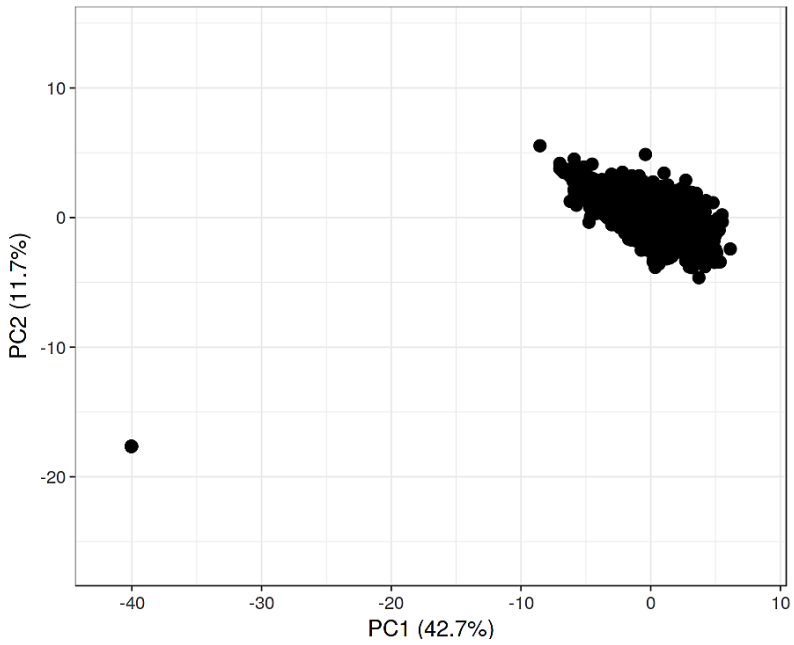

C. Correlation analysis of full gene sets *vs*. top-15 genes across independent datasets

Datasets	**Pearson *R* and *p* value of full buffa hypoxia signature *vs*. top-15 genes**
BRCA (TCGA) (Cancer Genome Atlas 2012)	*R = 0.87; p < 0.001*
LIHC (TCGA) (Cancer Genome Atlas Research Network. Electronic address and Cancer Genome Atlas Research 2017)	*R = 0.949; p = 0.0019*
METABRIC (Curtis *et al*. 2012)	*R = 0.901; p < 0.001*
Metastatic Melanoma (Van Allen *et al*. 2015)	*R = 0.899; p < 0.001*

Datasets	**Pearson *R* and *p* value of full Ragnum hypoxia signature *vs*. top-15 genes**
BRCA (TCGA) (Cancer Genome Atlas 2012)	*R = 0.9; p < 0.001*
LIHC (TCGA) (Cancer Genome Atlas Research Network. Electronic address and Cancer Genome Atlas Research 2017)	*R = 0.949; p <0.001*
METABRIC (Curtis *et al*. 2012)	*R = 0.88; p = 0.0027*
Metastatic Melanoma (Van Allen *et al*. 2015)	*R = 0.81; P < 0.0044*

Appendix 5 Tumour *vs*. normal tissue analysis of *RIMKLA* expression levels (TCGA datasets)

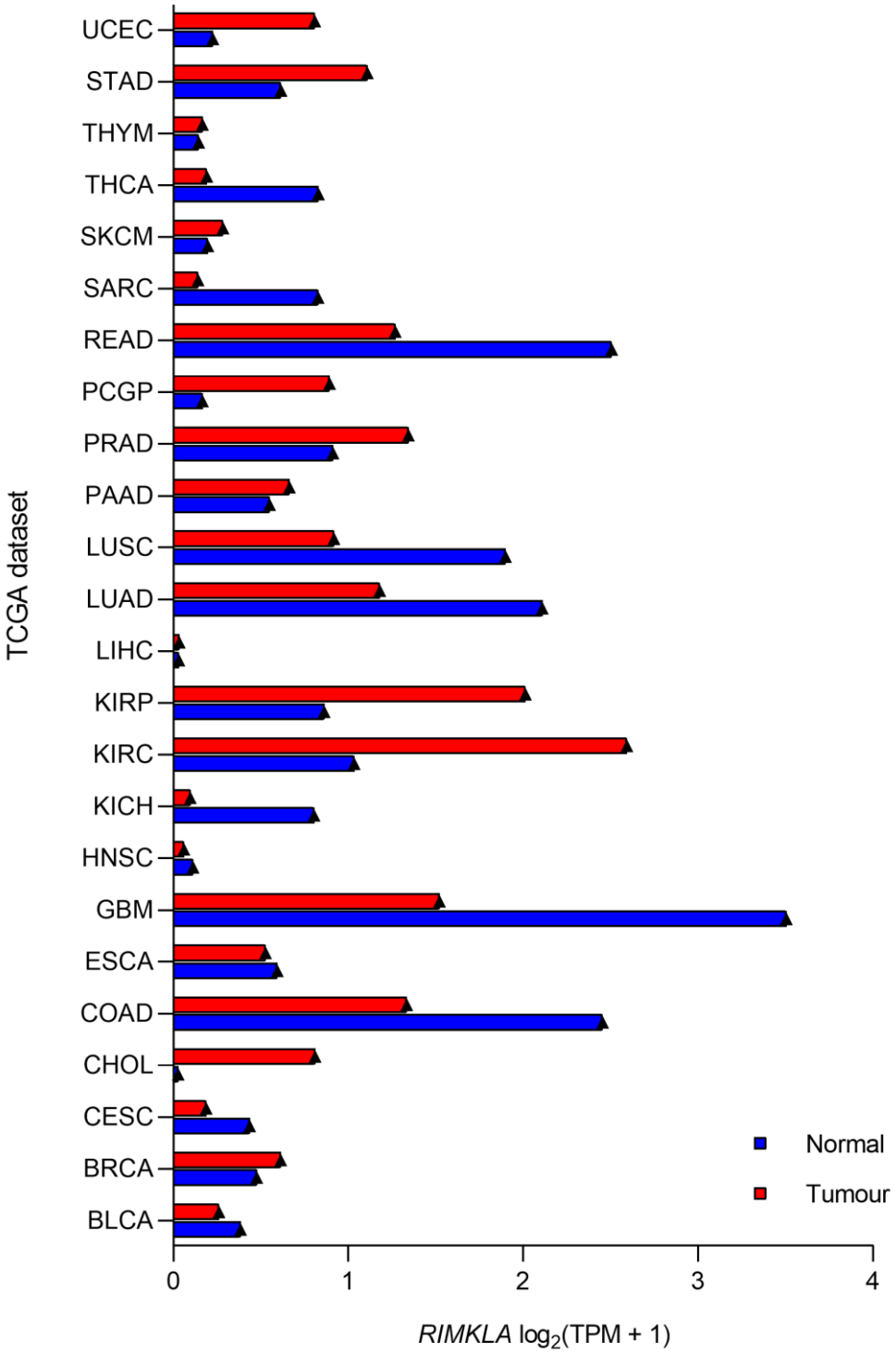

Appendix 6 Correlation analysis of published breast cancer HIF-target genes with the Buffa hypoxia signature in TCGA BRCA publicly available transcriptomic datasets

Data and graphs accessed and generated via cBioportal (Cerami *et al.* 2012).

A. *STC2 vs*. Buffa hypoxia score (TCGA BRCA PanCancer Atlas)

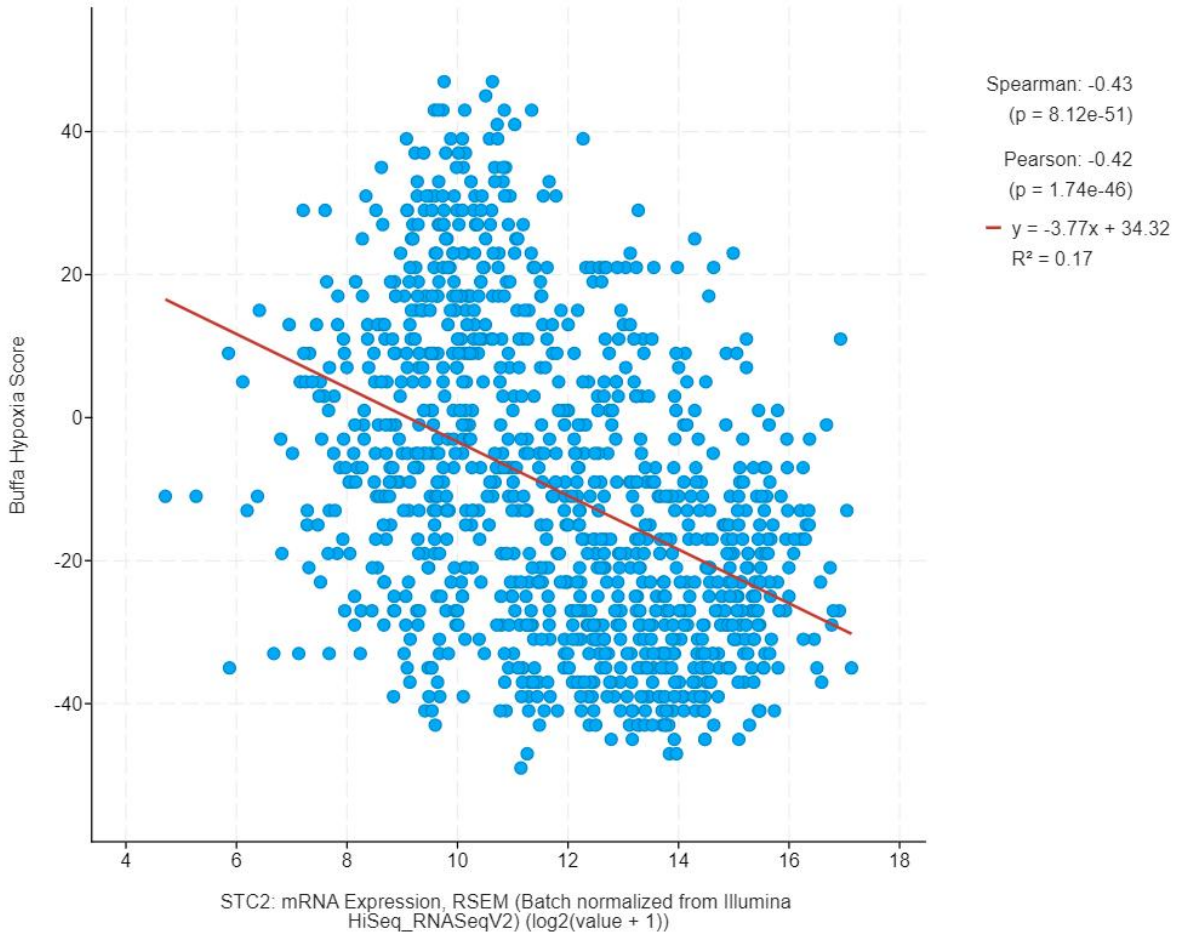

B. *KLF4 vs*. Buffa hypoxia score (TCGA BRCA PanCancer Atlas)

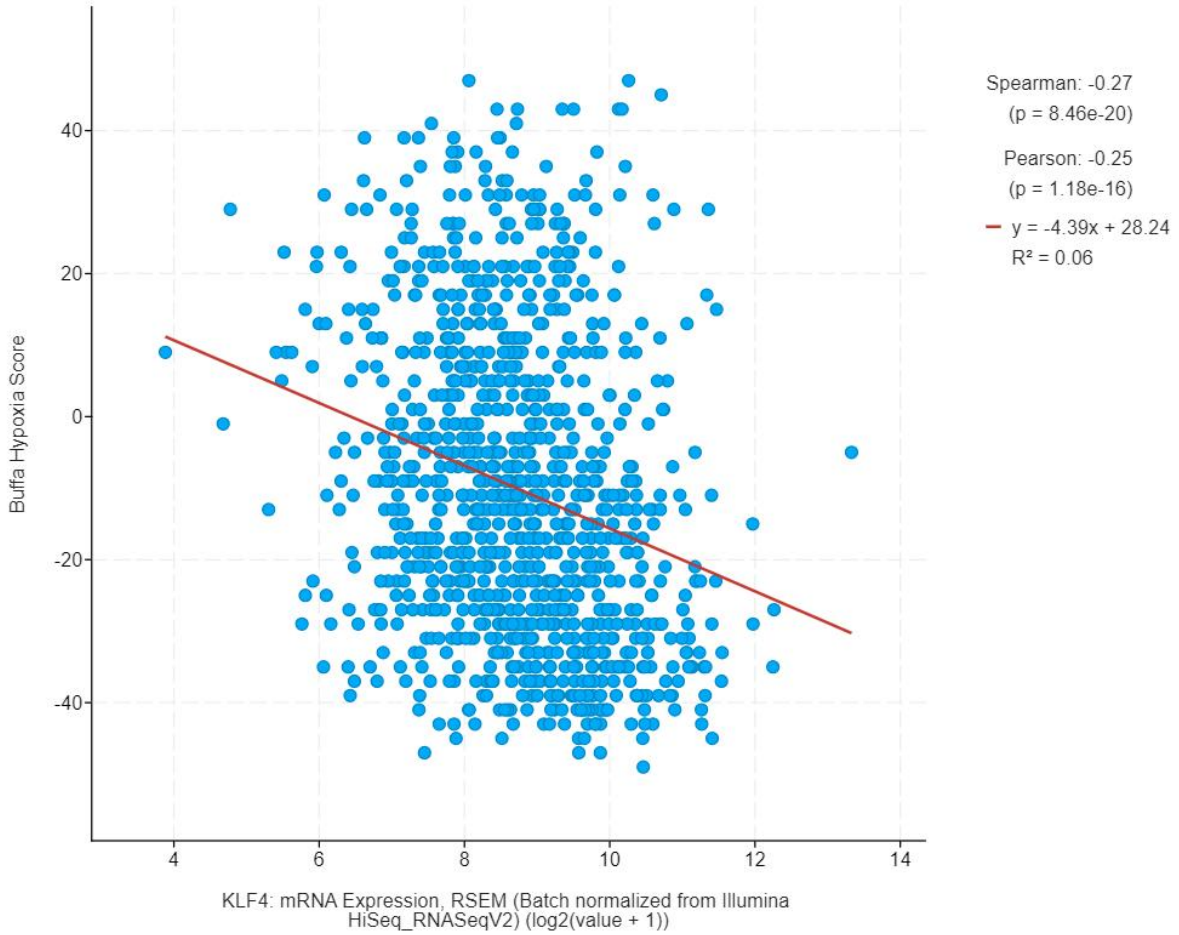

C. *SLC38A2 vs*. Buffa hypoxia score (TCGA BRCA PanCancer Atlas)

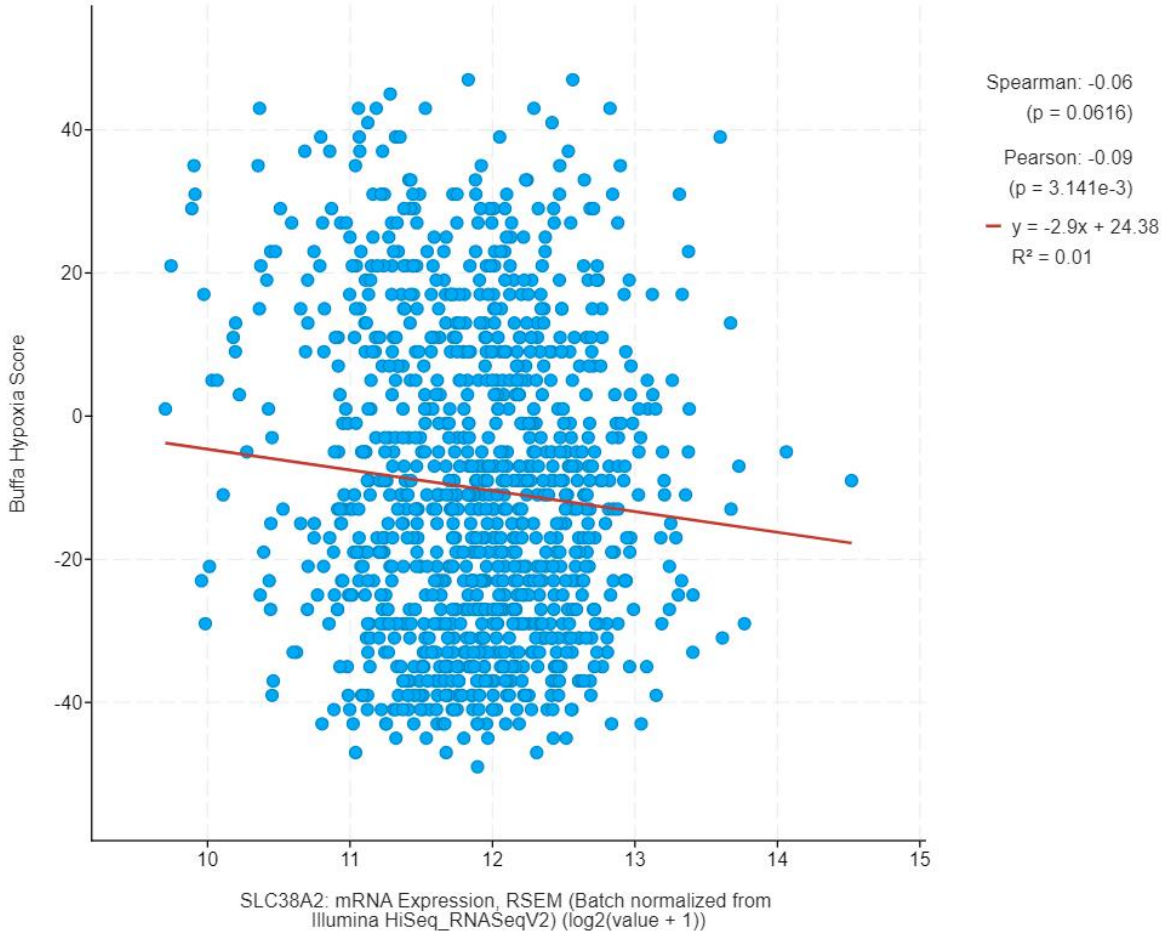

Appendix 7 FIJI/Image J script used for image analysis (foci quantification)

```
//Requires LOCI Plugin

dir = getDirectory("Choose a Directory");
list = getFileList(dir);
run("Input/Output...", "jpeg=100 gif=-1 file=.csv copy_column copy_row save_column save_row");

setBatchMode(true);

for (loop=0; loop<lengthOf(list);loop++){
if(endsWith(list[loop],".czi")){ //Edit File format for images i.e. czi or nd2
//open(dir+list[loop]);

updateResults();
run("Clear Results");
IJ.renameResults("Results","Final");

run("Bio-Formats", "open=["+dir+list[loop]+"] color_mode=Default rois_import=[ROI manager] view=Hyperstack stack_order=XYCZT series_2");

Title = getTitle();

//run("Smooth", "stack");
run("Split Channels");

selectWindow("C2-"+Title); // Dapi Channel Number
run("Smooth");
setAutoThreshold("Otsu dark");
//run("Threshold...");
setOption("BlackBackground", false);
run("Convert to Mask");
run("Fill Holes");
run("Watershed");
run("Set Measurements...", "area redirect=None decimal=3");
run("Analyze Particles...", "size=50-300 exclude clear add");
num_Cells = roiManager("Count");
roiManager("Measure");
IJ.renameResults("Results","Final");
run("Flatten");
rename("flat");

run("ROI Map");
roiManager("Reset");

selectWindow("C1-"+Title); //Foci Channel Number
run("Smooth");
run("Find Maxima...", "prominence=50 strict output=[Point Selection]"); // Alter prominence for Foci
//run("Find Maxima...", "noise=15 output=[Point Selection]"); // Alter noise parameter to find foci, test with process>find maxima
roiManager("Add");
selectWindow("flat");
roiManager("select", 0);
run("Flatten");
saveAs("Jpeg", dir+Title+".jpg");
close();

selectWindow("Roi Map");
roiManager("select", 0);
run("Set Measurements...", "min redirect=None decimal=3");
run("Measure");

for (i=1; i<num_Cells+1; i++){
    foci = 0;
    for (j=0; j<nResults; j++) {
        cell = getResult("Min", j);
        if(cell == i){
            foci++;
        }
    }
IJ.renameResults("Results","Temp");
IJ.renameResults("Final","Results");
setResult("Foci", i-1, foci);
IJ.renameResults("Results","Final");
IJ.renameResults("Temp","Results");
}
close("Results");
IJ.renameResults("Final","Results");

saveAs("Results", dir+Title+"_Results.csv");
run("Close All");
close("Results");
roiManager("Reset");
}
}

setBatchMode(false);
```

The script was created and kindly provided by Dr Rhodri Wilson, University of Oxford.

Appendix 8 Presentations from this Thesis

- European Association of Cancer Research (EACR) annual congress, Rotterdam, Netherlands – 2024 (Poster Presentation): "Loss of *RIMKLA* sensitises cancer cells to hypoxia"

- Oncology Departmental Seminar Series, University of Oxford – 2024 (Oral Presentation): "Loss of *RIMKLA* sensitises cancer cells to hypoxia"

- Oncology Departmental Poster Presentation Series, University of Oxford – 2023 (Poster Presentation) : "Loss of *RIMKLA* sensitises cancer cells to hypoxia"

- Department of Oncology Annual Student Symposium, University of Oxford – 2022 (Oral Presentation): "The impact of hypoxia dynamics on therapy response of breast cancer cells"

- Department of Oncology Annual Student Symposium, University of Oxford – 2021 (Poster Presentation): "The impact of acute hypoxia on the effects PARP inhibitors"